# The Hydrological System and Climate of Brewster Glacier, Tititea Mt Aspiring National Park, Southern Alps, Aotearoa New Zealand, in the Context of Climate Change.

By

**Alexandra Winter-Billington**

*Supervisor: Dr Andrew Mackintosh*

A thesis submitted to Victoria University of Wellington in partial fulfilment of the requirements for the degree of

**Masters of Science**

**in Physical Geography**

Victoria University of Wellington

2008

***"…science is done for the sake of the characteristic pleasure which accompanies the act of discovery and is therefore a kind of play."***

**Kaiser, 1952**

# Abstract

Temporal and spatial variability of stream discharge is directly related to variation in local climate, and this in turn is related to both regional and global atmospheric circulation and climate change. The relationship is complicated in glacierised catchments. This study aims to identify relationships between discharge from Brewster Glacier proglacial stream and both local atmospheric variables and national atmospheric circulation patterns. An attempt is made to quantify these relationships using statistical models and tests in order that prediction of discharge with climate change could be made using local weather forecasts and national circulation indices. The nature of the subglacial drainage system is also investigated with particular focus on its structural evolution from summer to autumn.

It is found that shortwave radiation, wind speed and relative humidity are consistently the most important variables in prediction of discharge and that wind speed is most important during summer while air temperature is most important in autumn. It is concluded that the importance of precipitation is greater than indicated by the results which were influenced by covariance in the records. A multiple regression model for summer discharge predicts up to 85% of variation in the proglacial stream hydrograph and for autumn 60%. Low overall energy inputs during autumn result in lesser sensitivity of discharge to variation in environmental conditions. It is concluded that the subglacial drainage system is highly arborescent over both summer and autumn and that little, if any, evolution occurs through these seasons. A qualitative relationship is established between discharge production at Brewster Glacier proglacial stream and national atmospheric circulation indices; highest average discharge occurs during northwesterly cyclonic conditions, when the turbulent heat fluxes and precipitation dominate discharge production, and lowest during southeasterly anticyclones when total energy inputs are low. The multiple regression models are used to estimate changes in discharge over the next 20 years given predicted changes in air temperature and precipitation, and it is found that the models lack the sensitivity required for accurate predictions.

# Acknowledgments

I was honoured and grateful to receive the following scholarships in support of this project:

- The Royal Geological Society of New Zealand Wellman Research Award; in commemoration of Harold Wellman's contribution to the study of geology in Aotearoa New Zealand.
- The Institute of Geological and Nuclear Sciences of New Zealand Sarah Beanland Memorial Scholarship; marking the inspiration provided by Dr Sarah Beanland to young geological scientists.
- The Victoria University of Wellington Tu Horomata Scholarship, in association with the Awhina Postgraduate Association of Victoria University; in support of postgraduate students of Maori decent.

Heartfelt thanks also go to Dr Andrew Mackintosh and Dr Brian Anderson for their tireless footwork, intellectual generosity and willingness, enthusiasm in their contribution to this project and for their patience. Thanks also to Tim Kerr for providing data, expertise and again footwork, intellectual generosity and patience; Dorothea Stumm, Ian Willis and Jordy Hendrix and Brett Mullan of NIWA for providing data; Lynley Hargreaves, Becky Goodsell, my mum Christine Winter, Yasmine El Orfi, Stefan and Franz and Graham Lyons for their generous contributions to the fieldwork; and finally the New Zealand Snow and Ice Research Group for support and feedback.

## Photographs

All photographs in this report were taken by the author unless otherwise stated.

# Contents

# List of Figures

## Chapter 1: Introduction



## Chapter 2: Methodology



## Chapter 3: Results

### *Section 1:*

***Section 4:***

***Section 5:***



***Section 6:***



***Section 7:***

***Section 8:***

***Section 9:***



***Section 10:***

**Chapter 4: Discussion**



**Appendix 1**

**<u>Appendix 2</u>**

# List of Tables

## Chapter 1: Introduction



## Chapter 3: Results

***Section 1:***



***Section 4:***



***Section 6:***



***Section 7:***

***Section 8:***

***Section 9:***



***Section 10:***

**Chapter 4: Discussion**



**Appendix 2**

# Chapter 1: Introduction

## Glaciers and Climate Change

Global Warming is arguably the greatest threat facing human kind and the global environment today. The Intergovernmental Panel on Climate Change (IPCC) has predicted a 'worse case scenario' average global temperature increase of 2.4-6.4°C by the end of this century (Bernstein et al., 2007). Predicted impacts range from widespread sea-level rise (0.09-0.88m [Watson et al., 2001], 0.13m from valley glaciers alone [Gregory and Oerlemans, 1998]) and regionally increased rainfall, to intense regional drought and forest fires (Bernstein et al., 2007). Comparisons of geologic and recent climate trends reveal that present day warming is the result of both natural and anthropogenic forcings and that, whilst such signals can be differentiated, climate change is enormously complicated (Bernstein et al., 2007).

Glaciology has moved to the fore in the study of causes, trends and impacts of climate change. Glacier behaviour is a measurable echo of climate variation and as such it is an invaluable indicator of both past and present climate change.

Glaciers exist only where the climate is conducive, requiring snowfall sufficient to accumulate a permanent base and summer temperatures insufficient to completely melt this base (Menzies, 1995). Whether or not this occurs depends on the combination of specific long-term atmospheric conditions together with a multitude of local geographic variables, as depicted in Figure 1.

Climatic variables dominate the diagram in Figure 1 and are the most changeable. Altitude, latitude and relief, geothermal heat, basal and surface debris are either very slow to change or highly sporadic in their changeability (Menzies, 1995), whilst variables such as precipitation, solar radiation and cloud cover change on time scales of days to millennia. These latter variables control the dynamics of a glacier - its specific mass, geometry and movement over time; a change in any one of them will result in a change of the dynamics and/or geometry of the affected glaciers at a comparable scale (Paterson, 1994).

For a glaciers' response to climate change to be comprehended, predicted or reconstructed, the minutiae of glacial and climatic dynamics must be well understood and the same is true if climate changes are to be predicted or reconstructed from past glacier behaviour (Paterson, 1994). As climate change is modelled by extrapolating real-time glaciological and

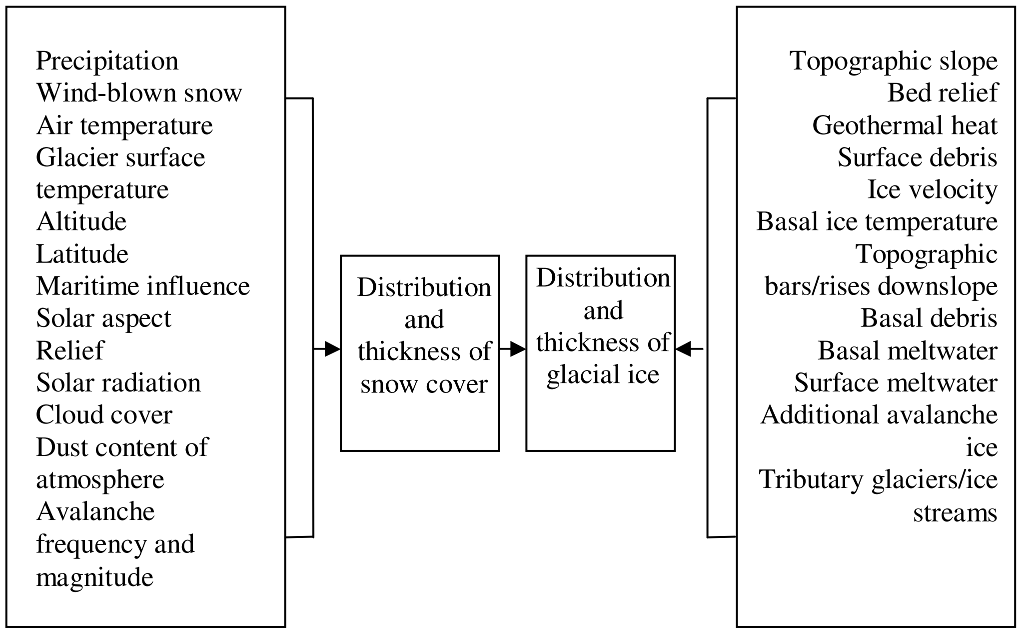


**Figure 1. A generalised linkage diagram exhibiting the relationships between external geographical and atmospheric variables, glacier mass balance and ice mass thickness and extent. (from Menzies, 1995)**

climatological data, models can represent only such small portion of the cryosphere and climate as the data from which they are derived (Oerlemans, 2001; Arnold et al., 1998). Local and regional responses to climate change are estimated in this way (Evans, 2004), whilst a comprehensive picture of climate change and its impacts on the cryosphere requires samples and precise modelling from a wide variety of glaciological regions to be combined for inter-regional and global models (Barry, 2006; Hock, 2005).

Most studies of glaciers in relation to climate change focus on mass balance (Oerlemans, 2005; Baisheng et al., 2003; Moore and Demuth, 2001; Oerlemans, 2000; Oerlemans & Reichert, 2000; Dyurgerov & Meier, 2000; Raper et al.; 2000; Gregory and Oerlemans, 1998). A number of studies relating mass balance changes of Aotearoa New Zealand glaciers to climatic patterns have been completed (Anderson et al., 2006; Fitzharris et al., 2006; Chinn et al., 2005; Clare et al., 2002; Hooker & Fitzharris, 1999; Lamont et al., 1999; Fitzharris et al., 1997; Neale & Fitzharris, 1997; Fitzharris et al., 1992a; Hessell, 1983). However, as knowledge of the influence of the ice/water interface on glacier dynamics has increased, and population stress on water resources has increased, more interest has been shown in water in the glacial system (Ramage et al., 2006; Hock, 2005; Jansson et al., 2003; Moore & Demuth, 2001; Munro, 2000; Fountain & Walder, 1998).

## Glacial Hydrology and a Changing Global Climate

By producing variation in ice flow velocity and distribution, and ablation rates, the ice-water interface has proven to be a significant complication to the glacier-climate relationship. Subglacial hydraulics influence ice flow dynamics (Clarke, 2005; Evans, 2005; Sharp, 2005; Alley et al., 2003; Lingle and Fatland, 2003; Flowers & Clarke, 2000; Boulton & Hindmarsh, 1987); when the drainage system of a glacier is hydraulically inefficient – a common occurrence for temperate glaciers during winter through to the beginning of the melt season (Oerlemans, 2001) - water moves through channels more slowly than it enters. Localised build-up of water can thereby occur, alleviating basal pressure and allowing overlying ice to flow more rapidly until basal pressure is restabilised by meltwater dispersion and/or a reorganisation of the drainage system morphology (Raymond, 1987). Saturation of fine basal sediments can also lead to high velocity events by facilitating sediment deformation and thereby, ice motion (Harrison and Post, 2003; Kulessa and Murray, 2003).

Bingham et al. present an archetypical study of glacial hydrology and high velocity events in their 2006 paper. They conclude that short-term velocity events at the predominantly cold John Evans Glacier, Canada, result from swift input and pooling of supraglacial melt water to the high pressure, hydraulically inefficient subglacial hydrological system at the beginning of each melt season. The authors infer subsequently increased efficiency of the subglacial drainage system due to meltwater channel enhancement. Bingham et al. (2005) assert that the distribution of moulins and crevasses increases during summer, thereby increasing the area over which supraglacial melt input may effect high velocity events. They also assert that high velocity events enhance retreat rates resulting from climate change by increasing the downward mass transfer of ice into the ablation zone.

The submersion of a glacial snout in water renders it more vulnerable to ablation than grounded termini through destabilisation and calving, and submarine melt at higher rates than subaerial (Haresign and Warren, 2005; Motyka et al., 2003; Kirkbride, 1993). Increased rates of retreat can also result from extension of thermokarst systems and the internal drainage system of a retreating glacier. Such extension represents an increase of the surface area from which melt can occur and can precede collapse of the ice mass as a result of internal destabilisation (Hochstein et al., 1995; Kirkbride, 1993).

Understanding of glacial hydrology is also important for interpretation of glaciated landscapes, as the subglacial structure and movement of water leaves a distinct imprint on the landscape that can be interpreted for many purposes (Evans, 2004). For example, Swift et al. (2002), from the results of a study of the suspended sediment in the proglacial stream of Haut Glacier d'Arolla, Switzerland, determined that moraine deposits will vary in size and composition depending on the configuration of the subglacial hydrological system, where a channelised system of restricted distribution will produce a greater overall quantity of sediment but lower marginal deposition. Such information is useful for the reconstruction of past climates from the geomorphology of glaciated catchments.

The water draining from high alpine regions is counted on for consumption, irrigation and hydro electricity production by hundreds of millions of people globally. While change of glacial discharge would be welcome in some areas, others could be at risk from increased flood frequency if glacial discharge were to increase or water shortages were it to decrease (Evans, 2005; Sharp, 2005) (both such trends have been observed in glacierised catchments due respectively to increased melt and decreasing glacier mass [Huntington, 2006]). Paul et al. (2004) estimate that global alpine glacier retreat rates have increased by seven times between 1850 and 1999 and suggest that retreat will continue to accelerate into the future. The IPCC predicts that the Hindu-Kush, Himalaya and Andes regions will suffer water shortages with climate change over the next century (Bernstein et al., 2007). In Aotearoa New Zealand, summer melt from glacierised catchments is relied upon for irrigation and hydro-electricity generation (Fitzharris et al., 1992b), although the predictions for this country are not as dire as they are for the former regions mentioned. Eastern Aotearoa New Zealand is predicted by the IPCC to be experiencing water shortages and subsequent decline in productivity by 2030 (Bernstein et al., 2007).

The probability, rate and cyclic variation of glacio-hydrological changes are therefore of import for town planning and hydrological forecasting (Schaefli et al., 2005; Singh et al., 2005; Baisheng et al., 2003; Walder and Driedger, 1995). Moore and Demuth (2001) present their findings and conclusions from study of Place Glacier, Canada. They state that with glacial retreat, discharge will initially increase due to the exposure of bare ice as snow and firn melt, reducing albedo and thereby increasing ice melt. But as ice volume decreases the authors conclude that a decline in discharge volume is inevitable. The research conducted by Baisheng et al. (2003) in the Tien Shan Mountains in China suggests that a positive relationship exists between glacier size and the sensitivity of response of both the glacier mass and runoff to climate change. Smaller glaciers showed a greater sensitivity in this model; response to climate variations occurred comparatively quickly and streamflow exhibited a pattern of higher peak discharge, faster flow attenuation and greater overall decrease in runoff over a thousand year period. The implication of such studies is that discharge from glacierised catchments is becoming increasingly irregular and is likely to cause problems for downstream communities as climate change continues to take effect, for which detailed hydrological forecasts can aid preparation.

## Glacial Hydrology

The specific characteristics of any hydrological system are given by the catchment's geography, geology and climate (Barry, 1992). In a glacierised catchment, the system is complicated so that the rules governing stream response are less straightforward than they are in a non-glacierised catchment. Where precipitation and groundwater are the primary sources of water in a non-glacierised catchment, a glacierised catchment has the addition of supraglacial, englacial and subglacial ice melt, snow and firn melt. Furthermore, the passage of water through a glacierised catchment is comparatively convoluted with a number of possible spatial and temporal drainage pathways (Menzies, 1995).

The bulk of water precipitated onto a glacier during cold months falls as snow and is stored as snow, firn or ice for periods ranging from days to hundreds of years (Fitzharris et al., 1992b) (Figure 2). Ripe snow and firn (as defined by Davie, 2003) store liquid water in interstitial cavities until further energy input forces melting beyond the storage capacity of the medium and output occurs with a time lag dependent on the density and transmissivity of the pack. Campbell et al.'s 2006 study of the effect of the supraglacial snowpack on melt water delivery

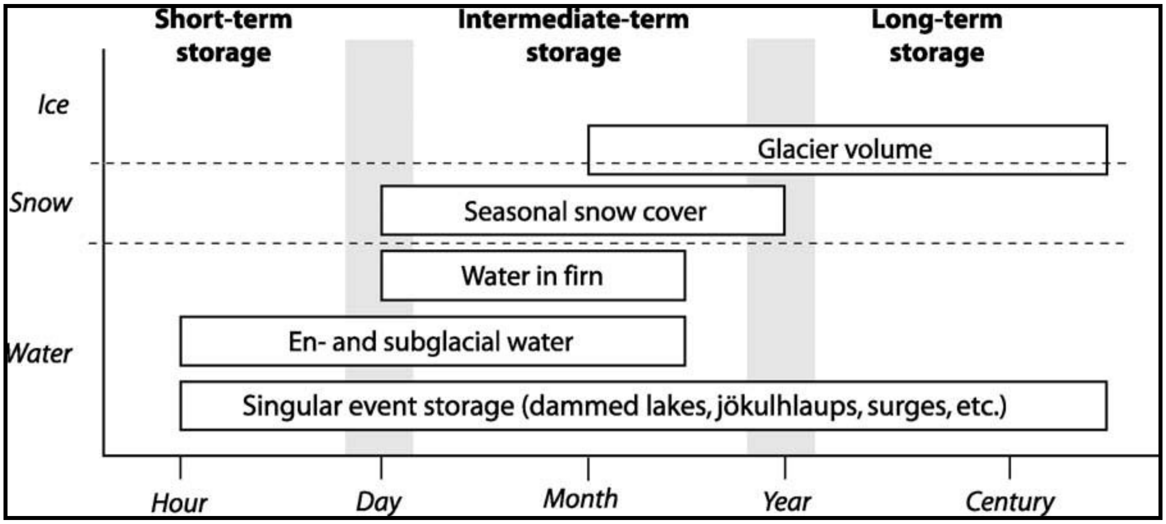


**Figure 2. Schematic graph showing different forms of glacier storage and their corresponding time-scales (from Jansson and Hock, 2003).**

to the subglacial drainage system of Haut Glacier d'Arolla showed that during cold months, the snowpack considerably slowed melt water flow, with transmission efficiency increasing through the melt season. Fountain (1996) also found that peak discharge occurred earlier once the winter snowpack had been removed, while flow of melt water through firn caused a comparatively short delay in streamflow response.

Pools of water form at the ice surface when air temperatures are above zero that may either refreeze, evaporate or eventually contribute to runoff. This depends largely on the season and short-term changes in environmental conditions (Jansson et al., 2003), where drainage of pools into the glacier is most frequent during summer (Menzies, 1995). Subglacial cavities in which water accumulates form on the lee side of topographic lumps; pressure melt of ice occurs on the stoss side of such protuberances and the newly formed liquid water, under pressure, flows downstream causing melt of lee side ice and thus creating a cavity. Growth of such cavities continues as long as high pressure water drains into them and closure occurs on cessation of this flow (Sharp, 2005; Hooke, 1989). Englacially, storage occurs in cavities resulting from blockages of channels due to plastic closure or ice accretion. In each case, release of stored water is favoured during warm months when temperatures and water flow induce disintegration of the blockages between cavities and hydraulically connected drainage pathways (Menzies, 1995). The idealised hydrological system of a temperate glacier and locations of water storage is depicted in Figure 3.

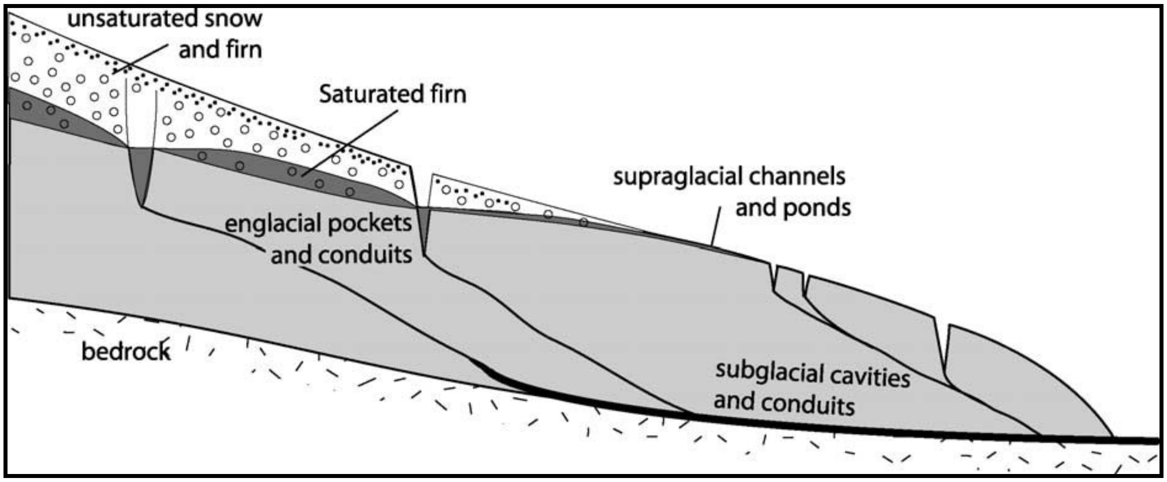


**Figure 3. The locations of water storage in a temperate glacier (from Jansson and Hock, 2003).**

In each case, melt will at some stage allow release of stored water. Melt occurs at every surface of the glacier where energy is received from the atmosphere, rain or flowing meltwater, ice overburden pressure, deformation pressure or geothermal heat (Menzies, 1995). Most melt of temperate glaciers, however, occurs at the glacier surface (Sharp, 2005). Energy inputs are greatest during spring and summer and this is therefore the period over which most runoff occurs.

Once released from storage, water is free to engage with the glacial drainage system. Little runoff occurs directly from a glacier surface. In most cases, water is routed through the glacier and is distributed spatially according to the drainage system's morphology and temporally depending on the subglacial equipotential surface, drainage channel morphology and pressure, and basal sediment type (Hooke, 1989). The subglacial equipotential surface corresponds to ice topography and overburden rather than bed topography (Sharp, 2005; Hubbard and Nienow, 1997; Hooke, 1989) and Shreve (1972) calculated that it may be up to 11 times and opposite that of ice flow directions. Overlying ice thickness, ice velocity, surface topography, input water flux and substrate type determine both the morphology of englacial and subglacial channels and pressure within these (Clarke, 2005).

An idealised glacial drainage network consists of capillary conduits microns to millimetres in diameter, moulins and crevasses that join sequentially to increasingly larger channels, finally coalescing into a few large channels normal to the flow of ice and equipotential surface

(Sharp, 2005; Hooke, 1989). Figure 4 illustrates the idealised drainage system of a temperate valley glacier.

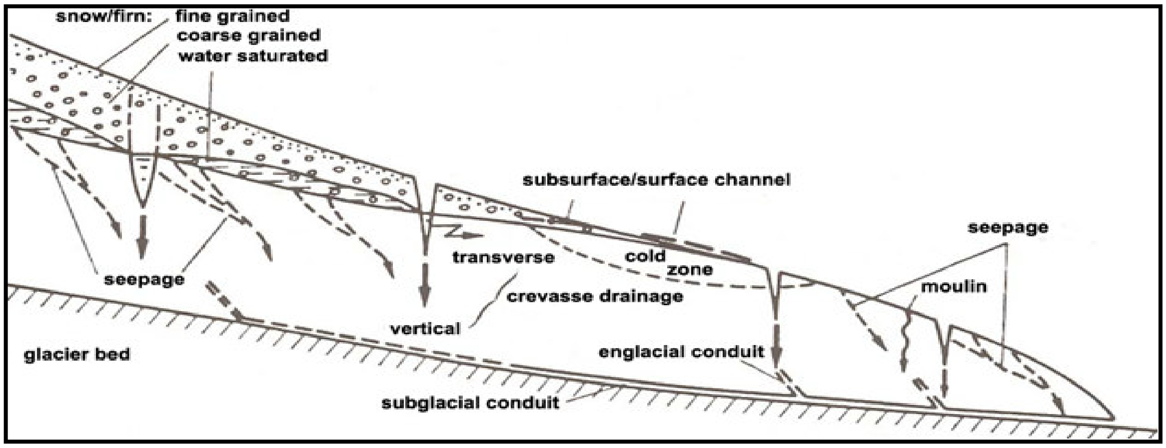


**Figure 4. Model of supraglacial, englacial and subglacial drainage routes (from Menzies, 1995).**

The actual morphology of glacial drainage systems in fact varies markedly both within and between ice masses and is rarely in a steady-state. Hubbard and Nienow (1997) have detailed the various theoretical drainage system configurations of alpine glaciers, starting with the distinction between arborescent and non-arborescent (also known as *fast* and *channelised* or *slow* and *distributed* respectively [Sharp, 2005]). Arborescent networks tend to consist almost entirely of hydraulically efficient, wide channels at low pressure with comparatively limited spatial distribution, while non-arborescent networks consist of hydraulically inefficient, small, widely distributed channels under high pressure and possibly some degree of film flow and/or linked-cavity flow (although combinations of all three can concurrently occur in either system type) (Hubbard and Nienow, 1997; Menzies, 1995). Non-arborescent drainage systems slow water flow more effectively than arborescent systems (Sharp, 2005) and small high pressure channels, linked cavities and film-flow prove more conducive to water back-up than large, low pressure channels. High velocity events are therefore more commonly associated with glaciers exhibiting non-arborescent drainage for at least some portion of the year, and this type of system produces a more highly modified version of the stream hydrograph than the arborescent type.

Numerous studies of Haut Glacier d'Arolla (Mair et al., 2002; Willis et al., 2002; Mair et al., 2001; Hubbard and Nienow, 1997) amongst a number of others (Bingham et al., 2006; Kavanaugh and Clarke, 2001; Hock and Hooke, 1983) have shown that some glacier's hydrological systems can, and commonly do, shift from non-arborescent to arborescent during the course of the melt season, as noted above. High atmospheric and water temperatures and large meltwater inputs during the ablation season are conducive to radial expansion and pressure reduction in drainage channels; during cooler months plastic flow of stable ice squeezes channels shut while ice accretion along open channel walls diminishes their size, together restricting flow and increasing pressure until an equilibrium with diminished input is attained (Hooke, 1989). Hooke (1989) details the ideal inverse relationship between discharge and conduit pressure resulting from a linear relationship between the energy available for conduit melt and discharge: conduit pressure increases as discharge decreases because the channels constrict. On a similar vein this author describes how melt of large conduits is differentially favoured as discharge increases because the ratio of discharge to channel wall area is higher in large channels than small and there is therefore more energy per wall unit area to be expended in melt and channel expansion. These assertions are qualified by Sharp (2005); he asserts that only in arborescent networks is the relationship between discharge energy flux and pressure inverse so in non-arborescent networks, flow occurs from large to small channels which equalises pressure in the network and discourages the growth of "master channels", whereas, he says, in arborescent systems flow tends to be from small to large channels producing a positive feedback loop in the development of the network arborescence. Neither state can remain steady in a temperate environment however. As surface entry points – moulins and crevasses – begin to close up with the onset of autumn, closure of internal channels by plastic deformation is favoured because runoff into the internal hydrological system decreases (the energy available to maintain open channels) while ice flow rates are maintained (Menzies, 1995). The process is revered in spring, as moulins and crevasses reopen, and larger quantities of melt water and rainwater flow into the drainage system. These processes contrive to adjust the degree of arborescence of the drainage system as air temperature, and therefore runoff, fluctuates over the course of the year.

## Glacial Hydrology and Climate

While some aspects of glacial hydrology are disconnected from climate, others are directly forced by it. The quantity of water in a catchment is dependent on the regional climate as it determines precipitation rates and major energy inputs, and the release of water from storage depends primarily on the state in which it is held and these two climatic factors (Oerlemans, 2001; Hannah et al., 2000). In general, runoff occurs in a pattern that follows the annual seasonal cycle of weather variation as precipitation, snow and ice changes from solid to liquid from winter to summer and vice versa, superimposed on a diurnal cycle dependent on daily incoming short-wave radiation and/or air temperature (Davie, 2003; Fitzharris et al., 1992b). Air temperatures exceeding zero degrees are all that is required for precipitation to fall in liquid form, and during summer, when the glacial drainage system is comparatively open, rainfall can pass through into the proglacial channel quickly and completely. Having said this, air temperatures at ground level can often be above zero degrees during snowfall events because of the atmospheric temperature lapse rate (2°C is the usual cut-off point for snow). Rain that falls during autumn and winter is likely to be refrozen and stored with subsequent snowfall until the weather warms again during spring (Oerlemans, 2001).

Significant energy input is required for melt, as discussed above, which, excluding basal heating (via geothermal and pressure melting), is provided by the climatic conditions at the ice/atmosphere boundary. The total energy available for melt – the surface energy flux (Ψ) - is given by the energy balance equation:

$$\Psi = Q(1-\alpha) + L_{in} + L_{out} + H_S + H_L + G + R$$

**Eq. 1**

where Q is incoming shortwave radiation and α is albedo, $L_{in}$ incoming and $L_{out}$ outgoing longwave radiation, $H_S$ the turbulent exchange of sensible heat with the atmosphere, $H_L$ the turbulent exchange of latent heat with the atmosphere, G the conduction or convection of sensible heat with the ground and R the heat input from rain (the precipitation heat flux) (from Oerlemans, 2001 and Davie, 2003). These energy fluxes and the processes of thermal exchange within the uppermost layer of ice and snow are depicted in Figure 5.

The shortwave radiation balance is largely a function of surface albedo, cloudiness and season and is generally found to be the most important term in the energy balance equation (Oerlemans, 2001; Fitzharris et al., 1992a). Longwave radiation emitted from earth, plants, clouds and the atmosphere is a fairly minor term, as incomings and outgoings tend to equate (Oerlemans, 2001). The sensible heat term is a function of the specific heat of the air mass, its density and its thermometric conductivity (Oke, 1978). The latent heat flux - a function of the density of the air mass, the eddy diffusivity for water vapour, the change the specific humidity

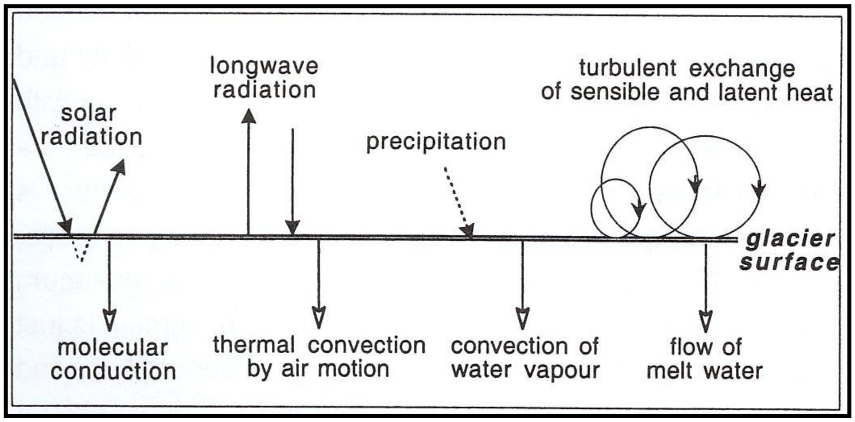


**Figure 5. The most important processes determining the energy flux at the glacier – atmosphere interface and the thermal structure of the upper layer of the glacier (from Oerlemans, 2001)**

of the air mass with height within the boundary layer and the latent heat of vaporisation - accounts for the heat exchanged during evaporation/sublimation or condensation of water vapour (Oke, 1978). Both the sensible and latent heat fluxes increase as atmospheric turbulence increases and together are known as the turbulent heat fluxes, accounting for a substantive portion of the energy available for melt. The precipitation heat flux is not usually of great importance (Oerlemans, 2001), although it may be more important in Aotearoa New Zealand than elsewhere due to the frequency of warm, intense precipitation events and the contribution of viscous heat provided by rainwater flowing over ice surfaces is unknown (Menzies, 1995).

Moore and Owens (1984) found that high snow melt events in Temple Basin catchment near the Main Divide of the Southern Alps occurred during warm, humid, windy conditions dominated by turbulent sensible and latent heat exchanges and that these heat transfers dominated the energy budget. Prowse and Owens (1982) have presented similar findings for the Craigieburn Range in the Southern Alps, where total net radiation contributed most to melt and the direction and strength of wind made a substantive difference to the effectiveness of air temperature by increasing the sensible heat transfer. Near Mueller hut in Aoraki Mt Cook National Park, Neale and Fitzharris (1997) found net radiation and the sensible heat flux to be the first and second most important sources of melt energy respectively, although they note that the turbulent latent heat flux became more important during northwesterly storms. During a short period of clear sky anticyclonic conditions at Franz Josef Glacier, Owens et al. (1986) found that shortwave radiation and the sensible heat flux were most important to melt, while

Marcus et al. (1985) found that at the same site the precipitation heat flux and latent heat dominated the energy balance equation during a heavy rainfall event.

The local climate of a glacierised catchment exists in a state of both positive and negative feedback with the resident ice mass. Air at a glacier surface is cooled as the ice absorbs sensible heat while albedo disallows the absorption of radiation, both of which encourage growth of the ice mass. Conversely, enhanced local katabatic winds resulting from the steep temperature gradient between the ice and surrounding, comparatively warm land (where bare land is adjacent), enhance melt rates (Oerlemans, 2001). The albedo of snow is significantly higher than that of ice and so a snowpack effectively protects ice from melt (Davie, 2003). It follows then that the former feedback loop is most important during periods of glacial advance, when extensive snow cover produces above average albedo, while the latter feedback is important during retreat phases when surrounding land is bare, the ice is less likely to be snow covered and therefore vulnerable to the resulting atmospheric turbulence. Braun and Escher-Vetter (1996) found that Vernagtferner glacier, Bavaria, exhibited a greater mass balance sensitivity to climate variation in years where winter snowfall was low, not only because of low accumulation but also because the comparatively high summer snowline that resulted left more ice exposed for melt. With similar results, Moore and Demuth (2001) found that discharge from the proglacial stream at Place Glacier, Canada, was higher overall and exhibited greater diurnal variation during low mass balance years indicating the sensitivity of the exposed ice to local atmospheric conditions.

Thresholds effected by climate exist within the glacial system that also affect the discharge regime. Swift et al. (2005) record a pattern of increasingly high peak discharge with decreasing baseflow with the tempered removal of the ablation area snowpack over the summer season of Haut Glacier d’Arolla, Switzerland. They attribute the pattern to a shift in the drainage system from hydraulically inefficient to hydraulically efficient and in the primary melt source from snow to ice. Hodgkins (2001) found a pattern of high discharge during summer with high variability and low diurnal variation and the opposite during winter on a glacier in Svalbard, with sensitivity of the hydrograph to meteorological variables increasing once englacial stores had drained.

As referred to obliquely above, seasonal variation in discharge is characteristic of streams from glacierised catchments. Chow (1964) relates the generalised pattern of discharge characteristics, presented in Table 1. Discharge tends to follow the annual insolation cycle, in a gradual progression from low in winter to high in summer and back again. Diurnal variability has been found to be greatest during summer and least during winter.

**Table 1. Seasonal change in glacier-runoff characteristics (from Chow, 1964)**

| Season | Snowpack thickness | Albedo | Diurnal fluctuation in streamflow | Amount of runoff | Characteristics of direct precipitation-runoff |
|---|---|---|---|---|---|
| **Winter** | Moderate to high | Very high | Nil | Slight | All precipitation stored |
| **Spring** | Highest | High | Slight | Moderate | Subdued, delayed |
| **Summer** | Moderate | Moderate to low | High | High | Slight delay |
| **Autumn** | Low | Low | Moderate | Moderate | No delay, very "flashy" |

It is clear that altogether the production of discharge from glacierised catchments is complicated and that quantifying the affect of the numerous relevant variables is a large task. Given that climate is the boundary condition of glacial hydrological systems that is changing all over the world, it is perhaps the relationship of discharge production with climate and weather that most urgently needs attention.

## Aotearoa New Zealand

There has been comparatively little investigation of glacial hydrology in Aotearoa New Zealand. The landmass has a maritime climate and is just 450km at its widest point, bounded by the Tasman Sea and the Pacific Ocean, and stretching from 34°S to 47°S latitudes. Of the approximately 3,155 known glaciers, six are found on Mt Ruapehu in the North Island, and the remainder in the Southern Alps of the South Island (Fitzharris et al., 1999). The Southern Alps are the major mountain ranges spanning the length of the South Island, with peak elevations from 2000m, culminating at 3750m at Aoraki Mt Cook, and perpendicular to the Southern Hemisphere westerly air flow belt. The glaciers on the western flank of the Southern Alps in particular exhibit high sensitivity to climate fluctuation with fast response times and a large dynamic response (Braithwaite, 2002); Franz Joseph Glacier, for example, has a response time of just 15 years (relating both to the climate regime and specific geometry of this glacier) (Oerlemans, 1997). Exceptionally high precipitation (around 12,000mm per year has been recorded just west of the Main Divide [Fitzharris et al., 1999]) and low seasonality result in significant dynamic response of glaciers to comparatively minor fluctuation of climatic variables (Anderson et al., 2008)

**Brewster Glacier**

The only comprehensive study of glacial hydrology of an alpine glacier in Aotearoa New Zealand was carried out in 2005 on Brewster Glacier (Willis et al., unpublished paper), a small, temperate alpine glacier in Tititea Mt Aspiring National Park (Figure 5). Brewster Glacier is an ideal study site given that it is easily accessed, has a simple geometry and this previous work has been carried out on its hydrology. It is by no means representative of New Zealand glaciers; at most it could be said to be representative of small alpine valley glaciers of southern aspect. Representativeness is not however something that can be easily achieved given the variety of glaciers in this country, and therefore any glacier that can physically be studied is of value to building a comprehensive understanding of the Aotearoa New Zealand cryosphere.

Brewster Glacier lies between 1660 and 2400 m a.s.l., has a simple geometry and is located on the Main Divide draining south from Mt Brewster (elevation 2515m). It is estimated to have an annual flow rate of around 30myr$^{-1}$ and response time of 50 years (Mackintosh, pers. com.). The glacier occupies an area of around 2.5km$^2$ equating to 70% of the 3.6km$^2$ catchment (Anderson et al., 2008). It has experienced positive mass balance for the last five years, after retreating around 500m since 1955 (Anderson et al., 2008) during which time a proglacial lake formed. The proglacial lake is now detached from the
glacier snout by a bedrock step by around 10 meters. The catchment consists entirely of exposed schist bedrock with a small amount of scree. Because of the paucity of fine sediments and gravel visible in the catchment, basal ice and in the proglacial channel and the angularity of loose sediments the subglacial substrate is inferred to be primarily bedrock. Anderson et al. (2008) describe the catchment climate as cool, wet, cloudy and windy. Precipitation measurements are sparse, but an estimation of 6354 mm yr$^{-1}$ for the years 2004 – 2006 has been made by Anderson et al. (2008).

Through dye tracing and GPS survey of the ice surface Willis et al. (unpublished paper) inferred that Brewster Glacier has a non-arborescent drainage system from late autumn to early spring and an arborescent one from late spring to early autumn, with the transition

**Figure 6. Brewster Glacier in the valley of Mt Brewster and fronted by Brewster Proglacial Lake.**

occurring during spring. This fits well with studies of Northern Hemisphere temperate high alpine valley glaciers and suggests that the hydrological system of this glacier may behave in a way comparable to its Northern Hemisphere counterparts. Anderson et al. (2008) have completed an energy balance model for the Brewster Glacier in which the authors attribute the greatest portion of discharge during the 2004-2005 and 2005-2006 summers to rainfall (54% and 57% respectively), then ice melt (34% and 32% respectively) and then snow melt (14% and 13% respectively) with total discharge of 7.3 cumecs and 7.9 cumecs respectively. They suggest that mass balance and discharge sensitivity to temperature is around 1.9m w.e. and 1 cumec/°C respectively. However, this model does somewhat misrepresent the hydrological system and could therefore be refined with further real-time analysis of the relationship between climatic variables and discharge. Because of the availability of these data sets and the accessibility of the glacier, Brewster is the obvious choice for further research into glacial hydrology.

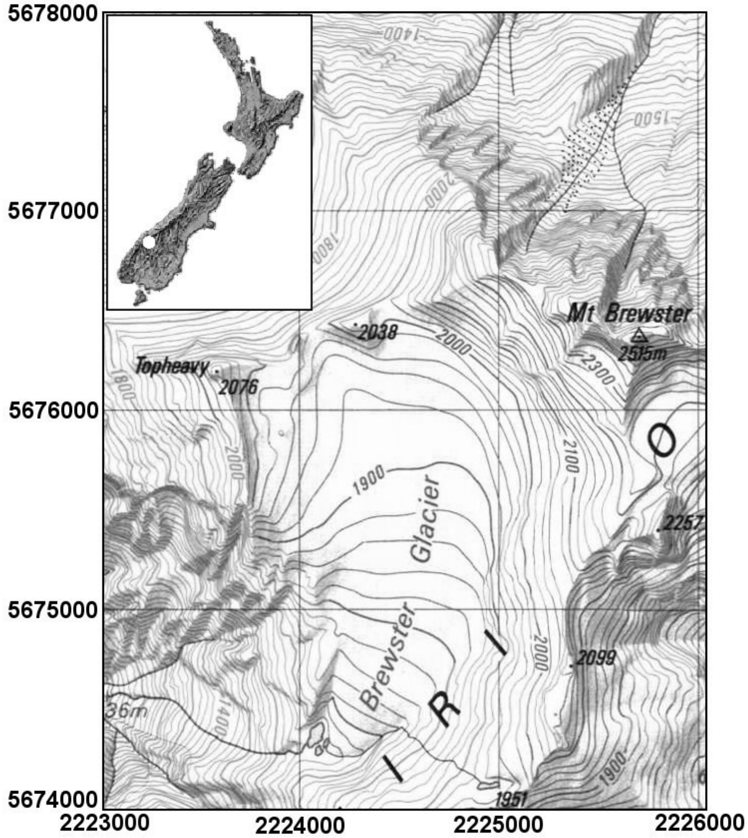


**Figure 7. The location and topography of Brewster Glacier and watershed (Land Information New Zealand, 1999).**

## Research Questions:

The overarching research objective for this project is to determine the strength of the relationship between weather and proglacial discharge in Brewster catchment. With this as the context, the following specific research questions have been adopted:

### Primary

- Which are the most important atmospheric variables influencing discharge from Brewster proglacial stream?
- What combination of atmospheric variables leads to highest/lowest discharge from the proglacial stream?

- Can a statistical model of atmospheric variables be used to reliably predict discharge?
- Can an atmospheric classification scheme be used to reliably predict discharge?
- Using a statistical model and atmospheric classification scheme, what changes to the discharge regime can be expected with predicted climate change?

**Secondary**

- What are the characteristics of the diurnal cycle of discharge from Brewster pro-glacial stream?
- Is there evidence of a seasonal evolution of the drainage system? If so, what are the characteristics of this evolution?
- Is there evidence in the diurnal hydrograph for an evolving influence of the supraglacial snowpack?
- What is the extent of hydrological storage in the glacier and how does it influence the hydrograph of the pro-glacial stream?
- How do the real-time results compare with Anderson et al. (2008) model of energy balance and discharge?

# Chapter 2: Methodology

At the heart of a scientific inquiry is, to quote Karl Popper, the "generally accepted problem-situation" (Popper, 1959). That is, an unknown that is known to be unknown. The problem is specific in space and time and may be clearly distinguished from both the known and unknown surrounding it. The question, answered by the scientific method, is how to approach the problem-situation such that its "true" nature may be revealed - independent of human perspective, interpretation, expectation and desire (Chalmers, 1982).

Briefly, the scientific method consists of 1. a question based on an observation (the problem-situation), 2. an hypothesis/es, 3. data collection in the form of either survey or experimentation, each an attempt to falsify the hypothesis/es, and 4. a conclusion/s drawn as to whether the hypothesis/es is supported or must be rejected (Chalmers, 1982). The process by which the data is collected must be repeatable and testable – the data must be independent of the observer, such that the same results can reasonably be expected to reproduce in repeat tests, and the conclusions must not breach any previously determined scientific law (Chalmers, 1982). Having said this, inference is a fundamental aspect of the acquisition of scientific knowledge – as Popper (1959) put it "conclusions are drawn by means of logical deduction". So part three of the process, the experiment or survey, must produce data of such quality and specificity that inference can be made with confidence.

Finding support for an hypothesis is not considered proof of its universality or reality, but only that it works in the current situation and for the time being, until further data refutes it or a substantial amount sufficiently verifies its accuracy that it can be accepted as a rule of nature (Popper, 1959). However, as Kaiser (1959) stated, "…it is absurd for physics (or any science) to consider that its proper task is to give an account of the nature of physical reality…, since if by some miracle it has been able to do so, it can never know that it has, and if it has not and has only an approximate account, it can never know the degree of approximation or correspondence." All conclusions drawn, he is saying, must be taken with a grain of salt.

In this study, the primary problem-situation, used as the foundational guide throughout the research process, is clear: what are the salient controls of the discharge regime at Brewster

Glacier and what will the impact of climate be on the volume of discharge? It is a question at the interface of geomorphological and glaciological investigation, or "process glaciology" as Chorley et al. (1984) call it. These authors assert that process glaciology may be either historically based (retrodictive) or functionally based (predictive). This study, of the current processes operating in a glacierised catchment and the probable effects of climate change on those processes, is clearly of the latter type. The predictive component of a functionally based inquiry invokes two of the concepts central to the study of geomorphology, namely *uniformity* and *systems*.

The principle of uniformity states that "the present is the key to the past" - that current geomorphological processes have and will occur consistently both in the past and future, as long as changes forced by climate, tectonic and anthropogenic activity are also accounted for (Chorley et al., 1984). The concept of uniformity is used in this research with respect to the response of Brewster proglacial stream to climate change. It is assumed that discharge will respond to changes in atmospheric conditions in the future in the same way that it has during the study period.

The concept of *systems* in geomorphology speaks to the interaction of the multiple components of a landscape and the mass and energy within that landscape. Understanding of an individual landform is derived from an understanding of the geomorphological system of which it is a part, while understanding of that system is derived from understanding of the landforms and component interactions within it. The model of a system that is adopted for this study is the *cascading* one, as defined in Chorley et al (1984): an exogenic system in which the input, throughput and output of energy and matter balance when accounting is done. In this case, it is assumed that the quantity of stored and discharged water in Brewster catchment is equal to the amount input (taking into consideration the duration of water storage as snow, ice and firn), and that the quantity of water discharged is in turn equal to that input minus that stored as snow, firn or ice. Given the high degree of storage of frozen water in a glacierised catchment, the input of energy is also of interest, and again it is assumed that the total energy input will be equal to that output, either as albedo, production of local winds or production of meltwater. A glacierised system as a cascading system is illustrated in Figure 8.

The broad aim of this study is to define the characteristics of one element of a glacierised catchment – the discharge – with relation to the system of which it is a part. For this to be achieved, the physical components and structure of the landscape must first be identified and subsequently the inputs, throughputs and outputs of mass and energy (Chorley et al., 1984), each of which to be either tested or controlled. In this case, these components can be defined according to previous work both at Brewster Glacier and on glacierised catchments in general.

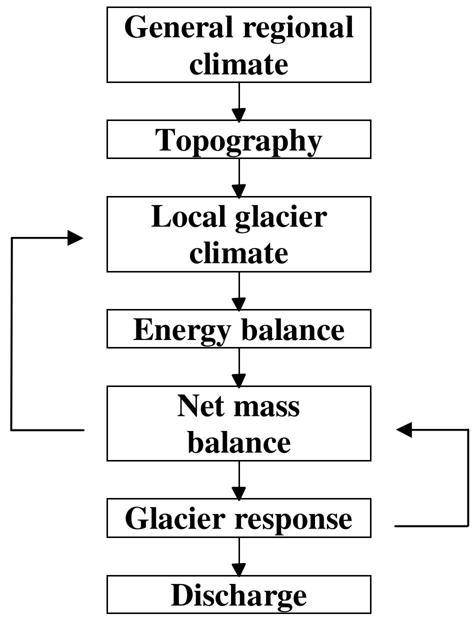


**Figure 8. Glacier behaviour and discharge as part of a cascading system with feedbacks (adapted from Andrews, 2006 and Menzies 1995).**

Energy inputs and outputs include shortwave radiation, longwave radiation, turbulent heat, precipitation heat and geothermal heat. Mass inputs include water in the form of vapour and precipitation, and sediment derived from either the bed or surrounding slopes. Mass outputs include liquid water and sediment.

Sediment transport in this particular system is demonstrably minimal and of little importance to the hydrological system, and therefore is counted as constant. Incoming and outgoing longwave radiation has been found to be such a minor term in glacial discharge production that it too is assumed to be constant, and there is no evidence that geothermal energy is of importance in this catchment. All other elements are changeable and affect the quantity and rate of discharge and must therefore be accounted for – measured.

The study site and subject largely precludes the use of experiment in data acquisition given its scale (national atmospheric circulation for example can hardy be reproduced in a laboratory situation), complexity (again, the laboratory is insufficient for recreation of the exact conditions of the glacier and climate) and ethical considerations (one would baulk at cutting a large trench into the glacier to examine its underside, for example). Survey is therefore the appropriate means of data collection.

There are established methods for the collection of meteorological and discharge data in a glacierised catchment, as follows:

*Precipitation*:
1. snow depth and density survey (Davie, 2003)
2. automated precipitation gauge (Davie, 2003)
3. automated lysimetre (Davie, 2003)

*Energy inputs and outputs*:
1. automatic weather station (Davie, 2003)
2. inference from atmospheric circulation indices (e.g. Andrews, 2006)

*Discharge*:
1. inference from atmospheric indices (e.g. Anderton, 1973)
2. direct measurement
    a. automated stage gauge (e.g. Francou et al.,1995)
    b. manual discharge gauge (e.g. Singh et al., 2005)
    c. automated discharge gauge (e.g. Moore and Demuth, 2001)

*Drainage system character*:
1. hydrograph analysis and inference (e.g. Hannah et al., 2003)
2. borehole channel pressure measurement (e.g. Gordon et al., 2001)
3. dye tracing (Hubbard and Nienow, 1997)

There are strengths and weaknesses to each method, but the choice of method is largely governed by the physical requirements of the study site. A precipitation gauge was installed and maintained by Tim Kerr of Canterbury University within meters of the margin of Brewster Glacier that converts all to liquid. Because delineation of the snowfall-rainfall components of precipitation are not required, the small catchment size and the convenience of a single gauge, this method is entirely appropriate (Davie, 2003). A climate station with gauges automatically recording values of relative humidity, air temperature, wind speed and incoming shortwave radiation every ten minutes was installed by Otago University at the base of Brewster Glacier in 2005. These meters provide detailed measurement of the atmospheric conditions in Brewster catchment.

The study site lends itself to both automated and manual discharge record. An automated stage gauge was preferred over an automated discharge gauge given the complexity and expense of the latter and the uncertainty about conditions during the accumulation season. Manual discharge measurement for calibration of this stage record was therefore deemed an appropriate method for long-term discharge data capture. The hand-held current meter method of discharge measurement was chosen given the nature of the proglacial stream (the channel being sufficiently small that such a method could be safe and sufficiently stable that it could produce accurate results).

As mentioned in the previous section, dye tracing experiments have been carried out at Brewster glacier previously by Willis et al. (unpublished paper). In this study, given that the results of Willis et al. were made available and the aim was to determine the relationship between atmospheric variables and discharge, further dye tracing tests were deemed unnecessary. Borehole measurements provide more detail as to the subglacial drainage channel structure than is required to answer the questions posed in the previous section, while hydrograph analysis is simple, requires no further data capture and provides sufficient information (Sharp, 2005) and was thus chosen for this project.

The established types of models used to reconstruct and predict behaviour of the inputs and outputs of hydrological systems are *physical* and *statistical*. In glaciology, the former is more common. Physical models have the advantage of having being able to account for the various inputs in three dimensions including variations in the state of each variable through time such that precise inference about the physical system can be made. Statistical models have the advantage of simplicity and retrospective diagnostics assuming a linear cause and effect relationship between the relevant variables. Arnold et al. (1998) argue that a statistical model can be useful for discharge prediction in a glacierised catchment but that statistical results cannot be transferred to other catchments or used for diagnostic analysis. However, the method has been used many times in a number of different locations with acceptable results (e.g. Hodgkins, 2001; Moore and Demuth, 2001; Salinger et al. 1983). Furthermore, a physical model of Brewster Glacier mass balance and runoff has already been developed by Anderson et al. (2008), and so the development of a statistical model in this study is also useful for comparison and thereby a greater depth of understanding of the system. Statistical modelling was therefore chosen for this study.

Successful and illuminating study of glacio-hydrological systems using atmospheric circulation indices has been completed by numerous authors (Moore and Demuth, 2001; Paterson, 1994; Brazel et al., 1992; Fitzharris et al., 1992b; Anderton, 1973). The fourth and fifth primary research questions set out in the previous section require national air pressure circulation data. Such data is recorded by a government network of automated gauges around the country maintained by the New Zealand National Institute of Water and Atmospheric Research (NIWA). Kidson (2000) created a set of national atmospheric circulation indices that NIWA uses to classify each twelve hourly period of recorded atmospheric circulation data. These data were available for use in this study and are sufficient to answer the research questions.

# Chapter 3: Results

## *Section 1: Discharge*

### 1.0 Method

Measurement of discharge from the main and auxiliary proglacial streams during the period 15th February to 9th March 2006, at approximately midday and/or 6pm, resulted in a total of 13 data points and 11 days of discharge data. Measurements were taken using a current meter of the type Oss PC1, calibrated by NIWA. The current meter has a maximum uncertainty of 0.2% at the 95% confidence level. The gauge records revolutions per second of a small propeller. Measurements were taken at 0.4 of water depth in the horizontal centre of ten sections into which the total width of the channel was divided.

#### 1.01 Gauging sites

Important characteristics of a metered channel are its stability and symmetry (Gardiner and Dackombe, 1983). The sampling locations were chosen primarily to satisfy these requirements, while also providing a safe distance from the glacier mouth. The auxiliary channel gauge site was around 10m from the glacier snout and the main channel site around 20m from it. The sites are identified in Figures 9 and 10.

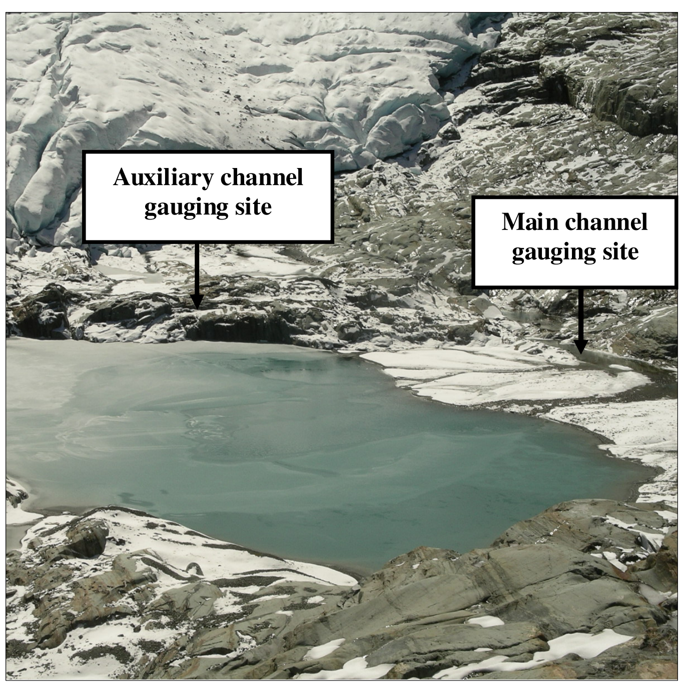


**Figure 9. The snout of Brewster Glacier and the discharge gauging sites.**

**Figure 10. The main channel discharge gauging site, with field assistants.**

## 1.1 Data quality and error

Without two current meters it was impossible to gauge both the main and auxiliary channels at the same time. There are therefore around two hours between measurement of one channel and the other. To obtain total discharge from the glacier, each measurement was designated as having been taken in the morning, afternoon or evening, and those from the main and auxiliary channels taken within the same period on the same day added together. The final discharge measurements are thus estimates for a time period during the day rather than point measurements.

The following graph (Figure 11) illustrates the measured depth profiles of the channel cross-section and the location of bedrock and gravel bed sections with respect to waters edge left bank (WELB), showing that the channel was both highly symmetrical and stable. There may have been some movement of gravel in the channel over the study period. However, variation in the gravel section of the channel is only slightly greater than that recorded in the bedrock sections, suggesting that the source of variation is mostly the result of variation in sampling positions and not changes in the channel itself.

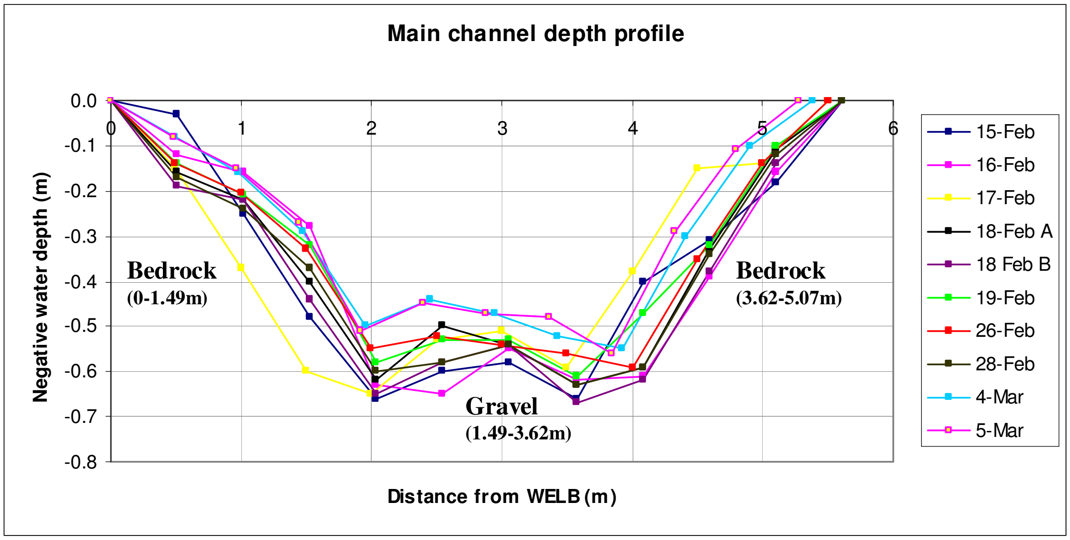


**Figure 11. Main channel depth profiles and location of gravel section of bed, over the period 15 February 2006 to 5 March 2006. The regularity of these profiles illustrates the symmetry and stability of the gauging site.**

The auxiliary channel was around 1.5m wide and composed entirely of bedrock. The cross-sectional profile of this site was asymmetric but deemed acceptable for gauging given its complete stability.

## 1.2 Calculations

Current meter measurements were transformed into velocity using the following equation provided with the equipment:

$$V = n * slope + constant$$

**Eq. 2**

Where $n$ is revolutions per second, and *slope* and *constant* are calibration constants that change according to the value of $n$. The velocity measurements were multiplied by the area of each section, giving discharge per section, which were then summed to give cubic meters per second discharge (cumecs) for the full channel cross-sectional area.

This was completed for both the main and auxiliary channels and the discharge from each added to give total discharge from the glacier, as described above. The assumption was made that a linear relationship must exist between discharge from the auxiliary and main channels. The graph below (Figure 12) presents the regression curve for discharge from these channels with an $R^2$ value of 0.84.

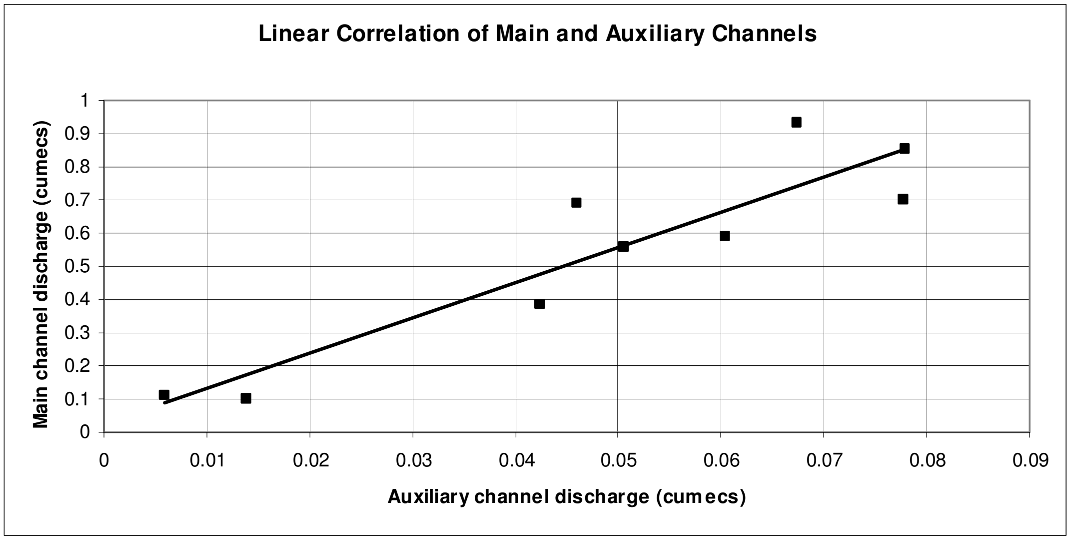


**Figure 12. Discharge from the main and auxiliary channels and a best fit curve with an $R^2$ value of 0.84. The equation for this curve was used to estimate values of discharge from each channel where direct measurements were not obtained.**

Where data points were missing from either channel, the corresponding value recorded at the other was entered to estimate the missing value using the linear equation, derived from the best fit curve, as follows

$$Y = 10.572x + 0.264$$

**Eq. 3**

## 1.3 Results

### 1.31 Calculated discharge

Table 2 presents the measured point and calculated total discharge and indicates which values were calculated using the regression equation above. The values show a marked decrease over the study period and considerable variation during the days on which two measurements were taken.

**Table 2. Measured and calculated discharge. Measurements of discharge in the main and auxiliary channels were taken within hours of each other so the final calculated values of discharge are given for a period of time during the day. The values followed by * were calculated using equation 3.1.2.**

| **Main channel** | | **Auxiliary channel** | | **Total** | |
|---|---|---|---|---|---|
| Date/time | Discharge | Date/time | Discharge | Date/time | Discharge |
| 15/02/06 15:05 | 0.91895 | 15/02/06 15:05 | 0.06052* | 15/02/06 Afternoon | 0.97947 |
| 16/02/06 18:35 | 0.75622 | 16/02/06 18:35 | 0.04513* | 16/02/06 Evening | 0.80135 |
| 17/02/06 13:30 | 0.59121 | 17/02/06 19:30 | 0.06043 | 17/02/06 Afternoon | 0.65164 |
| 18/02/06 12:05 | 0.69014 | 18/02/06 13:20 | 0.04601 | 18/02/06 Midday | 0.73615 |
| 18/02/06 18:20 | 0.93195 | 18/02/06 19:20 | 0.06744 | 18/02/06 Evening | 0.99939 |
| 19/02/06 11:45 | 0.55585 | 19/02/06 12:30 | 0.05067 | 19/02/06 Midday | 0.65602 |
| 19/02/06 18:50 | 0.85056* | 19/02/06 18:50 | 0.07796 | 19/02/06 Evening | 0.92852 |
| 26/02/06 12:25 | 0.38609 | 26/02/06 11:45 | 0.04244 | 26/02/06 Midday | 0.42853 |
| 28/02/06 12:30 | 0.69815 | 28/02/06 14:10 | 0.07776 | 28/02/06 Midday | 0.77591 |
| 4/03/06 18:55 | 0.11216 | 4/03/06 18:20 | 0.00593 | 4/03/06 Evening | 0.12753 |
| 5/03/06 16:25 | 0.10046 | 5/03/06 17:20 | 0.01395 | 5/03/06 Afternoon | 0.11441 |

# Chapter 3: Results

## *Section 2: Stage*

### 2.0 Measurement

Stage was recorded with an Odyssey capacitive water level probe hanging in a perforated 2.4 m galvanised steel pipe, set up by Brian Anderson and Andrew Mackintosh in February 2005. The gauge and pipe were bolted to a bedrock section of the main channel, approximately 10m from the glacier mouth (Figure 13). The metre recorded electrical conductivity of substance within the tube, indicating the ratio of air to water. The data was automatically logged as water depth.

**Figure 13. Brewster Proglacial Stream and the stage gauge pipe being bolted to bedrock.**

#### 2.01 Gauging site

The gauging site was chosen for its stability and location with respect from the glacier mouth. Although the bed was never visible due to the turbidity of the water, it was assumed to be solid bedrock. The site is identified in Figure 14.

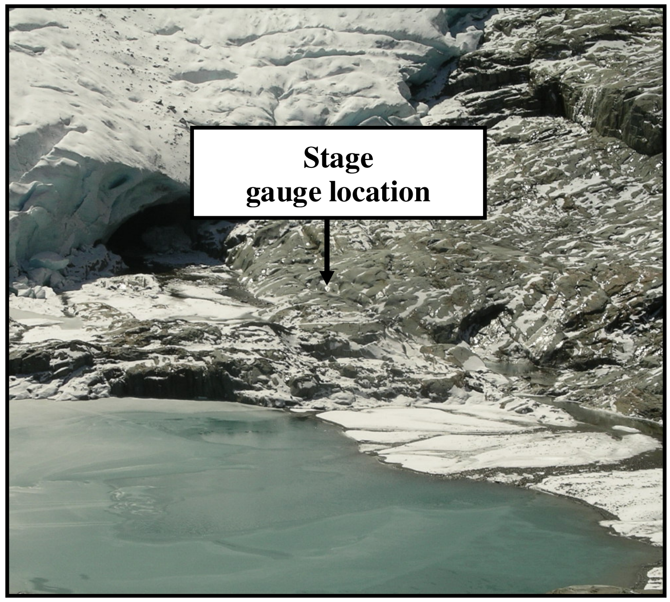


**Figure 14. Brewster Glacier proglacial stream and the location of the stage gauge.**

## 2.1 Data quality, error and corrections

On the 3rd of May, 2005 there was a sudden drop in stage from 724mm at 5.33pm to 260mm at 5.48pm, shown in Figure 15. Clearly something changed in either the gauge or the channel, as a drop in water level of this magnitude over a period of 15 minutes is too great and sudden to represent a real discharge event. Given that the gauge was bolted to bedrock and had not changed position when examined, and the size of the perforations largely preclude the entrance of gravel, nor had it been damaged, it was assumed that the change occurred in the channel itself. For a drop in stage to have been recorded, channel depth must have increased.

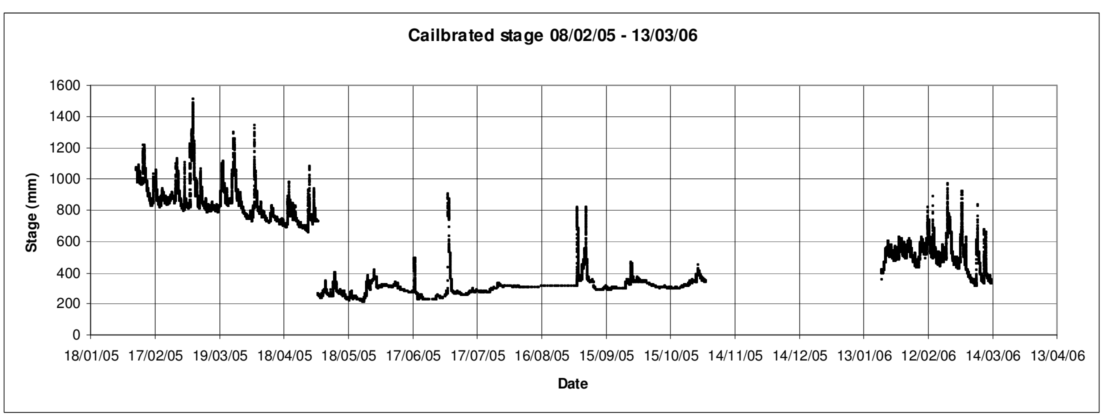


**Figure 15. The full calibrated stage record from February 8th 2005 to March 13th 2006. On the 3rd of May 2005 the gauge recorded a drop of 464mm and this is considered to be the result of a channel depth increase. No data was recorded over the period 31 October 2005 – 8 February 2006.**

An evacuation of gravel from the channel bed is a likely explanation, although the exact cause was undetermined. It is unfortunate that the channel was not as stable as required for accurate stage measurement – it is impossible to know whether or not small sediment input or removal events affected other parts of the record. It is assumed that no other such events occurred, although this may be spurious, and only the single obvious event was corrected for. In this case, 464mm, the difference between the pre- and post-drop values, was subtracted from the pre-drop data to make a continuous record, shown in Figure 16.

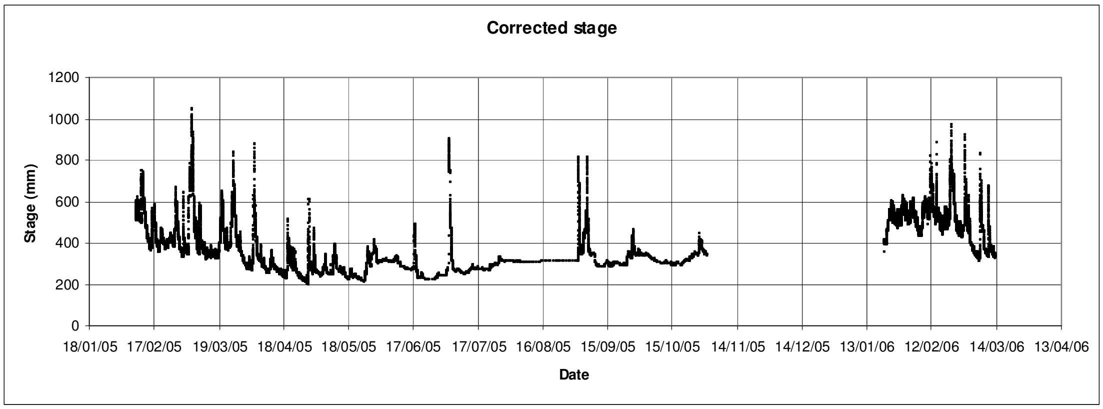


**Figure 16. The full stage record, as above, with 464mm subtracted from the pre-drop values to correct for the May 3rd 2005 event.**

From the 4th May to the 31st October 2005 the gauge recorded highly sporadically, with often only one or a few recordings per day, and with dubious accuracy. From the 20th of May to the 24th of April 2005, for example, a strange pattern of variation was recorded - lacking gradual variation and the typical hydrograph form of the rest of the record and with the systematic appearance of a gauge gone haywire (Figure 17).

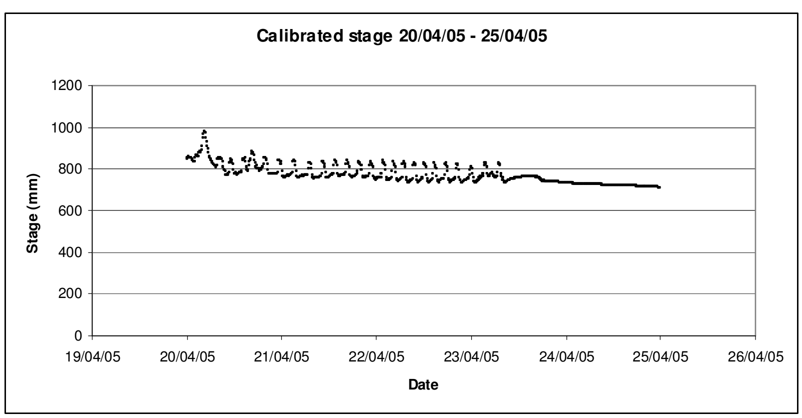


**Figure 17. Calibrated stage over the period 20/04/05 to 24/04/05 showing a suspect pattern of variation. This section and others like it were considered recording errors and removed from the record.**

As can be seen in the graph, there are more "wiggles" per day than could be accounted for by diurnal variation, so this section was attributed to a mechanical fault. Brian Anderson checked the gauge during this winter and found that it had become blocked by ice, which is a likely suspect for the odd recordings. Because of this and the fact that too few points were often recorded for calculation of either hourly or daily total data, the whole section was omitted. No data was recorded during the period from the 31st October 2005 to the 8th of February 2006. The final corrected record is shown in Figures 18 and 19, and the distribution of values in a boxplot in Figure 20.

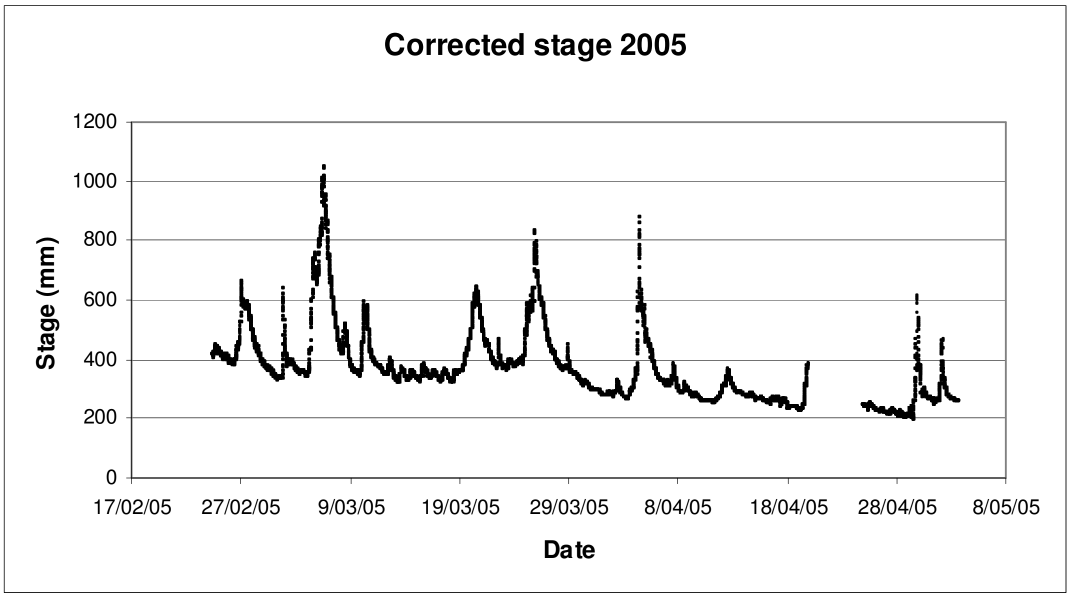


**Figure 18. The final corrected stage record for 2005.**

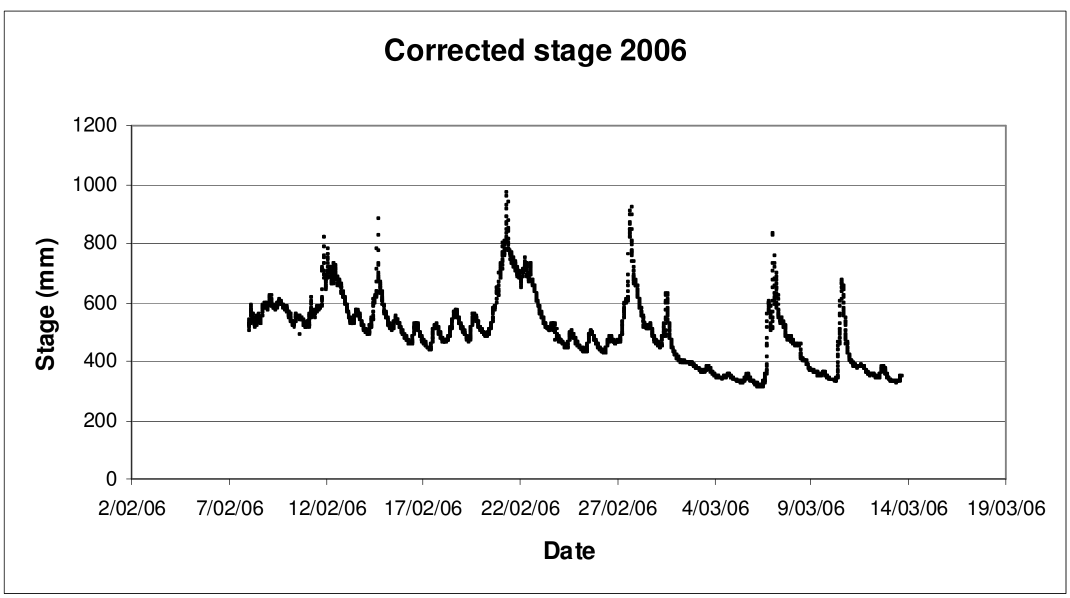


**Figure 19. The final corrected stage record for 2006.**

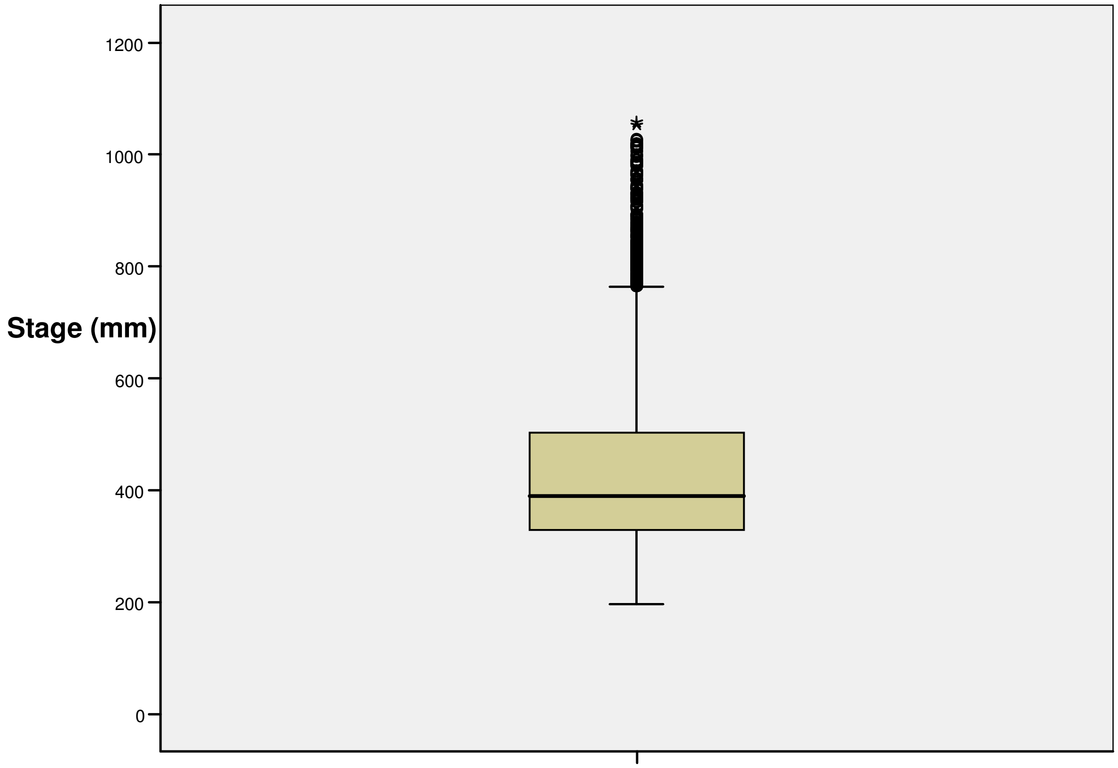


**Figure 20. Boxplot of the corrected stage record, showing a median value of 394mm and range from 197 – 1047mm. Circles represent outliers within one quartile an stars outliers within two quartiles.**

# Chapter 3: Results

## *Section 3: Ratings curve*

### 3.0 Method

A ratings curve is an approximation of discharge through time, assuming that there is a consistent relationship between water depth and volume. Best fit curves are created by finding the least squares between recorded stage and discharge values according to a mathematical function. This function is not required to be linear, and whichever fits best is chosen.

### 3.1 Reliability and limitations

The measurements of discharge were made when weather permitted (given safety issues) and there are therefore no measured values of peakflow. This is a problem because the relationship between stage and discharge is likely to change with discharge volume, as higher flow velocities may produce higher values of discharge without necessarily a marked change in stage.

Figure 21 shows measured discharge and stage plotted against time and the trendlines for each of these records. It shows that the trend of each record is different through time, indicating that there is an additional factor affecting the values of discharge that the stage record alone cannot account for. As a result, there must be a degree of unknown error in the calculated discharge record presented below.

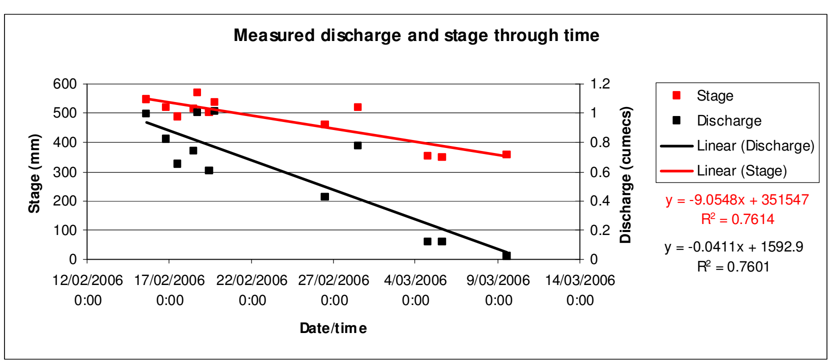


**Figure 21. Measured discharge and three hour average stage showing the different relationship that each record has with time.**

## 3.2 Results

Linear, exponential and power functions were trialled for the ratings curve, and the linear function (shown in Figure 22) was found to have the highest $R^2$ with a value of 0.96. However, this equation produced values of discharge below zero for all values of stage below around 340mm. The exponential curve, with an $R^2$ value of 0.81, produced a value of 1412 cumecs for the highest stage reading, 1047mm (Figure 23). This is too high given the channel size. The power curve had an $R^2$ value of 0.82 and produced the most reasonable range of values for discharge (presented below), and was therefore chosen for discharge calculation (Figure 23).

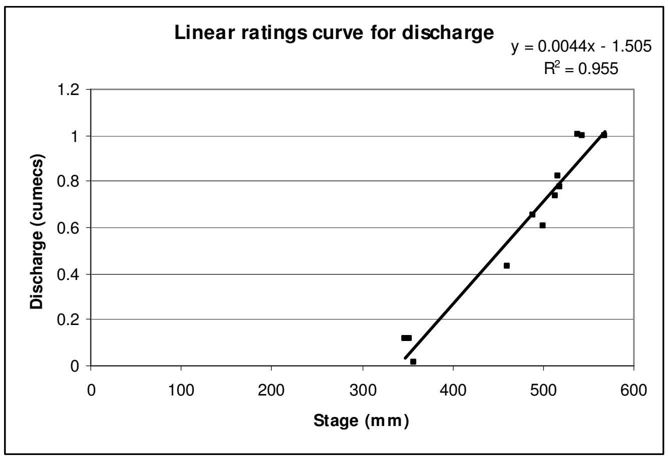


**Figure 22. Measured discharge and stage with a linear function ratings curve, with the ratings curve equation and $R^2$ value of 0.955 displayed. This curve produced values of discharge below 0 for all values of stage below 340mm.**

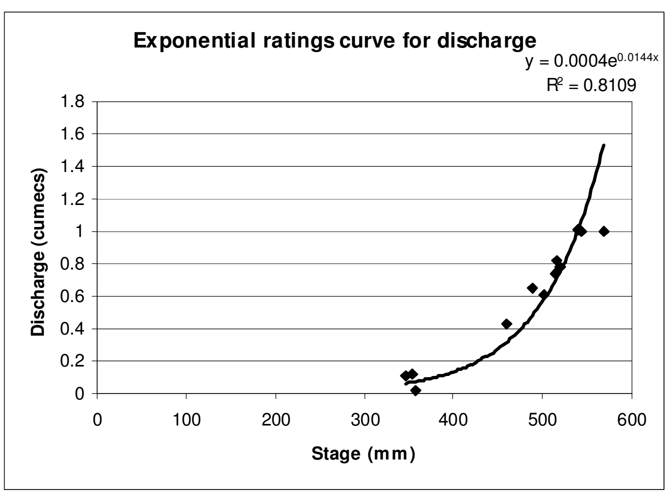


**Figure 23. Measured discharge and stage with an exponential function ratings curve, with the ratings curve equation and $R^2$ value of 0.8109 displayed. This curve produced a value for discharge of 1412 cumecs for stage value of 1047mm – well above what is reasonable given the stream characteristics.**

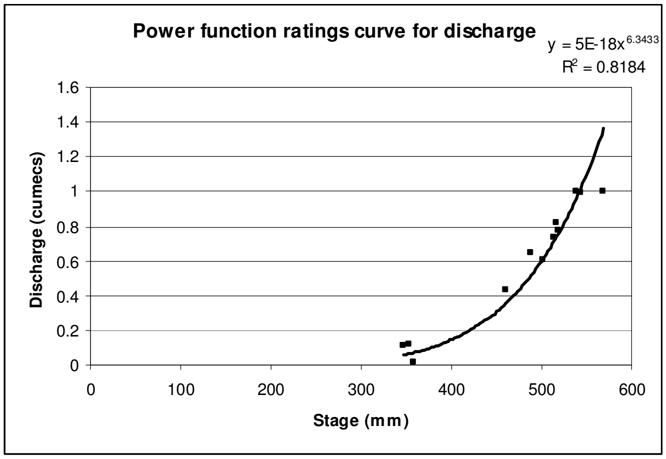


**Figure 24. Measured stage and discharge with the power function ratings curve chosen for discharge calculation, with curve equation and $R^2$ of 0.8184 displayed. This curve produced the most reasonable estimates of discharge and was used in calculation of a full discharge record.**

The following equation derived from the ratings curve in Figure 23 was used to calculate the full discharge record:

$$y = 5^{-18} * x^{6.3433}$$

**Eq. 4**

Discharge calculated using this equation is shown in Figures 24 and 25 with the stage record and measured values of discharge. A blow up of the sections with measured points is given in Figure 26 and illustrates a close yet inexact correspondence between the measured and rated values. The calculated values of discharge are described in a boxplot in Figure 27.

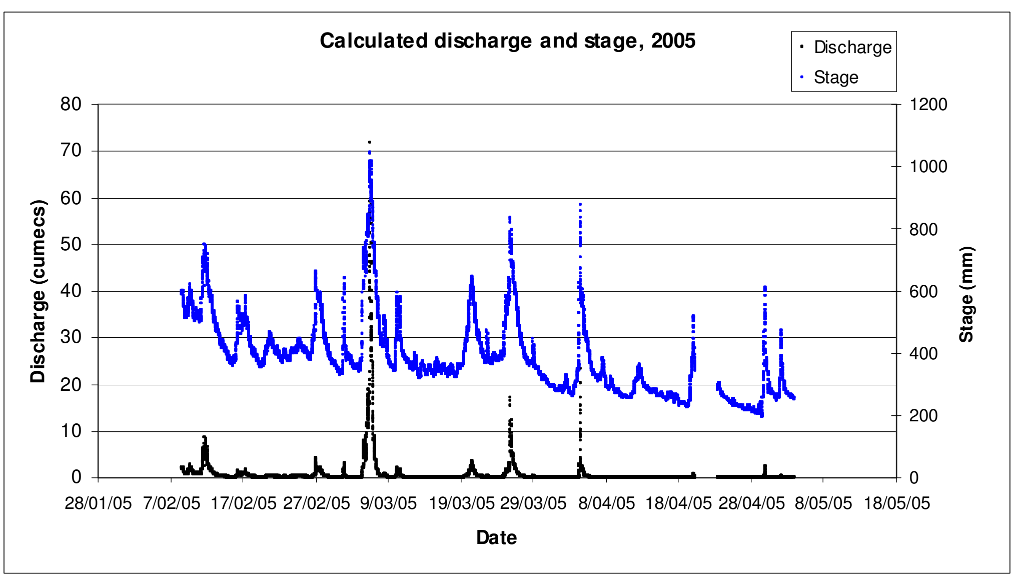


**Figure 25. Calculated discharge and stage for the period 08/02/05 – 03/05/05.**

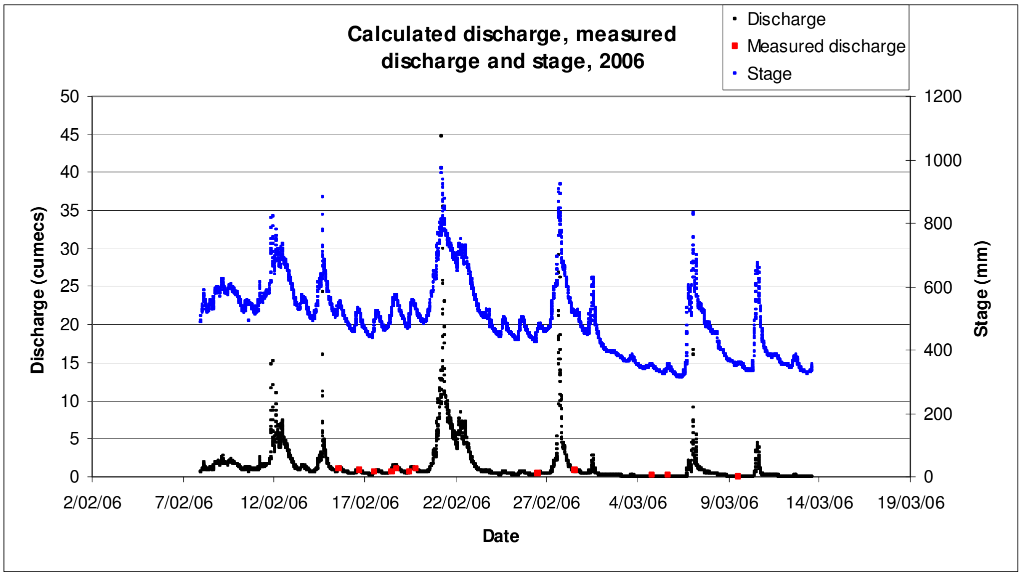


**Figure 26. Measured discharge, calculated discharge and stage for the period 08/02/06 – 13/03/06.**

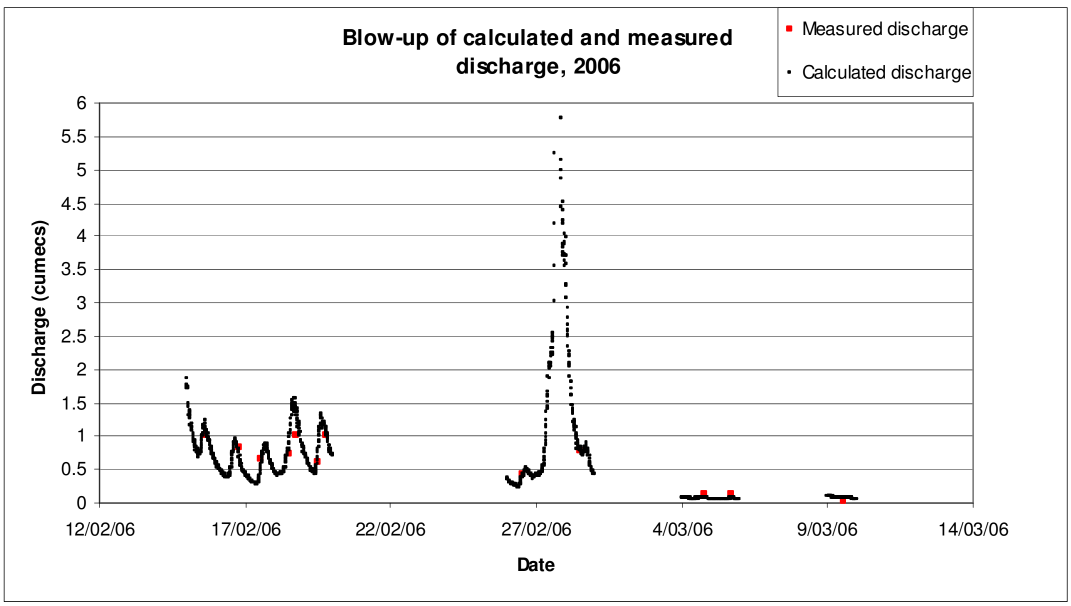


**Figure 27. Detail of calculated and measured discharge showing an imperfect, if close, agreement between the two data sets.**

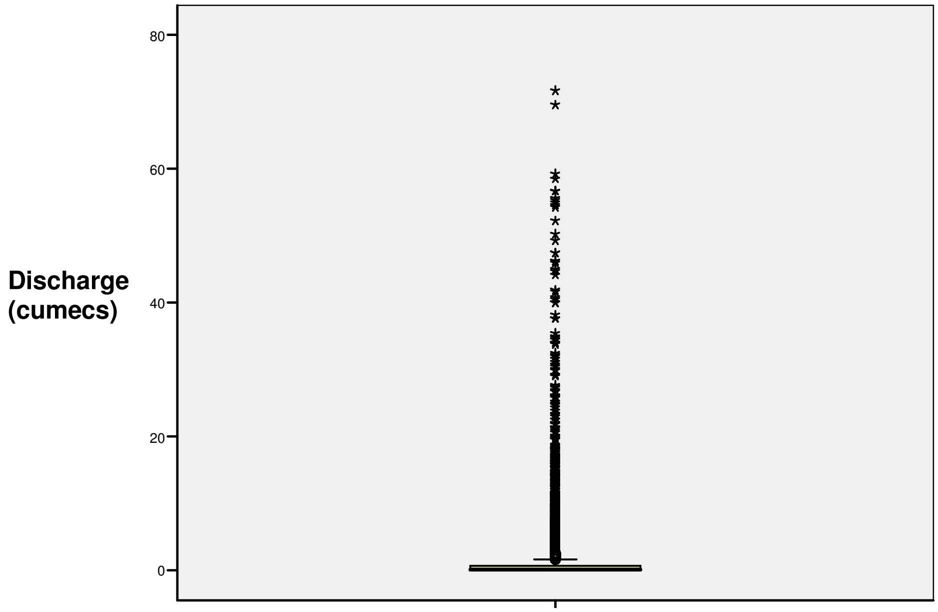


**Figure 28. Boxplot showing the distribution of values of the full calculated discharge record, summer and autumn 2005 and 2006, showing a very wide distribution of values. Circles indicate outliers within one quartile and stars outliers within two quartiles**

# Chapter 3: Results

## *Section 4: Streamflow Characteristics*

### 4.0 Stream character

The velocity profiles of the channel cross-section were highly variable and exhibited a relationship between the maximum flow velocity and the location in the channel cross-section at which this occurred. The values of maximum velocity show clustering from true right to true left and back again with decrease in maximum velocity of each sample, with the exception of flow measured on the 17th of February (Figure 28).

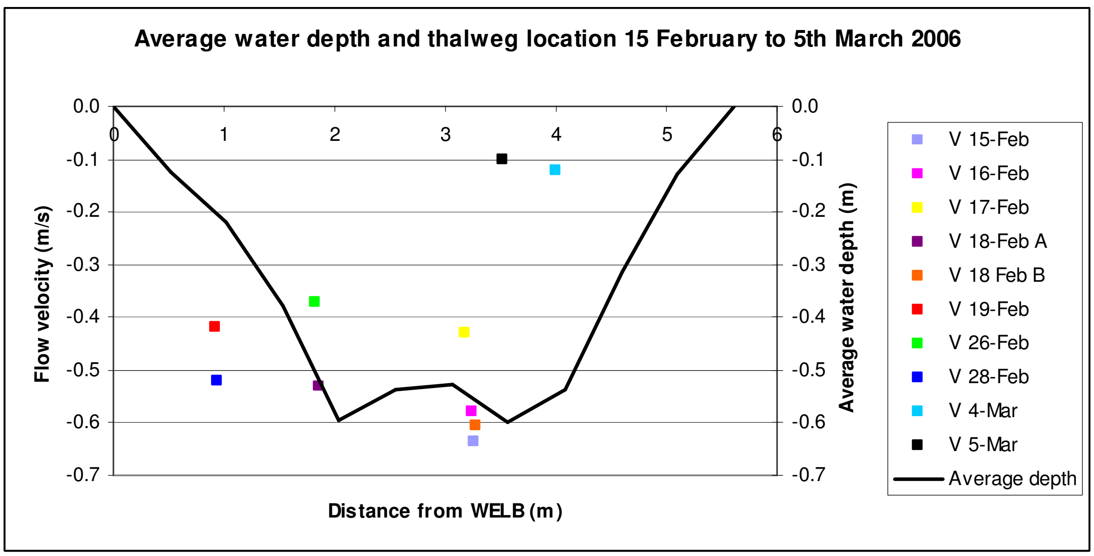


**Figure 29. The location of maximum point flow velocity for each sample in the main channel with respect to water depth, showing clustering of the maximum flow velocity location according to the value of maximum velocity.**

### 4.1 Overall streamflow

#### 4.10 Reliability and limitations

Analysis of the characteristics of streamflow in Brewster proglacial stream was done using the recorded values of stage, calculated discharge and the stage hydrograph forms. Measurements for winter and spring were not obtained and the data for summer and autumn cover a total of only seven months over two years. Ideally, several full years, or at least several full summer - autumn periods, would be available for analysis, especially for deduction of seasonal evolution of flow. Conclusions drawn from this data are therefore limited to the summer and autumn months.

### 4.11 Results

Table 3 presents the basic descriptive statistics for streamflow in the proglacial channel for 2005 and 2006, for the two seasons of the study and for the period over which the two yearly records overlap, from the 8th February to the 13th March. The following boxplots (Figures 29 - 34) show the distribution of values grouped in the same categories.

**Table 3. Descriptive statistics for stage (mm) and discharge (cumecs – calculated using the power curve given on page 36) for 2005 and 2006, for summer and autumn and the overlapping time period from February 8th to March 13th.**

| | | **Mean** | **Maximum** | **Minimum** |
|---|---|---|---|---|
| **2005** | Stage | 385 | 1047 | 197 |
| | Discharge | 0.720 | 71.680 | 0.002 |
| **2006** | Stage | 495 | 972 | 313 |
| | Discharge | 1.402 | 44.734 | 0.009 |
| **Summer** | Stage | 508 | 972 | 356 |
| | Discharge | 1.373 | 44.734 | 0.076 |
| **Autumn** | Stage | 366 | 1047 | 197 |
| | Discharge | 0.670 | 71.670 | 0.002 |
| **08/02/05 – 13/03/05** | Stage | 458 | 1047 | 319 |
| | Discharge | 1.379 | 71.680 | 0.038 |
| **08/02/06 – 13/03/06** | Stage | 495 | 972 | 313 |
| | Discharge | 1.403 | 44.734 | 0.034 |

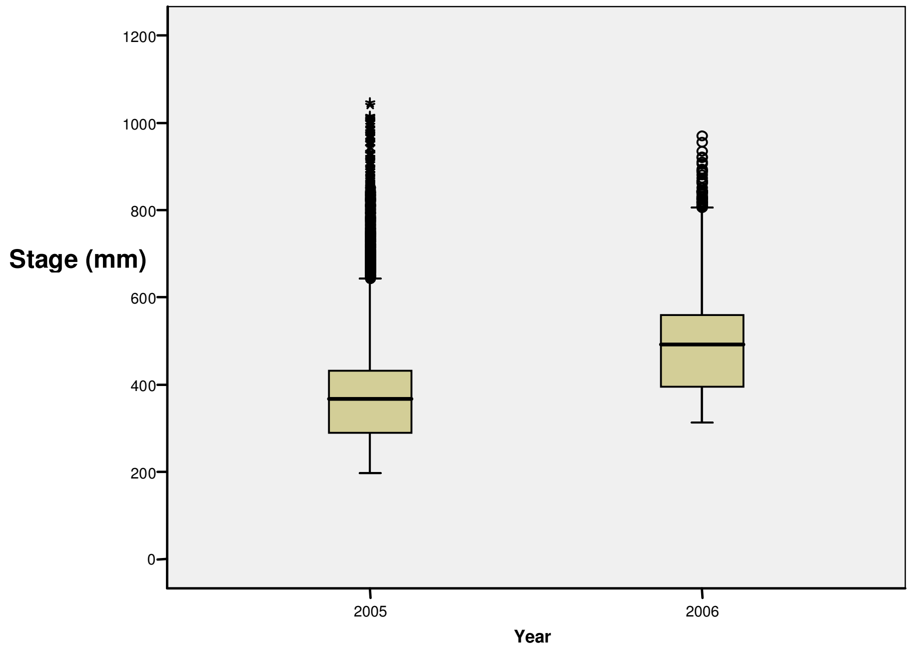


**Figure 30. Boxplots of stage in 2005 and in 2006, showing the distribution of values in each year. Circles represent outliers within one quartile and stars outliers within two quartiles.**

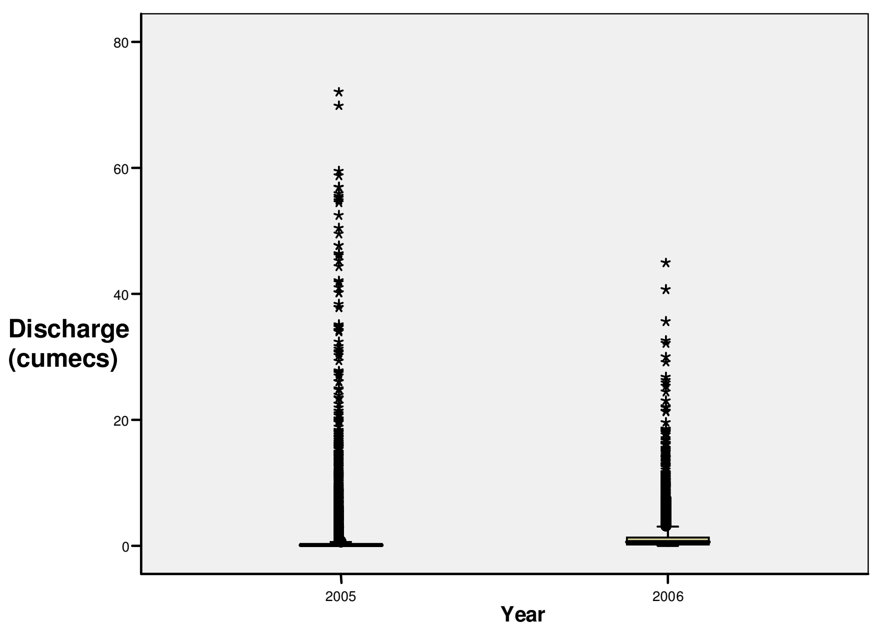


**Figure 31. Boxplots of discharge in 2005 and 2006, showing the distribution of values in each year. Circles represent outliers within one quartile and stars outliers within two quartiles.**

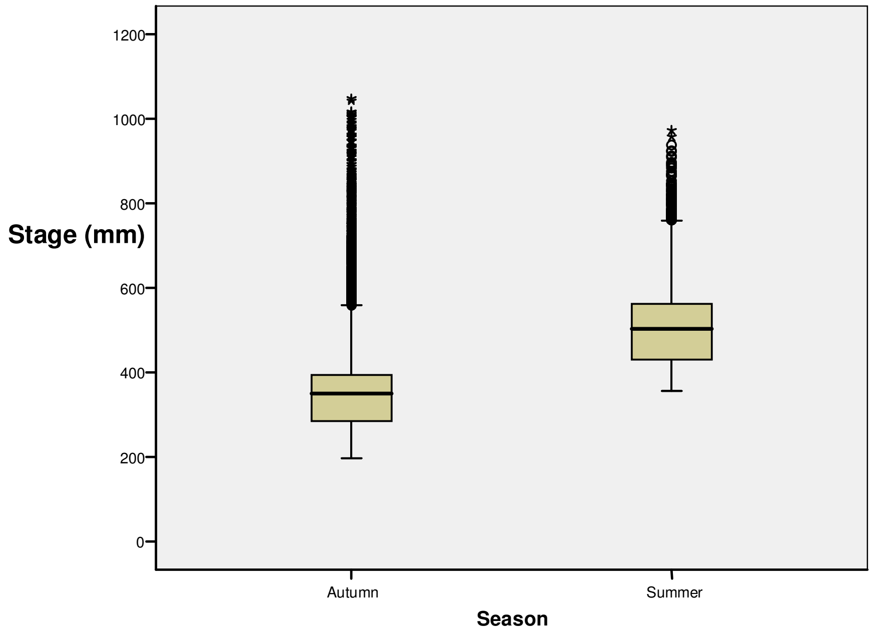


**Figure 32. Boxplots of stage in summer and autumn, showing the distribution of values in each season. Circles represent outliers within one quartile and stars outliers within two quartiles.**

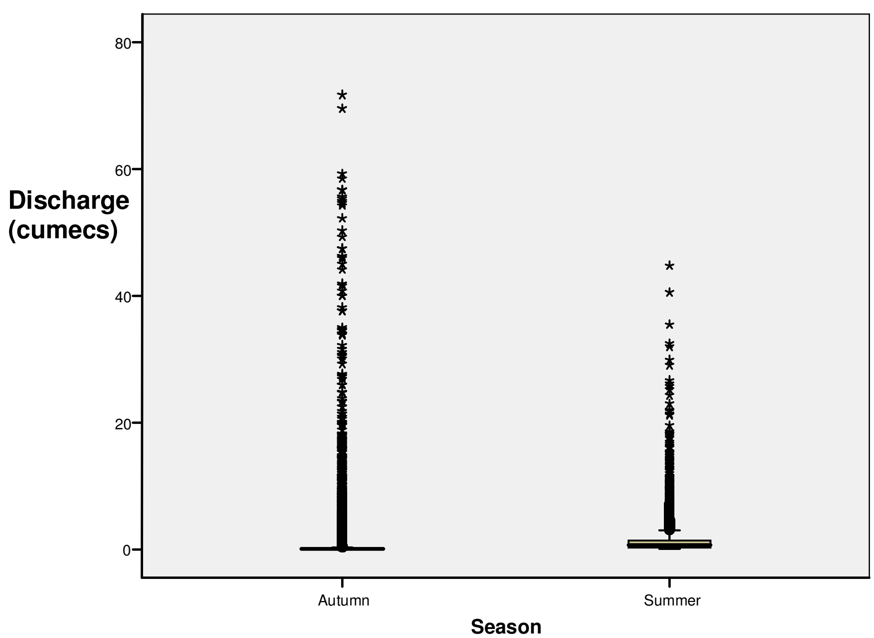


**Figure 33. Boxplots of discharge in summer and autumn, showing the distribution of values in each season. Circles represent outliers within one quartile and stars outliers within two quartiles.**

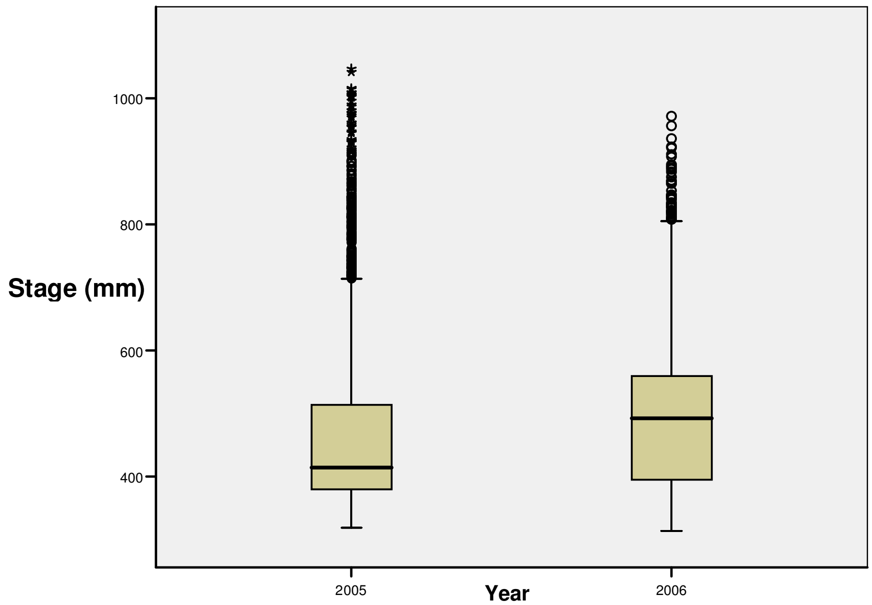


**Figure 34. Boxplots of stage from the 8th of February to the 13th of March in 2005 and 2006, showing the distribution of values over that same period. Circles represent outliers within one quartile and stars outliers within two quartiles.**

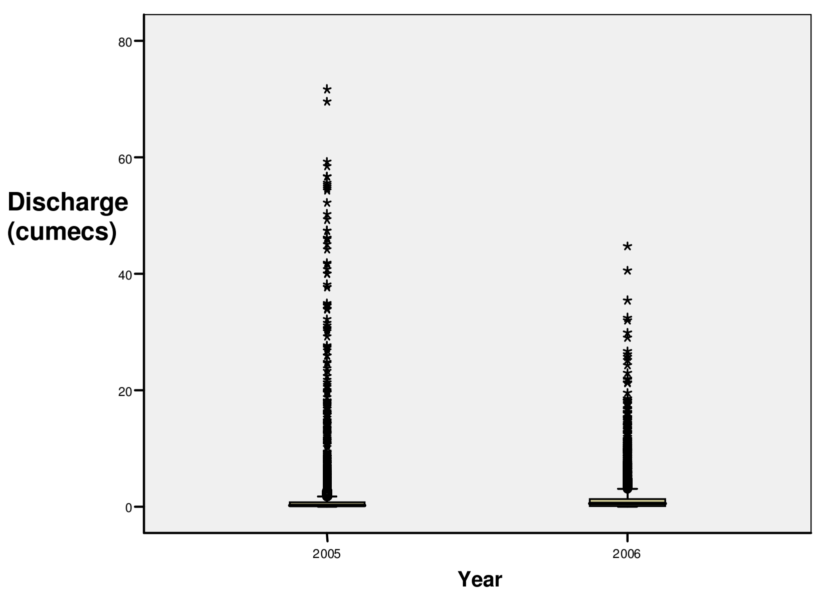


**Figure 35. Boxplots of discharge from the 8th of February to the 13th of March in 2005 and 2006, showing the distribution of values over that same period. Circles represent outliers within one quartile and stars outliers within two quartiles.**

The following flow duration curves show the percentage of time for which stage (Figure 35) and discharge (Figure 36) of a certain value is always exceeded (Davie, 2003).

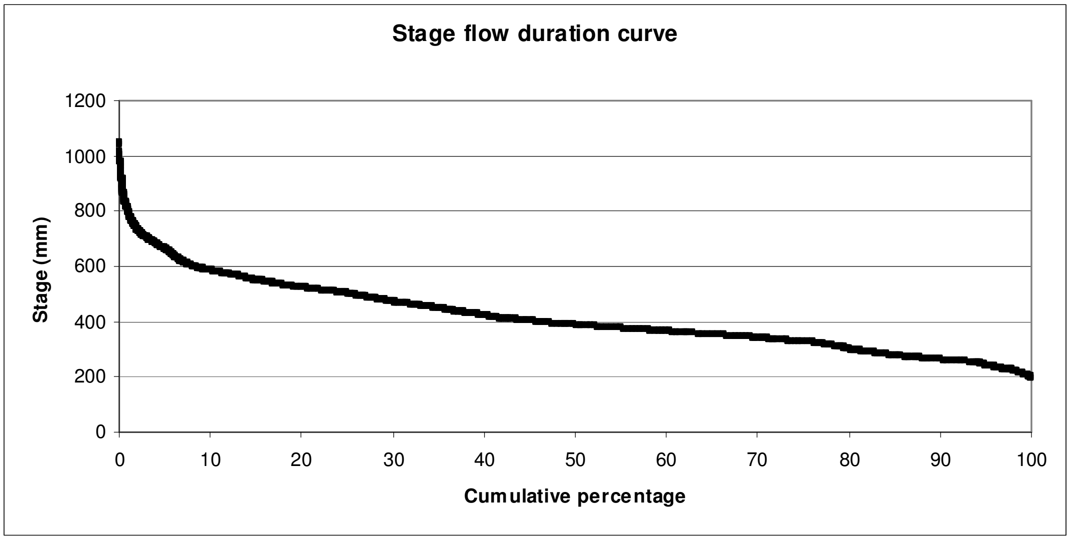


**Figure 36. Flow duration curve showing that stage exceeds 200mm 100% of the time, 663mm 5% of the time and 769mm 1% of the time.**

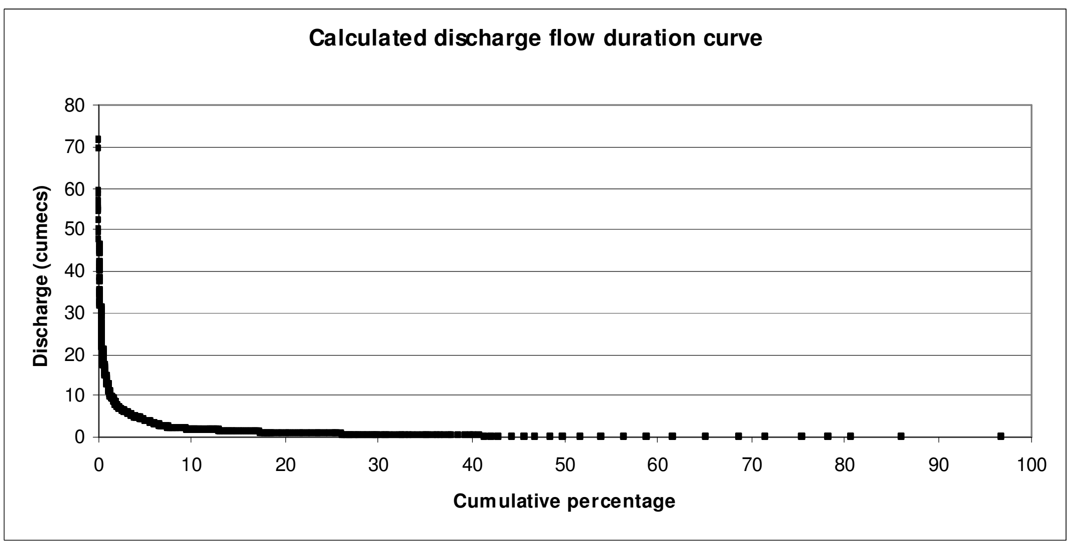


**Figure 37. Flow duration curve showing that discharge exceeds 0.005cumecs 100% of the time, 3.955 cumecs 5% of the time and 10 cumecs 1% of the time.**

Figures 37 and 38 show the daily moving average of stage over the study periods for 2005 and 2006, showing the overall decrease in water level over time with $R^2$ values of 0.53 and 0.61 respectively.

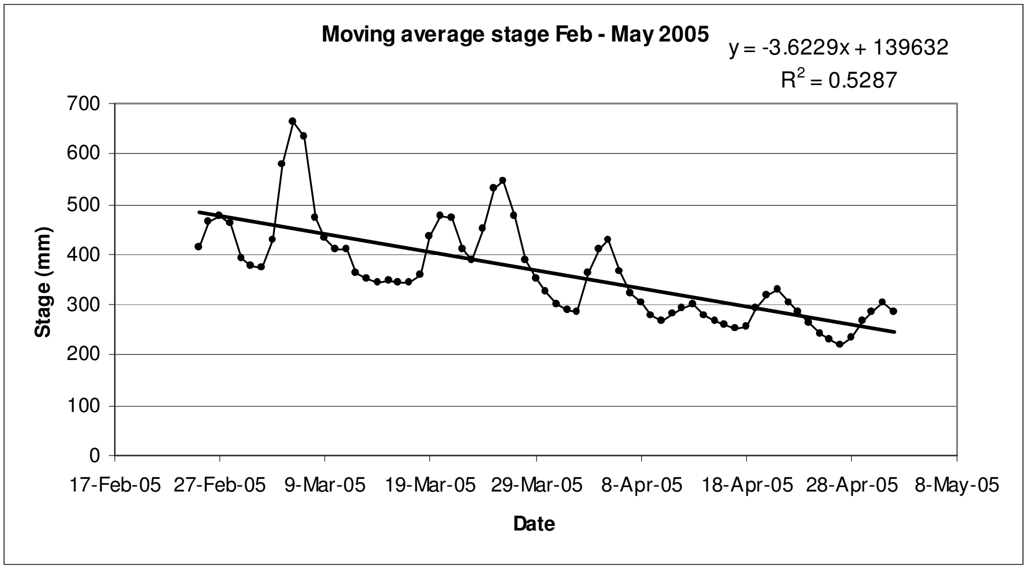


**Figure 38. Moving average stage 2005 with trendline and $R^2$ of 0.53, showing that around 50% of the variation in stage can be accounted for with time.**

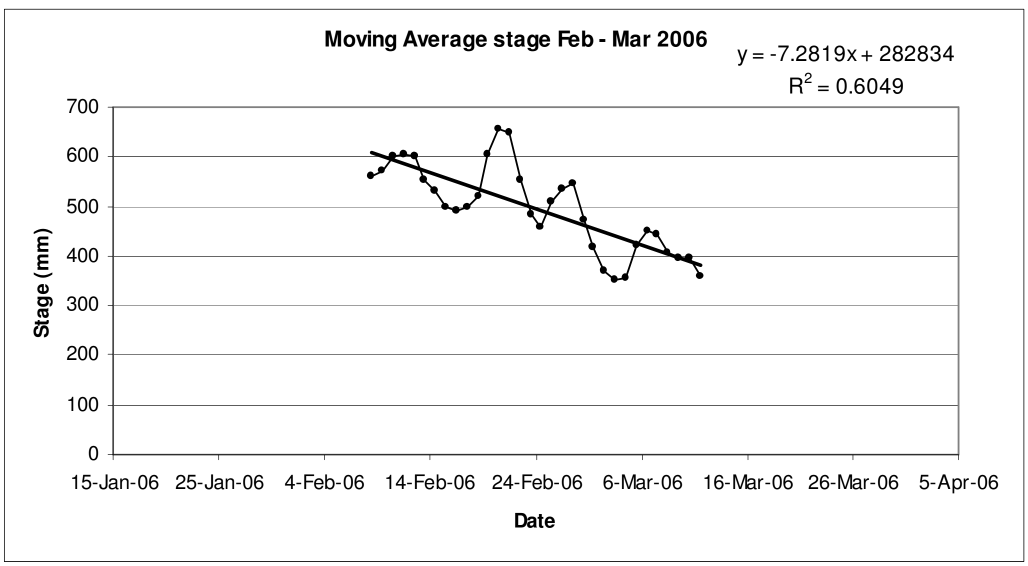


**Figure 39. Moving average stage 2006 with trendline and $R^2$ of 0.61, showing that around 60% of the variation in stage can be accounted for with time.**

## 4.2 Diurnal streamflow

### 4.21 Method

Diurnal characteristics of Brewster proglacial stream were ascertained from sections of the stage hydrograph in which distinct diurnal variation could be identified. Stage was used rather than discharge to avoid losing definition in the conversion. The chosen sections are characterised by consistent, approximately 12 hourly rises and falls in stage. Six sections of the record were found that met these criteria, which are highlighted in Figures 39 and 40. From these, the magnitude of daily variation, the timing of daily peaks and troughs and the change in these over time was distinguished in order to shed light on the nature of the stream and its evolution over the course of the year.

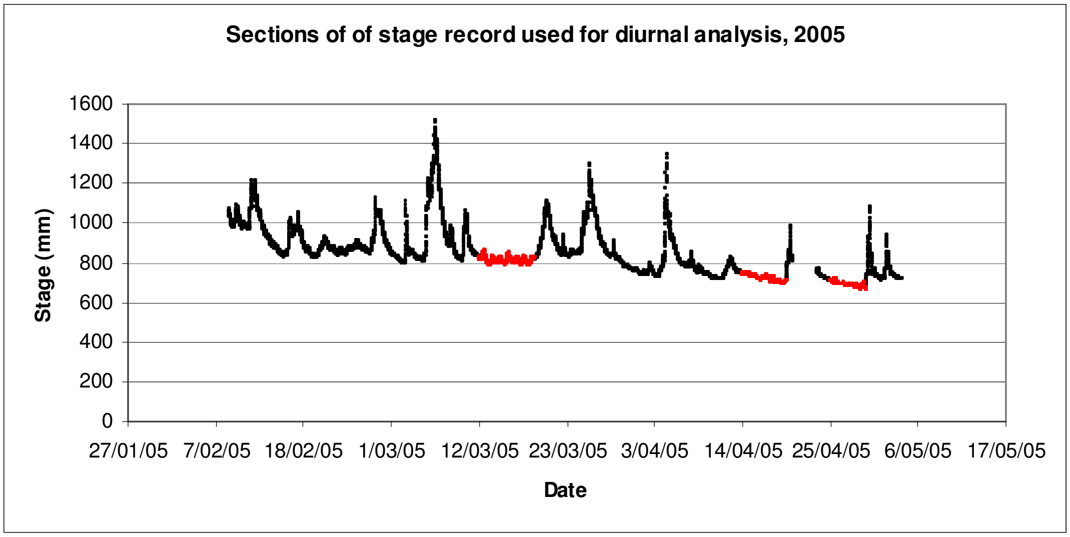


**Figure 40. The sections of the 2005 stage record used for diurnal characteristic analysis, highlighted in red.**

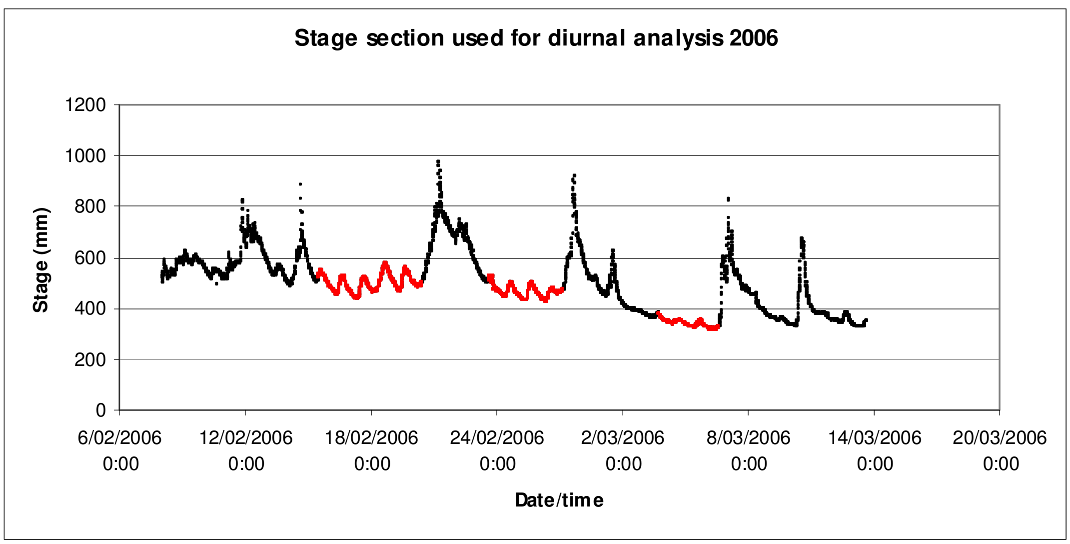


**Figure 41. The sections of the 2006 stage record used in diurnal characteristic analysis, highlighted in red.**

### 4.22 Results

Figures 41-46 and the adjoining tables describe the characteristics of diurnal variations in Brewster proglacial stream. The maximum diurnal variation of 105mm occurred during February 2006, and the maximum diurnal variation in 2005 of 76mm also occurred in the earliest record of the year, in March. The lowest diurnal variation of 5mm occurred during April 2005, and the lowest diurnal amplitude for 2006, 11mm, was in March, the latest record for that year. The timing of peaks in 2005 did not change and those in 2006 advanced by approximately one hour, while the troughs in both years advanced by approximately an hour overall. The duration of the rising limbs in 2005 decreased by three hours over the study period and in 2006 by one hour, while the duration of the falling limbs in 2005 increased by four hours and in 2006 by one hour.

**Figures 42 - 44. Sections of stage showing diurnal variations for 2005, with descriptive statistics.**

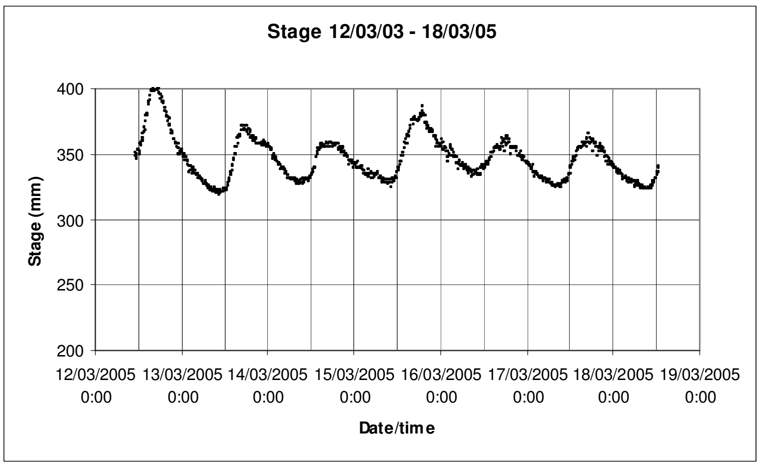


**Figure 42**.

| **Descriptive statistics 12/03/05 – 18/03/05** | |
|---|---|
| Max diurnal variation (mm) | 76 |
| Min diurnal variation (mm) | 26 |
| Mean diurnal variation (mm) | 44 |
| Average duration rising limb (hours) | 8 |
| Average duration falling limb (hours) | 16 |
| Timing of peak (hours) | 17:00 – 19:00 |
| Timing of trough (hours) | 09:00 – 12:00 |

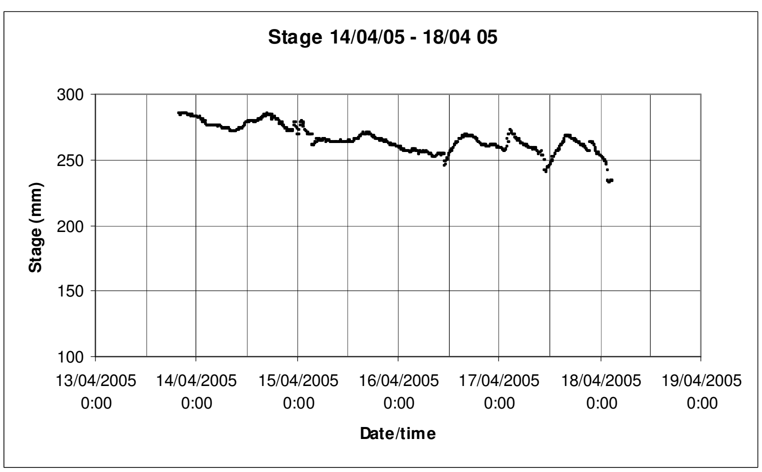


**Figure 43.**

| **Descriptive statistics 14/04/05 – 18/04/05** | |
|---|---|
| Max diurnal variation (mm) | 22 |
| Min diurnal variation (mm) | 5 |
| Mean diurnal variation (mm) | 15 |
| Average duration rising limb (hours) | 6 |
| Average duration falling limb (hours) | 18 |
| Timing of peak (hours) | 17:00 – 18:00 |
| Timing of trough (hours) | 10:00 – 12:00 |

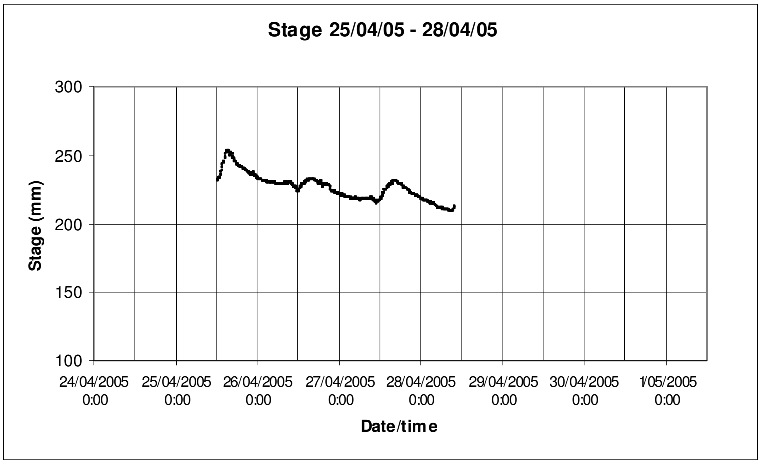


**Figure 44.**

| **Descriptive statistics 25/04/05 – 28/04/05** | |
|---|---|
| Max diurnal variation (mm) | 26 |
| Min diurnal variation (mm) | 6 |
| Mean diurnal variation (mm) | 15 |
| Average duration rising limb (hours) | 5 |
| Average duration falling limb (hours) | 20 |
| Timing of peak (hours) | 16:00 – 18:00 |
| Timing of trough (hours) | 12:00 – 13:00 |

**Figures 44-46. Sections of stage showing diurnal variations 2006, with descriptive statistics.**

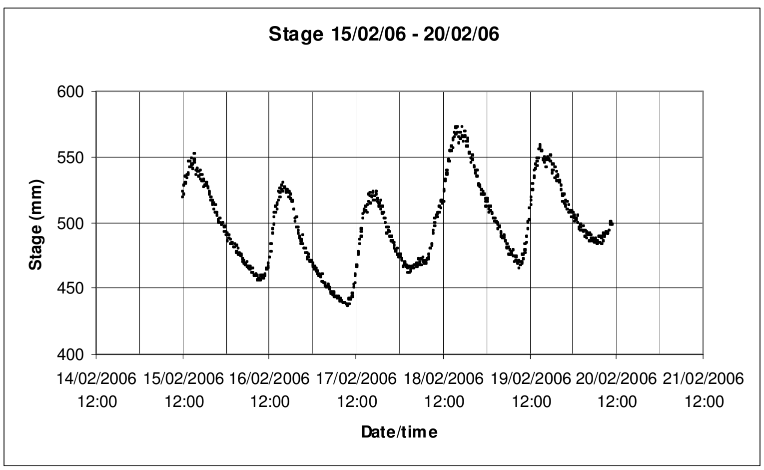


**Figure 45.**

| **Descriptive statistics 15/02/06 – 20/02/06** | |
|---|---|
| Max diurnal variation (mm) | 105 |
| Min diurnal variation (mm) | 55 |
| Mean diurnal variation (mm) | 84 |
| Average duration rising limb (hours) | 8 |
| Average duration falling limb (hours) | 16 |
| Timing of peak (hours) | 15:00 – 18:00 |
| Timing of trough (hours) | 05:00 – 11:00 |

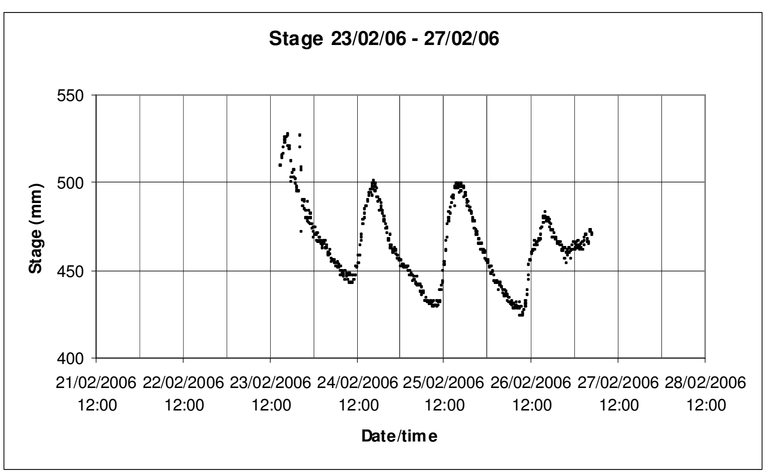


**Figure 46.**

| **Descriptive statistics 23/02/06 – 27/02/06** | |
|---|---|
| Max diurnal variation (mm) | 82 |
| Min diurnal variation (mm) | 53 |
| Mean diurnal variation (mm) | 67 |
| Average duration rising limb (hours) | 7 |
| Average duration falling limb (hours) | 17 |
| Timing of peak (hours) | 16:00 – 18:00 |
| Timing of trough (hours) | 10:00 – 11:00 |

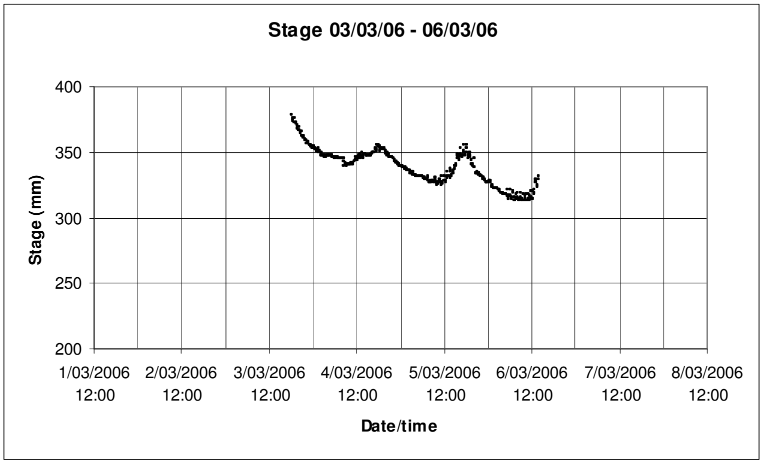


**Figure 47.**

| **Descriptive statistics 03/03/06 – 06/03/06** | |
|---|---|
| Max diurnal variation (mm) | 42 |
| Min diurnal variation (mm) | 11 |
| Mean diurnal variation (mm) | 28 |
| Average duration rising limb (hours) | 7 |
| Average duration falling limb (hours) | 17 |
| Timing of peak (hours) | 18:00 – 19:00 |
| Timing of trough (hours) | 11:00 – 13:00 |

## 4.3 Baseflow and peak flow

### 4.30 Method

Different hydrologists distinguish the baseflow component of discharge in different ways. A great degree of precision was not required in this analysis, so the simple method outlined by Pilgrim and Cordery (1992) in which baseflow and peakflow are separated by joining the low points of the hydrograph between peak flow events with straight lines was used here. The two components of discharge are illustrated in Figures 47 and 48.

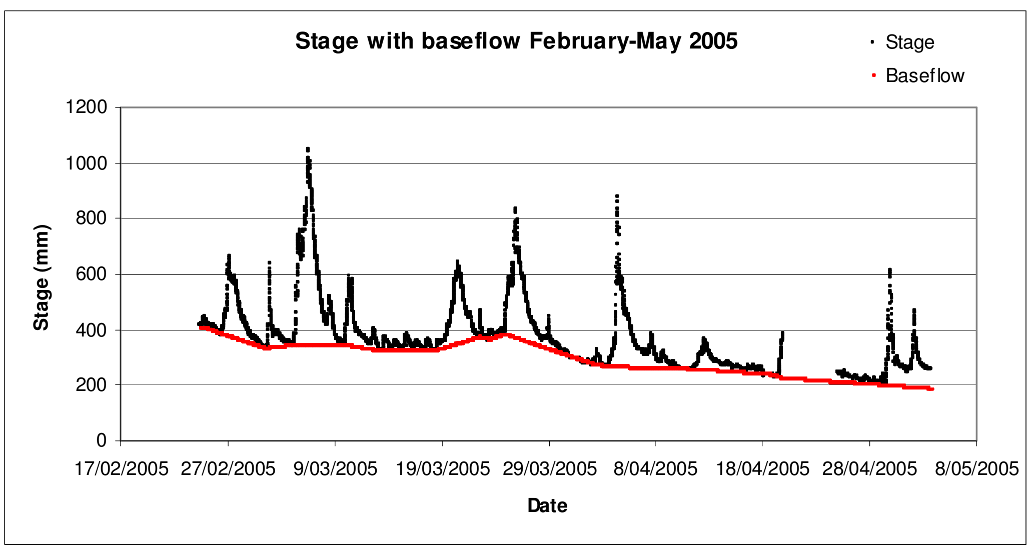


**Figure 48. The stage record for 2005 showing peakflow (volume above red line) and baseflow (volume below red line).**

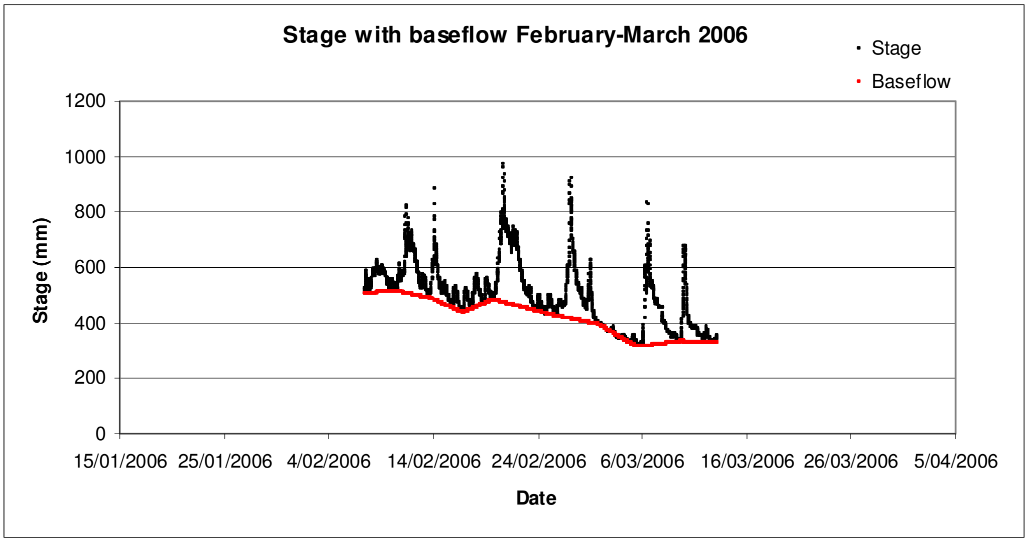


**Figure 49. The stage record for 2006 showing peakflow (volume above red line) and baseflow (volume below red line).**

## 4.32 Results

Descriptive statistics for peakflow in 2005 and 2006 are shown in Table 4 and for baseflow in 2005, 2006 and the overlapping period from the 8th of February to the 13th March in Table 5.

**Table 4. Peakflow descriptive statistics**

| | | **2005** | **2006** |
|---|---|---|---|
| **Largest peak flow event** | | | |
| | **Season** | Autumn | Autumn |
| | **Length** | 115 hr | 89 hr |
| | **Duration rising limb** | 34 hr | 10 hr |
| | **Duration falling limb** | 57 hr | 79 hr |
| | **Ratio of rising to falling limb** | 0.60 | 0.13 |
| | **Amplitude (mm stage)** | 705 | 529 |
| **Smallest peakflow event** | | | |
| | **Season** | Autumn | Summer |
| | **Length** | 184 hr | 43 hr |
| | **Duration rising limb** | 20 hr | 14 hr |
| | **Duration falling limb** | 164 hr | 29 hr |
| | **Ratio of rising to falling limb** | 0.12 | 0.48 |
| | **Amplitude (mm stage)** | 94 | 109 |

**Table 5. Baseflow descriptive statistics (stage – mm; discharge – cumecs)**

| | **2005** | | **2006** | | **08/02/05 – 13/03/05** | | **08/02/06 – 13/03/06** | |
|---|---|---|---|---|---|---|---|---|
| | Stage | Discharge | Stage | Discharge | Stage | Discharge | Stage | Discharge |
| **Max** | 406 | 0.176 | 514 | 0.786 | 406 | 0.176 | 443 | 0.306 |
| **Min** | 185 | 0.001 | 313 | 0.034 | 319 | 0.038 | 313 | 0.034 |
| **Change over study period** | -221 | -0.004 | -178 | -0.001 | -87 | 0.000 | -117 | 0.000 |

# Chapter 3: Results

## *Section 5: Precipitation*

### 5.0 Measurements

Precipitation data was collected using a Dataflow Systems Odyssey capacitance water level probe model ODYWL20. The gauge comprised an open topped PVC tube that permitted entry of both liquid and solid forms of precipitation. The tube was primed with an antifreeze solution of monopropylene glycol–methylated spirits so that all forms of precipitation were converted to liquid upon entering it. Increased water volume resulted in a higher value of capacitance which was automatically converted by the sensor into a record of water level. Measurements showed the change in water level and thereby the depth in water equivalent of any precipitation since the last record. The gauge was installed, monitored and maintained continually since February 2005 by Tim Kerr of Canterbury University, who provided the data, and Brian Anderson of Victoria University.

### 5.1 Calculations

Over time, the gauge sensor demonstrated an inverse sensitivity to temperature, recording increased water level when the water temperature dropped and decreased water level when the water temperature rose, while there had in fact been no change in water level. Inquiry to the manufacturer proved that the sensor relies on water temperature stability (Kerr, pers. com.), which cannot be held in a mountain situation. This sensitivity produced a distinct pattern in the data that was identifiable by its consistency, diurnal regularity and close correlation to temperature changes (Figure 49).

As the graph shows, the precipitation record “wiggled” in response to temperature changes with a gentle downward trend between each substantive increase in water level. This graph also shows that real precipitation events could be distinguished from the background noise created by the sensors sensitivity to temperature.

A subjective method for correcting this error was developed by Tim Kerr. Firstly, the periods of small “wiggles” that corresponded with changes in temperature were removed. The gradual downward trend of these periods - which could be the result of slow, steady

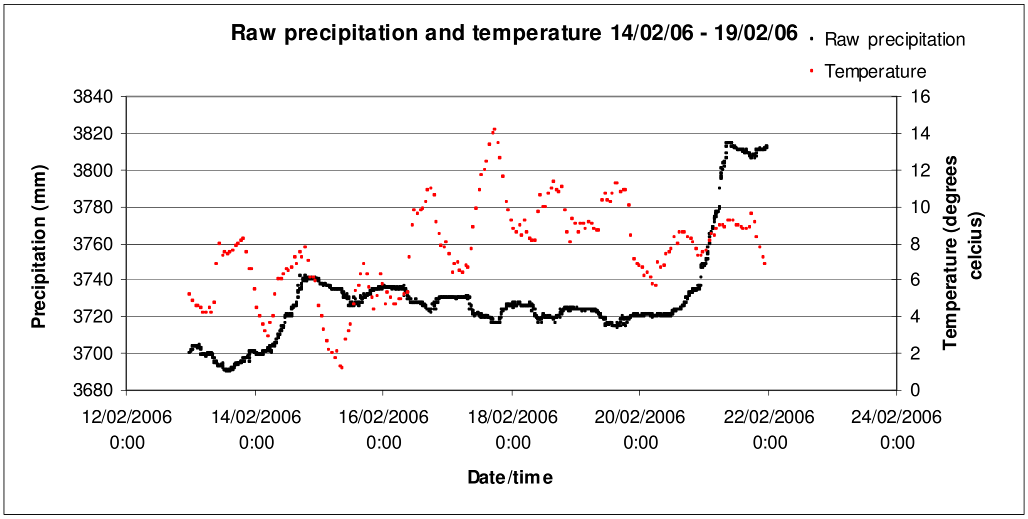


**Figure 50. Precipitation and temperature for the period 14 February to 19 February 2006, showing the close inverse relationship between temperature variation and "wiggles" in the precipitation record.**

evaporation from the gauge or a continuous gradual leak (though no leak was observed), or a secondary effect of the temperature sensitivity, were offset so that the values at the end and beginning of consecutive precipitation events were equal. The remaining data was then compared to the temperature record from the climate station located at the base of the glacier, the record of a tipping bucket rainfall gauge (maintained by Otago University, with data provided by Dorothea Stumm) situated on the shore of the proglacial lake and to the record of rainfall at the nearest local government weather station, in Haast, to evaluate the likelihood of the remaining patches of data being precipitation or artefacts of temperature variation. Where there was a significant decrease in temperature, a corresponding increase in gauge value and no suggestion of precipitation in the tipping bucket record or Haast record, the data was removed. This left only data that could be called precipitation with confidence.

The resulting record of cumulative precipitation was then calibrated using the following formula:

$$y = (x-o)/s$$

**Eq. 5**

where $x$ is the raw logged value for precipitation, $o$ is the initial offset value and $s$ is the initial slope value as determined from manually measured values (Kerr, pers. com.)

## 5.2 Data quality and errors

A thin layer of oil is usually maintained in precipitation gauges to avoid evaporation. However it was found by researchers at Canterbury University that oil coated the capacitance sensor, producing inaccurate records and was therefore not included (Kerr, pers. com.). Hence evaporation is not accounted for in the automatic precipitation record. This may have resulted in an underestimation of precipitation during warm periods. Furthermore, the precipitation gauge was not shielded from wind and this is likely to have resulted in an undercatch, especially of snow and light rain.

The temperature sensitivity almost certainly had an effect on the record during precipitation events as well as dry periods. A sensitivity test was undertaken in the models presented in Chapter 3.8 which proved that a small change in the values of precipitation (from five millimeters and above) does affect the results. Unfortunately, no method has been found to quantify this effect as the magnitude of each "wiggle" with a given temperature change was quite variable. Almost certainly this resulted in overestimation of precipitation during periods of decreasing temperature and underestimation during periods of increasing temperature. It is also possible that some precipitation events were not recorded as such at all, having been cancelled out by the effect of coincident temperature variation. Overall, it is likely that the final corrected record underestimates the frequency of precipitation events and that the magnitude of each event is somewhat distorted.

## 5.3 Results

Figures 50 and 51 show the final hourly and cumulative precipitation records for the study period, as used in further analysis.

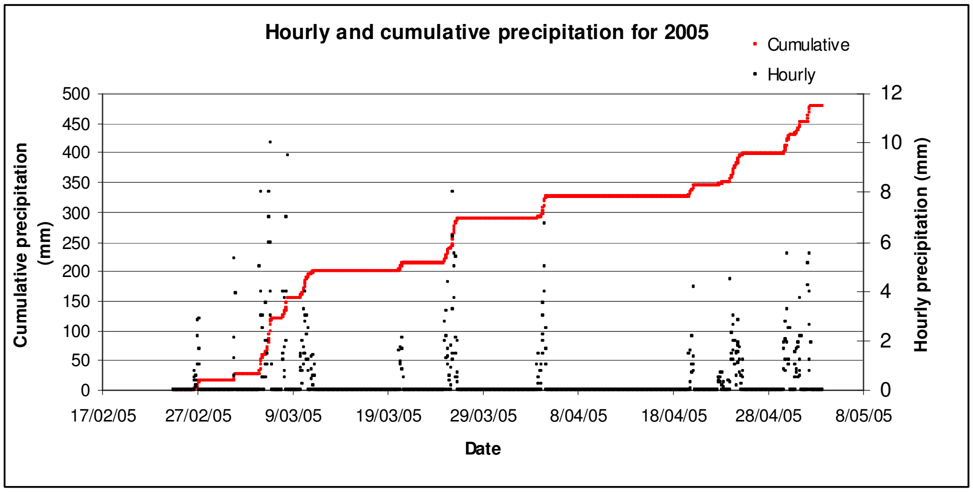


**Figure 51. The final corrected hourly and cumulative precipitation record for the 2005 study period.**

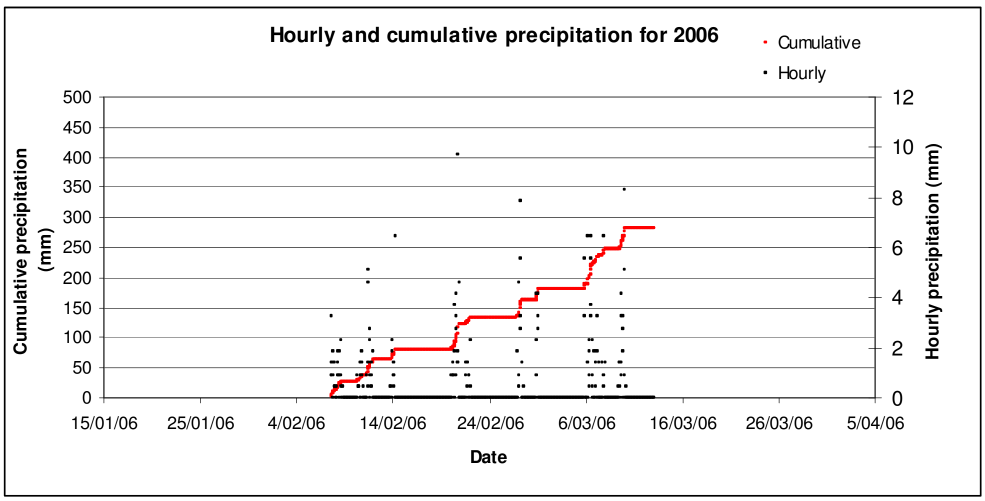


**Figure 53. The final corrected hourly and cumulative precipitation record for the 2006 study period.**

# Chapter 3: Results

## *Section 6: Atmospheric variables*

### 6.0 Data

Relative humidity, shortwave radiation, atmospheric pressure, wind speed and air temperature were recorded at an automated climate station. This station, located beside the proglacial lake approximately 200m from the glacier terminus (Figure 52), was installed by researchers of Otago University in February 2005 and data from the 24$^{th}$ of February 2005 was provided by Dorothea Stumm. Analysis of the atmospheric variables therefore only covers the period from the 24$^{th}$ of February 2005, rather than the 8$^{th}$ of February as for analysis of the stage record.

**Figure 53. Brewster Glacier with the climate station, located around 200m from the glacier, circled.**

### 6.1 Measurement

Wind speed was measured with an A200m Vector Anemometer, at 3.5m height. Air temperature and relative humidity were measured on a SKH 2031 Sky Temperature and Humidity probe, at 3m height, and incoming shortwave radiation on an LI-COR –

PY200SA pyranometer also at 3m above ground. Measurements were taken every 30 seconds in all cases excepting that of wind speed for which measurements were hourly. Atmospheric pressure at Brewster was derived from measurements taken at the nearby Haast weather station, provided by NIWA. These were transformed using the following equation:

$$P = Po \exp(-m * g * h / (R * T))$$

**Eq. 6**

where *Po* is atmospheric pressure at sea-level, the constant *m* equals 0.02895kg/mol, the constant *g* equals 9.81ms$^{-2}$, *h* is elevation of the site - 1724.086m in this case, the constant *R* equals 8.314 J/Kmol, and *T* is air temperature in Kelvins (Anderson, pers. com.).

### 6.3 Results

The following tables (Tables 6-9) describe the distribution of values in the atmospheric variable data sets for 2005 and 2006 and for the overlapping time period from the 24$^{th}$ February to the 13$^{th}$ of March. Graphs of the full data sets are in Appendix 1.

**Table 6. Descriptive statistics for atmospheric variables 2005.**

| | Air temperature (degrees C) | Relative humidity (%) | Wind speed (m/s) | Shortwave radiation (w/m$^2$) | Atmospheric pressure (hPa) |
|---|---|---|---|---|---|
| Mean | 4.45 | 80.02 | 3.37 | 119.48 | 822.81 |
| Minimum | -6.71 | 11.43 | 0.20 | 0.00 | 799.28 |
| Maximum | 12.34 | 100.00 | 16.20 | 891.78 | 835.83 |
| Standard deviation | 3.50 | 19.92 | 2.26 | 193.61 | 6.22 |

**Table 7. Descriptive statistics for atmospheric variables 2006.**

| | Air temperature (degrees C) | Relative humidity (%) | Wind speed (m/s) | Shortwave radiation (w/m$^2$) | Atmospheric pressure (hPa) |
|---|---|---|---|---|---|
| Mean | 4.45 | 85.14 | 3.41 | 154.52 | 822.38 |
| Minimum | -4.45 | 28.49 | 0.20 | 0.00 | 803.76 |
| Maximum | 14.14 | 100.00 | 10.85 | 981.46 | 836.76 |
| Standard deviation | 3.69 | 17.54 | 1.91 | 244.35 | 6.99 |

**Table 8. Descriptive statistics for atmospheric variables over the period 24/02/05 – 13/03/05**

| | Air temperature (degrees C) | Relative humidity (%) | Wind speed (m/s) | Shortwave radiation ($w/m^2$) | Atmospheric pressure (hPa) |
|---|---|---|---|---|---|
| Mean | 4.64 | 87.01 | 3.42 | 123.13 | 821.82 |
| Minimum | -2.33 | 26.95 | 0.82 | 0.00 | 808.93 |
| Maximum | 10.50 | 100.00 | 16.20 | 891.78 | 833.14 |
| Standard deviation | 3.00 | 15.14 | 2.53 | 195.39 | 5.55 |

**Table 9. Descriptive statistics for atmospheric variables over the period 24/02/06 – 13/03/06**

| | Air temperature (degrees C) | Relative humidity (%) | Wind speed (m/s) | Shortwave radiation ($w/m^2$) | Atmospheric pressure (hPa) |
|---|---|---|---|---|---|
| Mean | 2.30 | 84.48 | 3.76 | 145.41 | 819.93 |
| Minimum | -4.45 | 28.49 | 0.20 | 0.00 | 803.76 |
| Maximum | 9.76 | 100.00 | 10.85 | 934.44 | 836.76 |
| Standard deviation | 3.20 | 17.95 | 2.25 | 231.57 | 7.77 |

There is no record of albedo for either year, but photographic evidence of snow cover (Figures 53 and 54) provided a qualitative proxy record. The glacier was fully snow covered by mid-February of 2006 but still bare in the ablation zone by that time in 2005, indicating that albedo would have been higher in 2006 than in 2005.

**Figure 54. Brewster Glacier from the southwest in the first week of February 2005, with bare ice in the ablation zone indicating comparatively low albedo.**

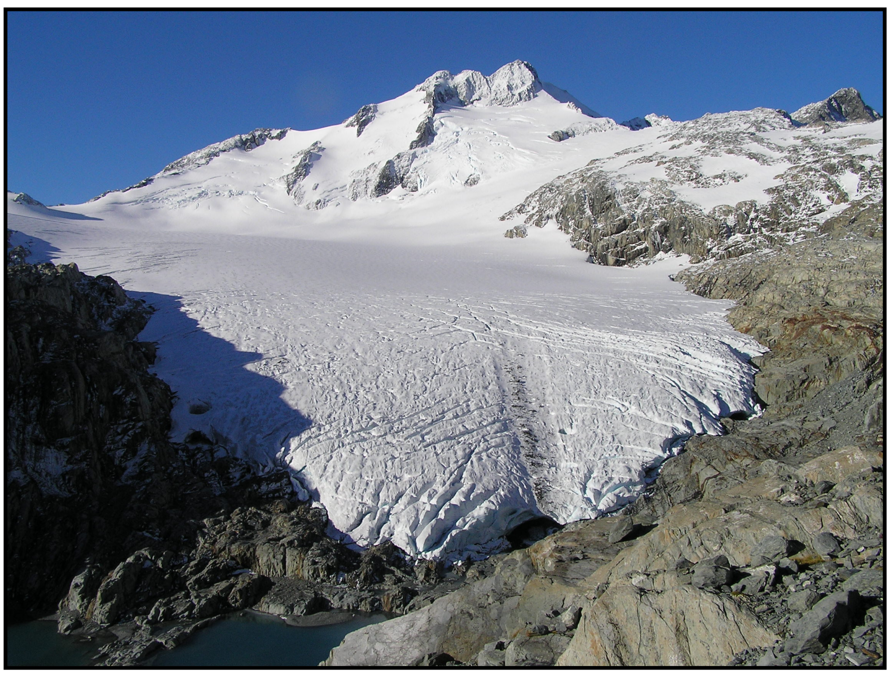

**Figure 55. Brewster Glacier from the south in the second week of February 2006, with a full snow cover indicating comparatively high albedo (*photo courtesy of Andrew Mackintosh*).**

# Chapter 3: Results

## *Section 7: Single regressions and linear relationships*

### 7.0 Single linear regressions

#### 7.01 Method

Single linear regressions were carried out with the atmospheric variables as predictors of stage. The full data set was used first and then summer and autumn data separately, using average hourly values to include as much information as possible and then daily totals for a more general picture.

It was expected that there would be a lag period for the response of stream flow to atmospheric variation, but when trials with lag times of one to ten hours were done the $R^2$ values remained the same for all except relative humidity with a lag time of three hours, in that case with a change from 0.40 to 0.30. The $R^2$ values given are therefore those found between stage and the atmospheric variables at the same point in time.

Regressions were then performed on the atmospheric variables as predictors of each other to establish relationships between them and as a test of covariance, using only daily total data for the full data set and then summer and autumn separately. This part of the analysis was not done with hourly average data because the aim was to distinguish general relationships between these variables and not the detail that is relevant in the discharge analysis. Stage was graphed with each atmospheric variable for a qualitative analysis of the correlation between patterns in the records.

#### 7.02 Results

The $R^2$ values for each of the hourly regressions are given in Table 10 and for the daily in Table 11. Wind speed and stage during summer had the highest $R^2$ values in both analyses at 0.42 and 0.73 respectively, and daily total precipitation was notably correlated with stage in summer with a value of 0.62 and 0.36 in autumn.

**Table 10. $R^2$ values for hourly average stage against each atmospheric variable**

| | Full data $R^2$ | Summer $R^2$ | Autumn $R^2$ |
|---|---|---|---|
| **Air temperature** | 0.10 | 0.00 | 0.04 |
| **Relative humidity** | 0.15 | 0.19 | 0.14 |
| **Wind speed** | 0.07 | 0.42 | 0.13 |
| **Shortwave radiation** | 0.00 | 0.01 | 0.01 |
| **Atmospheric pressure** | -0.04 | -0.14 | -0.13 |
| **Precipitation** | 0.15 | 0.27 | 0.22 |

**Table 11. $R^2$ values for daily total stage against each atmospheric variable**

| | Full data $R^2$ | Summer $R^2$ | Autumn $R^2$ |
|---|---|---|---|
| **Air temperature** | 0.12 | 0.00 | 0.21 |
| **Relative humidity** | 0.22 | 0.29 | 0.24 |
| **Wind speed** | 0.11 | 0.73 | 0.05 |
| **Shortwave radiation** | 0.01 | 0.19 | 0.06 |
| **Atmospheric pressure** | -0.04 | 0.00 | -0.14 |
| **Precipitation** | 0.25 | 0.62 | 0.36 |

The $R^2$ values for the atmospheric variables as predictors of each other are shown for the full data set in Table 12, for summer in Table 13 and autumn in Table 14.

**Table 12: $R^2$ values for daily totals of all predictor variables**

| | **T** | **H** | **W** | **S** | **P** | **R** |
|---|---|---|---|---|---|---|
| **T** | 1 | -0.015 | -0.031 | 0.072 | 0.037 | -0.018 |
| | **H** | 1 | 0.049 | -0.035 | -0.088 | 0.21 |
| | | **W** | 1 | -0.167 | -0.099 | 0.48 |
| | | | **S** | 1 | 0.088 | -0.35 |
| | | | | **P** | 1 | -0.116 |
| | | | | | **R** | 1 |

**Table 13: $R^2$ values for daily totals of all predictor variables for summer**

| | **T** | **H** | **W** | **S** | **P** | **R** |
|---|---|---|---|---|---|---|
| **T** | 1 | -0.024 | -0.015 | 0.007 | 0.049 | 0.006 |
| | **H** | 1 | 0.294 | -0.795 | -0.006 | 0.411 |
| | | **W** | 1 | -0.357 | 0.009 | 0.625 |
| | | | **S** | 1 | 0.002 | -0.487 |
| | | | | **P** | 1 | -0.014 |
| | | | | | **R** | 1 |

**Table 14: $R^2$ values for daily totals of all predictor variables for autumn**

| | **T** | **H** | **W** | **S** | **P** | **R** |
|---|---|---|---|---|---|---|
| **T** | 1 | -0.029 | -0.019 | 0.051 | 0.021 | -0.024 |
| | **H** | 1 | 0.037 | -0.338 | -0.135 | 0.188 |
| | | **W** | 1 | -0.13 | -0.111 | 0.466 |
| | | | **S** | 1 | 0.13 | -0.369 |
| | | | | **P** | 1 | -0.143 |
| | | | | | **R** | 1 |

The correlation between the full data wind speed and precipitation records was of particular note with an $R^2$ of 0.48, and between shortwave radiation and precipitation at -0.35. During summer, relative humidity correlated to shortwave radiation with a coefficient of -0.78 and to precipitation with a coefficient of 0.41, wind speed correlated to shortwave radiation with a coefficient of -0.36 and to precipitation with a coefficient of 0.63, and shortwave radiation correlated to precipitation with a coefficient of -0.49. In the analysis of the autumn data, relative humidity correlated with shortwave radiation with a coefficient of-0.34, wind speed to precipitation with a coefficient of 0.47, and shortwave radiation to precipitation with a coefficient of -0.37. All other $R^2$ values were below |0.3|.

**7.1 Investigating relationships**

Figures 55-60 are graphs of stage with each atmospheric variable for summer and autumn 2005 and 2006. Coincident events can be seen in these graphs, with positive and negative relationships quite clear in some cases (between stage and precipitation or stage and atmospheric pressure respectively, for example).

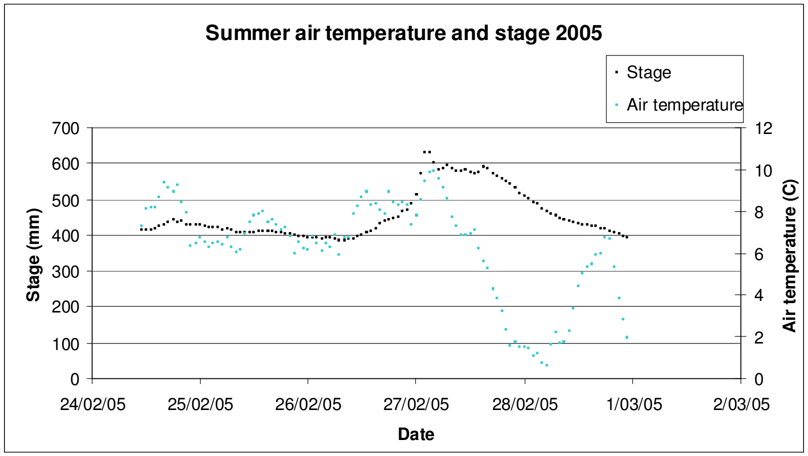

Figure 56a. Summer stage and air temperature 2005.

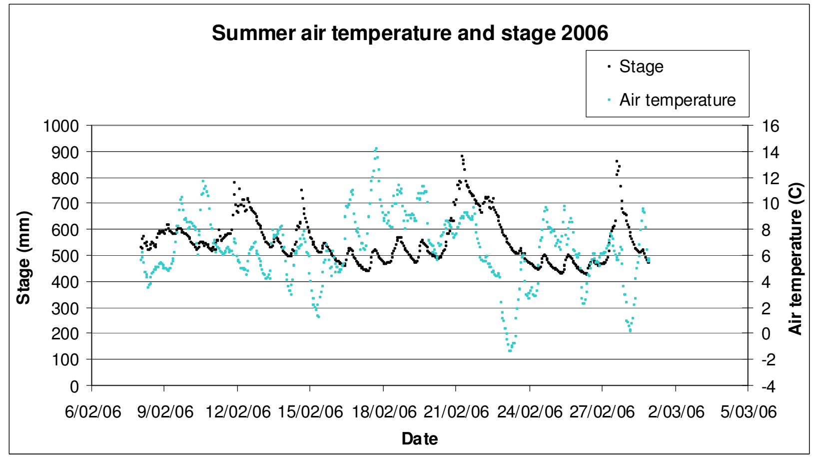

Figure 56b. Summer stage and air temperature 2006.

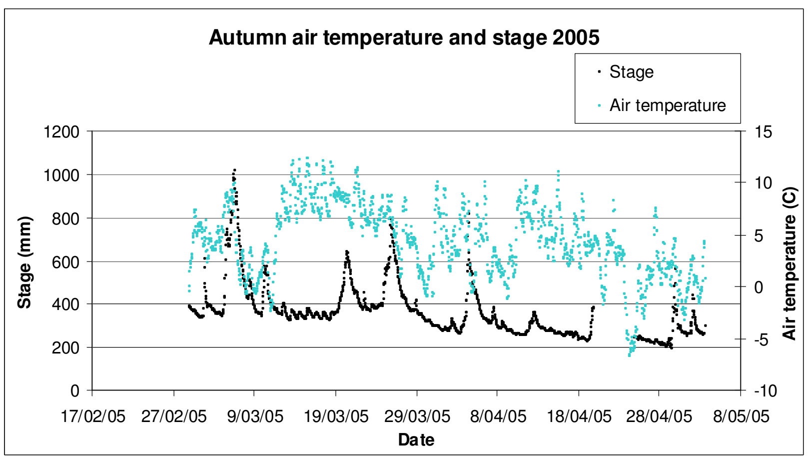

Figure 56c. Autumn stage and air temperature 2005.

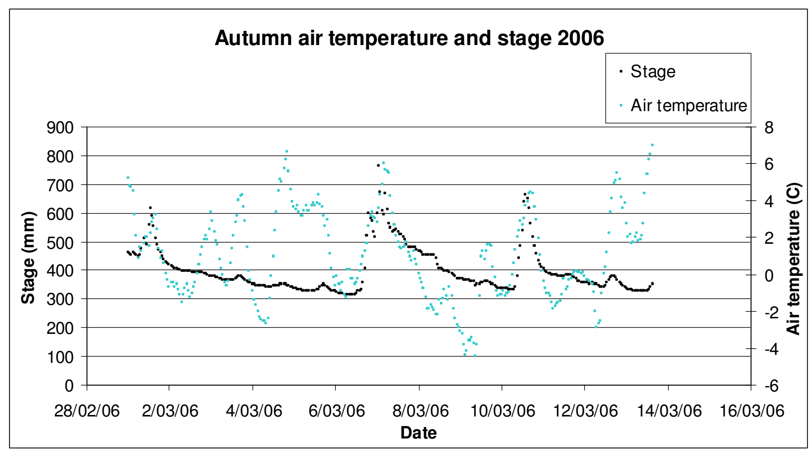

Figure 56d. Autumn stage and air temperature 2006.

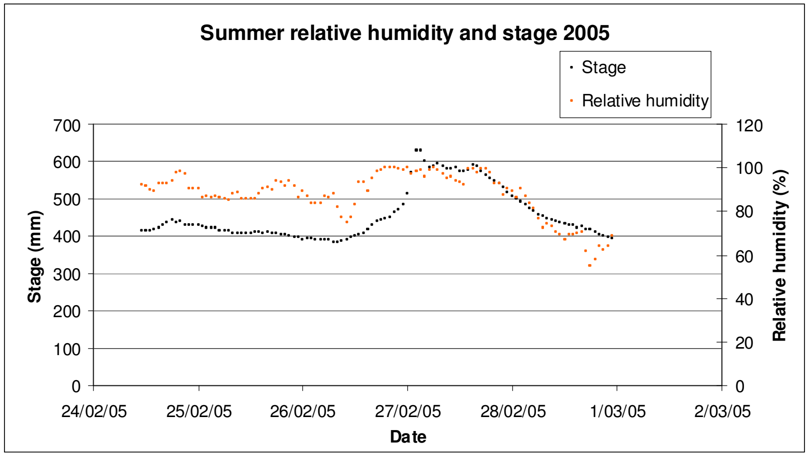


**Figure 57a. Summer stage and relative humidity 2005.**

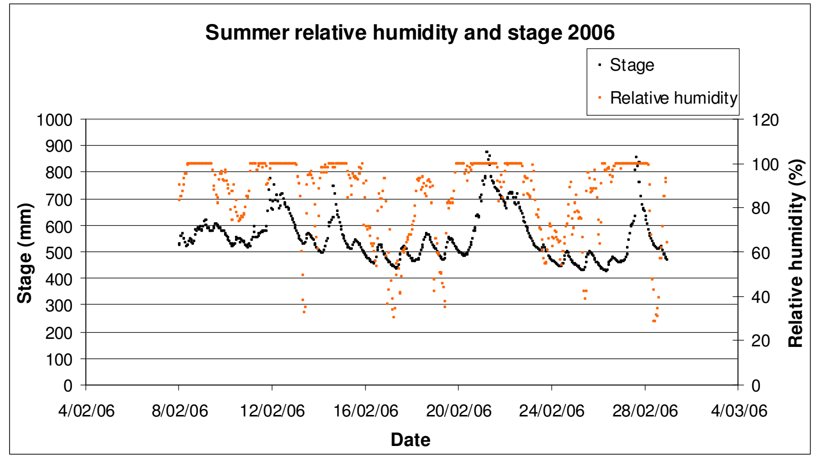


**Figure 57b. Summer stage and relative humidity 2006.**

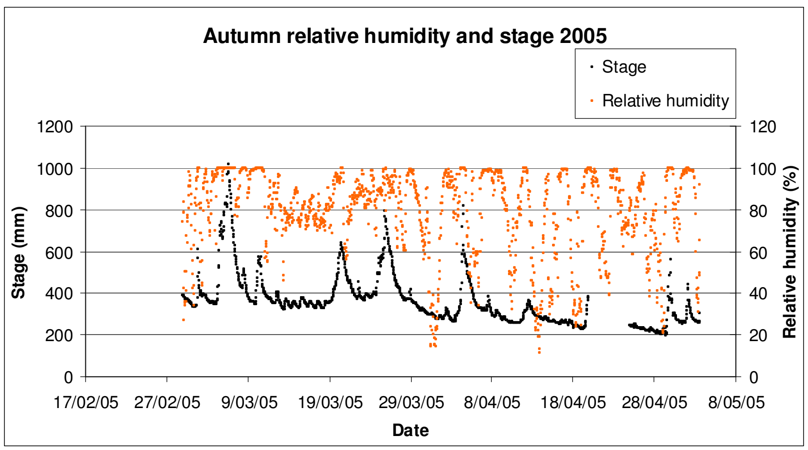


**Figure 57c. Autumn stage and relative humidity 2005.**

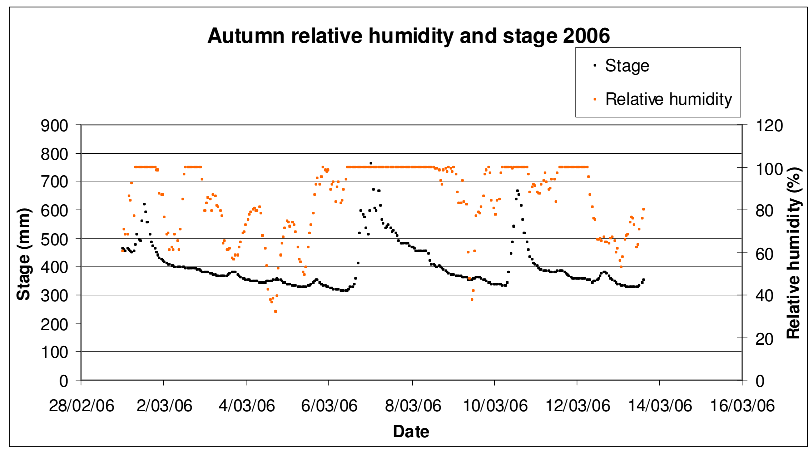


**Figure 57d. Autumn stage and relative humidity 2006.**

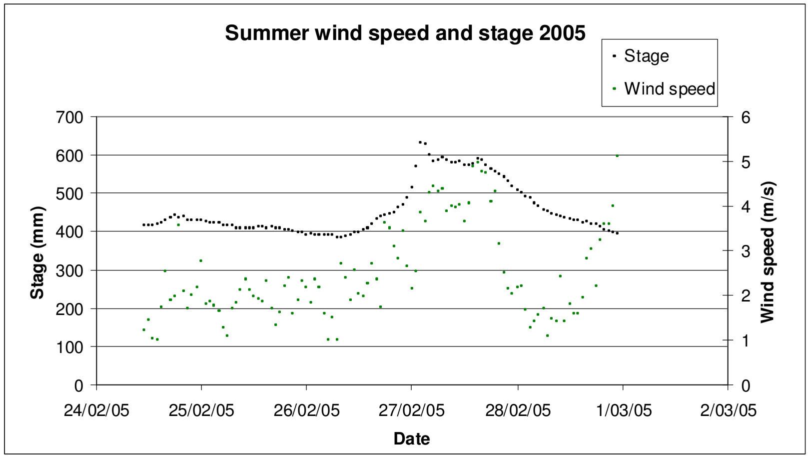


**Figure 58a. Summer stage and wind speed 2005.**

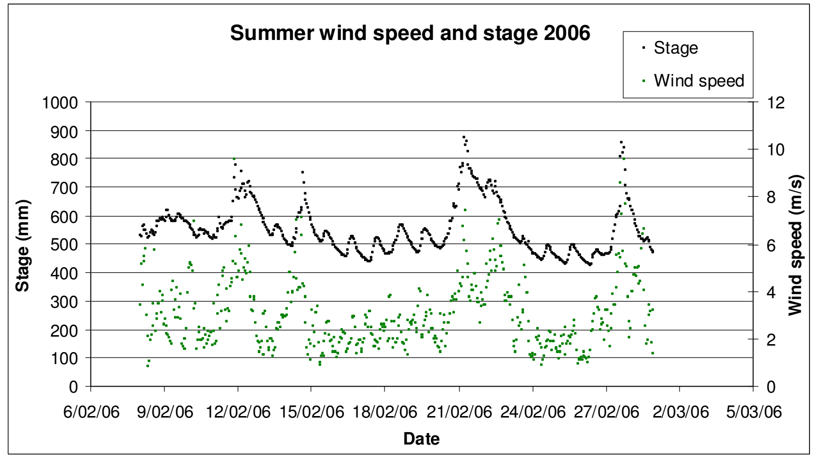


**Figure 58b. Summer stage and wind speed 2006.**

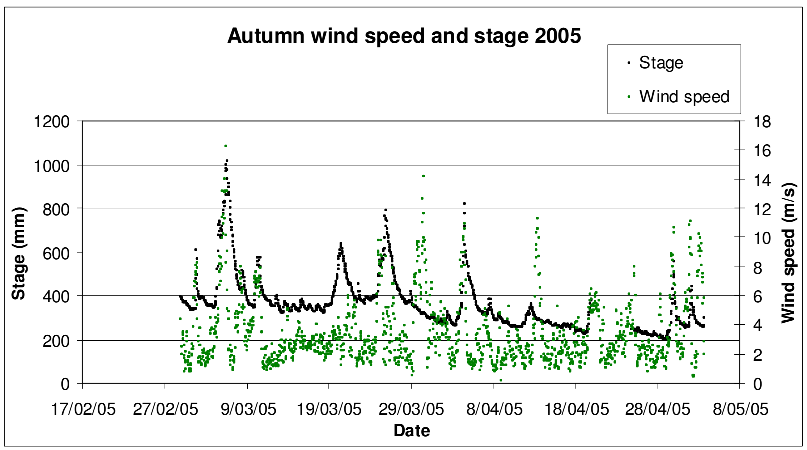


**Figure 58c. Autumn stage and wind speed 2005.**

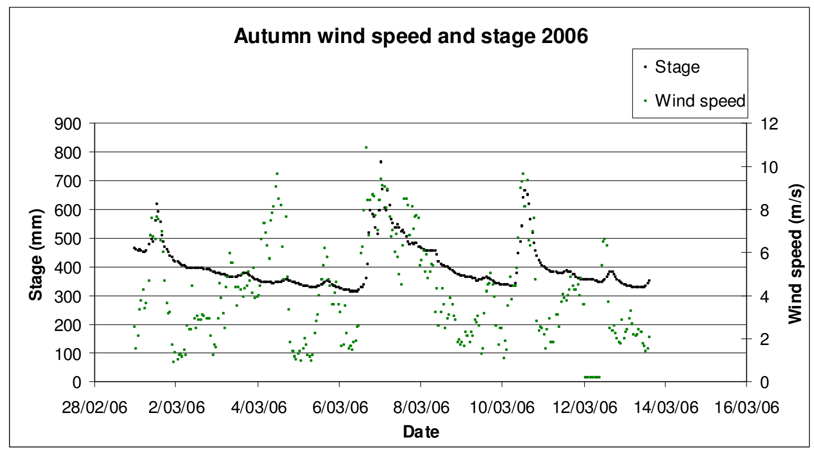


**Figure 58d. Autumn stage and wind speed 2006.**

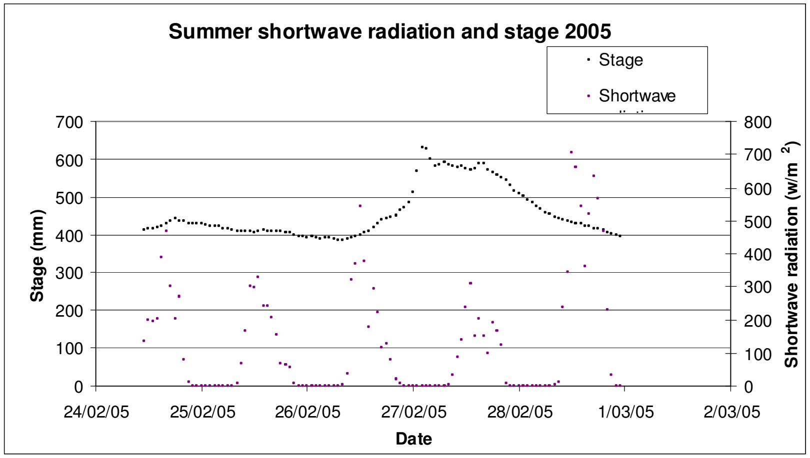


Figure 59a. Summer stage and shortwave radiation 2005.

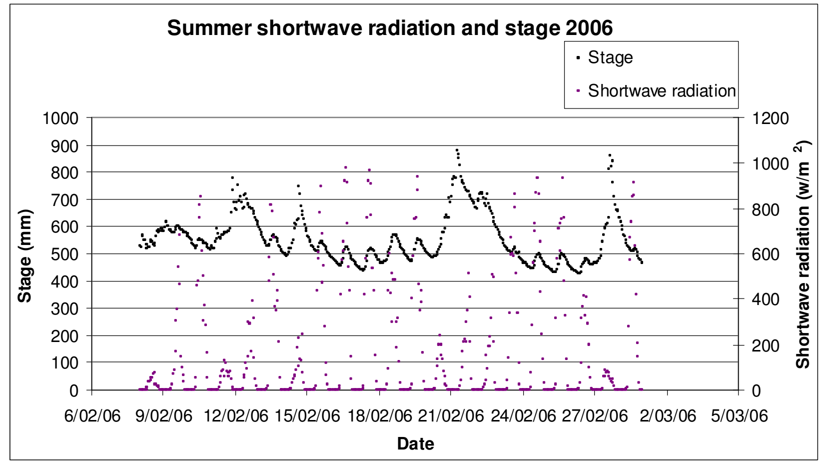


Figure 59b. Summer stage and shortwave radiation 2006.

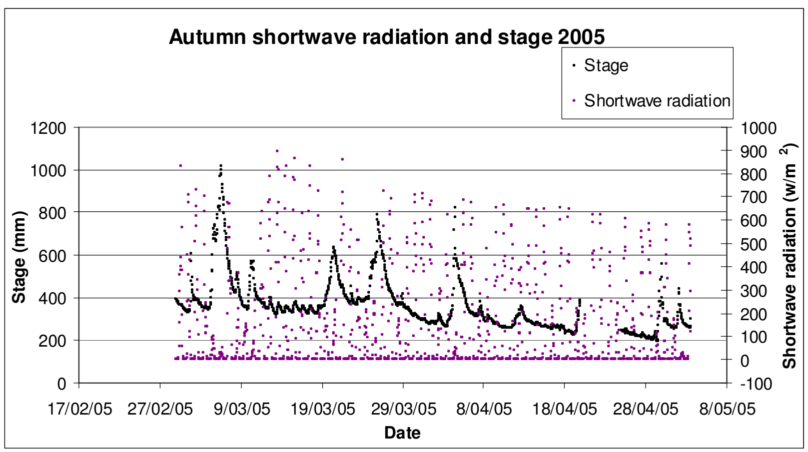


Figure 59c. Autumn stage and shortwave radiation 2005.

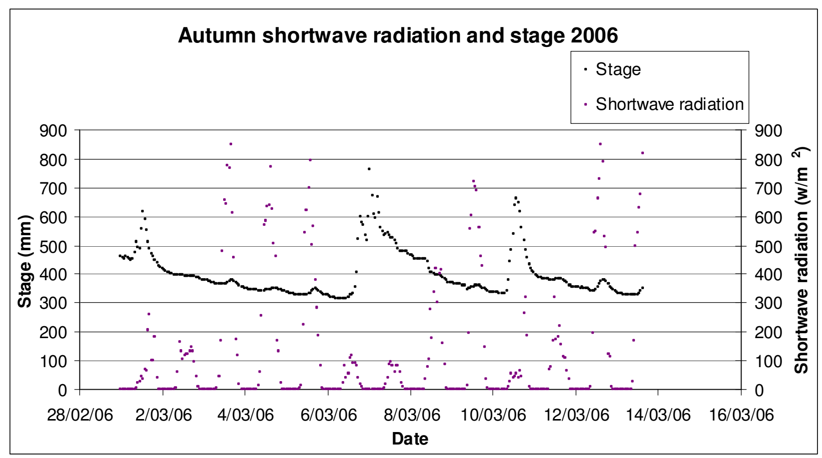


Figure 59d. Autumn stage and shortwave radiation 2006.

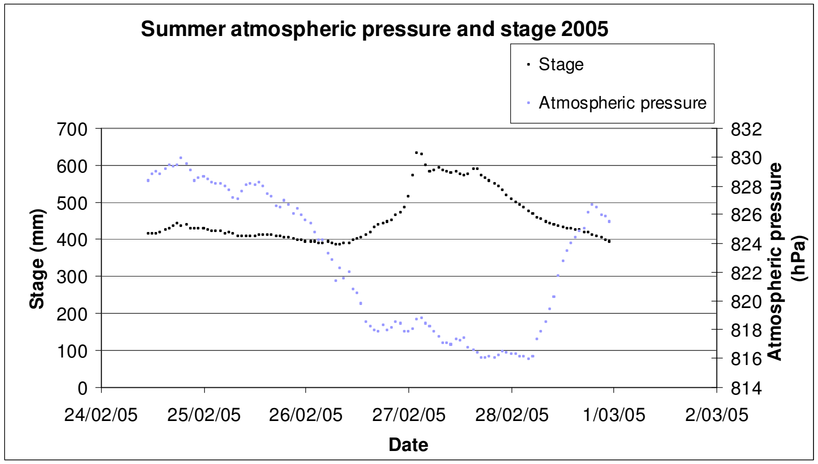


Figure 60a. Summer stage and atmospheric pressure 2005.

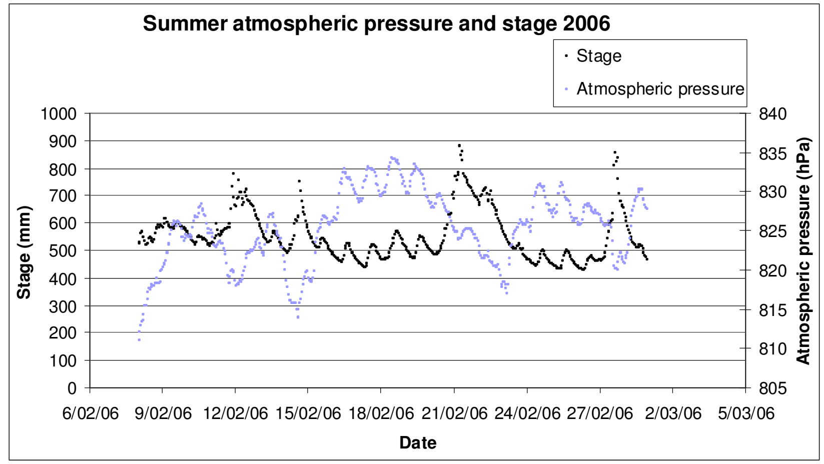


Figure 60b. Summer stage and atmospheric pressure 2006.

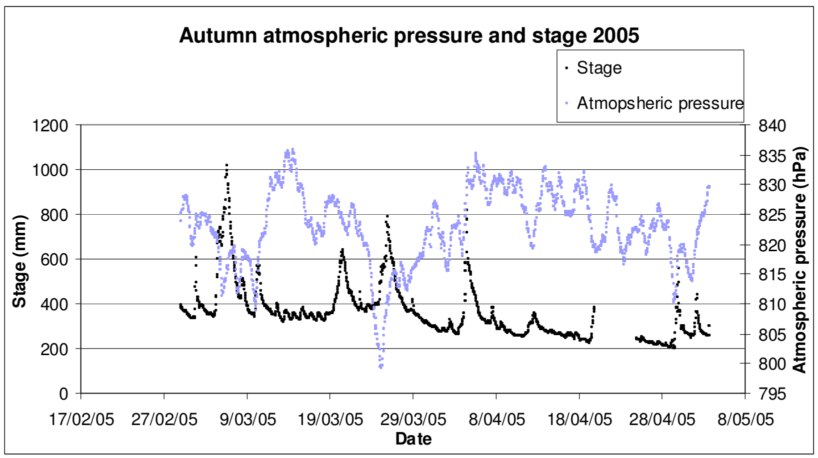


Figure 60c. Autumn stage and atmospheric pressure 2005.

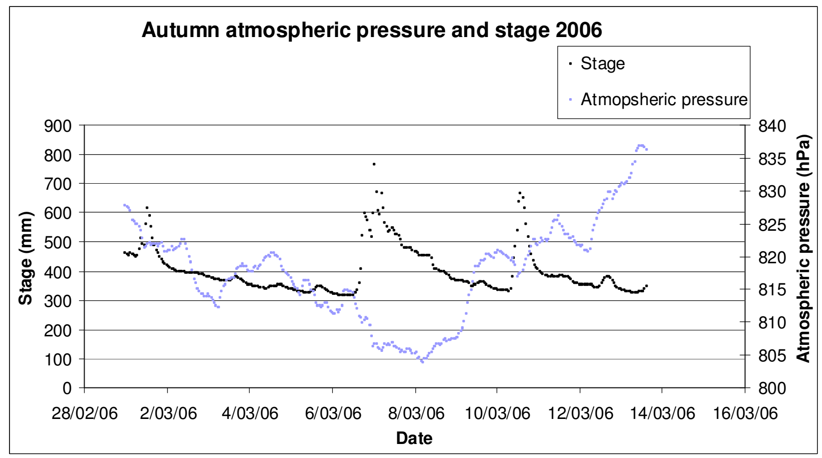


Figure 60d. Autumn stage and atmospheric pressure 2006.

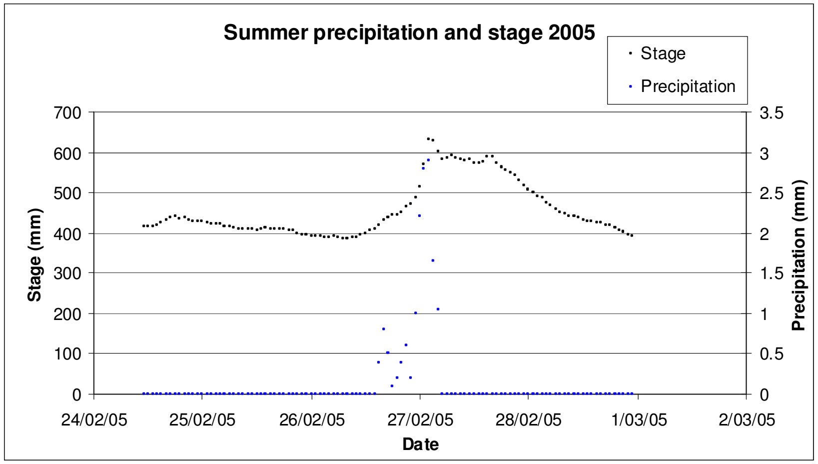


Figure 61a. Summer stage and precipitation 2005.

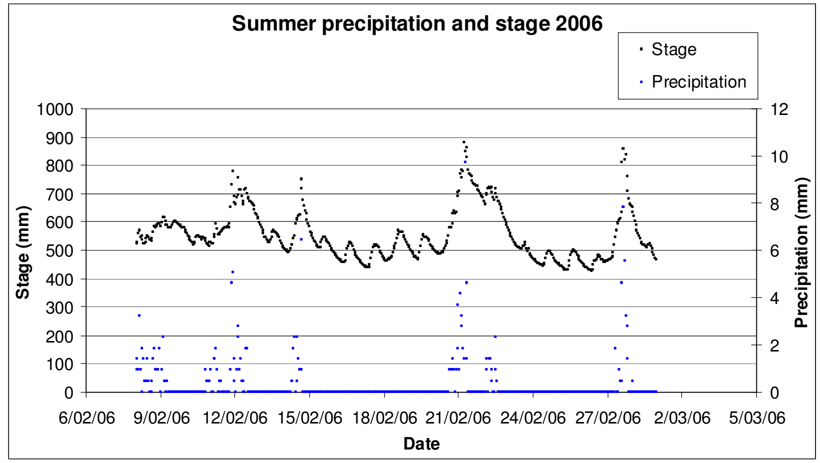


Figure 61b. Summer stage and precipitation 2006.

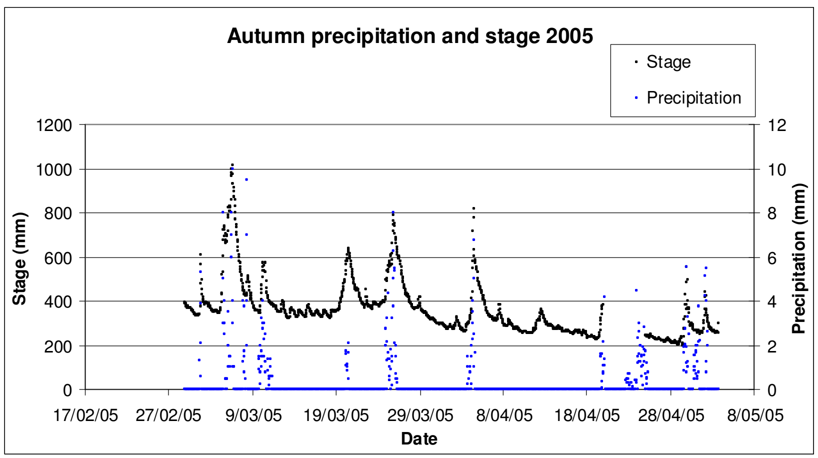


Figure 61c. Autumn stage and precipitation 2005.

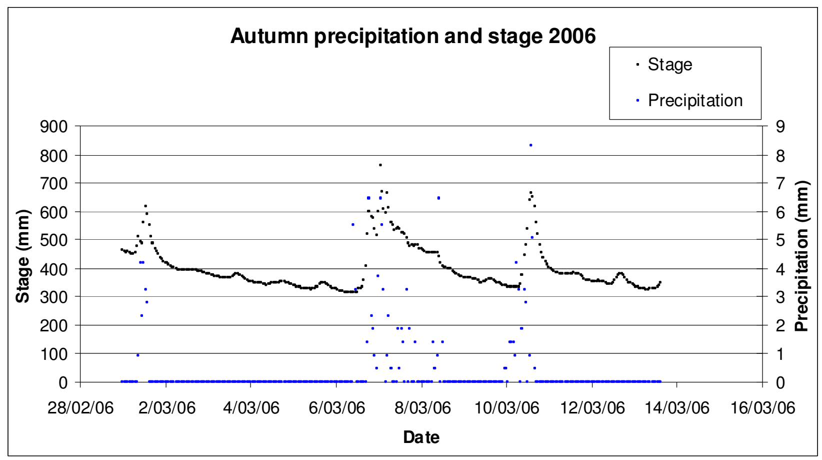


Figure 61d. Autumn stage and precipitation 2006.

# Chapter 3: Results

## *Section 8: Multiple regression models*

### 8.0 Method

Multiple regression models use a number of independent variables to predict the response in a given dependent variable, using the formula

$$y_i = ß_0 + ß_1 x_{i1} + ß_2 x_{i2} + \ldots + ß_p x_{ip} + \epsilon_i$$

**Eq. 3.8.1**

where y is the dependent variable, $ß_0$ the intercept, $ß_1$ through $ß_p$ the slope of the line for each independent variable, $x_1$ through $x_p$ the independent variables and $\epsilon_i$ the error term (or constant), all for case *I* (Gelman and Hill, 2007).

In a multi-dimensional representation of all the variables included, the model adjusts to find the best fit of all predictor lines acting together to give a response in the dependent variable. The output statistics are the best fit ß coefficients for each independent variable and the error term. The multiple regression analysis was carried out using SPSS v15 and all terminology and definitions used here are the same as given in the program.

'Enter' and 'stepwise' types of multiple regression models were employed. The 'enter' method includes all independent variables as dictated manually, giving only an indication of each variable's significance to the model in the accompanying statistics. The stepwise method creates a number of models in which independent variables are added sequentially according to a number of selection criteria. Firstly is the relative importance of each independent variable in predicting variation in the dependent variable, determined by the beta statistic. Secondly is the statistical significance of the contribution a variable makes to the model, and thirdly is the statistical soundness of a variable's contribution to the model (given by the VIF and tolerance statistics as measures of covariance, explained below). That is, the first model produced will include the one independent variable that contributes most to prediction of variation in the dependent variable where that contribution is also statistically significant. The next variable added will be chosen given its relative importance to prediction of variation in the dependent variable, its statistical significance and also the degree of covariance it has with the previous variable. In this way, subsequent models are built until the model that best fits all the criteria, of predictive power, statistical significance and statistical soundness, is complete.

Stage was again used in the multiple regression analysis to avoid any loss of detail by converting that data set into discharge. The 'enter' method produced higher adjusted $R^2$ values than the 'stepwise' method and was therefore used for producing black box predictive equations. The 'stepwise' method produced statistically sound models that could be used in diagnostic analysis.

Models were made for the full data set, for summer and autumn alone, and for each of these divided into periods of precipitation ("wet") and periods of no precipitation ("dry"), in order to tease out relationships between the atmospheric conditions and stage in different conditions.

### 8.1 Model assumptions

Multiple regression models make the following assumptions:

1. the model residuals have an approximately normal distribution, as shown in a P-P scatterplot of model residuals;
2. the model residuals have approximately constant variance, as shown by the scatterplot of studentised versus standardised predicted residuals;
3. the observations in each data set are internally independent (where internal dependence is known as *autocorrelation*); that is, each observation value is independent of the observation values around it, as shown by the Durban-Watson statistic;
4. each independent variable is unrelated to the others (where a linear relationship between independent variables is known as *covariance*); that is, each observation of a variable is independent of the observations of the other variables, as shown by the tolerance and VIF statistics.

Models were made only with daily total data. The hourly average models invariably exhibited too high a degree of autocorrelation in the independent variables to be valid. This is unsurprising. It is intuitively clear that the most important factor in determining the value of discharge 'now' is discharge a moment ago, a minute ago, an hour ago or even twelve hours ago. While water production is ultimately the result of atmospheric, ice and snow conditions, the nature of a stream is to flow moment to moment irrespective of the conditions, with short-term atmospheric variation taking time to be exhibited as streamflow. Short-term variation is furthermore superimposed upon the steadier, antecedent baseflow, and long-term environmental variation takes even longer to exhibit itself in streamflow and is then muted as a long-term trend. The degree to which flow is related hour by hour is too much for a multiple regression model. Even the daily total data did not uniformly meet the model criteria. In some cases, the degree of autocorrelation in the dependent variable was still too high. Fortunately, it was found that taking a random sample of 90%, 80%, 70% or 60% of the data corrected this problem (where this procedure has been employed it will be indicated in the model title as either 90%, 80%, 70% or 60%).

It was not possible to create valid models for summer dry periods. The full summer data set includes only 23 data points which when divided in two became non-normal and covariant and no solution for this was found. However, while this precluded diagnostic analysis of the variable relationships, the equation for prediction of stage was still valid as a black box result.

### 8.2 Statistics

The statistics used in this analysis are as follows (with definitions derived from SPSS v15):

**Adjusted $R^2$ ($AR^2$)**: The $R^2$ of the model adjusted for the number of independent variables.

**ANOVA:** The ANOVA statistics show how well the model accounts for variation in the dependent variable, where a value of significance below 0.05 indicates statistical significance in the model's predictive capacity.

**Durban-Watson (DW)**: The degree of autocorrelation of the dependent variable. This statistic is expressed as a value between 0 and 3, where values between 1.72 and 2.28 indicate no autocorrelation, values between 1.51 and 1.72 and between 2.28 and 2.49 indicate autocorrelation of low significance, and values below 1.51 or above 2.49 indicate significant autocorrelation.

**ß**: The gradient of the line of independent variables within the model.

**Beta**: The relative contribution of each variable to the model, where greater magnitude indicates greater importance.

**Sig**: The significance of the contribution of each variable to the model, where a value under 0.05 indicates statistical significance.

**Zero-order, partial and part correlations (Z, Pt, P)**: The correlation of an independent variable with the dependent variable where (respectively) 1. no other variables are held constant, 2. one other variable is held constant, and 3. more than one other variable is held constant, giving an indication of actual correlation between the dependent and independent variables.

**Tolerance**: A value between 0 and 1 that indicates the degree of covariance of the independent variables, where a value of 0.2 for example indicates that 80% of the variation in the dependent variable that is explained by the given independent variable is also explained by other variables in the model, and vice versa in the case of a value of 0.8.

**VIF**: A statistic indicating the significance of covariance, where a value above 2 indicates unacceptability.

## 8.3 Results

### 8.31 Linear multiple regression models

In all the models stage is the dependent variable and the independent variables (predictors) are as follows, all in daily total:

T – temperature (°C)
H – relative humidity (%)
W – wind speed (m/s)
S – shortwave radiation (W/m$^2$)
P – atmospheric pressure (hPa)
R – precipitation (mm)

For the 'enter' models used to create predictive equations for stage the adjusted $R^2$ value, ANOVA statistics and equation are presented, followed by plots of predicted and measured stage. The autocorrelation and covariance statistics and the model parameters for included and excluded variables are presented for the 'stepwise' models. The 'goodness-of-fit' statistics, normal p-p plots for residuals and scatterplots of studentised residuals versus standardised predicted residuals for each 'stepwise' model are in Appendix 2. There is a high degree of covariance between the wind speed and precipitation data sets (which will be examined in Chapter 4) so in some cases two models were made, one in which all variables were input and one in which wind speed was manually excluded.

As mentioned above, no valid model for summer dry periods was created. A number of 'enter' type models were made in order to ascertain the source of the problem in this data set, the statistics for which are shown here.

### Model Aa: Full data 60% 'stepwise'

**Model 5 adjusted $R^2$ 0.612**

**Table 15: Autocorrelation and Covariance statistics for model Aa**

| **Durban-Watson** | | 1.509 | **Covariance Statistics** | |
|---|---|---|---|---|
| **Model** | | | Tolerance | VIF |
| **1** | Relative humidity | | 1.000 | 1.000 |
| **2** | Relative humidity | | .993 | 1.007 |
| | Air temperature | | .993 | 1.007 |
| **3** | Relative humidity | | .974 | 1.027 |
| | Air temperature | | .975 | 1.026 |
| | Wind Speed | | .960 | 1.042 |
| **4** | Relative humidity | | .622 | 1.607 |
| | Air temperature | | .884 | 1.131 |
| | Wind Speed | | .840 | 1.191 |
| | Shortwave radiation | | .500 | 2.000 |
| **5** | Relative humidity | | .589 | 1.699 |
| | Air temperature | | .884 | 1.132 |
| | Wind Speed | | .540 | 1.852 |
| | Shortwave radiation | | .448 | 2.233 |
| | Precipitation | | .396 | 2.525 |

**Table 16: Model parameters and coefficients for model Aa: Full data 60% 'stepwise'.**

| Model | | Unstandardized Coefficients | | Standardized Coefficients | | | 95% Confidence Interval for B | | Correlations | | |
|---|---|---|---|---|---|---|---|---|---|---|---|
| | | B | Std. Error | Beta | t | Sig. | Lower Bound | Upper Bound | Zero-order | Partial | Part |
| 1 | (Constant) | 1302.234 | 1713.466 | | .760 | .450 | -2120.809 | 4725.277 | | | |
| | Relative humidity | 4.363 | .856 | .538 | 5.099 | .000 | 2.654 | 6.073 | .538 | .538 | .538 |
| 2 | (Constant) | -992.860 | 1605.571 | | -.618 | .539 | -4201.337 | 2215.618 | | | |
| | Relative humidity | 4.645 | .760 | .572 | 6.114 | .000 | 3.127 | 6.163 | .538 | .610 | .570 |
| | Air temperature | 16.111 | 3.717 | .406 | 4.334 | .000 | 8.683 | 23.540 | .357 | .479 | .404 |
| 3 | (Constant) | -2809.422 | 1584.365 | | -1.773 | .081 | -5976.523 | 357.679 | | | |
| | Relative humidity | 4.315 | .711 | .531 | 6.065 | .000 | 2.892 | 5.737 | .538 | .610 | .524 |
| | Air temperature | 17.687 | 3.479 | .445 | 5.084 | .000 | 10.732 | 24.641 | .357 | .542 | .440 |
| | Wind Speed | 28.642 | 8.538 | .296 | 3.355 | .001 | 11.575 | 45.708 | .310 | .392 | .290 |
| 4 | (Constant) | -8068.840 | 2301.686 | | -3.506 | .001 | -12671.345 | -3466.335 | | | |
| | Relative humidity | 5.824 | .837 | .717 | 6.954 | .000 | 4.149 | 7.498 | .538 | .665 | .566 |
| | Air temperature | 14.548 | 3.437 | .366 | 4.232 | .000 | 7.674 | 21.421 | .357 | .476 | .344 |
| | Wind Speed | 37.765 | 8.591 | .390 | 4.396 | .000 | 20.585 | 54.945 | .310 | .490 | .358 |
| | Shortwave radiation | .631 | .210 | .345 | 3.000 | .004 | .210 | 1.052 | -.120 | .359 | .244 |
| 5 | (Constant) | -6904.621 | 2224.057 | | -3.105 | .003 | -11353.398 | -2455.844 | | | |
| | Relative humidity | 5.294 | .817 | .652 | 6.478 | .000 | 3.660 | 6.929 | .538 | .642 | .500 |
| | Air temperature | 14.322 | 3.263 | .361 | 4.389 | .000 | 7.794 | 20.849 | .357 | .493 | .339 |
| | Wind Speed | 20.866 | 10.169 | .216 | 2.052 | .045 | .525 | 41.207 | .310 | .256 | .158 |
| | Shortwave radiation | .821 | .211 | .449 | 3.890 | .000 | .399 | 1.243 | -.120 | .449 | .300 |
| | Precipitation | 83.504 | 30.029 | .341 | 2.781 | .007 | 23.437 | 143.571 | .439 | .338 | .215 |

**Table 17: Excluded variables for model Aa: Full data 60% 'stepwise'.**

| Model | | Beta In | t | Sig. | Partial Correlation | Tolerance | VIF |
|---|---|---|---|---|---|---|---|
| 1 | Air temperature | .406 | 4.334 | .000 | .479 | .993 | 1.007 |
| | Wind Speed | .236 | 2.281 | .026 | .276 | .978 | 1.023 |
| | Shortwave radiation | .315 | 2.486 | .016 | .299 | .642 | 1.559 |
| | Atmospheric pressure | -.147 | -1.353 | .181 | -.168 | .926 | 1.080 |
| | Hourly rainfall | .248 | 2.165 | .034 | .263 | .800 | 1.251 |
| 2 | Wind Speed | .296 | 3.355 | .001 | .392 | .960 | 1.042 |
| | Shortwave radiation | .166 | 1.356 | .180 | .170 | .572 | 1.749 |
| | Atmospheric pressure | -.213 | -2.241 | .029 | -.274 | .906 | 1.104 |
| | Hourly rainfall | .322 | 3.282 | .002 | .385 | .782 | 1.279 |
| 3 | Shortwave radiation | .345 | 3.000 | .004 | .359 | .500 | 2.000 |
| | Atmospheric pressure | -.138 | -1.474 | .146 | -.185 | .835 | 1.198 |
| | Hourly rainfall | .187 | 1.451 | .152 | .183 | .442 | 2.261 |
| 4 | Atmospheric pressure | -.151 | -1.724 | .090 | -.217 | .833 | 1.201 |
| | Hourly rainfall | .341 | 2.781 | .007 | .338 | .396 | 2.525 |
| 5 | Atmospheric pressure | -.107 | -1.247 | .217 | -.160 | .797 | 1.254 |

# Model Ab: Full data 'enter' – derived from model Aa

**Table 18: ANOVA for model Ab**

| Model | | Sum of Squares | df | Mean Square | F | Sig. |
|---|---|---|---|---|---|---|
| 1 | Regression | 586995477.470 | 6 | 97832579.578 | 28.103 | .000 |
| | Residual | 323747973.588 | 93 | 3481161.006 | | |
| | Total | 910743451.059 | 99 | | | |

**Table 19: Adjusted R2 and equation for stage for model Ab**

| |
|---|
| **Adjusted $R^2$** 0.622 |
| **Equation**: $y = 14.958T + 4.681H + 10.927W + 0.871S – 0.695P + 115.576R + 8226.321$ **Eq. 3.8.2** |

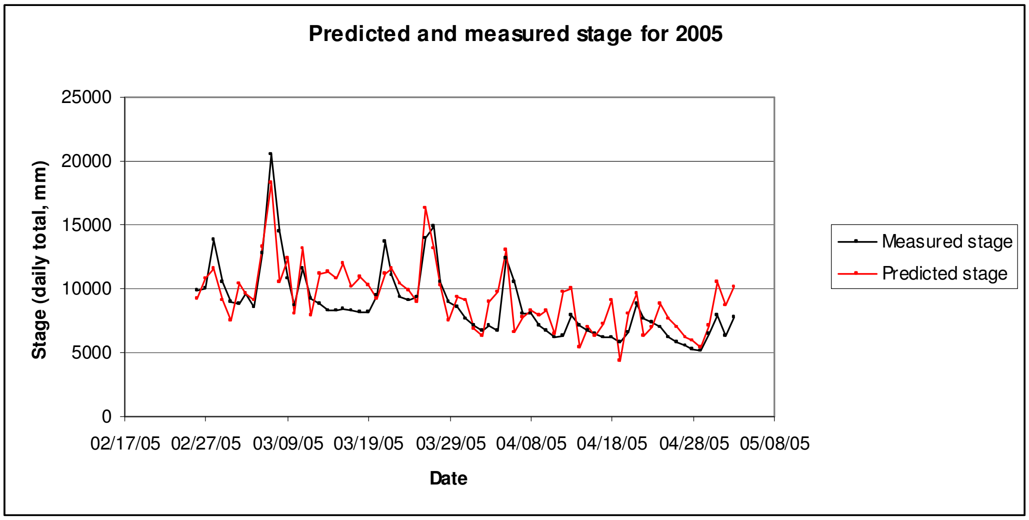


**Figure 62. Measured stage and predicted stage for 2005 from model Ab.**

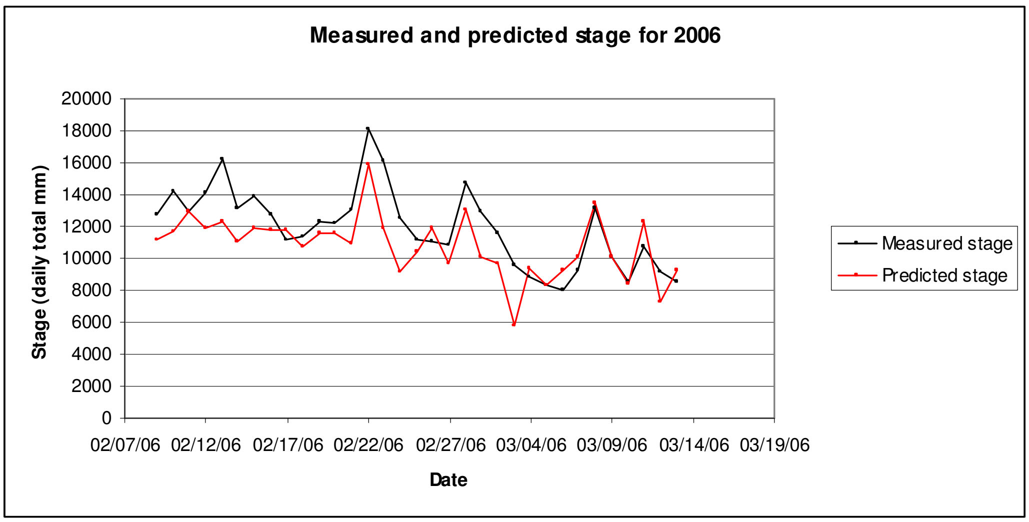


**Figure 63. Measured and predicted stage for 2006 from model Ab.**

## Model Ba: Summer 90% 'stepwise'

**Adjusted $R^2$ 0.726**

**Table 20: Autocorrelation and Covariance statistics for model Ba**

| **Durban-Watson** | | 1.647 | **Covariance Statistics** | |
|---|---|---|---|---|
| **Model** | | | Tolerance | VIF |
| **1** | Wind Speed | | 1.000 | 1.000 |

**Table 21: Model parameters for model Ba: Summer 90% ‘stepwise’**

| Model | | Unstandardized Coefficients | | Standardized Coefficients | | | 95% Confidence Interval for B | | Correlations | | |
|---|---|---|---|---|---|---|---|---|---|---|---|
| | | **B** | **Std. Error** | **Beta** | **t** | **Sig.** | **Lower Bound** | **Upper Bound** | **Zero-order** | **Partial** | **Part** |
| **1** | (Constant) | 7585.011 | 734.782 | | 10.323 | .000 | 6052.283 | 9117.738 | | | |
| | Wind Speed | 73.641 | 9.794 | .859 | 7.519 | .000 | 53.211 | 94.071 | .859 | .859 | .859 |

**Table 22: Excluded variables for model Ba: Summer 90% ‘stepwise’.**

| Model | | Beta In | t | Sig. | Partial Correlation | Tolerance | VIF |
|---|---|---|---|---|---|---|---|
| **1** | Air temperature | .095 | .815 | .425 | .184 | .986 | 1.015 |
| | Relative humidity | .089 | .631 | .536 | .143 | .674 | 1.483 |
| | Shortwave radiation | .159 | 1.079 | .294 | .240 | .596 | 1.677 |
| | Atmospheric pressure | .015 | .132 | .897 | .030 | .993 | 1.008 |
| | Precipitation | .276 | 1.514 | .147 | .328 | .370 | 2.706 |

## Model Bb: Summer 'enter'

**Table 23: ANOVA for model Bb**

| Model | | Sum of Squares | df | Mean Square | F | Sig. |
|---|---|---|---|---|---|---|
| 1 | Regression | 85521649.038 | 6 | 14253608.173 | 23.117 | .000 |
| | Residual | 9865373.220 | 16 | 616585.826 | | |
| | Total | 95387022.258 | 22 | | | |

**Table 24: Adjusted R2 and equation for stage for model Bb**

| |
|---|
| **Adjusted $R^2$** 0.858 |
| **Equation:** $y = 2.926T + 4.397H + 60.257W + 0.811S + 0.715P + 79.624R - 18762.603$ **Eq. 3.8.3** |

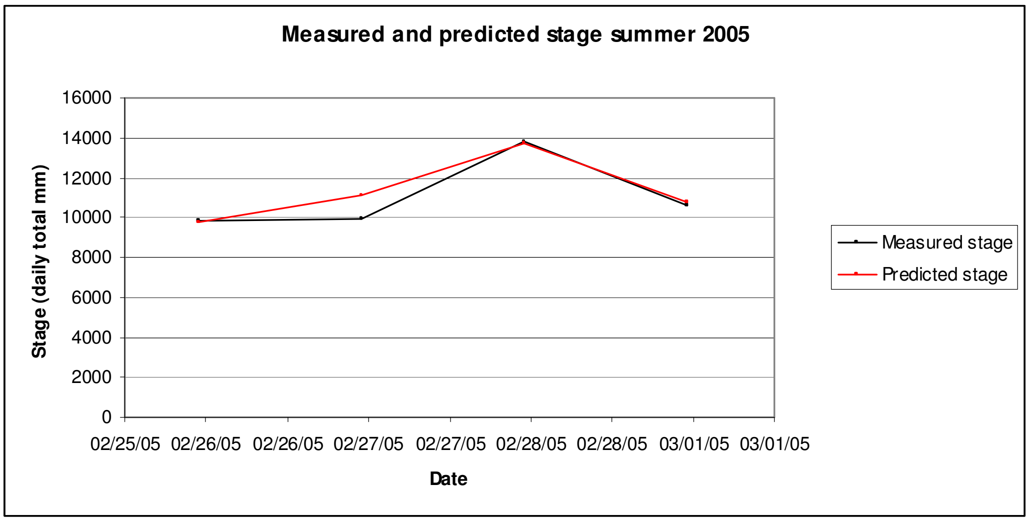


**Figure 64. Measured and predicted stage for summer 2005 from model Bb.**

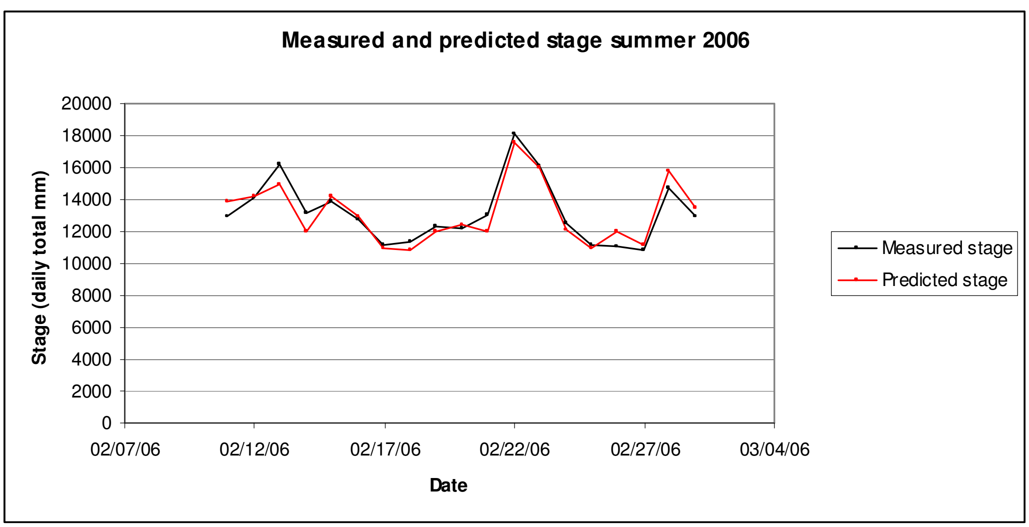


**Figure 65. Measured and predicted stage for summer 2006 from model Bb.**

## Model Ca: Autumn 60% 'stepwise'

**Model 4 adjusted R2 0.572**

**Table 25: Autocorrelation and Covariance statistics for model Ca**

| **Durban-Watson** | 1.554 | **Covariance Statistics** | |
|---|---|---|---|
| **Model** | | Tolerance | VIF |
| **1** | Precipitation | 1.000 | 1.000 |
| **2** | Precipitation | .975 | 1.025 |
| | Air temperature | .975 | 1.025 |
| **3** | Precipitation | .804 | 1.243 |
| | Air temperature | .966 | 1.035 |
| | Relative humidity | .805 | 1.243 |
| **4** | Precipitation | .611 | 1.636 |
| | Air temperature | .964 | 1.037 |
| | Relative humidity | .669 | 1.494 |
| | Shortwave radiation | .517 | 1.933 |

**Table 26: Model parameters and coefficients for model Ca: Autumn 60% 'stepwise'**

| Model | | Unstandardized Coefficients | | Standardized Coefficients | | | 95% Confidence Interval for B | | Correlations | | |
|---|---|---|---|---|---|---|---|---|---|---|---|
| | | B | Std. Error | Beta | t | Sig. | Lower Bound | Upper Bound | Zero-order | Partial | Part |
| 1 | (Constant) | 7912.284 | 362.658 | | 21.817 | .000 | 7183.110 | 8641.458 | | | |
| | Precipitation | 112.970 | 20.710 | .619 | 5.455 | .000 | 71.330 | 154.610 | .619 | .619 | .619 |
| 2 | (Constant) | 6805.186 | 514.223 | | 13.234 | .000 | 5770.703 | 7839.669 | | | |
| | Precipitation | 121.725 | 19.558 | .667 | 6.224 | .000 | 82.379 | 161.071 | .619 | .672 | .658 |
| | Air temperature | 11.061 | 3.869 | .306 | 2.859 | .006 | 3.277 | 18.845 | .202 | .385 | .302 |
| 3 | (Constant) | 2259.668 | 1671.520 | | 1.352 | .183 | -1104.928 | 5624.263 | | | |
| | Precipitation | 97.854 | 20.082 | .536 | 4.873 | .000 | 57.430 | 138.278 | .619 | .583 | .481 |
| | Air temperature | 12.080 | 3.626 | .334 | 3.332 | .002 | 4.782 | 19.378 | .202 | .441 | .329 |
| | Relative humidity | 2.423 | .854 | .312 | 2.839 | .007 | .705 | 4.141 | .492 | .386 | .280 |
| 4 | (Constant) | -1295.574 | 2132.586 | | -.608 | .547 | -5590.823 | 2999.675 | | | |
| | Precipitation | 124.519 | 21.839 | .682 | 5.702 | .000 | 80.532 | 168.505 | .619 | .648 | .533 |
| | Air temperature | 11.737 | 3.439 | .325 | 3.413 | .001 | 4.810 | 18.665 | .202 | .453 | .319 |
| | Relative humidity | 3.329 | .887 | .429 | 3.753 | .000 | 1.543 | 5.116 | .492 | .488 | .351 |
| | Shortwave radiation | .594 | .239 | .324 | 2.490 | .017 | .114 | 1.075 | -.283 | .348 | .233 |

**Table 27: Excluded variables for mode Ca: Autumn 60% 'stepwise'.**

| Model | | Beta In | t | Sig. | Partial Correlation | Tolerance | VIF | Minimum Tolerance |
|---|---|---|---|---|---|---|---|---|
| **1** | Air temperature | .306 | 2.859 | .006 | .385 | .975 | 1.025 | .975 |
| | Relative humidity | .276 | 2.287 | .027 | .316 | .813 | 1.231 | .813 |
| | Wind Speed | .181 | 1.014 | .316 | .146 | .404 | 2.474 | .404 |
| | Shortwave radiation | .152 | 1.064 | .293 | .153 | .626 | 1.598 | .626 |
| | Atmospheric pressure | -.199 | -1.666 | .102 | -.236 | .866 | 1.155 | .866 |
| **2** | Relative humidity | .312 | 2.839 | .007 | .386 | .805 | 1.243 | .804 |
| | Wind Speed | .093 | .546 | .588 | .080 | .389 | 2.568 | .380 |
| | Shortwave radiation | .124 | .920 | .362 | .134 | .622 | 1.608 | .622 |
| | Atmospheric pressure | -.185 | -1.656 | .105 | -.237 | .864 | 1.157 | .843 |
| **3** | Wind Speed | .167 | 1.044 | .302 | .154 | .380 | 2.631 | .324 |
| | Shortwave radiation | .324 | 2.490 | .017 | .348 | .517 | 1.933 | .517 |
| | Atmospheric pressure | -.089 | -.782 | .438 | -.116 | .755 | 1.325 | .703 |
| **4** | Wind Speed | .204 | 1.352 | .183 | .200 | .377 | 2.655 | .300 |
| | Atmospheric pressure | -.135 | -1.242 | .221 | -.184 | .736 | 1.359 | .505 |

## Model Cb: Autumn 'enter'

**Table 28: ANOVA for model Cb.**

| Model | | Sum of Squares | df | Mean Square | F | Sig. |
|---|---|---|---|---|---|---|
| 1 | Regression | 344298956.591 | 6 | 57383159.432 | 20.431 | .000 |
| | Residual | 196603047.476 | 70 | 2808614.964 | | |
| | Total | 540902004.067 | 76 | | | |

**Table 29: Adjusted R2 and equation for autumn stage for model Cb.**

| |
|---|
| **Adjusted $R^2$** 0.605 |
| **Equation:** $y = 12.010T + 3.238H + 8.853W + 0.603S - 1.906P + 103.357R + 35758.874$ **Eq. 3.8.4** |

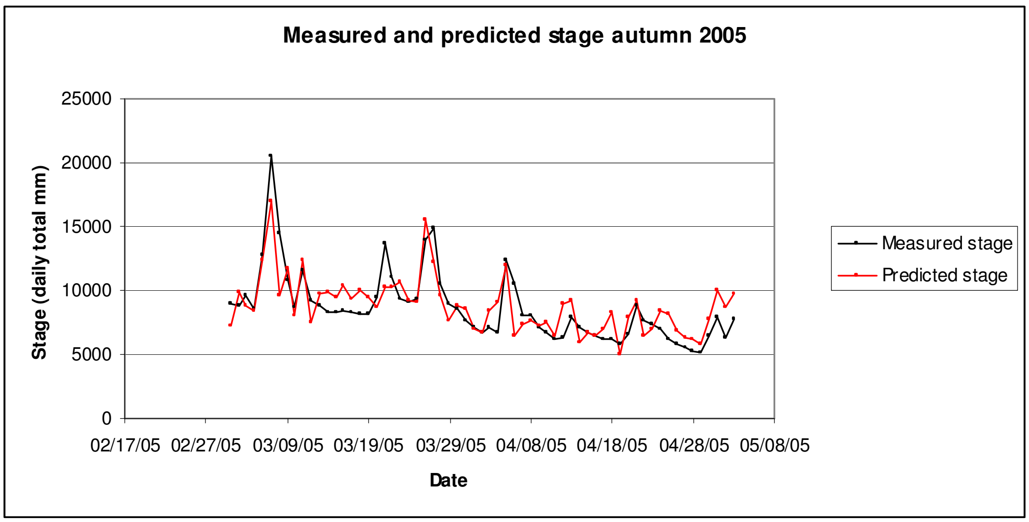


**Figure 66. Measured and predicted stage autumn 2005 from model Cb.**

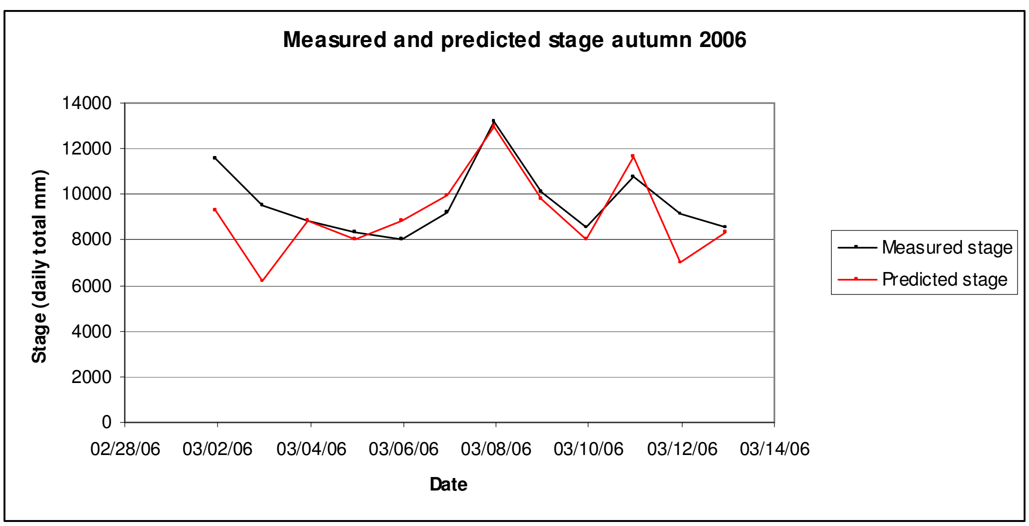


**Figure 67. Measured and predicted stage autumn 2006 from model Cb.**

## Model D: Full data wet 'stepwise'

**Model 4 adjusted R2 0.748**

**Table 30: Autocorrelation and Covariance statistics for model D**

| **Durban-Watson** | | 1.982 | **Covariance Statistics** | |
|---|---|---|---|---|
| **Model** | | | Tolerance | VIF |
| **1** | Air temperature | | 1.000 | 1.000 |
| **2** | Air temperature | | .940 | 1.064 |
| | Relative humidity | | .940 | 1.064 |
| **3** | Air temperature | | .932 | 1.073 |
| | Relative humidity | | .796 | 1.257 |
| | Precipitation | | .847 | 1.181 |
| **4** | Air temperature | | .910 | 1.098 |
| | Relative humidity | | .640 | 1.563 |
| | Precipitation | | .660 | 1.516 |
| | Shortwave radiation | | .536 | 1.865 |

**Table 31: Model parameters and coefficients for model D: Full data wet 'stepwise'**

| Model | | Unstandardized Coefficients | | Standardized Coefficients | | | 95% Confidence Interval for B | | Correlations | | |
|---|---|---|---|---|---|---|---|---|---|---|---|
| | | **B** | **Std. Error** | **Beta** | **t** | **Sig.** | **Lower Bound** | **Upper Bound** | **Zero-order** | **Partial** | **Part** |
| **1** | (Constant) | 8702.284 | 632.926 | | 13.749 | .000 | 7424.065 | 9980.504 | | | |
| | Air temperature | 28.561 | 5.327 | .642 | 5.361 | .000 | 17.803 | 39.320 | .642 | .642 | .642 |
| **2** | (Constant) | -4332.578 | 3502.928 | | -1.237 | .223 | -11412.259 | 2747.103 | | | |
| | Air temperature | 24.138 | 4.780 | .543 | 5.050 | .000 | 14.478 | 33.798 | .642 | .624 | .526 |
| | Relative humidity | 6.198 | 1.645 | .405 | 3.768 | .001 | 2.874 | 9.523 | .538 | .512 | .392 |
| **3** | (Constant) | -2087.548 | 3441.091 | | -.607 | .548 | -9047.812 | 4872.716 | | | |
| | Air temperature | 25.132 | 4.537 | .565 | 5.539 | .000 | 15.955 | 34.310 | .642 | .664 | .545 |
| | Relative humidity | 4.611 | 1.690 | .301 | 2.729 | .009 | 1.193 | 8.029 | .538 | .400 | .269 |
| | Precipitation | 62.409 | 26.006 | .257 | 2.400 | .021 | 9.806 | 115.012 | .379 | .359 | .236 |
| **4** | (Constant) | -12453.772 | 3409.996 | | -3.652 | .001 | -19356.947 | -5550.596 | | | |
| | Air temperature | 22.391 | 3.612 | .503 | 6.199 | .000 | 15.079 | 29.703 | .642 | .709 | .480 |
| | Relative humidity | 7.892 | 1.483 | .515 | 5.323 | .000 | 4.890 | 10.894 | .538 | .654 | .412 |
| | Precipitation | 116.852 | 23.178 | .481 | 5.041 | .000 | 69.931 | 163.774 | .379 | .633 | .391 |
| | Shortwave radiation | 1.252 | .250 | .529 | 5.000 | .000 | .745 | 1.759 | -.020 | .630 | .387 |

**Table 32: Excluded variables for Model D: Full data wet 'stepwise'.**

| Model | | Beta In | t | Sig. | Partial Correlation | Tolerance | VIF |
|---|---|---|---|---|---|---|---|
| **1** | Relative humidity | .405 | 3.768 | .001 | .512 | .940 | 1.064 |
| | Wind Speed | .375 | 3.540 | .001 | .488 | 1.000 | 1.000 |
| | Shortwave radiation | -.028 | -.228 | .821 | -.036 | 1.000 | 1.000 |
| | Atmospheric pressure | -.125 | -1.033 | .308 | -.161 | .986 | 1.015 |
| | Hourly rainfall | .371 | 3.497 | .001 | .484 | 1.000 | 1.000 |
| **2** | Wind Speed | .249 | 2.248 | .030 | .339 | .802 | 1.247 |
| | Shortwave radiation | .278 | 2.338 | .025 | .351 | .688 | 1.453 |
| | Atmospheric pressure | -.029 | -.265 | .793 | -.042 | .926 | 1.080 |
| | Hourly rainfall | .257 | 2.400 | .021 | .359 | .847 | 1.181 |
| **3** | Wind Speed | .107 | .588 | .560 | .095 | .296 | 3.374 |
| | Shortwave radiation | .529 | 5.000 | .000 | .630 | .536 | 1.865 |
| | Atmospheric pressure | .015 | .141 | .888 | .023 | .897 | 1.115 |
| **4** | Wind Speed | .119 | .833 | .410 | .136 | .296 | 3.375 |
| | Atmospheric pressure | -.041 | -.489 | .628 | -.080 | .881 | 1.135 |

**Model E: Full data dry 60% 'stepwise'**

**Model 2 adjusted R2 0.478**

**Table 33: Autocorrelation and Covariance statistics for model E.**

| **Durban-Watson** | | 1.620 | **Covariance Statistics** | |
|---|---|---|---|---|
| **Model** | | | Tolerance | VIF |
| **1** | Shortwave radiation | | 1.000 | 1.000 |
| **2** | Shortwave radiation | | .810 | 1.234 |
| | RH % | | .810 | 1.234 |

**Table 34: Parameters for model E: Full data dry 60% 'stepwise'**

| Model | | Unstandardized Coefficients | | Standardized Coefficients | | | 95% Confidence Interval for B | | Correlations | | |
|---|---|---|---|---|---|---|---|---|---|---|---|
| | | **B** | **Std. Error** | **Beta** | **t** | **Sig.** | **Lower Bound** | **Upper Bound** | **Zero-order** | **Partial** | **Part** |
| **1** | (Constant) | 6348.242 | 911.980 | | 6.961 | .000 | 4490.599 | 8205.885 | | | |
| | Shortwave radiation | .613 | .210 | .459 | 2.919 | .006 | .185 | 1.041 | .459 | .459 | .459 |
| **2** | (Constant) | -106.472 | 1753.334 | | -.061 | .952 | -3682.422 | 3469.477 | | | |
| | Shortwave radiation | .952 | .191 | .712 | 4.977 | .000 | .562 | 1.343 | .459 | .666 | .641 |
| | Relative humidity | 2.818 | .692 | .583 | 4.070 | .000 | 1.406 | 4.229 | .272 | .590 | .524 |

**Table 35: Excluded variables for model E: Full data dry 60% 'stepwise'**

| Model | | Beta In | t | Sig. | Partial Correlation | Tolerance | VIF | Minimum Tolerance |
|---|---|---|---|---|---|---|---|---|
| 1 | Air temperature | .190 | 1.125 | .269 | .198 | .858 | 1.166 | .858 |
| | Relative humidity | .583 | 4.070 | .000 | .590 | .810 | 1.234 | .810 |
| | Wind Speed | -.130 | -.820 | .419 | -.146 | .998 | 1.002 | .998 |
| | Atmospheric pressure | -.075 | -.468 | .643 | -.084 | .994 | 1.006 | .994 |
| 2 | Air temperature | .252 | 1.870 | .071 | .323 | .848 | 1.179 | .734 |
| | Wind Speed | .089 | .627 | .536 | .114 | .846 | 1.182 | .687 |
| | Atmospheric pressure | .003 | .022 | .983 | .004 | .972 | 1.028 | .793 |

## Model Fa: Summer wet 'stepwise'

**Adjusted R2 0.550**

**Table 36: Autocorrelation and Covariance statistics for model Fa.**

| **Durban-Watson** | | 1.693 | **Covariance Statistics** | |
|---|---|---|---|---|
| **Model** | | | Tolerance | VIF |
| **1** | Wind Speed | | 1.000 | 1.000 |

**Table 37: Parameters for model Fa: Summer wet 'stepwise'.**

| Model | | Unstandardized Coefficients | | Standardized Coefficients | | | 95% Confidence Interval for B | | Correlations | | |
|---|---|---|---|---|---|---|---|---|---|---|---|
| | | **B** | **Std. Error** | **Beta** | **t** | **Sig.** | **Lower Bound** | **Upper Bound** | **Zero-order** | **Partial** | **Part** |
| **1** | (Constant) | 6996.889 | 1820.866 | | 3.843 | .003 | 2989.191 | 11004.588 | | | |
| | Wind Speed | 80.395 | 20.294 | .767 | 3.961 | .002 | 35.727 | 125.062 | .767 | .767 | .767 |

**Table 38: Excluded variables for model Fa: Summer wet 'stepwise'.**

| **Model** | | **Beta In** | **t** | **Sig.** | **Partial Correlation** | **Tolerance** | **VIF** |
|---|---|---|---|---|---|---|---|
| **1** | Air temperature | .382 | 2.038 | .069 | .542 | .827 | 1.210 |
| | Relative humidity | .250 | 1.285 | .228 | .376 | .938 | 1.067 |
| | Shortwave radiation | .014 | .068 | .947 | .021 | .967 | 1.034 |
| | Atmospheric pressure | .134 | .675 | .515 | .209 | .995 | 1.005 |
| | Precipitation | .204 | .857 | .412 | .262 | .679 | 1.473 |

## <u>Model Fb: Summer wet 'stepwise' (excluding wind speed)</u>

**Adjusted $R^2$ 0.267**

**Table 39: Autocorrelation and covariance statistics for model Fb.**

| **Durban-Watson** 1.956 | | **Covariance Statistics** | |
|---|---|---|---|
| **Model** | | Tolerance | VIF |
| **1** | Precipitation | 1.000 | 1.000 |

**Table 40: Parameters for model Fb: Summer wet 'stepwise' excluding wind speed**

| Model | | Unstandardized Coefficients | | Standardized Coefficients | | | 95% Confidence Interval for B | | Correlations | | |
|---|---|---|---|---|---|---|---|---|---|---|---|
| | | B | Std. Error | Beta | t | Sig. | Lower Bound | Upper Bound | Zero-order | Partial | Part |
| 1 | (Constant) | 12561.213 | 802.365 | | 15.655 | .000 | 10795.220 | 14327.206 | | | |
| | Hourly rainfall | 109.946 | 47.446 | .573 | 2.317 | .041 | 5.518 | 214.374 | .573 | .573 | .573 |

**Table 41: Excluded variables for model Fb: Summer wet 'stepwise' excluding wind speed.**

| Model | | Beta In | t | Sig. | Partial Correlation | Tolerance | VIF | Minimum Tolerance |
|---|---|---|---|---|---|---|---|---|
| 1 | Air temperature | .001 | .003 | .998 | .001 | 1.000 | 1.000 | 1.000 |
| | Relative humidity | .161 | .526 | .611 | .164 | .701 | 1.426 | .701 |
| | Shortwave radiation | .389 | 1.254 | .238 | .369 | .604 | 1.655 | .604 |
| | Atmospheric pressure | .395 | 1.637 | .133 | .460 | .908 | 1.101 | .908 |

## Model G: Summer dry 'stepwise'

This model produced no results. The significance of the independent variables was too low for any to be entered using the stepwise method, and no valid model could be created using the 'enter' method. The following table shows the adjusted $R^2$ value and significance values for various enter-type models, showing the source of this lack of validity.

**Table 42: Adjusted $R^2$, values of significance and covariance for the summer dry data set enter-type models.**

| | **Independent variable input** | **Variable significance** | **VIF** |
|---|---|---|---|
| **Model 1** | Air temperature | 0.441 | 1.386 |
| **Adjusted R2 0.548** | Relative humidity | 0.024 | 2.957 |
| **ANOVA sig. 0.073** | Wind speed | 0.028 | 1.195 |
| | Shortwave radiation | 0.014 | 2.688 |
| | Atmospheric pressure | 0.655 | 1.282 |
| **Model 2** | | | |
| **Adjusted R2 0.589** | Shortwave radiation | 0.009 | 2.848 |
| **ANOVA sig. 0.017** | Relative humidity | 0.018 | 2.529 |
| | Wind speed | 0.014 | 1.041 |
| **Model 3** | | | |
| **Adjusted R2 0.181** | Wind speed | 0.094 | 1.000 |
| **ANOVA sig. 0.094** | | | |

## Model H: Autumn wet 'stepwise'

**Model 6 adjusted R2 0.741**

**Table 43: Autocorrelation and covariance statistics for model H.**

| Durban-Watson 2.201 | | Covariance Statistics | |
|---|---|---|---|
| **Model** | | Tolerance | VIF |
| **1** | Wind speed | 1.000 | 1.000 |
| **2** | Wind speed | .954 | 1.049 |
| | Air temperature | .954 | 1.049 |
| **3** | Wind speed | .561 | 1.782 |
| | Air temperature | .945 | 1.059 |
| | Shortwave radiation | .562 | 1.780 |
| **4** | Wind speed | .483 | 2.069 |
| | Air temperature | .940 | 1.063 |
| | Shortwave radiation | .545 | 1.833 |
| | Relative humidity | .653 | 1.531 |
| **5** | Wind speed | .188 | 5.330 |
| | Air temperature | .939 | 1.065 |
| | Shortwave radiation | .544 | 1.839 |
| | Relative humidity | .631 | 1.584 |
| | Precipitation | .251 | 3.985 |
| **6** | Air temperature | .944 | 1.059 |
| | Shortwave radiation | .590 | 1.694 |
| | Relative humidity | .733 | 1.365 |
| | Precipitation | .646 | 1.547 |

**Table 44: Parameters for model H: Autumn wet 'stepwise'**

| Model | | Unstandardized Coefficients | | Standardized Coefficients | | | 95% Confidence Interval for B | | Correlations | | |
|---|---|---|---|---|---|---|---|---|---|---|---|
| | | B | Std. Error | Beta | t | Sig. | Lower Bound | Upper Bound | Zero-order | Partial | Part |
| 1 | (Constant) | 4932.982 | 1430.979 | | 3.447 | .002 | 2001.753 | 7864.211 | | | |
| | Wind speed | 48.751 | 12.779 | .585 | 3.815 | .001 | 22.575 | 74.928 | .585 | .585 | .585 |
| 2 | (Constant) | 4577.350 | 1233.376 | | 3.711 | .001 | 2046.672 | 7108.028 | | | |
| | Wind speed | 40.736 | 11.236 | .489 | 3.625 | .001 | 17.681 | 63.791 | .585 | .572 | .477 |
| | Air temperature | 19.628 | 5.924 | .447 | 3.313 | .003 | 7.473 | 31.783 | .552 | .538 | .436 |
| 3 | (Constant) | -56.428 | 1967.994 | | -.029 | .977 | -4101.699 | 3988.842 | | | |
| | Wind speed | 64.476 | 13.043 | .773 | 4.944 | .000 | 37.667 | 91.286 | .585 | .696 | .579 |
| | Air temperature | 21.095 | 5.300 | .480 | 3.980 | .000 | 10.200 | 31.990 | .552 | .615 | .466 |
| | Shortwave radiation | 1.119 | .394 | .444 | 2.838 | .009 | .308 | 1.930 | -.168 | .486 | .333 |
| 4 | (Constant) | -10403.324 | 3996.946 | | -2.603 | .015 | -18635.188 | -2171.460 | | | |
| | Wind speed | 51.156 | 12.426 | .614 | 4.117 | .000 | 25.564 | 76.748 | .585 | .636 | .427 |
| | Air temperature | 20.197 | 4.696 | .460 | 4.301 | .000 | 10.525 | 29.869 | .552 | .652 | .446 |
| | Shortwave radiation | 1.292 | .354 | .512 | 3.652 | .001 | .564 | 2.021 | -.168 | .590 | .378 |
| | Relative humidity | 5.371 | 1.868 | .369 | 2.875 | .008 | 1.524 | 9.218 | .556 | .499 | .298 |
| 5 | (Constant) | -10445.210 | 3656.014 | | -2.857 | .009 | -17990.853 | -2899.568 | | | |
| | Wind speed | 16.560 | 18.241 | .199 | .908 | .373 | -21.087 | 54.206 | .585 | .182 | .086 |
| | Air temperature | 20.603 | 4.299 | .469 | 4.793 | .000 | 11.731 | 29.476 | .552 | .699 | .454 |
| | Shortwave radiation | 1.337 | .324 | .530 | 4.125 | .000 | .668 | 2.006 | -.168 | .644 | .391 |
| | Relative humidity | 6.144 | 1.738 | .422 | 3.535 | .002 | 2.557 | 9.731 | .556 | .585 | .335 |
| | Precipitation | 97.760 | 40.313 | .459 | 2.425 | .023 | 14.558 | 180.962 | .575 | .444 | .230 |
| 6 | (Constant) | -10388.289 | 3642.602 | | -2.852 | .009 | -17890.368 | -2886.210 | | | |
| | Air temperature | 20.891 | 4.272 | .475 | 4.890 | .000 | 12.093 | 29.689 | .552 | .699 | .462 |
| | Shortwave radiation | 1.255 | .310 | .497 | 4.046 | .000 | .616 | 1.893 | -.168 | .629 | .382 |
| | Relative humidity | 6.731 | 1.608 | .462 | 4.187 | .000 | 3.420 | 10.042 | .556 | .642 | .395 |
| | Precipitation | 126.385 | 25.031 | .593 | 5.049 | .000 | 74.832 | 177.938 | .575 | .711 | .477 |

**Table 45: Excluded variables for model H: Autumn wet 'stepwise'.**

| Model | | Beta In | t | Sig. | Partial Correlation | Tolerance | VIF |
|---|---|---|---|---|---|---|---|
| **1** | Air temperature | .447 | 3.313 | .003 | .538 | .954 | 1.049 |
| | Relative humidity | .331 | 1.851 | .075 | .336 | .677 | 1.476 |
| | Shortwave radiation | .383 | 1.977 | .058 | .356 | .567 | 1.763 |
| | Atmospheric pressure | -.081 | -.478 | .636 | -.092 | .850 | 1.176 |
| | Hourly rainfall | .277 | .921 | .365 | .174 | .260 | 3.840 |
| **2** | Relative humidity | .289 | 1.884 | .071 | .347 | .673 | 1.486 |
| | Shortwave radiation | .444 | 2.838 | .009 | .486 | .562 | 1.780 |
| | Atmospheric pressure | -.105 | -.725 | .475 | -.141 | .848 | 1.179 |
| | Hourly rainfall | .319 | 1.250 | .223 | .238 | .260 | 3.849 |
| **3** | Relative humidity | .369 | 2.875 | .008 | .499 | .653 | 1.531 |
| | Pressure | -.041 | -.308 | .761 | -.061 | .820 | 1.219 |
| | Hourly rainfall | .336 | 1.496 | .147 | .287 | .260 | 3.851 |
| **4** | Atmospheric pressure | .039 | .323 | .749 | .066 | .775 | 1.290 |
| | Hourly rainfall | .459 | 2.425 | .023 | .444 | .251 | 3.985 |
| **5** | Atmospheric pressure | .000 | .000 | 1.000 | .000 | .758 | 1.319 |
| **6** | Atmospheric pressure | -.029 | -.280 | .782 | -.057 | .840 | 1.190 |
| | Wind Speed | .199 | .908 | .373 | .182 | .188 | 5.330 |

### Model I: Autumn dry 65% ‘stepwise’

**Model 3 adjusted $R^2$ 0.352**

**Table 46: Autocorrelation and Covariance statistics for model I.**

| **Durban-Watson** 1.914 | | **Covariance Statistics** | |
|---|---|---|---|
| **Model** | | Tolerance | VIF |
| **1** | Relative humidity | 1.000 | 1.000 |
| **2** | Relative humidity | .839 | 1.192 |
| | Shortwave radiation | .839 | 1.192 |
| **3** | Relative humidity | .810 | 1.235 |
| | Shortwave radiation | .827 | 1.209 |
| | Atmospheric pressure | .924 | 1.082 |

**Table 47: Parameters for model I: Autumn dry 65% 'stepwise'**

| Model | | Unstandardized Coefficients | | Standardized Coefficients | | | 95% Confidence Interval for B | | Correlations | | |
|---|---|---|---|---|---|---|---|---|---|---|---|
| | | B | Std. Error | Beta | t | Sig. | Lower Bound | Upper Bound | Zero-order | Partial | Part |
| 1 | (Constant) | 4937.343 | 1411.354 | | 3.498 | .001 | 2058.868 | 7815.818 | | | |
| | Relative humidity | 1.633 | .752 | .363 | 2.171 | .038 | .099 | 3.166 | .363 | .363 | .363 |
| 2 | (Constant) | 1390.502 | 1795.807 | | .774 | .445 | -2277.025 | 5058.029 | | | |
| | Relative humidity | 2.469 | .743 | .550 | 3.325 | .002 | .953 | 3.986 | .363 | .519 | .503 |
| | Shortwave radiation | .558 | .199 | .464 | 2.808 | .009 | .152 | .964 | .244 | .456 | .425 |
| 3 | (Constant) | 52677.057 | 23117.047 | | 2.279 | .030 | 5397.388 | 99956.726 | | | |
| | Relative humidity | 2.173 | .711 | .484 | 3.059 | .005 | .720 | 3.627 | .363 | .494 | .435 |
| | Shortwave radiation | .608 | .188 | .506 | 3.231 | .003 | .223 | .993 | .244 | .515 | .460 |
| | Atmospheric pressure | -2.580 | 1.160 | -.329 | -2.224 | .034 | -4.952 | -.208 | -.346 | -.382 | -.317 |

**Table 48: Excluded variables for model I: Autumn dry 65% 'stepwise'.**

| Model | | Beta In | t | Sig. | Partial Correlation | Tolerance | VIF | Minimum Tolerance |
|---|---|---|---|---|---|---|---|---|
| **1** | Air temperature | .283 | 1.713 | .097 | .299 | .967 | 1.034 | .967 |
| | Wind Speed | .173 | 1.030 | .311 | .185 | .996 | 1.004 | .996 |
| | Shortwave radiation | .464 | 2.808 | .009 | .456 | .839 | 1.192 | .839 |
| | Atmospheric pressure | -.272 | -1.616 | .117 | -.283 | .937 | 1.067 | .937 |
| **2** | Air temperature | .154 | .939 | .355 | .172 | .855 | 1.169 | .743 |
| | Wind Speed | .087 | .557 | .582 | .103 | .952 | 1.050 | .803 |
| | Atmospheric pressure | -.329 | -2.224 | .034 | -.382 | .924 | 1.082 | .810 |
| **3** | Air temperature | .129 | .835 | .411 | .156 | .851 | 1.175 | .729 |
| | Wind Speed | -.008 | -.050 | .960 | -.010 | .871 | 1.148 | .776 |

### 8.32 Relative importance

The relative importance of each variable as a predictor in the 'stepwise' models is given by the beta statistic, which is a standardised version of the ß statistic allowing for direct comparison. The following table (Table 49) presents the beta values for each model with the rank in importance of each variable indicated with a colour code. The Table gives and idea of which variables contributed most to the models overall and how their contribution varied depending on the subset of data.

**Table 49. The beta statistic and rank of relative importance (by colour) of each predictor variable in the models. Shortwave radiation and relative humidity stand out as being of high importance in a large number of models and wind speed stands out for its importance in the summer models.**

| | T | H | W | S | P | R |
|---|---|---|---|---|---|---|
| **Full data** | 0.361 | 0.652 | 0.216 | 0.449 | 0 | 0.341 |
| **Summer** | 0 | 0 | 0.859 | 0 | 0 | 0 |
| **Autumn** | 0.325 | 0.429 | 0 | 0.324 | 0 | 0.682 |
| **FD wet** | 0.503 | 0.515 | 0 | 0.529 | 0 | 0.481 |
| **FD dry** | 0 | 0.583 | 0 | 0.712 | 0 | / |
| **SD wet** | 0 | 0 | 0.767 | 0 | 0 | 0 |
| **AD wet** | 0.475 | 0.462 | 0 | 0.497 | 0 | 0.593 |
| **AD dry** | 0 | 0.484 | 0 | 0.506 | -0.329 | / |

**Key: Ranks from 1, most important to 6, least important**

| 1 | 2 | 3 | 4 | 5 | 6 |
|---|---|---|---|---|---|

### 8.33 Change in beta

A change in the beta value of a variable with the addition of a subsequent variable is an indication that when combined, those variables alter each others predictive capacity - their influence on discharge production. For example, if the beta value for precipitation increased when temperature was added to the model, then temperature had a positive effect on the influence of precipitation in discharge production.

The following tables and graphs (Table 50 and Figure 67 through Table 55 and Figure 72) present the beta values in models beginning with one predictor and subsequently including a second predictor thus showing the effect of the second on the first. The data sets used for this part of analysis were the same as those that were used for the regression models above.

**Table 50. The beta statistics for air temperature in multiple regression models for stage in which air temperature is the constant predictor and each other variable is added as a predictor individually, indicating the influence of these subsequent variables on the predictive capacity of air temperature. Also shown is the change in the Beta statistic represented by the new value.**

| Model | FDDT | | SDDT | | ADDT | |
|---|---|---|---|---|---|---|
| **Variable added** | Beta | Δ | Beta | Δ | Beta | Δ |
| **T** | 0.373 | 0 | -0.008 | 0 | 0.231 | 0 |
| **H** | 0.424 | 0.051 | 0.553 | 0.561 | 0.308 | 0.077 |
| **W** | 0.436 | 0.063 | 0.869 | 0.877 | 0.277 | 0.046 |
| **S** | 0.435 | 0.062 | -0.443 | -0.435 | 0.298 | 0.067 |
| **P** | 0.432 | 0.059 | -0.056 | -0.048 | 0.275 | 0.044 |
| **R** | 0.455 | 0.082 | 0.790 | 0.798 | 0.298 | 0.067 |

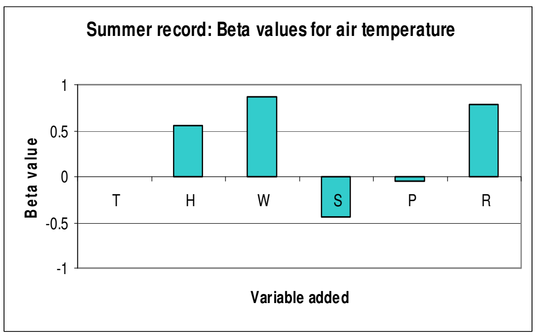


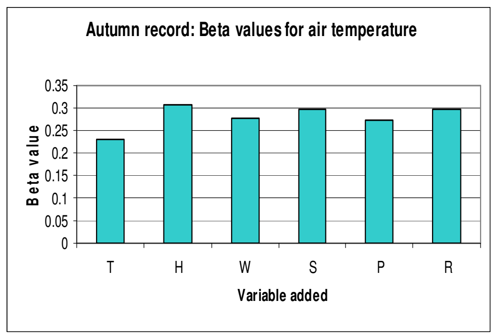


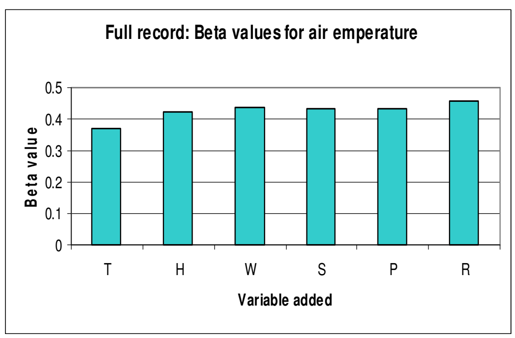


**Figure 68. The beta values for air temperature in a multiple regression model for stage in which air temperature is the constant predictor and subsequent variables are added singly as predictors, showing the influence of those subsequent variables on the predictive capacity of air temperature.**

**Table 51. The beta statistics for relative humidity in a multiple regression model for stage in which relative humidity is the constant predictor and other variables are added as predictors one by one, indicating the influence of these subsequent variables on the predictive capacity of relative humidity. Also shown is the change in the Beta statistic represented by the new value.**

| Model | FDDT | | SDDT | | ADDT | |
|---|---|---|---|---|---|---|
| **Variable added** | Beta | Δ | Beta | Δ | Beta | Δ |
| **T** | 0.559 | 0.038 | 0.553 | 0.012 | 0.534 | 0.045 |
| **H** | 0.521 | 0 | 0.541 | 0 | 0.489 | 0 |
| **W** | 0.473 | -0.048 | 0.108 | -0.433 | 0.433 | -0.056 |
| **S** | 0.709 | 0.188 | 0.722 | 0.181 | 0.504 | 0.015 |
| **P** | 0.493 | -0.028 | 0.54 | -0.001 | 0.405 | -0.084 |
| **R** | 0.378 | -0.143 | 0.065 | -0.476 | 0.287 | -0.202 |

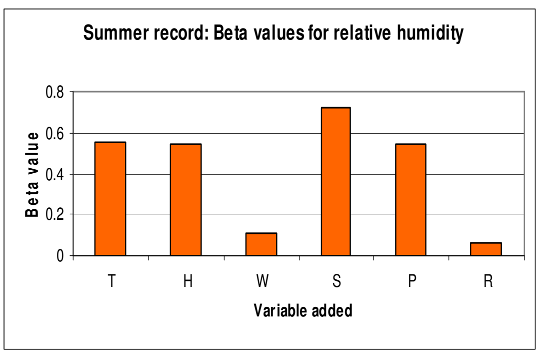


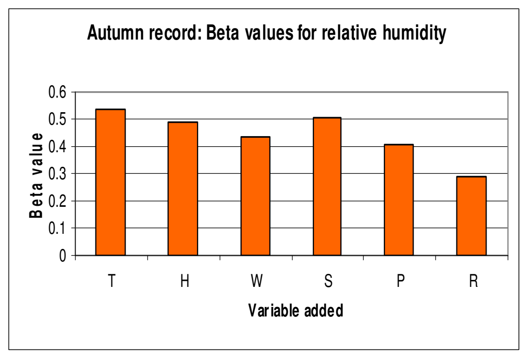


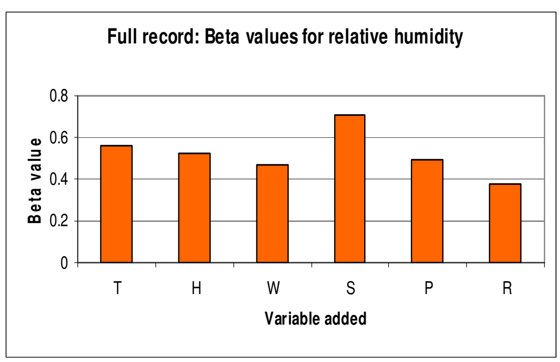


**Figure 69. The beta values for relative humidity in a multiple regression model for stage in which relative humidity is the constant predictor and subsequent variables are added singly as predictors, showing the influence of those subsequent variables on the predictive capacity of relative humidity.**

**Table 52. The beta statistics for wind speed in a multiple regression model for stage in which wind speed is the constant predictor and other variables are added as predictors one by one, indicating the influence of these subsequent variables on the predictive capacity of wind speed. Also shown is the change in the Beta statistic represented by the new value.**

| Model | FDDT | | SDDT | | ADDT | |
|---|---|---|---|---|---|---|
| **Variable added** | Beta | Δ | Beta | Δ | Beta | Δ |
| **T** | 0.392 | 0.07 | 0.869 | 0.012 | 0.477 | 0.026 |
| **H** | 0.22 | -0.102 | 0.798 | -0.059 | 0.389 | -0.062 |
| **W** | 0.322 | 0 | 0.857 | 0 | 0.451 | 0 |
| **S** | 0.348 | 0.026 | 0.923 | 0.066 | 0.411 | -0.04 |
| **P** | 0.274 | -0.048 | 0.859 | 0.002 | 0.368 | -0.083 |
| **R** | -0.024 | -0.346 | 0.631 | -0.226 | 0.085 | -0.366 |

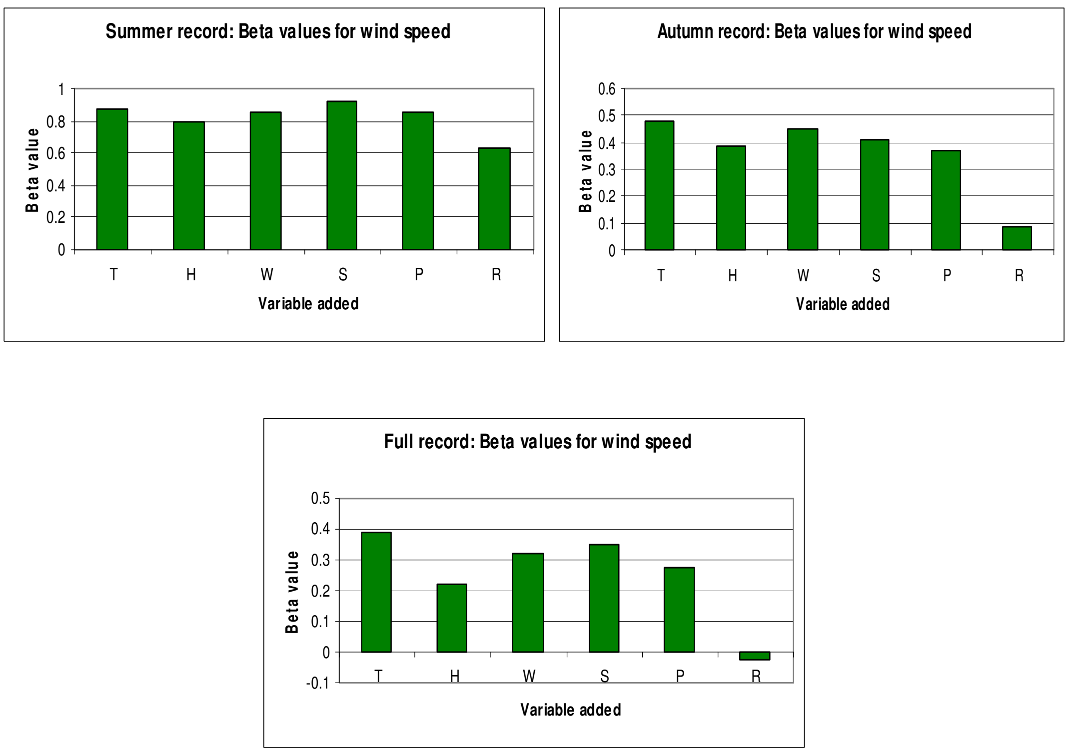


**Figure 70. The beta values for wind speed in a multiple regression model for stage in which wind speed is the constant predictor and subsequent variables are added singly as predictors, showing the influence of those subsequent variables on the predictive capacity of wind speed.**

**Table 53. The beta statistics for shortwave radiation in a multiple regression model for stage in which shortwave radiation is the constant predictor and other variables are added as predictors one by one, indicating the influence of these subsequent variables on the predictive capacity of shortwave radiation. Also shown is the change in the Beta statistic represented by the new value.**

| Model | FDDT | | SDDT | | ADDT | |
|---|---|---|---|---|---|---|
| **Variable added** | Beta | Δ | Beta | Δ | Beta | Δ |
| **T** | -0.205 | -0.132 | -0.443 | -0.002 | -0.318 | -0.063 |
| **H** | 0.331 | 0.404 | 0.203 | 0.644 | 0.027 | 0.282 |
| **W** | 0.067 | 0.14 | 0.11 | 0.551 | -0.122 | 0.133 |
| **S** | -0.073 | 0 | -0.441 | 0 | -0.255 | 0 |
| **P** | -0.002 | 0.071 | -0.039 | 0.402 | -0.139 | 0.116 |
| **R** | 0.328 | 0.401 | 0.207 | 0.648 | 0.173 | 0.428 |

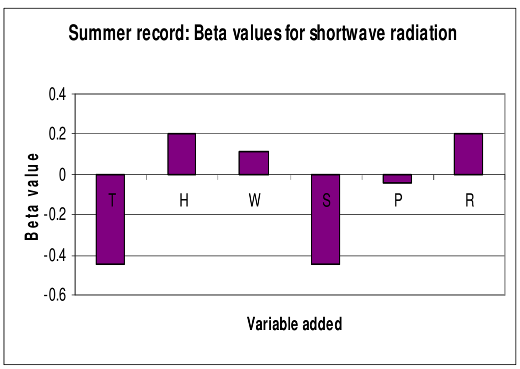


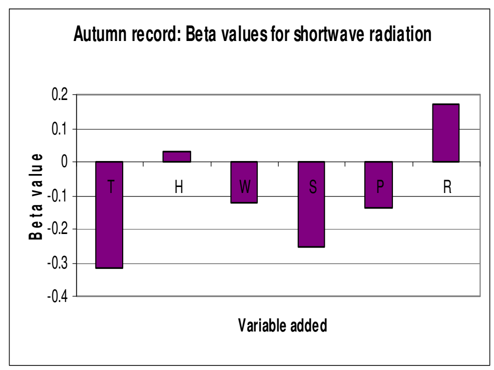


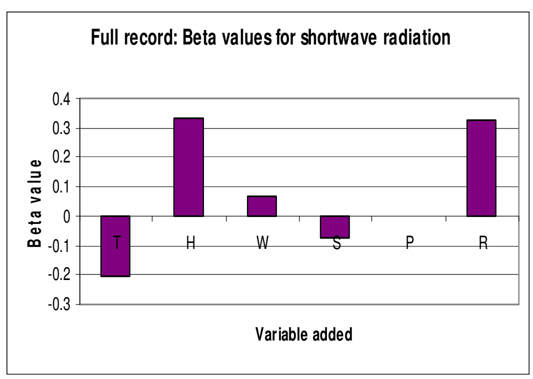


**Figure 71. The beta values for shortwave radiation in a multiple regression model for stage in which shortwave radiation is the constant predictor and subsequent variables are added singly as predictors, showing the influence of those subsequent variables on the predictive capacity of shortwave radiation.**

**Table 54. The beta statistics for atmospheric pressure in a multiple regression model for stage in which atmospheric pressure is the constant predictor and other variables are added as predictors one by one, indicating the influence of these subsequent variables on the predictive capacity of atmospheric pressure. Also shown is the change in the Beta statistic represented by the new value.**

| Model | FDDT | | SDDT | | ADDT | |
|---|---|---|---|---|---|---|
| **Variable added** | Beta | Δ | Beta | Δ | Beta | Δ |
| **T** | -0.317 | -0.081 | -0.056 | -0.001 | -0.412 | -0.029 |
| **H** | -0.094 | 0.142 | -0.014 | 0.041 | -0.243 | 0.140 |
| **W** | -0.147 | 0.089 | 0.024 | 0.079 | -0.270 | 0.113 |
| **S** | -0.236 | 0 | -0.439 | -0.384 | -0.334 | 0.049 |
| **P** | -0.236 | 0 | -0.055 | 0 | -0.383 | 0 |
| **R** | -0.045 | 0.191 | 0.039 | 0.094 | -0.188 | 0.195 |

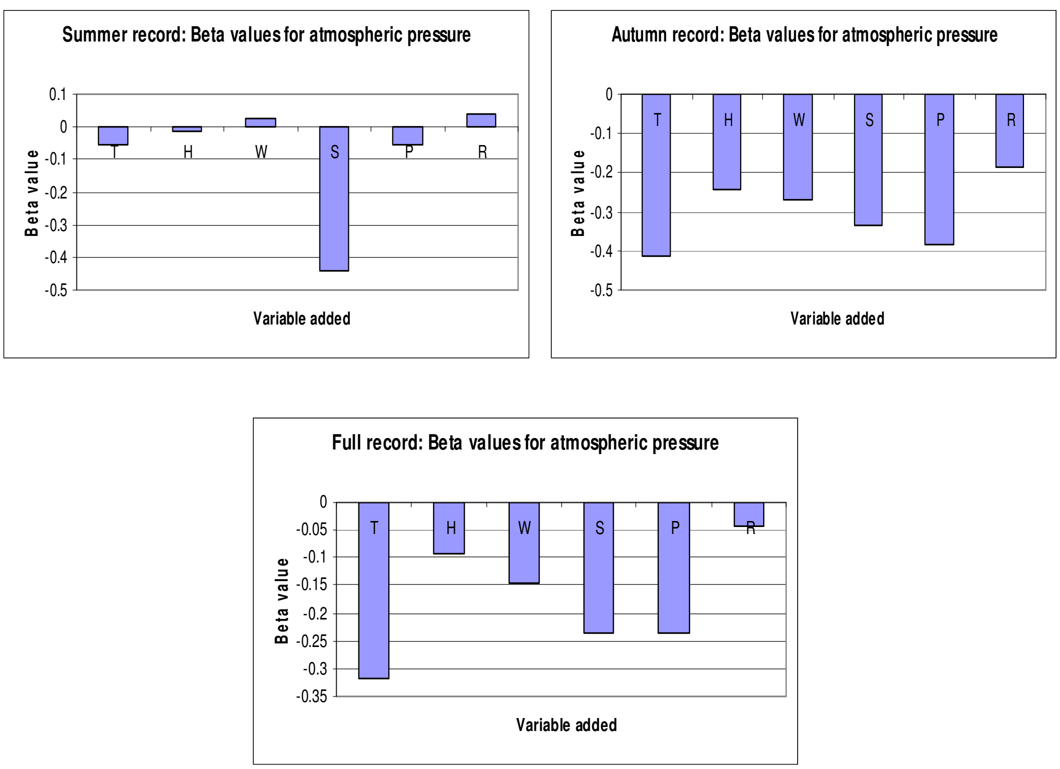


**Figure 72. The beta values for atmospheric pressure in a multiple regression model for stage in which atmospheric pressure is the constant predictor and subsequent variables are added singly as predictors, showing the influence of those subsequent variables on the predictive capacity of atmospheric pressure.**

**Table 55. The beta statistics for precipitation in a multiple regression model for stage in which precipitation is the constant predictor and other variables are added as predictors one by one, indicating the influence of these subsequent variables on the predictive capacity of precipitation. Also shown is the change in the Beta statistic represented by the new value.**

| Model | FDDT | | SDDT | | ADDT | |
|---|---|---|---|---|---|---|
| **Variable added** | Beta | Δ | Beta | Δ | Beta | Δ |
| **T** | 0.551 | 0.067 | 0.79 | 0.006 | 0.644 | 0.031 |
| **H** | 0.309 | -0.175 | 0.743 | -0.041 | 0.496 | -0.117 |
| **W** | 0.5 | 0.016 | 0.285 | -0.499 | 0.557 | -0.056 |
| **S** | 0.678 | 0.194 | 0.929 | 0.145 | 0.716 | 0.103 |
| **P** | 0.465 | -0.019 | 0.789 | 0.005 | 0.546 | -0.067 |
| **R** | 0.484 | 0 | 0.784 | 0 | 0.613 | 0 |

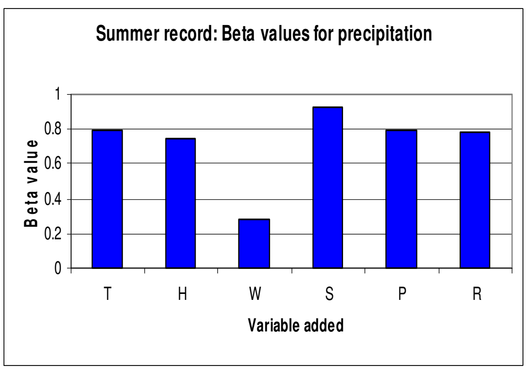


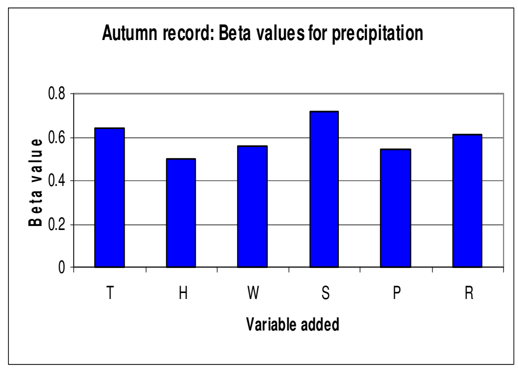


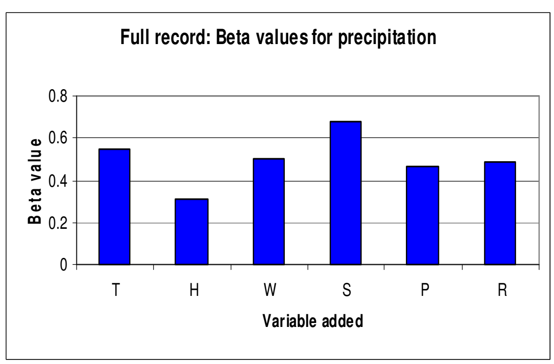


**Figure 73. The beta values for precipitation in a multiple regression model for stage in which precipitation is the constant predictor and subsequent variables are added singly as predictors, showing the influence of those subsequent variables on the predictive capacity of precipitation.**

### 8.34 Stream flow response time

While trialling models using hourly data, it was found that the best fit models (given the adjusted $R^2$ value) were often those in which some time lag of response in streamflow was assigned. That is, in predicting stage ‘now’ the values for atmospheric variables at some time previous, from one to nine hours ago, often produced the best models.

While the models using hourly data violated the multiple regression model assumptions, these results do still give an indication at least of the time that the stream took to respond to atmospheric variability during different times of the year and given different environmental conditions. The lag times that resulted in the best fit for each model are given in Table 56.

**Table 56. The lag time for stream response**

| Model | Lag time (hours) |
|---|---|
| Full data | 4 |
| Summer | 1 |
| Autumn | 4 |
| Full data precipitation | 5 |
| Full data dry | 6 |
| Summer precipitation | 0 |
| Summer dry | 4 |
| Autumn precipitation | 3 |
| Autumn dry | 9 |

# Chapter 3: Results

## *Section 9: Atmospheric Circulation Patterns*

### 9.0 Method

In his 2000 paper, Kidson defined twelve synoptic weather types (classes) for Aotearoa New Zealand based on the location of the 1000hPa isobar and surface temperature and precipitation anomalies. The twelve classes are divided into three “groups” of Blocking, Zonal and Trough type circulations. In this analysis, a statistical significance test was used to distinguish relationships between the twelve synoptic weather classes and the three grouped circulation types with the measured stage record at Brewster proglacial stream.

Every twelve hours from mid 2000 Aotearoa New Zealand weather has been classified into one of the twelve classes by NIWA. That data was used here to assign a class to every twelve hour period of stage at Brewster Glacier. The distribution of stage in each class was examined and the Wilcoxon Signed Ranks test of significance used to determine if there is a significant difference between the stage values in each circulation class and group. The tests were also carried out on the precipitation record for Brewster catchment in order to see if a relationship exists between precipitation at Brewster Glacier and national atmospheric circulation patterns.

Again, SPSS v15 was employed for this analysis and so the terminology used in that program is used here. None of the twelve hour periods within the study come under the 1:TSW classification so that class was omitted from the tests.

#### 9.01: The classes

The following are the twelve atmospheric circulation classes followed with the group to which they belong and their broadly defined characteristics:

1: TSW – trough southwesterly (“Trough” group): Characterised by moderate to weak southeasterly airflow over the South Island and weak southwesterlies over the northern tip of the North Island, with a low pressure system focussed to the southeast of the North Island. Associated with strongly negative temperature anomalies and weakly positive precipitation anomalies.

2: T – trough ("Trough" group). Characterised by moderate southwesterly airflow changing across the Main Divide to northeasterly, with the 1000hPa isobar located over the central South Island. Associated with strongly negative temperature anomalies and weakly positive precipitation anomalies.

3: SW – southwesterly ("Trough" group). Characterised by strong southwesterly airflow with the 1000hPa isobar to the southeast of the South Island and anomalously high pressure over the main landmasses. Associated with strongly negative temperature anomalies and weakly positive precipitation anomalies.

4: NE – northeasterly ("Blocking" group). Characterised by weak northwesterly airflow, with anomalously high pressure over the country, a trough located over the Tasman Sea and a ridge over the southwest Pacific Ocean. Associated with strongly positive temperature anomalies and moderately positive precipitation anomalies, particularly over the southwest coast of the South Island.

5: R – ridge ("Blocking" group). Characterised by moderate to weak northwesterly air flow, a trough located to the northeast of the country and a ridge latterly spanning the South Island. Associated with strongly positive temperature anomalies and moderately positive precipitation anomalies, particularly over the southwest coast of the South Island.

6: HW – high westerly ("Blocking" group). Characterised by strong southwesterly airflow over the lower South Island and strong southeasterly airflow from around 45°S latitude north, with a high pressure system over the Tasman Sea. Associated with strongly positive temperature anomalies and moderately positive precipitation anomalies, particularly over the southwest coast of the South Island.

7: HE – high easterly ("Blocking" group). Characterised by strong northwesterly airflow over the whole country, intensifying southward, and a high pressure system located to the east of the North Island. Associated with strongly positive temperature anomalies and moderately positive precipitation anomalies, particularly over the southwest coast of the South Island.

8: W – westerly ("Zonal" group). Strong westerly airflow over the whole country, intensifying southward, with a high pressure system to the north of the North Island. Associated with moderately positive temperature anomalies in the South Island, near normal temperatures in the North Island, weakly positive precipitation anomalies at the southwest of the South Island and strongly positive precipitation anomalies elsewhere in the country.

9: HNW – high northwesterly ("Zonal" group). Characterised by strong northwesterly airflows with a high pressure system over the Tasman Sea and anomalously high pressure over the main landmasses. Associated with moderately positive temperature anomalies in the South Island, near normal temperatures in the North Island, weakly positive precipitation anomalies at the southwest of the South Island and strongly positive precipitation anomalies elsewhere in the country.

10: TNW – trough northwesterly ("Trough" group). Characterised by moderate northwesterly airflow with a high pressure system over the western Pacific Ocean and weakly positive high pressure anomalies over the main landmasses, decreasing south. Associated with strongly negative temperature anomalies and weakly positive precipitation anomalies.

11: HSE – high southeasterly ("Blocking" group). Characterised by a high pressure system located over and to the east of the South Island, with weak northeasterly airflow over the country and high pressure anomalies. Associated with strongly positive temperature anomalies and moderately positive precipitation anomalies, particularly over the southwest coast of the South Island.

12: H – high ("Zonal" group). Characterised by a high pressure system over and to the west of the North Island, with moderate to weak southwesterly airflow over the country and very high pressure anomalies. Associated with moderately positive temperature anomalies in the South Island, near normal temperatures in the North Island, weakly positive precipitation anomalies at the southwest of the South Island and strongly positive precipitation anomalies elsewhere in the country.

## 9.1 Results

### 9.11: Stage in classes

Table 57 presents the descriptive statistics for stage in the eleven classes, and these data are also presented in a box plot (Figure 73). These are followed by the results of the Kruskal-Wallis test in Table 58, from which those classes with significance above the 95% confidence level are summarised in Table 59 and those with values of significance between the 95% and 90% confidence levels in Table 60. The tests were repeated for stage in the three circulation groups as defined above; the results are presented in Table 61 and the distribution in each group displayed in boxplots in Figure 74.

**Table 57. Stage in the eleven Kidson 2000 classes ranked according to average magnitude (from 1 - greatest to 11 - lowest), with range and standard deviation also shown.**

| Class | n | Mean (mm) | Rank | Range (mm) | Standard Deviation (mm) |
|---|---|---|---|---|---|
| **2:T** | 10 | 465 | 4 | 318-596 | 97.7 |
| **3:SW** | 21 | 486 | 2 | 276-966 | 181.6 |
| **4:NE** | 9 | 466 | 3 | 339-628 | 111.8 |
| **5:R** | 7 | 354 | 10 | 257-550 | 93.4 |
| **6:HW** | 14 | 414 | 7 | 257-578 | 100.2 |
| **7:HE** | 17 | 433 | 5 | 232-690 | 133.6 |
| **8:W** | 17 | 417 | 6 | 198-797 | 182.5 |
| **9:HNW** | 27 | 387 | 8 | 212-818 | 150.3 |
| **10:TNW** | 6 | 491 | 1 | 382-665 | 106.7 |
| **11:HSE** | 45 | 352 | 11 | 240-585 | 89.0 |
| **12:H** | 29 | 377 | 9 | 231-654 | 109.7 |

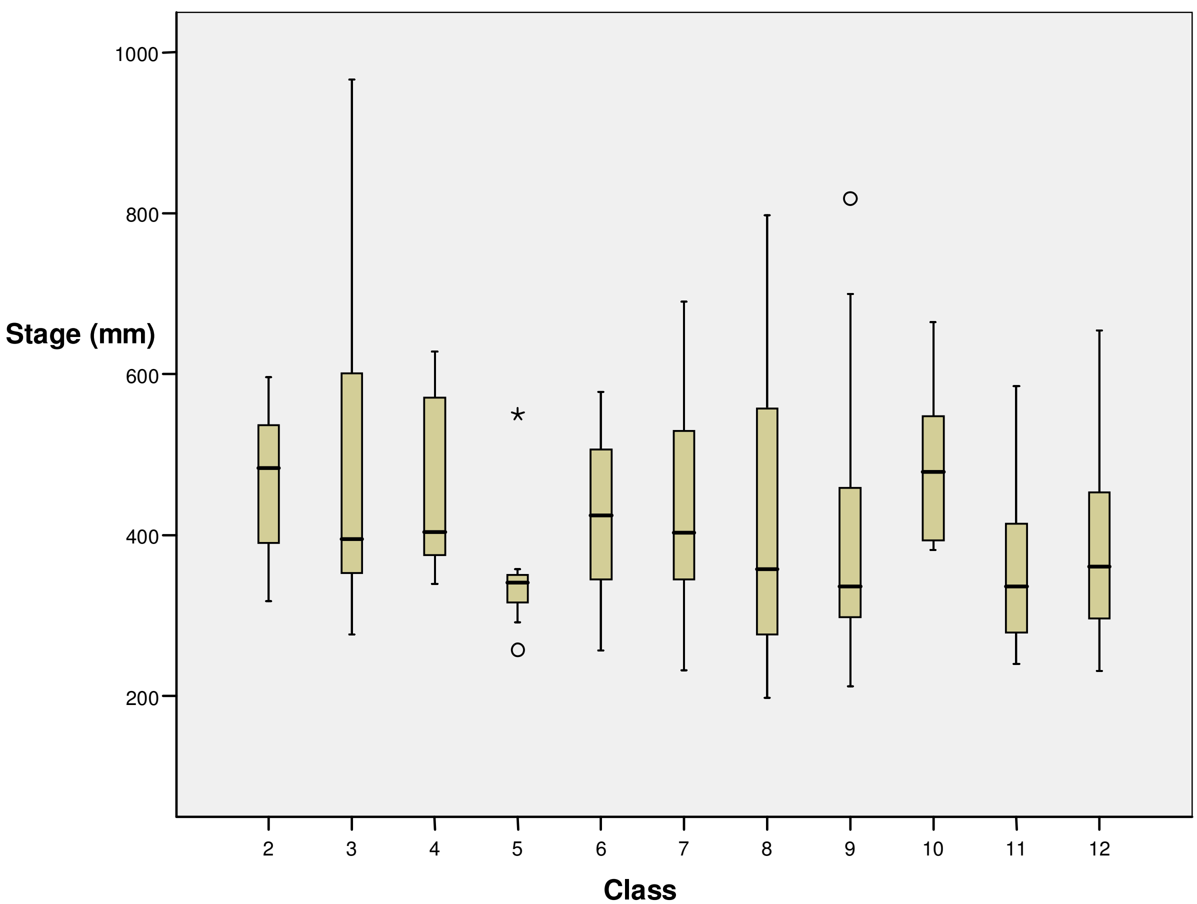


Key: 2 = T 3 = SW 4 = NE 5 = R 6 = H 7 = HE 8 =W 9 = HNW 10 = TNW 11 = HSE 12 = H

**Figure 74. Boxplot of stage in Kidson 2000 atmospheric circulation classes. Circles represent outliers within one quartile and stars outliers within two quartiles.**

**Table 58. Wilcoxon Signed Ranks Test for stage in classes; Asymptotic significance of Z statistic. Those results indicating statistical significance are in bold type.**

| Class | 3 | 4 | 5 | 6 | 7 | 8 | 9 | 10 | 11 | 12 |
|---|---|---|---|---|---|---|---|---|---|---|
| **2** | 0.074 | 0.374 | 0.176 | **0.047** | **0.047** | 0.721 | 0.114 | 0.600 | **0.013** | **0.013** |
| | **3** | 0.214 | 0.091 | **0.004** | 0.248 | 0.112 | **0.016** | 0.173 | **0.005** | **0.001** |
| | | **4** | 0.176 | 0.066 | 0.139 | 0.678 | 0.173 | 0.463 | **0.038** | **0.038** |
| | | | **5** | 0.237 | **0.043** | 0.091 | **0.043** | **0.028** | 0.237 | 0.237 |
| | | | | **6** | 0.826 | 0.198 | 0.875 | 0.249 | 0.245 | 0.096 |
| | | | | | **7** | 0.983 | 0.122 | 0.075 | **0.048** | 0.094 |
| | | | | | | **8** | 0.053 | 0.753 | 0.286 | 0.157 |
| | | | | | | | **9** | 0.249 | 0.195 | 0.943 |
| | | | | | | | | **10** | 0.116 | **0.046** |
| | | | | | | | | | **11** | 0.256 |

Key: 2 = T 3 = SW 4 = NE 5 = R 6 = H 7 = HE 8 =W 9 = HNW 10 = TNW 11 = HSE 12 = H

**Table 59. Statistically significant difference between stage in classes at the 95% confidence level:**

| **High stage** | **Low stage** |
|---|---|
| Trough | High westerly |
| Trough | High easterly |
| Trough | High south-easterly |
| Trough | High |
| Trough north westerly | Ridge |
| Trough north westerly | High |
| High westerly | South westerly |
| High easterly | Ridge |
| High easterly | High south-easterly |
| High north westerly | Ridge |
| South westerly | High north westerly |
| South westerly | High south easterly |
| South westerly | High |
| North easterly | High south easterly |
| North easterly | High |

**Table 60: Statistically significant difference between stage in classes at the 90% confidence level:**

| High stage | Low stage |
|---|---|
| Trough | South westerly |
| South westerly | Ridge |
| North easterly | High westerly |
| Westerly | Ridge |
| Westerly | High north westerly |
| High westerly | High |
| Trough north westerly | High easterly |
| High easterly | High |

## 9.12: Stage in groups

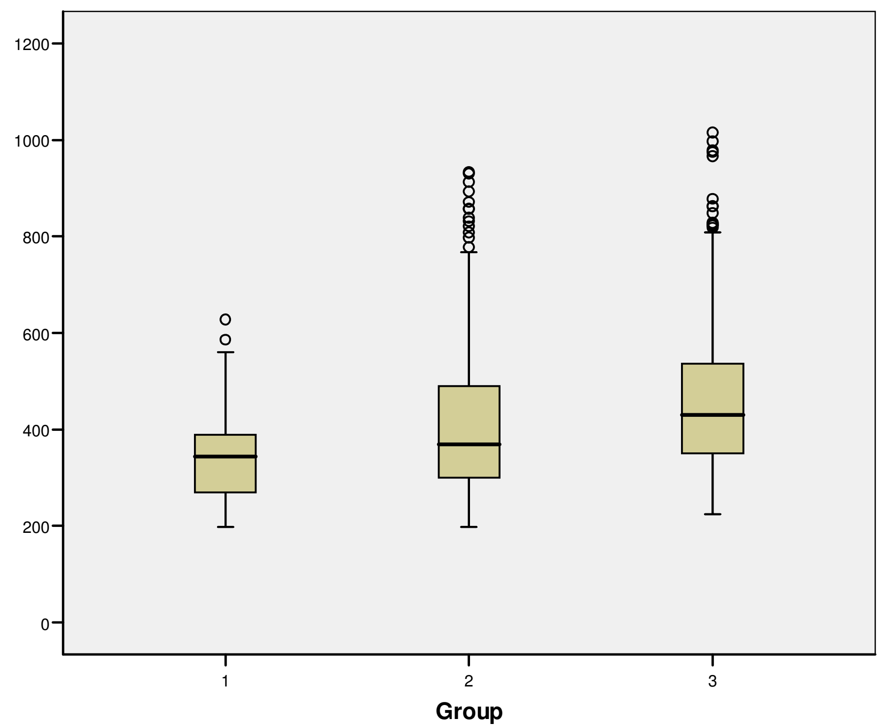


Key: 1 = Trough 2 = Blocking 3 = Zonal

**Figure 75. Boxplot of stage in Kidson 2000 atmospheric circulation groups. Circles represent outliers within one quartile and stars outliers within two quartiles.**

**Table 61. Wilcoxon Signed Ranks Test for stage in groups; Asymptotic significance of Z statistic. Those results that indicate statistical significance are in bold type.**

| Group | Blocking | Zonal |
|---|---|---|
| **Trough** | 0.122 | **0.017** |
| **Blocking** | | 0.857 |

### 9.13: Precipitation in classes

Table 62 presents the eleven classes ranked according to average twelve-hourly precipitation, and the maximum value of precipitation recorded during the same circulation. Table 63 presents Kidson's three circulation groups again ranked according to average precipitation at Brewster Glacier.

**Table 62. Mean twelve-hourly precipitation in the eleven Kidson 2000 classes ranked according to magnitude (from 1 - greatest to 11 - lowest), with maximum hourly precipitation recorded also shown.**

| Class | Average (mm) | Rank | Maximum (mm) |
|---|---|---|---|
| **2 (T)** | 8.3 | 2 | 21.2 |
| **3 (SW)** | 7.1 | 3 | 31.9 |
| **4 (NE)** | 1.8 | 10 | 9.1 |
| **5 (R)** | 1.9 | 9 | 13.4 |
| **6 (HW)** | 2.1 | 8 | 20.8 |
| **7 (HE)** | 2.2 | 7 | 17.6 |
| **8 (W)** | 8.5 | 1 | 34.0 |
| **9 (HNW)** | 5.9 | 4 | 30.8 |
| **10 (TNW)** | 2.9 | 5 | 12.5 |
| **11 (HSE)** | 0.8 | 11 | 25.5 |
| **12 (H)** | 2.3 | 6 | 26.8 |

**Table 63. The three circulation groups of Kidson 2000 ranked according to average precipitation, with maximum hourly precipitation recorded during also shown.**

| | Average (mm) | Rank | Maximum (mm) |
|---|---|---|---|
| **Trough** | 6.7 | 3 | 31.9 |
| **Blocking** | 1.5 | 1 | 25.5 |
| **Zonal** | 5.1 | 2 | 34.0 |

# Chapter 3: Results

## *Section 10: Brewster proglacial discharge and predicted climate change*

The relevant literature asserts that changes in glacial discharge depend on the combination of many atmospheric variables, temporal and spatial variability of these, the physiology of the glacier and its drainage system (Hannah et al., 2000; Raper et al., 2000; Gregory and Oerlemans, 1998). A precise estimate of the change in discharge at Brewster glacier with climate change would account for changes in each applicable atmospheric variable, the influence these variables have on each other in discharge production, and changes in the morphology of the glacier – particularly its size. The only data used in this analysis were predicted changes in air temperature and precipitation for Aotearoa New Zealand over the next 100 years assuming constancy of all other parameters (an erroneous assumption).

Given that changes in glacier mass and morphology are critical to discharge production, estimation of the change in discharge using only air temperature and precipitation estimations beyond a few years from the time of discharge measurement would be seriously flawed. Therefore, estimations are made only for the period 2007 – 2020, which may also be pushing it but might at least indicate the trend in discharge given temperature and precipitation changes.

### 10.0 Method 1

The 'rough and ready' method attempted first to estimate changes in discharge used the relationship between high, medium and low temperature and corresponding stage. Figure 75 shows the distribution of stage when broken into these categories (relative to the range of values in the air temperature record) and Table 64 shows that the difference in stage in each of these sets is significantly different in each case. A best fit curve was created from the average temperature and corresponding average stage for each of these sets, showing a change of approximately 11mm stage, or 0.02 cumecs (4% of average calculated discharge), per 1°C (Figure 76).

The IPCC has predicted an average global temperature increase of around 0.2°C per decade for the next two decades (Bernstein et al., 2007). NIWA has predicted a change of around 2°C for Aotearoa New Zealand by 2100 using the IPCC

A1B scenario (Mullan, pers. com.), which works out approximately the same. The best-fit equation derived from the graph in Figure 76,

$$Y = 11.231x + 357.18$$

**Eq. 7**

was used to estimate stage (and thereby discharge) for the years 2008-2020 using a temperature change of 0.02°C per year with a baseline of average (recorded) stage for 2006 and 2007. The results for this are shown in Figure 77.

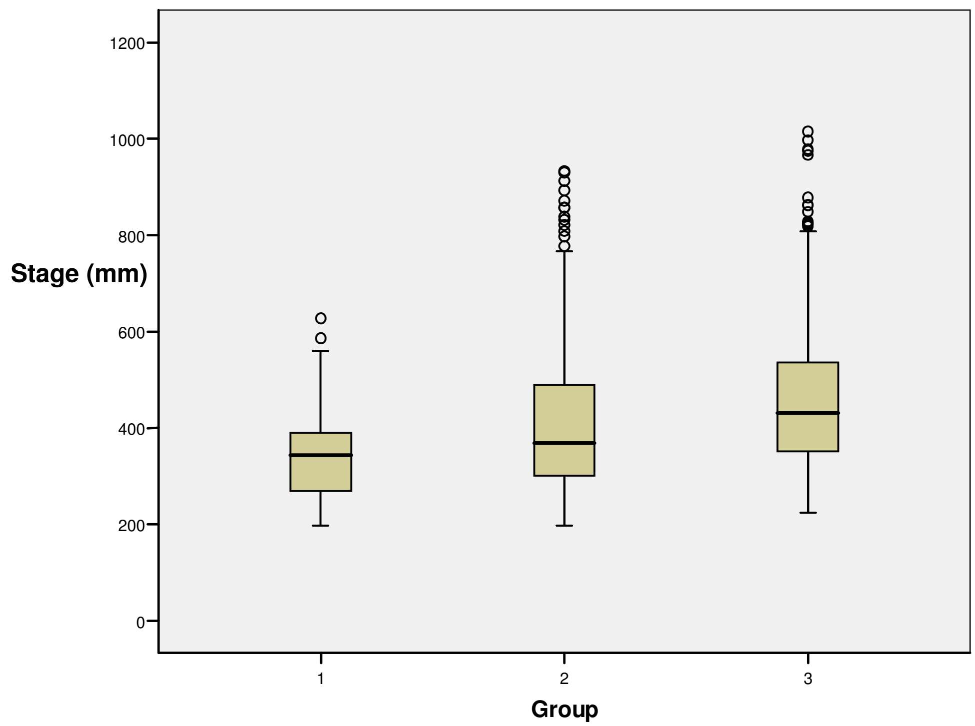


**Figure 76. Boxplot of stage divided into groups of 1: low, 2: medium and 3: high air temperature showing the distribution of stage when defined by air temperature. Circles represent outliers within one quartile.**

**Table 64. The asymptotic z-score values for stage in groups of low, medium and high air temperature, showing that the difference in the distribution of each group is statistically significant.**

| Group | Low | Medium |
|---|---|---|
| **High** | 0.000 | 0.000 |
| **Low** | | 0.014 |

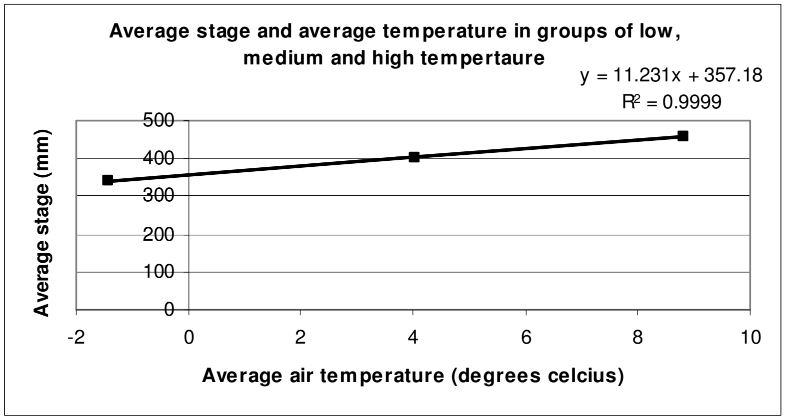


**Figure 77. The average air temperature for low, medium and high groups against the corresponding average stage, with a regression line, $R^2$ value of 0.99 and regression line equation. This curve was used to estimate changes in stage with changes in temperature from 2008 – 2020.**

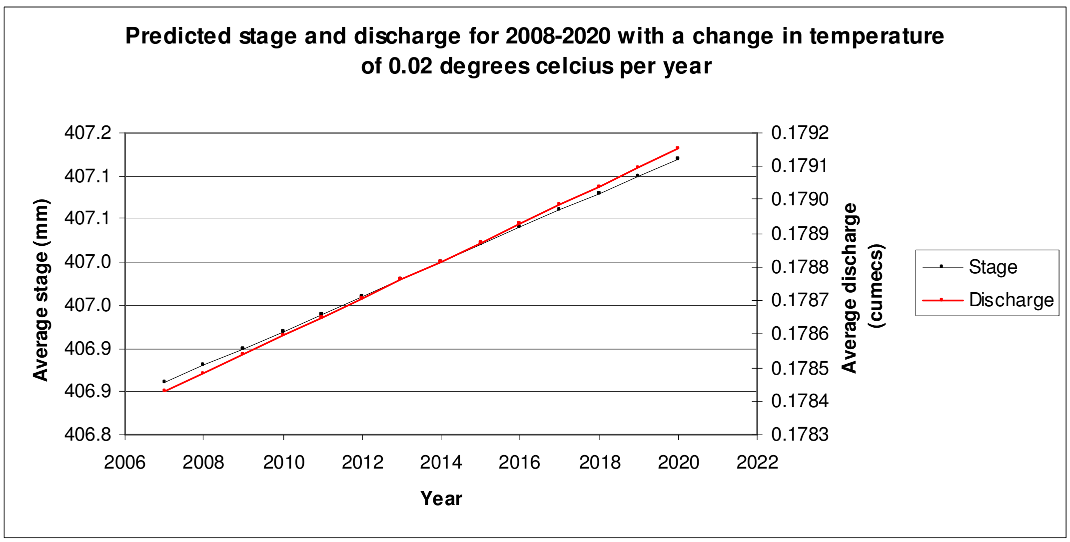


**Figure 78. Predicted stage and discharge for 2008-2020 given a temperature change of 0.02°C per year, estimating an increase in average stage and discharge of around 0.5mm and 0.0007 cumecs respectively between 2007 and 2020.**

### 10.1 Method 2

Monthly average change in temperature and precipitation for a 5km gridpoint encompassing Brewster catchment has been predicted NIWA for the periods 2030-2049 (nominally 2040) and 2080-2099 (nominally 2090) and provided for this analysis. The values are the averaged output of twelve different climate models using the IPCC 2007 A1B emissions scenario with 1971-2000 as the baseline and statistically downscaled over Aotearoa New Zealand. In this analysis, monthly average daily total values for temperature and precipitation recorded at Brewster were used as the baseline (a method supported by the suppliers - Mullan, pers. com.).

The NIWA predicted changes for temperature to 2040 and 2090 were multiplied by 24 to produce a daily total change and these then added to the baseline values for the months February, March, April and May (the months for which reliable measurements exist). A best fit line was then interpolated from the three resulting points for each month, giving linear equations for changes from the 2006-2007 average (Figure 78), as follows:

**February**

$$y = 0.7613x - 1377 \quad \textbf{Eq. 8}$$

**March**

$$y = 0.6279x - 1180.7 \quad \textbf{Eq. 9}$$

**April**

$$y = 0.6187x - 1160.7 \quad \textbf{Eq. 10}$$

**May**

$$y = 0.6081x - 1220 \quad \textbf{Eq. 11}$$

These regression equations were used to estimate values for daily total air temperature (the sum of values recorded at fifteen minute intervals over a twenty-four hour period) for February, March, April and May for every year up 2020 (Figures 79a – 79d).

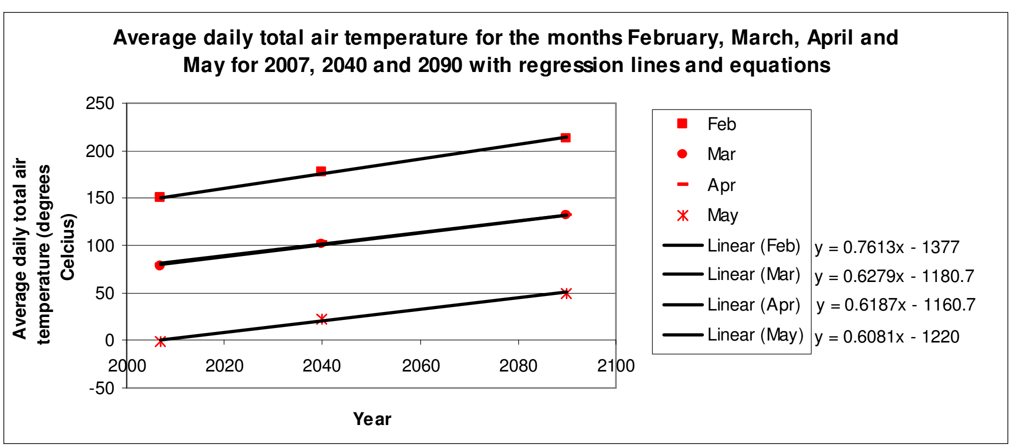


**Figure 79. Value of average daily total air temperature for 2007 (recorded), 2040 and 2090 (estimated from 2007 values with predicted air temperature changes provided by NIWA), with regression lines and equations.**

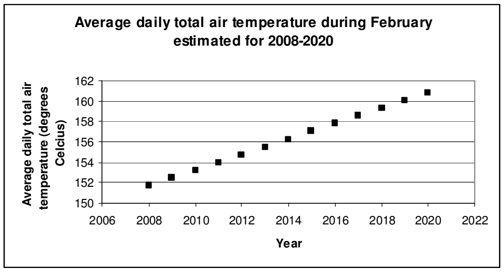


**a.**

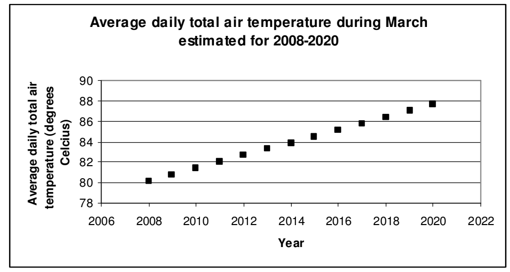


**b.**

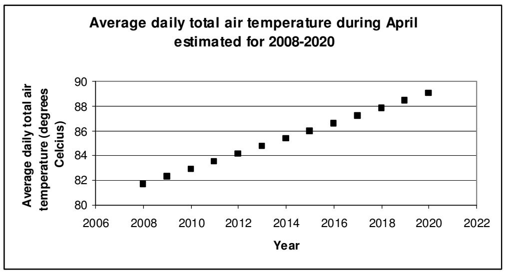


**c.**

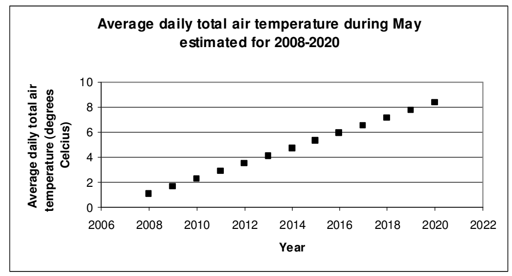


**d.**

**Figure 80a – 80d. Estimated average daily total air temperature for the months of February (a) March (b), April (c) and May (d) from 2008 to 2020.**

Changes in precipitation were provided as percentages, so the percentage of the baseline precipitation values was found for 2040 and 2090 and added to the baseline values. The percentage change is positive in each case, but of a lower magnitude in February and April between 2007 and 2090 than between 2007 and 2040. This indicates a changing trend in precipitation in this region as climate change advances. Given that this analysis hoped only to estimate changes between now and 2020, the change in precipitation between 2007 and 2040 was deemed more useful than the overall change between 2007 and 2090. Therefore, only the two values for 2007 and 2040 were used to create regression lines and equations for estimation of precipitation for February, March, April and May for the period 2007 – 2020 (Figure 80), as follows:

**February**

$$Y = 0.0093x - 12.95$$

**Eq. 12**

**March**

$$Y = 0.0019x + 5.6009$$

**Eq. 13**

**April**

$$Y = 0.0106x - 16.313$$

**Eq. 14**

**May**

$$Y = 0.0206x - 18.903$$

**Eq. 15**

The values of average daily total precipitation estimated from these regression lines are presented in Figure 81a – 81d.

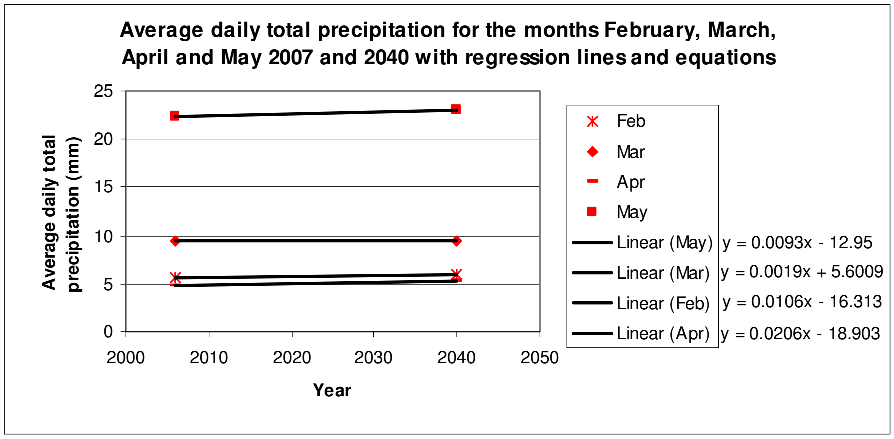


**Figure 81. Value of average daily precipitation for 2007 (recorded) and 2040 (estimated from 2007 values with predicted precipitation changes provided by NIWA), with regression lines and equations.**

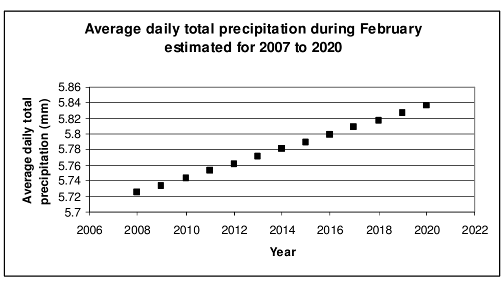


**a.**

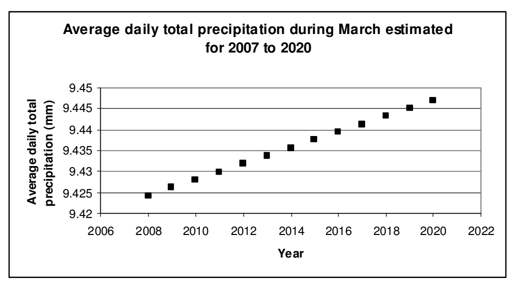


**b.**

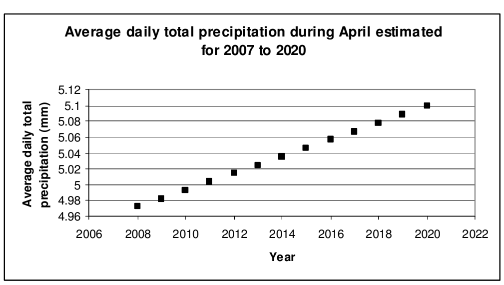


**c.**

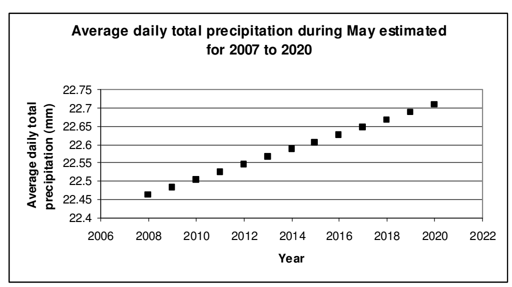


**d.**

**Figure 82a – 82d. Estimated average daily total precipitation for the months February (a), March (b), April (c) and May (d) from 2008 to 2020.**

The estimated values for temperature and precipitation were input to the Full data (Ab), Summer (Bb) and Autumn (Cb) regression equations presented in Chapter 3.8 with all other values held constant at the 2007 level, giving an estimation of stage from 2007 to 2020. Because the equation for conversion of stage into discharge is of the power type, calculation of daily total stage into discharge produces vastly overestimated values for discharge. Therefore, the results are given for stage only, as presented in Figures 82, 83 and 84.

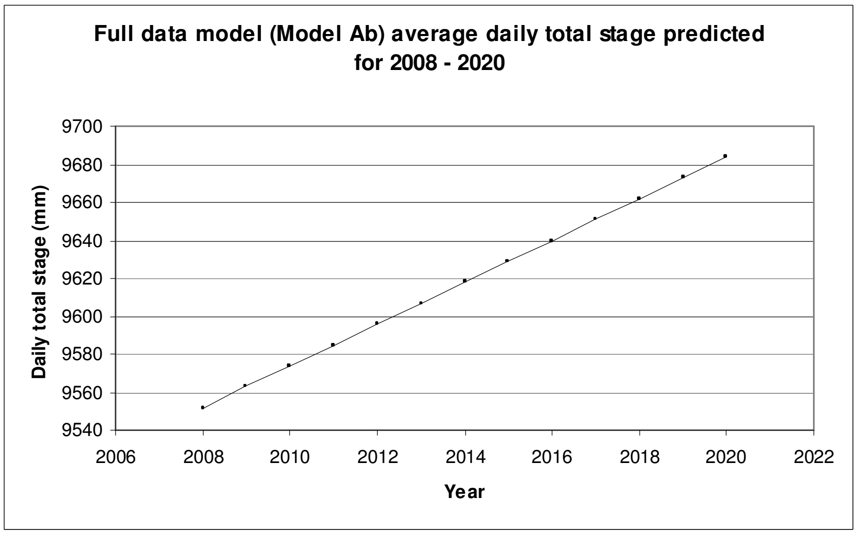


**Figure 83. Daily total stage predicted for each year from 2007 to 2020 using the Full data enter type regression model (Ab) of Chapter 3.8, estimating a daily total increase in stage of around 12.33 mm per year and around 160.30 mm by 2020.**

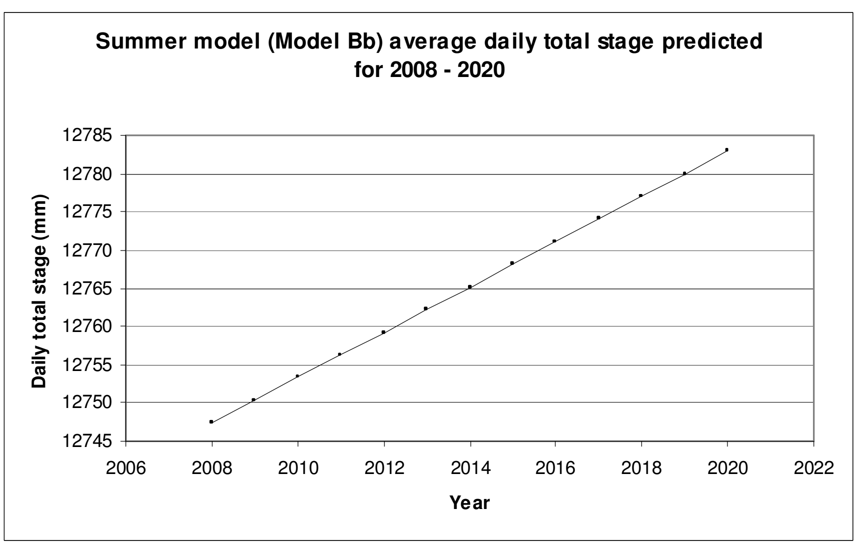


**Figure 84. Daily total stage predicted for summer of each year from 2007 to 2020 using the Summer Enter type regression model (Bb) of Chapter 3.8, suggesting increased daily total stage of around 3.23 mm per year and around 41.99 mm by 2020.**

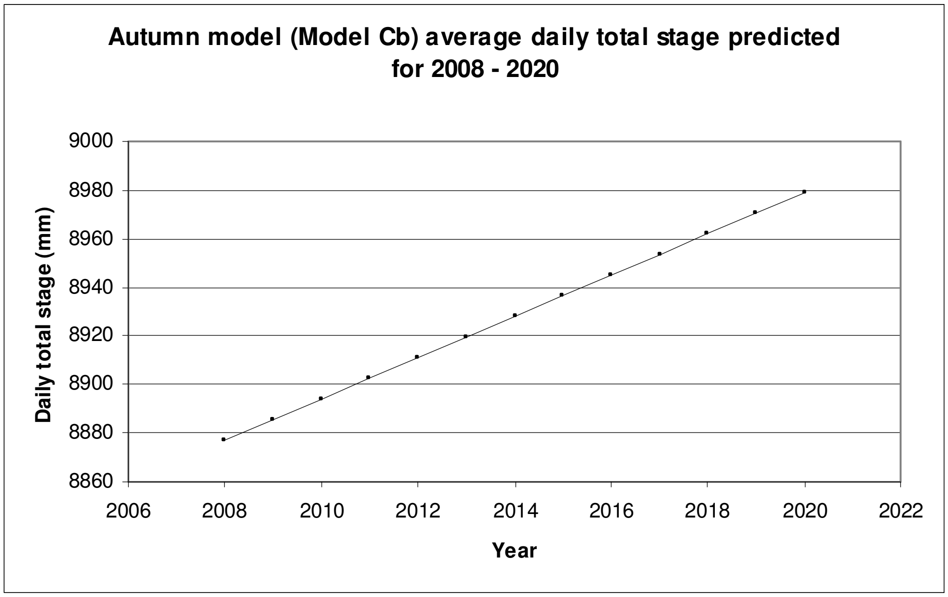


**Figure 85. Daily total stage predicted for autumn of each year from 2007 to 2020 using the Autumn Enter type regression model (Cb) of Chapter 3.8, suggesting increased daily total stage of around 9.62 mm per year and around 125.12 mm by 2020.**

## 10.2 Prediction Comparison

To compare the results of Method 1 with those of Method 2, the predicted daily total stage values of Method 2 were divided by 24 to give the average, and then converted into discharge. These values and those of Method 1 are presented in Table 65 for comparison.

**Table 65. Comparison of the annual and total increase in stage from 2007 to 2020 predicted using Methods 1 and 2.**

| | Method 1 (cumecs) | Method 2 (stage mm) | | |
|---|---|---|---|---|
| | | Full data | Summer | Autumn |
| **Annual increase in average** | 0.04 | 12.33 | 3.23 | 9.62 |
| **Total increase in average between 2007 and 2020** | 0.50 | 160.30 | 41.99 | 125.12 |

# Chapter 4: Discussion

In this section the results presented in Chapter 3 are discussed in an attempt to draw out detail of the discharge regime and drainage system of Brewster Glacier. Special attention is given to those data that are related directly to the aims of this project but other relationships that became apparent in the course of analysis are also discussed. In large part this discussion follows the order in which the results are presented, excepting where different sections relate together to a single problem.

## Section 1: Discharge characteristics of Brewster proglacial stream

### 1.0 Stream flow characteristics

#### 1.01 Stream character

The record of channel cross-sectional velocities showed, unexpectedly, the stream thalweg migrating through the channel with little relationship to channel depth or curvature (Figure 28). This is a known phenomenon. McConchie (pers. com.) recorded a similar state in a stream in the Rimutaka Forest Park of Aotearoa New Zealand (Figures 85 and 86), and suggests that it is more common than hydrological theory would attest.

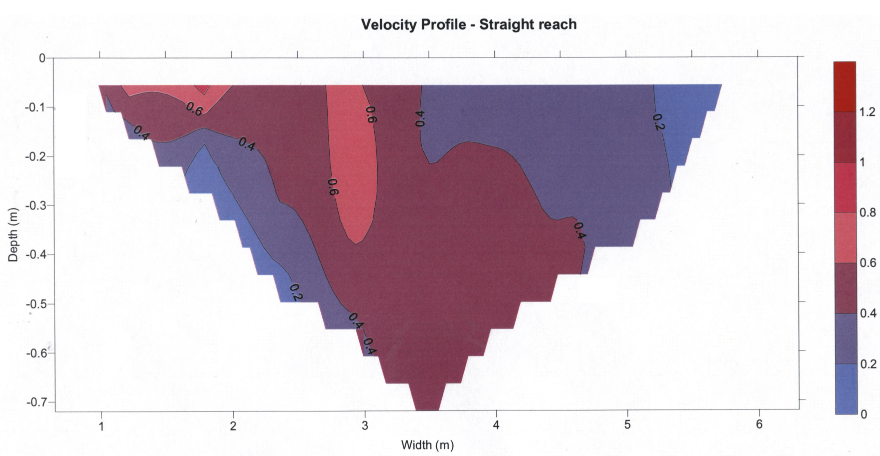


**Figure 86. Velocity profile of a straight reach of a river in the Rimutaka Ranges showing a velocity distribution that does not correlate with channel depth (McConchie, unpublished data.).**

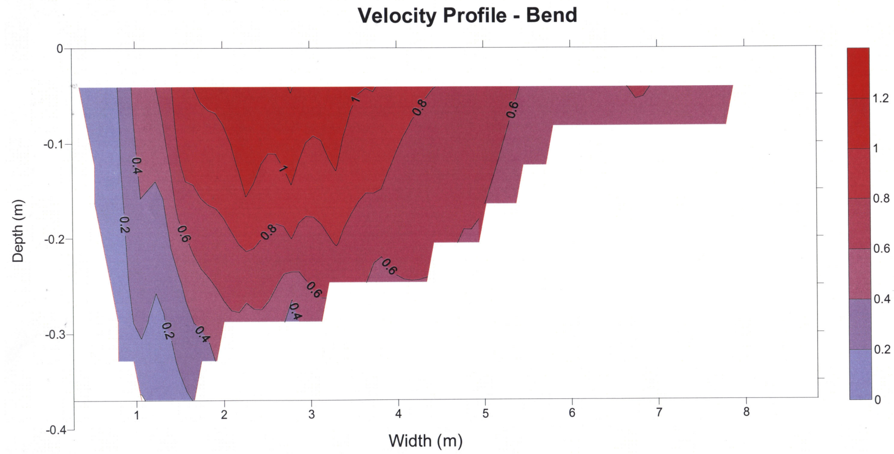


**Figure 87. Velocity profile of a bend in a river in the Rimutaka Ranges showing a velocity distribution that does not correlate with either channel depth or curvature (McConchie, unpublished data).**

Popular textbooks state that a stream thalweg will be at the outside of a curve in a stream channel and/or where the channel is deepest (Mosley and McKercher, 1992; Scheidegger, 1992; Chorley et al., 1984). In Brewster proglacial stream the migration seemed to instead be related to flow velocity as much as, if not more than, channel depth and curvature. Excepting only the 17th of February, the thalweg was located at the true right of the channel – the outside of a gentle curve – when maximum flow velocity was above $0.58ms^{-1}$, on the true left when maximum velocity was between $0.53ms^{-1}$ and $0.37ms^{-1}$ and again on the true right when maximum velocity was below $0.12ms^{-1}$. The channel had two deep points, one to the left and one to the right of the horizontal centre. The wall at waters edge left bank was more gradually sloping and smoother than that at waters edge right bank, which was almost vertical and more craggy and rough. McConchie (pers. com.) suggests that streamflow can behave like a car driving at different speeds. Taking a corner 100km/hr will force the car to the outside of the bend, while at 30km/hr the car is comfortable at any place upon the road, even at the inside of the bend. It seems the proglacial stream was behaving in this manner. At high and low flows waters edge right bank was the path of least resistance where, in the case of high flows, the roughness of the channel wall was overcome by high velocities while at low flows most of the outer wall was above water and therefore did not retard flow. When flows were moderate, however, there was insufficient velocity to overcome the effect of the roughness of the outside wall so fastest flow occurred closer to waters edge left bank where the channel was just as deep but friction was lesser.

### 1.02 Streamflow

It is unlikely that the calculated discharge record is an accurate representation of streamflow from the proglacial stream. Peak flows were amplified by the ratings curve equation (Figures 24 and 25). The maximum values for discharge calculated using the linear equation (1.9 cumecs for the highest value of stage) were well below what people versed in hydrology from both Victoria and Canterbury Universities assert they have observed or would expect (Mackintosh, pers. com.), and the maximum value of 71 cumecs calculated using the chosen equation is not outside the bounds of possibility (Table 3). However low flows were also exaggeratedly diminished – the equation produced a value of 0.002 cumecs for the lowest value of stage, 197mm. While this value was recorded in late autumn when flows could be expected to be low it stretches the limits of the imagination, let alone measurement. It is probable that an equation with a smaller exponent would more accurately represent streamflow in Brewster Proglacial Stream. This is supported by the flow duration curves presented in Figures 35 and 36. The curve for stage is gradual while that for discharge pivots steeply near 5%, with a shape that is clearly an artefact of the equation used for its calculation. It was for this reason and the fact that the discharge record was calculated from the directly measured stage record that it was primarily the stage data that were used for further analysis.

The stage record suggested characteristic variability in Brewster proglacial stream relating to total energy inputs and little change in the configuration of the drainage system through the study period. Stage ranged from 197mm to 1047mm in 2005 and 313mm to 972mm in 2006 (Table 3). From the 8$^{th}$ February to the 13$^{th}$ March each year – the single period of overlap - stage ranged 319mm to 1047mm in 2005 and 313mm to 922mm in 2006. Baseflow ranged in 2005 from 185mm to 406mm and 313mm to 514mm in 2006 (Table 5). In 2005, the overall decrease in baseflow was approximately 221mm and in 2006 around 178mm. During the overlapping period baseflow ranged from 319mm to 406mm in 2005 and 313mm to 443mm in 2006. The similarity between values for full stage and baseflow during the overlapping time period in particular suggests that intra-annual streamflow variation is consistent inter-annually. There does not appear to be a pattern in the occurrence of peak or low flow events: both occurred in both summer and autumn and the ratio of rising limb to falling limb changed with no regularity (Table 4). Given that there was also no overall increase in the magnitude of precipitation events, this suggests that there was no considerable change in the configuration of the hydrological system that might otherwise have caused peak flows to attenuate through the study period. An overall decrease in baseflow over the study period was to be expected from a temperate glacier (see Richards et al., 1996, for example), and in this case it could, given no change in the form of peak flow events, be attributed solely to a reduction in energy inputs to the system causing progressively less melt and less rainfall on a day to day basis.

In the stage record, a pattern of small peak flow events superimposed on the falling limb of most major peak flow events was identified (Figures 18 and 19). These events occurred on the 8th February 2005, 14:36; 22nd of March 2005, 16:23; 29th March 2005, 1:03; 7th of April 2005, 17:03; 22nd of February 2006, 8:27; 1st of March 2006, 14:07 and the 8th of March 2006, 10:37. Those on the 8th of March 2005 and in 2006 were each concurrent with 'blips' in the precipitation record, but the others were not nor were similar patterns in the other atmospheric records identified that could account for the 'blips' in the stage record (Figures 55-60). Given the fact that those 'blips' that did correlate with the precipitation record had a similar graphic form as those that did not, the most likely explanation is that there was a pattern to precipitation events, where a secondary, comparatively small event occurred as storms passed away - though identifying the cause is beyond the scope of this project - and some precipitation events were removed from the record erroneously (a distinct possibility given the refinement process of the precipitation record – see discussion in Chapter 3.5).

### 1.02 Diurnal variation of streamflow

Daily peak flow occurred between 3pm and 7pm, the rising limb lasting five to eight hours, and low flow between 5am and 1pm with the falling limb lasting sixteen to twenty hours (Figures 41-46). The ratio of the rising to falling limbs suggests that after a swift melt/discharge production initiation and peak, the effect of daily insolation receipt lingered after its own zenith, such that attenuation of melt occurred more slowly and gradually than its instigation.

Davie (2003) asserts that a positive feedback exists between melt water quantity and transmission speed. He describes three stages to snow melt: first, a warming phase in which the temperature of the snowpack is raised to 0°C; second, a "ripening" phase during which time melt occurs but water remains in the interstitial cavities of the snowpack; and third, an output phase, during which any additional energy produces water output. A positive feedback loop causes the warming and ripening phases to occur with a steep gradient with constant energy input: melt occurs at the surface; the resulting water trickles into the snowpack and refreezes releasing latent heat, thereby further warming the pack. This first phase may not be as relevant to Aotearoa New Zealand snowpacks, which are usually near or at 0°C. It is likely then that during summer, Brewster Glacier snowpack is often, if not always, ripe, so that energy input from the beginning of the day takes very little time to generate liquid output. Water output over the course of the morning would therefore be relatively large and fast, accounting for the steep gradient of the rising limb of the diurnal hydrograph. Attenuation of melt production in the afternoon may then occur less quickly again because this 'ripeness' results in a great sensitivity to energy input. A significant zone of bare ice will be exposed during the summer and autumn months (as it was in 2005 - see Figure 53) and as temperate glacier ice is also, by definition, at or near 0°C (Oerlemans, 2001), all incoming energy should be directly available for melt. Furthermore local, thermally driven katabatic winds are likely to have been an important source of turbulent energy exchange during the late afternoon and early evening and melt from this source is likely to have contributed to the low gradient of the falling limbs of the diurnal hydrographs.

The stage records appear to show a strong relationship between diurnal fluctuation and air temperature. Flow magnitude fluctuated 39mm on average over the course of a day. The largest diurnal variation observed in this data set was a fall of 105mm between 5pm on the 18$^{th}$ of February 2006 and 10am on the 19$^{th}$ of February 2006, but the amplitude of diurnal fluctuation during March (the only month for which records exist for both 2005 and 2006) was noticeably lower in 2006 (Figures 41 and 46). Average air temperature for the overlapping period of atmospheric record – from the 24$^{th}$ of February to the 13$^{th}$ of March - was significantly higher in 2005 at 4.8°C, than it was in 2006, at 2.4°C, while shortwave radiation was higher over the same period in 2006, at 149.3wm$^{-2}$, than in 2005, at 124.5wm$^{-2}$. Moore and Demuth (2001) found that diurnal variability in discharge from Place Glacier, Canada, correlated to daily fluctuations in air temperature and the results of this study suggest that the diurnal variation seen in the Brewster record also relates to daily temperature fluctuation and not radiation fluctuation. This finding is supported by the work of Anderson et al. (2008), in which the authors found that the sensible heat flux was an important contributor to ablation at Brewster Glacier. A reason cited by Oke (1978) for the importance of shortwave radiation in diurnal discharge production is the changing value of albedo during the course of the day: in the mornings and evenings, the albedo from ice and/or snow is higher than it is at midday when the surface is wet with melt water. If the ice and snow surfaces at Brewster Glacier are typically ripe for most of the twenty-four hours of a day, this effect may be less pronounced, accounting for the lesser importance of shortwave radiation at the site.

The diurnal signal in streamflow became more suppressed as the seasons progressed. Variation in the earliest records of both years was greater than that in following months, and the diurnal pattern was more distinct. A decrease in the diurnal variation of discharge from temperate glaciers due to overall energy attenuation is well documented (Menzies, 1995). Figure 87 shows the mean diurnal variation in runoff of a glacier in the Austrian Alps over the Northern Hemisphere spring-autumn period. Such a pattern can reasonably be expected to occur in the proglacial streams of Aotearoa New Zealand as well, and the apparent seasonal progression observed in this study is likely to represent one part of such a broader pattern.

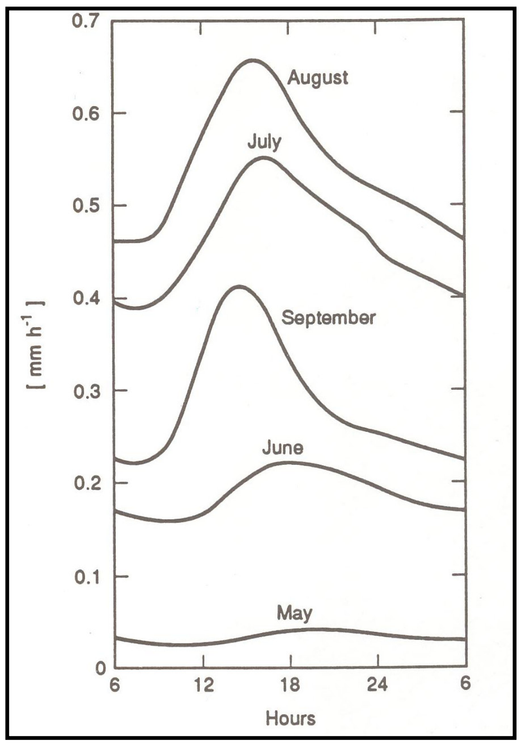


**Figure 88. Mean diurnal variation in runoff, 1974-1978, for Verngtbach (Austrian Alps), over the period May-September (from Menzies, 1995).**

There are four possible causes for the progressive suppression of the diurnal signal: 1. the drainage system was freezing up and becoming less hydraulically efficient, 2. diurnal variability in atmospheric conditions was decreasing, 3. air temperatures were more frequently dropping below zero so that melt was progressively decreasing and solid precipitation was occurring, and/or 4. snow cover on the glacier was becoming more extensive, causing higher albedo, less melt and suppressing the connectivity of water flow between the glacier surface and proglacial channel. Sharp (2005) asserts that the major factors in decreasing diurnal discharge variation are the increased depth of the supraglacial snowpack which slows transmission of water, and the closure of englacial and subglacial drainage channels, both resulting from decreased energy input. Evidence for increased diurnal discharge variability as the ratio of firn to snow cover increases was found by Moore and Demuth (2001) in their study of Place Glacier. Sharp (2005) also suggests that as a drainage system begins to freeze up during autumn and the major channels empty of water, pressure in them decreases and drainage from high pressure minor channels is thereby initiated. The rate and quantity of discharge is then controlled by drainage from these smaller auxiliary channels which occurs more slowly and at lower magnitude than it does from the large.

Figures in Chapter 3, Section 7.1 show that variability of atmospheric conditions did not decrease over the course of either year, but that overall air temperature and shortwave radiation input did. Given this and the fact that the form of peak flow events showed no seasonal progression, as discussed above, the first possible cause for diminishing diurnal variability in stage stated above may be discounted, and the second largely so at least as a primary cause of this phenomenon. Having said that, Klok and Oerlemans (2002) note that diurnal variation at Morteratschgletscher, Switzerland was barely distinguishable on cloudy days where the pattern was distinct on clear ones. While it was not measured, it is possible that increased cloudiness in autumn contributed to some degree to the attenuation of the diurnal signal through its effect on radiation receipt, and this would also have decreased in autumn as a result of the solar angle and increasing albedo as snow cover increased.

If the drainage system did not close up to any substantive degree but melt input did decrease, the likelihood that flow from secondary englacial channels increased is indeed high and this may also have contributed to the change in the form of the diurnal signal. Figure 42 shows the stage hydrograph from the 14$^{th}$ to the 18$^{th}$ of April 2005. The diurnal signal is comparatively mute in this graph. The source of this suppression could not be identified in the precipitation or air temperature records (Figures 55c and 60c respectively) (no precipitation was recorded during the period and air temperatures were consistently above zero degrees) and so it may well be the result of a weak diurnal signal confused by an extending snowpack and input of water from high pressure subsidiary channels. This, combined with lower air temperatures and decreased rainfall - together creating the conditions outlined in the 3rd and 4th explanations given above - sufficiently explains the decreased diurnal variability observed in Brewster Proglacial Stream.

### 1.03 Seasonal evolution of streamflow

There is a clear seasonal signal in the stage record. Graphs of moving average stage were created to examine the overall pattern in stage through time (Figures 37 and 38). In these, the $R^2$ value is 0.53 in 2005 and 0.61 in 2006, with gradients of -3.6 and -7.3 respectively. Average stage for both years combined was 536mm in summer and 364mm in autumn (Table 3) - a 32% decrease. From the 8th February to the 13th of March baseflow decreased 87mm in 2005 and 117mm in 2006 (Table 5), as mentioned above. The similarity of the change in each year suggests that a decrease around this magnitude is characteristic of the stream and that a linear relationship exists between time, at the seasonal resolution, and discharge magnitude. An overall decrease in discharge almost always occurs in temperate glacierised catchments from the end of summer, for the same reasons that diurnal variation decreases (Menzies, 1995).

Fitzharris (1979) suggests that a unique streamflow signature exists in South Island rivers resulting simply from altitude and the storage time of snow in upper Southern Alps catchments. Rivers draining from high altitude catchments (in which there is a permanent snowbase and winter snowfall is high) tend to have a minima during July, the month of lowest insolation. Streams issuing from low altitude catchments (in which there is no permanent snow base and snowfall is perennial) have the earliest peaks, around October, while streamflow from high altitude catchments tends to peak around November. Brewster Glacier, at around average altitude on the Main Divide, with a permanent snowbase and in the vicinity of Wanaka, Wakatipu, Hawea and Shotover, cited in Fitzharris (1979) for having November streamflow peaks, is likely to be one of those with a November streamflow peak. If that is the case, the record of streamflow presented in this study is a mid-section of the decrease towards a July minima.

It was expected that if the drainage system channels were constricting with progression of the seasons, the ratios of rising limb to falling limb of peak flow events would increase, as the time for water transmission from the glacier surface to the channel increased and intensity of melt decreased. This was not observed in the data (Table 4), supporting the hypothesis that the arborescence of the drainage system did not change significantly during the study period.

**<u>Section 2: Atmospheric variables and discharge from Brewster proglacial stream</u>**

## 2.0 Single linear regressions

### 2.01 Method reliability and limitations

As mentioned in the results (Chapter 3, Section 7.01) no lag time for response in stream flow was evident in the single regressions, but lag times did become important in the multiple regressions, as discussed below. In reality, there must be a lag time for response of streamflow to changes in energy inputs, and the superficiality of single linear regressions is highlighted by this lack of sensitivity.

### 2.02 Results

There was a significant difference between the hourly average data and daily total data $R^2$ values for stage and each atmospheric variable (Tables 10 and 11). The difference is the result of smoothing that summing the daily data produced. Small aberrations, such as the collapse of an ice barrier between a blocked moulin and a supraglacial pool, or the collapse of a subglacial channel wall (as observed during the study period) would produce sudden, short-lived perturbations in stage uncorrelated with atmospheric variables at the hourly scale. These events and others like them are related to atmospheric conditions, but must have a ‘preparation’ period during which atmospheric energy is absorbed with little distinguishable effect until a threshold is passed and the event occurs. In such cases stage would indeed be more highly correlated with the daily atmospheric conditions than hourly. The results for the daily total data were therefore more useful in finding generalised relationships, while the hourly average data were interesting in that they gave an indication of how often such small input events occurred.

The highest $R^2$ values were each found in the summer analysis, these being between stage and wind speed for both the hourly and daily data (0.42 and 0.73 respectively), and between stage and precipitation for the daily data (0.62). The coefficient for summer stage and precipitation in the hourly analysis was 0.27, and in the daily analysis the coefficient for stage and relative humidity was 0.29. The strongest relationships during autumn showed up in the daily analysis, these being between stage and temperature (0.21), relative humidity (0.24) and precipitation (0.36) with the value for stage and precipitation in the hourly analysis being 0.22. In the full data analysis, the $R^2$ values were highest between stage and relative humidity (0.22) and precipitation (0.25), higher again in the daily analysis than the hourly. All other $R^2$ values were below 0.20 showing weak relationships.

Relative humidity and precipitation are closely linked. In the graphs in Chapter 3, Section 7.1 (Figures 56 and 60), it can be seen that relative humidity was always high when precipitation events were occurring. However, there were also times when relative humidity was high and no precipitation was recorded. It is possible that these humidity events actually represent precipitation events that were erroneously removed from the record, or they may be entirely independent. In this analysis of correlation, relative humidity is likely to have acted as a proxy for precipitation at least in part, contributing to the high $R^2$ values.

Consistently higher $R^2$ values in summer than in autumn suggest one or both of two things: 1. that the drainage system was more arborescent during summer, and/or 2. atmospheric conditions were more conducive to rainfall and melt production in summer than in autumn. Given the above discussion relating to the form of peak flow events and the seasonal evolution of the air temperature and precipitation records, the second explanation is more likely. The high $R^2$ values between stage and wind speed highlight the importance of the turbulent energy flux at the glacier surface and between stage and relative humidity the latent heat flux, both of which will be elaborated on below.

### 2.02a Wind speed

Numerous authors have shown the effectiveness of wind speed in increasing melt at snow and ice surfaces (Sturman and Tapper, 2006; Moore and Owens, 1984; Oerlemans and Grisogono, 2002; Oerlemans and van den Broeke, 2002; Oerlemans et al., 1999; Paterson, 1994; Prowse and Owens, 1982). Wind speed only contributes to melt production when air temperatures are above zero degrees (Moore and Owens, 1984), as it does not itself input energy but only enhances the turbulent heat fluxes. The exchange of sensible and latent heat is greatest when the temperature gradient at an ice surface is large, and even more so when air in the boundary layer is turbulent. Fitzharris et al. (1992a), in a comparative study of energy balance at Aotearoa New Zealand snow and ice surfaces, suggest that in this country's maritime climate, turbulent energy transfers dominate.

The type of wind, whether driven by large scale pressure gradients or by local thermal gradients, is unimportant, and high air temperatures and radiation receipt therefore feedback positively in melt production by contributing to the development of katabatic winds. During summer particularly, when ground surrounding a glacier is often exposed, anabatic winds on surrounding bedrock slopes develop during the day and reach peak strength in late afternoon and early evening. Because the ice surface itself is never above 0°C, these winds flow up and around the glacier and can then become entrained in a local katabatic flow back down over the ice surface itself (Figure 88 depicts the most common pattern of wind flow over a glacier surface). This phenomenon is most pronounced when the boundary layer atmosphere is well stratified. Oerlemans and Grisogono (2002), Oerlemans and van den Broeke (2002) and Oerlemans et al. (1999) in particular have documented the importance of locally derived katabatic winds in melt production when the temperature gradient of the boundary layer is stable.

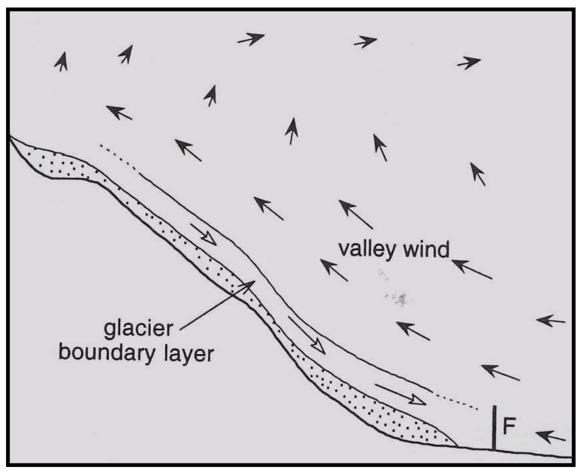


**Figure 89. The basic structure of wind circulation in a glacierised valley (Oerlemans, 2001).**

In this study, the $R^2$ values for wind speed and stage vary considerably between the hourly and daily analyses. The hourly value changes from 0.07 to the daily value of 0.11 in the full data analysis, for the summer data from 0.42 to 0.73 and for the autumn data from 0.13 to 0.05 (Tables 10 and 11). The marked change in the summer values suggests a high frequency of short-term runoff events that confuse the relationship between the turbulent energy exchange and discharge, which in turn suggests a comparatively high degree of instability in the structure of the glacial drainage system during summer. When discharge was measured in the field, small ‘icebergs’ floating down the proglacial stream and the collapse of an inner wall of the stream mouth were observed. It was inferred that such collapses of the drainage system structure occurred frequently, and it is likely that this also resulted in the release of temporarily pooled water throughout the channel system.

The difference in the $R^2$ values for summer and autumn is an indication of the importance of wind speed when combined with high heat energy input. The seasonal change is well illustrated in Figures 57a-57d. The agreement of patterns in each data set is much more striking in the summer record than in the autumn, with each peak in wind speed corresponding to a peak in stage. Air temperatures in the summer 2005 record never dropped below zero, while they did in the autumn. In the latter season, there were two peaks in wind speed (Figure 57c) at times when air temperatures were below zero (Figure 55c) that corresponded with low values of stage, while all but one high wind speed event occurred concurrently with high stage events when air temperatures were above 0°C. In 2006, corresponding peaks in wind speed (Figure 57d) and stage only occurred when air temperatures were also above zero (Figure 55d).

Air temperature and wind speed were negatively correlated with each other in each of the full data, summer and autumn single linear regressions, but with very weak $R^2$ values (-0.031, -0.015 and -0.019 respectively). The consistency of the negativity indicates that there was a trend of high wind speed with low air temperature, despite the low magnitude of the values. As noted above, high air temperatures and high wind speeds can be associated with each other as the local thermal gradient is enhanced (Moore and Owens, 1984, for example), but during storms are likely to be negatively correlated. Anecdotal evidence suggests that katabatic winds are indeed a noticeable feature of Brewster catchment but occur in all conditions (as on Morteratschgletscher and noted by Klok and Oerlemans (2002)), and some of the precipitation (storm) events that occurred during the study period did so in concert with relatively high air temperatures (on the 5$^{th}$ of March 2005 for example). This explains why the $R^2$ values for air temperature and wind speed are of low magnitude and suggests that while most often high wind speeds occurred in association with cool storms, strong katabatic winds in association with high air temperatures were also relatively frequent in the catchment.

### 2.02b Atmospheric pressure

Atmospheric pressure was an odd variable to use as a predictor because it does not cause water production itself and is not included in energy balance equations except sometimes in calculation of the latent heat flux (Takeuchi et al., 1999). It is one step further removed from discharge than the other variables, and a proxy for atmospheric conditions rather than a causative factor. It was included in this analysis in order to determine if it can be used as a predictor of discharge given the relative ease of pressure data acquisition.

While the single regression $R^2$ values are low (Tables 10 and 11), there is a clear pattern of peaks in stage with troughs in pressure (Figures 59a-59d) – almost every peak in stage corresponded to a trough in pressure. This rules out the possibility that pressure acts as a proxy for shortwave radiation, as this latter is more likely to be high when pressure is high. It also provides an argument for its acting as a proxy for precipitation, relative humidity and/or air temperature, as these are often high when pressure is low. The $R^2$ values between atmospheric pressure and air temperature are positive in each of the full data, summer and autumn analyses (Tables 12-14), while those between atmospheric pressure and precipitation and atmospheric pressure and relative humidity are negative. This suggests that atmospheric pressure is a proxy record for precipitation and relative humidity in this analysis and not air temperature.

There is little consistency in the actual values for each corresponding peak/trough in the pressure and stage records; for example, in Figure 59c, Autumn 2005, there is a high stage event beginning on the 5$^{th}$ of March reaching a height of around 1000mm. The corresponding trough in pressure dips to around 810 hPa. Then, on the 25$^{th}$ of March another high stage event peaked at around 800mm corresponding to a trough just below 800 hPa. Were the two variables directly correlated, the lower of the two pressure troughs would correlate to the higher of the two peaks in stage. This accounts for the low $R^2$ values and suggests two things: 1. that the correlating patterns are indeed the result of the negative relationship between pressure and precipitation and relative humidity and 2. that there is a certain value of pressure below which precipitation and/or melt almost invariably occurs, but the magnitude of the trough does not determine the amount of precipitation that falls or melt that occurs.

### 2.02c Relative humidity

Relative humidity is an important contributor to the energy balance equation as a measure of the provision and removal of latent heat (Sharp, 2005). When the vapour pressure gradient is negative, condensation or rime ice forms on ice surfaces, releasing the latent heat of vaporisation – 7.5 times the latent heat of fusion required for melt of snow or ice (Hock, 2005). When the vapour pressure gradient is positive, the latent heat of both fusion and of vaporisation is used in the process of evaporation and/or sublimation, cooling the ice surface. Paterson (1994) asserts that the condensation of just one gram of water on an ice surface releases enough energy to melt eight grams of ice. The energy involved in either condensation or evaporation/sublimation is greatest when the vapour pressure gradient is steep (Oerlemans, 2001). Sublimation is not an important process in the mid-latitudes (Paterson, 1994), and so will not be discussed further.

Both absolute and relative humidity are a function of air temperature in a relationship approximating a positive power function (Chow, 1964). More melt water is produced when both air temperature and relative humidity are high because the capacity of the air to hold water is greater when warm, so that high relative humidity indicates a high absolute value of water content. When air temperature is low and relative humidity is high the actual moisture content of the air is relatively low (Sturman and Tapper, 2006). The flux away from snow and ice surfaces is greatest during the day and the flux toward the surface is greatest during night, correlating to air temperature (Sturman and Tapper, 2006).

The $R^2$ values between stage and relative humidity for the full data, summer and autumn analyses are each high and consistent, and slightly higher for summer than for autumn (0.29 and 0.24 respectively in the daily analysis, 0.19 and 0.14 in the hourly, Tables 10 and 11). While less distinctive than some others, there is a clear pattern of peaks in stage with concomitant peaks in relative humidity (Figures 56a-56d). As mentioned above, this is an indication of the importance of the latent heat flux in generating melt. When air temperatures were above zero (as they often were in the autumn record and always were in the summer record) and relative humidity was high, condensation is likely to have occurred on the ice surfaces and when air temperatures were below zero and relative humidity was high rime ice may have formed, in both cases releasing latent heat and precipitating melt production if not causing it directly. The slightly higher $R^2$ value for summer suggests that the process of condensation either produced more melt or occurred more frequently than it did in autumn, and there is in fact no further indication that the formation of rime ice in autumn was important in melt production (given the concurrence of temperatures below zero, high relative humidity and low stage, on the 25$^{th}$ of April 2005 and the 9$^{th}$ of March 2006 for example).

Relative humidity has a high negative correlation with shortwave radiation in both the summer and autumn analyses (-0.78 and -0.34 $R^2$ values respectively) and high positive correlations with precipitation in each season (0.41 and 0.12 respectively). These are likely to be indicative of the same wet, cloudy conditions that are conducive to high relative humidity.

### 2.02d Precipitation

Precipitation's contribution to discharge has a number of forms. Firstly in the provision of water to the catchment in either liquid form, in which case the effect on streamflow is swift where refreezing does not occur, or in solid form in which case a delay in the response of streamflow will occur. Secondly, warm rain that falls on a snow or ice surface at freezing is cooled and thereby releases sensible heat (Sharp, 2005), and where the snow or ice is below freezing precipitation is cooled first to the freezing point and then beyond, in which case it releases first sensible and then latent heat. The released energy is absorbed and causes an increase in the snow or ice temperature and/or melt. Finally, rainfall held by snow in liquid form can reduce the albedo of that surface, inducing higher radiation absorption (Oke, 1978).

Precipitation is not generally thought of as an important contributor to the energy balance of glaciers. However, in maritime climates, where warm, intense and prolonged rainfall events occur, it can be significant (Hock, 2005). For example, Hay and Fitzharris (1988) recorded a rainfall event at Ivory Glacier, Aotearoa New Zealand in which 37% of the energy available for ablation was provided by the precipitation heat flux.

Precipitation is generally assumed to fall as snow when air temperatures are below around 2°C (Makintosh, pers. com.). On contact with ice and snow surfaces at 0°C, it can remain frozen even when the air is at this temperature. In this study it was assumed that precipitation falling with air temperatures above 2°C was in liquid form and below 2°C in solid form.

The $R^2$ values for precipitation and stage in the full data single regressions are lower than were expected, but quite high for each of the seasons in the hourly regressions (0.27 for summer and 0.22 for autumn) and substantively higher for each season in the daily regressions (0.62 for summer and 0.36 for autumn) (Tables 10 and 11). The higher correlation between stage and precipitation during summer than autumn indicates that most precipitation occurred as rainfall during summer and temperatures were high enough for that rain to remain in liquid form as it travelled through the glaciers drainage system. The lower coefficients in the hourly analysis than the daily may be an indication of the time it took for rain to travel through the glacier's drainage system and of temporary storage therein, and/or of a lag time for the heat of rain to have effected melt.

Precipitation is negatively correlated with shortwave radiation in both summer and autumn (-0.49 and -0.37 respectively), positively correlated with relative humidity in each season (0.41 and 0.19 respectively) as discussed above, and positively correlated with wind speed in each season (0.63 and 0.47 respectively) (Tables 12-14). The negative relationship precipitation has with shortwave radiation is an indication of the high degree of cloudiness during precipitation events. A higher $R^2$ value between relative humidity and precipitation during summer than in autumn suggests that air temperature was generally higher during summer than autumn, allowing for greater air moisture content in general and during precipitation events in particular. Positive correlation between precipitation and wind speed was unexpected; the lack of a wind shield on the precipitation gauge was expected to result in low catch during high wind events. Figures 57 and 60 illustrate this positive relationship. For every precipitation event, wind speed is also relatively high. The results suggest that the precipitation gauge may have worked effectively even during windy conditions, although it is impossible to know how much more precipitation may have been recorded had a wind shield been incorporated in the design. High wind speed and precipitation are both features of low pressure systems, and these results only confirm that the experience of high winds during storm events in Brewster catchment were accurate.

### 2.02e Shortwave radiation

Shortwave radiation contributes to the net radiation term of the energy balance equation (Oerlemans, 2001). It causes snowpack ripening, snow and ice melt where directly absorbed and its transferral of energy to air masses and bare ground (producing a thermal gradient and katabatic winds through the process discussed above) can also indirectly influence melt rates. In cloudy conditions and at night direct radiation receipt at ground level is minimal, and thus the term is most important on clear days. It is much more important to melt during summer than any other season both because of the solar angle and the fact that bare ice has a lower albedo than snow. Snow absorbs only around 1-2% of incoming shortwave radiation, with an albedo of 0.7-0.9 compared to only around 0.3-0.5 for ice (Paterson, 1994). Furthermore the thermal conductivity of ice is higher than that of snow, such that absorbed energy is transmitted to greater depths of an ice surface than a snow one (Hock, 2005). Even a thin layer of snow over an ice surface can significantly reduce melt rates.

More than any other term, the importance of shortwave radiation in a particular catchment is affected by aspect. Brewster catchment is south facing, and as a result, the seasonal change in solar angle could be expected to have a noticeable effect of the receipt of shortwave radiation.

Shortwave radiation has the lowest $R^2$ values of all the input variables (0.00, 0.01 and 0.01 in the hourly analysis and 0.01, 0.19 and 0.06 in the daily) (Tables 10 and 11). This is somewhat surprising, as shortwave radiation is frequently cited as the most important energy source for melt production (Sturman and Tapper, 2006; Hock, 2005; Arnold et al., 1998; Neale and Fitzharris, 1997; Owens et al., 1986 for example), and is elaborated on below in discussion of the multiple regression analysis. The higher value for the daily summer analysis (0.19) than the autumn (0.06) is indicative both of relatively high radiation receipt during clear sky periods and increasingly extensive snow cover and albedo through time. The only strong correlations between shortwave radiation and the other atmospheric variables are negative and exist between shortwave radiation and relative humidity, precipitation and wind speed, indicating that the latter are highest during cloudy periods.

### 2.03f Air temperature

Marcus et al. (1985) assert that the effects of precipitation and air temperature on melt are not independent. These authors state that high ablation occurs when both precipitation and air temperature are high and that highest ablation occurs during warm rainfall events, while accumulation occurs when both precipitation and air temperature are low. These assertions are supported by the results of this study as discussed above. Air temperature effects melt by contributing to both the sensible and latent heat fluxes – warm air provides sensible energy for melt and also for evaporation, the latter of which results in higher vapour pressure gradients in the boundary layer and thus the strength of the latent heat flux (Huntington, 2006; Sturman and Tapper, 2006). Moore and Owens (1984) found in a regression analysis that 56% of the variance in air temperature and 60% of the variance in vapour pressure was explained by the average temperature of the corresponding air mass, increasing to 77% and 78% respectively with the addition of average air mass temperature lagged by one hour. The transfer of sensible heat to or from snow and ice surfaces depends on the intensity, direction and turbulence of the temperature gradient in the boundary layer (Sturman and Tapper, 2006).

Like shortwave radiation, air temperature has low $R^2$ values in the single regression models - the highest is for the autumn daily totals at 0.21 (Table 11). Figures 55a-55d present the stage and temperature records and show the least agreement in pattern of all the graphs. There are some high temperature events that very distinctly coexist with high stage events however, and this suggests that high temperatures are a factor in melt production when combined with other conditions conducive to melt such as high relative humidity or high wind speed. The $R^2$ values for air temperature and relative humidity are consistently negative, indicative of the greater capacity of air to hold moisture when it is warm. Similarly the $R^2$ values for air temperature and wind speed are consistently negative and likely to be indicative of storm conditions. The significance of these relationships will be discussed further in the following sections.

## 2.1 Multiple linear regressions

### 2.11 Method reliability and limitations

It is likely that reliable predictions using the multiple regression method could only ever be made for daily total discharge/stage and not for any higher resolution because of the high degree of autocorrelation in the discharge and stage records. This is satisfactory; the equations produced by the models using daily total values show a high degree of agreement with the measured record.

Covariance between precipitation and wind speed has been a problem, and was first assumed to be the result of undercatch by the precipitation gauge during high winds as this is a common problem in mountain catchments, as documented by a number of authors (for example Xia and Xu, 2007; Sieck et al., 2007; Duchon and Essenberg, 2001). However, as discussed above, positive correlation between the precipitation and wind speed records indicates that in fact the covariance was a natural phenomenon and not entirely an artefact of the gauge. Nevertheless, the result is that the importance of the two variables in discharge production was muted by the presence of the other, as identified in discussion of the model results below.

Testing for the reliability of the equations outside of the study period was not possible due to the lack of independent data sets. The equations generated by the model were tested for reliability by comparing predicted values to the same measured values that the equation is generated from. Naturally, there is going to be a high degree of correlation between these values. It is highly unlikely that the correlation would be as high with a discharge record taken in the future.

As mentioned above, the lack of high and low flow measured discharge data points has limited the accuracy of the ratings curve, and the discharge values are especially questionable at the extremes. For this reason, stage was used for the analysis, and reliability of discharge predictions made using the models is limited.

Finally, for practical application – for use to hydro-power generation for example - prediction of a full years discharge would be most useful. As the following analysis shows, the relationship between discharge and atmospheric variables varies considerably between just autumn and summer, and the shape of the hydrograph (as well as anecdotal evidence) suggests that it will vary markedly during winter and spring as well. In Brewster catchment, as with many glacierised catchments, there is very little water flow during winter. The proglacial lake is largely frozen and the channel itself entirely obscured by a layer of snow and ice. This is prohibitive to the record of stage for one thing (as discovered during the course of this study, where the stage gauge became blocked by ice and failed to record (Anderson, pers. com.)), and is also likely to have a significant impact on the response of the proglacial stream to any influx of water. For annual discharge prediction, the changing physical characteristics of the catchment and drainage system in particular would need to be accounted for.

### 2.12 Results – predictive models

The $R^2$ values for the 'enter' models are 0.63 for the full data record, 0.86 for the summer record and 0.61 for the autumn record. While having the highest $R^2$ value, the summer predictions may be least reliable as the total number of data points is only 23. Having said this, the high value may instead (or as well) indicate a comparative simplicity in the relationship between atmospheric variables and discharge during summer. If this is the period in which the drainage system is most arborescent, most precipitation is in liquid form, least refreezing of precipitation and melt occurs, and least supraglacial, englacial and subglacial storage occurs, then the response of streamflow to variation in atmospheric conditions would indeed be most straightforward. The lower coefficient for autumn could be an indication of increasingly retarded flow pathways. Water may be hindered in its journey from precipitation to discharge by the form in which it is precipitated, by poor conditions for melt, by closing moulins, englacial and subglacial channels, by increasing pressure in these channels and by refreezing. The proposition that the drainage system morphology became more restricted is not supported by the changing form of the diurnal hydrograph, as discussed above, but this does not rule it out altogether as a possibility. The low $R^2$ value for the autumn 'enter' model is almost certainly the result of low water input, increasing transmission retardation by a snowpack, increasing degrees of refreezing and storage, but there may also have been some degree of channel constriction occurring in late autumn that is not obvious in the form of the hydrographs but that the models were sensitive to.

As mentioned above, atmospheric pressure does not itself cause melt or precipitation but only brings about the conditions required for this. It is interesting therefore that the predictive capacity of the models is invariably higher when atmospheric pressure is included as a predictor. This suggests that the variable adds weight to important patterns in the data; for example, high wind speeds are generally associated with low pressure circulation and, given that the importance of wind speed is diminished in the models by the presence of the covariant precipitation record, the inclusion of atmospheric pressure may have given weight to this pattern that would not otherwise be accounted for. However, some authors suggest that low atmospheric pressure increases the latent heat flux (Takeuchi et al., 1999), so it is possible that inclusion of the variable in the models increases representation of this energy flux and thereby increases their accuracy.

The error term (Constant) in the Full Data model (Ab, Table 19) is $|2109.990|$, in the Summer model (Bb, Table 24) $|1484.136|$ and in the Autumn model (Cb, Table 29) $|3460.622|$. The low value for the summer model supports the hypothesis that it was not limited by a lack of data but that discharge was controlled more directly by atmospheric conditions in summer than it was in autumn. The actual magnitude of the error terms is the amount of unexplained variation added automatically to the models per 1mm variation in stage to increase their accuracy. This gives a sense of how well the models would predict stage or discharge during a different study period – which these values indicate would be fairly poorly.

**2.13 Results – diagnostic models**

Each of the 'stepwise' models met the assumption criteria outlined in Chapter 3, Section 8.1 and illustrated by the 'goodness-of-fit' statistics and Figures in Appendix 2. The diagnosis used the included and excluded model parameters in Chapter 3, Section 8.31.

No Summer Dry ‘stepwise’ model could be produced. Table 42 presents the statistics for three ‘enter’ models that were made in order that the source of error could be examined. It shows that when all the variables were included as predictors, only shortwave radiation made a statistically significant contribution to prediction of stage, but had too high a VIF value. When the three variables with the lowest values of significance – shortwave radiation, relative humidity and wind speed - were included as predictors alone, they each become too highly covariant. Finally, when wind speed – the variable of these latter three with the lowest value of significance and lowest VIF statistic - was used as a predictor alone, its value of significance increased beyond the model’s 95% criteria. There were only twelve days in the summer record during which no precipitation occurred (and only thirteen on which precipitation did occur). No doubt these models would benefit from extra data, but the fact that a model could be constructed using only the thirteen data points for the Summer Wet model indicates that the lack of data alone is not the cause of the problems in the Summer Dry model. The summer data for relative humidity and shortwave radiation correlate by -0.795 (Table 13). As discussed above, this is indicative of the tendency for relative humidity to be high during cloudy conditions. Also discussed above is the importance of wind speed combined with a latent or sensible heat source, as opposed to alone. It was these two physical relationships between the variables that precluded the creation of a multiple regression model.

The results of the Summer Dry ‘enter’ models hint at shortwave radiation and wind speed (net radiation and the turbulent convective heat flux) being the most important melt producers during dry periods respectively, and perhaps more sensitive to variation in relative humidity (the turbulent latent heat flux) than air temperature (the sensible heat flux) but because the models do not meet the criteria for robustness, are inconclusive.

The error term varies greatly between the models (Chapter 3, Section 8.31). The lowest, |106.472|, was given for the Full Data Dry model (E) (Table 34), while the greatest, |12453.772|, was given for the Full Data Wet model (D) (Table 31). This is an important indication of the degree to which variation in stage was controlled by atmospheric conditions during the specified period, even where the adjusted $R^2$ value is high; it may be that with inclusion of the error term a model worked well in accounting for the variation in stage, but that value represents causative factors that are unknown and cannot be diagnosed.

### 2.13a Wind speed

Wind speed was included as a predictor in three stepwise models: the Full Data model (Aa) (Table 16) as the fifth and least important variable, the Summer model (Ba) (Table 21) as the first and sole variable and in the Summer Wet model (Fa) (Table 37) again as the first and sole variable. Clearly the turbulent heat flux was of great importance to melt production at Brewster Glacier during summer. Moore and Owens (1984) assert that wind speed can often be more important in melt production than air temperature because high air temperatures result in more stable temperature stratification in the boundary layer which discourages transfer of both latent and sensible heat. As discussed above, a strong temperature gradient and stable stratification of the boundary layer is conducive to production of katabatic winds (as discussed above), and this goes some way to explaining why wind speed has such importance in the summer models and not the autumn ones.

In the excluded variables for model Ca, Autumn, the value for significance of wind speed was high (0.316), the partial correlation value low (0.146) and the tolerance and VIF statistics (0.404 and 2.474 respectively) indicate covariance with the precipitation record (Table 27). In Model H, Autumn Wet, wind speed was included as the first predictor in the 'stepwise' process, and then removed at the sixth stage after the successive inclusion of relative humidity and then precipitation caused its VIF statistic to increase beyond the acceptable limit (Table 44). The exclusion of wind speed from the Autumn Dry model (Model I) however could obviously not have been the result of covariance with precipitation and in this case the statistics for covariance were indeed acceptable, but the value of significance for wind speed was high – the final value being 0.960 (Table 48).

In autumn, air temperatures were more often near or below zero than they were in summer. Given that wind speed only makes an effective contribution to the exchange of energy when air temperatures are above zero, it is likely that its importance to melt production diminished in autumn because high wind speed events less often occurred in concert with high air temperatures. The two variables are negatively correlated (Tables 12-14), indicating the concurrence of cold air and high winds during storms. Furthermore, with the development of a snowpack in autumn surface roughness would have diminished, decreasing the effectiveness of wind speed in producing turbulent exchanges of energy (Klok and Oerlemans, 2002; Stull, 1988) and the high, positive $R^2$ value for precipitation and wind speed (0.466) indicates that wind speed was anyhow typically low when no precipitation was occurring (Table 14).

Therefore, with runoff more frequently driven by net radiation and the latent heat flux during clear periods (indicated by the relative importance of these variables in the Autumn Dry model) and by precipitation and air temperature during precipitation events, wind speed was far less important in autumn than it was during summer.

It is important to note that the climate station recording wind speed was below the glacier rather than on it. It is possible that a katabatic wind on the glacier itself was quite different to wind around the proglacial lake. Given that relative humidity was important in the Autumn Dry model, it seems unlikely that variation in wind speed had no effect on melt. Perhaps wind speed around the proglacial lake was so different to those on the glacier itself that the record did not correlate to variation in discharge and it was for this reason alone that it was not included in the model.

### 2.13b Atmospheric pressure

Atmospheric pressure is included in only one stepwise multiple regression model, Model I (Chapter 3, Section 8.31), Autumn Dry. Possibly, atmospheric pressure acted as a proxy for the air temperature or wind speed records and added weight to the relative humidity record. However, if this were the case it could be expected that the covariance between these records would be high, but there was only a slight increase in the tolerance value for relative humidity with inclusion of atmospheric pressure (Table 46), and the value of tolerance of air temperature as an excluded variable for the third model (Table 48) was in fact slightly lower once atmospheric pressure had been added to the final model than it was previously. The turbulent latent heat flux tends to increase when atmospheric pressure is low, as it increases the vapour pressure gradient (Takeuchi et al., 1999). Therefore, it is likely that it was this effect that was represented by atmospheric pressure in the model. Given that autumn was typically cooler than summer and that relative humidity was invariably lower during dry periods than wet, it is possible that the effectiveness of relative humidity was quite highly sensitive to variations in pressure during this period where in other conditions it was much less so.

In Model Aa, Full Data, atmospheric pressure is the only excluded variable and has a significance of 0.217 and partial correlation of -0.160. In the Summer model, Ba, it is excluded with a significance of 0.897 and partial correlation of 0.030. The statistics are similar in each of the other models from which it is excluded. Clearly, it does not provide much information that the other variables do not, but, as noted above, enough to aid prediction in the ‘enter’ type models.

### 2.13c Relative Humidity

Relative humidity was the most frequently included variable in the multiple regression models (along with shortwave radiation) (Table 49) indicating the importance of the latent heat flux in producing melt on Brewster Glacier. In the Full Data model, Aa, relative humidity was the first variable entered with a partial correlation of 0.538 (Table 16). This value increased with the addition of air temperature and shortwave radiation, remained the same with the addition of wind speed and decreased slightly with the final addition of precipitation. In the full data analysis of correlation (Table 12), relative humidity had a weak positive relationship with air temperature ($R^2$ of -0.015), a weak negative relationship with shortwave radiation (-0.035) and a fairly high correlation with precipitation (0.21). The model parameters show that the beta statistic for relative humidity increased substantially – from 0.531 to 0.717 - with the inclusion of shortwave radiation at the fourth stage.

In the Autumn model, Ba, relative humidity was entered in the third stage with a partial correlation of 0.386 (Table 21). This value increased to 0.488 with the subsequent inclusion of shortwave radiation. The $R^2$ value for relative humidity and shortwave radiation in autumn is -0.338 and again the beta statistic for relative humidity increased with the inclusion of shortwave radiation in this model. With a partial correlation of 0.512 and beta value of 0.301, relative humidity was entered at the second stage to the Full Data Wet model, D, and both values decreased with the inclusion of precipitation and increased once more with the subsequent inclusion of shortwave radiation (Table 31). In the Full Data Dry model, E, relative humidity was entered with shortwave radiation in the second and final stage with a partial correlation of 0.590, increasing the partial correlation of the latter from 0.459 to 0.666 (Table 34). Relative humidity was entered at the fourth stage to the Autumn Wet model, H, with a partial correlation of 0.499, decreasing the partial correlation of wind speed by 0.06, increasing the partial correlation of air temperature by 0.041 and increasing the partial correlation value of shortwave radiation by 0.104 (Table 44). Again, the relative importance of shortwave radiation increased with the inclusion of relative humidity as a predictor. The removal of wind speed in the final stage of this model increased the partial correlation value of relative humidity from 0.585 to 0.642. In the Autumn Dry model, I, relative humidity was the first entered variable with a partial correlation of 0.363, this value increasing to 0.519 with the inclusion of shortwave radiation in the second stage and decreasing slightly with inclusion of atmospheric pressure in the third and final stage (Table 47).

There is clearly a strong relationship between relative humidity and shortwave radiation. The two variables are negatively correlated, so the results indicate that the latent heat flux increased in relative importance to melt production as net radiation diminished - as it would have in cloudy conditions, and this further indicates that when high, net radiation is important enough in melt production to substantively mute any effect of the latent heat flux. The results also indicate that relative humidity is more effective at producing runoff when shortwave radiation is low. This is because when shortwave radiation is high the vapour pressure gradient is weaker than it is when shortwave radiation low; high shortwave radiation is conducive to evaporation rather than condensation such that the latent heat flux is diminished.

The $R^2$ values between relative humidity and air temperature are consistently negative, although very low in each case (-0.015 for full data, -0.024 for summer, -0.029 for autumn), indicating a weak but persistent relationship (Tables 12-14). Absolute humidity increases with air temperature given an increase in evaporation but relative humidity increases as air temperature drops, as the air then has a lower capacity to hold water vapour. The increase in the partial correlation and beta values for relative humidity and air temperature with the inclusion of the other in the Full Data and Autumn models respectively (Aa and Ca) (Tables 16 and 26), suggests the increasing relative importance of the latent heat flux as the sensible heat flux diminishes and vice versa. The beta value for air temperature decreased with the inclusion of relative humidity however in Models D and H (Full Data Wet and Autumn Wet) although maintaining a higher beta magnitude - indicating that the latent heat flux made a considerable contribution to melt production during precipitation events but that the sensible heat flux was in fact the more important of the two (Tables 31 and 44). Furthermore, air temperature greatly influences the latent heat flux – as Takeuchi et al. (1999) state, the latent heat exchange will be small in cold conditions even when the air is both turbulent and humid. So with a negative relationship between the two it makes sense that they should diminish each others relative importance when included together in a model.

The $R^2$ value for relative humidity and wind speed in the autumn record is 0.037 (Table 14). The increased partial correlation of relative humidity with the exclusion of wind speed at the sixth stage of Model H is indicative that similar information was provided by each record (Table 44). It is clear in Figures 56a-56d and 57a-57d that wind speed and relative humidity were both high during precipitation events - indicating storm conditions - and indeed the VIF statistic for wind speed increased beyond the acceptable limit with inclusion of relative humidity in the fourth stage. At the same time the beta value for wind speed decreased confirming that the two variables were providing a lot of the same information about the latent heat flux. At this stage the beta value for wind speed was still higher than that for relative humidity but with the inclusion of precipitation as a predictor in the fifth stage this value decreased by 0.415 and the VIF statistic increased over 5. This suggests that wind speed alone provided information about both the sensible and latent heat fluxes, air temperature – added in the second stage and decreasing the beta value for wind speed - was also providing information about the sensible heat flux, relative humidity alone provided information about the latent heat flux that was then compounded by the inclusion of precipitation such that altogether the information provided by wind speed was outdone by the information about both energy sources provided by the other three variables.

Relative humidity was excluded from Model Ba, Summer, with a significance of 0.536 and partial correlation of 0.143 (Table 22), and from the Summer Wet model, Fa, with a significance of 0.228 and partial correlation of 0.376 (Table 38). The $R^2$ value for relative humidity and wind speed (the sole predictor in these two models) is 0.294 (Table 13) but in both multiple regression models the statistics for excluded variables show that the covariance between the two was acceptably low; therefore it was only the lack of significance that caused relative humidity to be excluded from the models. The statistics for correlation in summer (Table 13) show that relative humidity was negatively correlated with shortwave radiation and air temperature, indicating that relative humidity was high during storm conditions in summer as it was in autumn. Wind speed is also negatively correlated with both air temperature and shortwave radiation, indicating the same. These results suggest that during summer the most important source of variation was the degree of turbulence in the boundary layer and not the absolute amount of latent heat available at any point in time. As discussed above, this is likely to be because air temperatures were invariably above zero degrees in summer, so that wind speed was always a contributor to the energy exchange, while in autumn it became less effective as air temperatures dropped making the absolute quantity of energy available more significant.

### 2.13d Precipitation

In Figures 60a-60d there is a very clear concurrence of precipitation events and peaks in stage, but also a great deal of variability in the stage record when no precipitation was falling. The latter variable was included as a predictor in four of the six models in which it was input (Table 49). It was fourth in importance in the Full Data model (Aa) (Table 16), highest in importance in the Autumn model (Ca) (Table 26), fourth in the Full Data Wet model (D) (Table 31) and highest in the Autumn Wet model (H) (Table 44). The covariance between precipitation and wind speed is clearly the reason for the exclusion of the former variables from the summer models, indicated by the fact that it was included as the sole predictor in Model Fb, Summer Wet Excluding Wind Speed, in which wind speed was manually omitted (Table 40).

Precipitation appeared to be important in the autumn models, and this is likely to be because of the incidence of rainfall and because the vapour pressure gradient tends to be high during precipitation events, but, as stated above, the importance of precipitation in summer was likely to have been greater than indicated in the models. The $R^2$ values for precipitation and relative humidity are positive in every case, albeit somewhat lower for autumn than summer, this most likely being the result of lower air temperatures during autumn (Table 13 and 14). The $R^2$ value for stage and precipitation in autumn is lower than that in summer, 0.36 as opposed to 0.62, which suggests that perhaps as much as half the precipitation during autumn fell in solid form. Together these results provide further evidence for the importance of the latent heat flux and possibly also the precipitation heat flux as the year advanced. As air temperature and shortwave radiation diminished, the relative importance of other sources of energy naturally increased.

### 2.13e Shortwave Radiation

Shortwave radiation has the lowest of all the $R^2$ values with stage (Tables 10 and 11) but was frequently the most important predictor in the multiple regression models and together with relative humidity, most often included in the models (Table 49). The explanation for this is best illustrated in Figure 58d. In that graph the diurnal variation in shortwave radiation and the small perturbations in stage that correspond are visible, while no such association between shortwave radiation and other peakflow events is evident. The same pattern (inversed) is evident in the atmospheric pressure record, but it is given far less importance in the multiple regression models than shortwave radiation. However, shortwave radiation has a noticeably greater impact on stage when acting in concert with wind speed and precipitation (as indicated by the beta variables in models including each, as discussed above) and it is likely that the importance of this variable was enhanced in the multiple regression models because it was included with those others, where atmospheric pressure does not increase in effectiveness in combination with other variables and thus received no such enhancement.

Contrarily, shortwave radiation had the lowest significance and partial correlation of all the excluded variables in the Summer Wet model (Table 37) (0.947 and 0.021 respectively). Air temperature has a relatively low value of significance and high value of partial correlation (0.69 and 0.542 respectively). Wind speed (the sole predictor in the Summer Wet model) and shortwave radiation were negatively correlated with comparatively high magnitude in each of the single regressions; air temperature and wind speed were negatively correlated with relatively low magnitude and shortwave radiation and air temperature were positively correlated with relatively low magnitudes (Tables 12-14). These statistics are a record of cloudy, warm, humid conditions during which the turbulent sensible heat flux was the most important contributor to the energy balance.

It is also interesting that shortwave radiation has the lowest value of significance in Model G (Table 42), enter type models for dry summer days. The G models are invalid given high values of covariance, but the statistics nevertheless point to the importance of net radiation in melt production during clear summer days.

### 2.13f Air temperature

Like shortwave radiation, air temperature has low $R^2$ values in the single regression models - the highest is for the autumn daily totals at 0.21. As mentioned above with reference to the single linear regressions, the pattern of air temperature and stage show little agreement in the graphs (Figures 55a-55d). However, air temperature was included as the third ranking variable in the Full Data (Aa) and Autumn (Ca) models, in which it was input second in each case, and the Full Data Wet (D) and Autumn Wet (H) models, in which it was input first and second respectively (Table 49). This indicates that overall, like shortwave radiation, air temperature's importance as a predictor increased when included with other variables and therefore that its capacity to produce discharge increased when combined with other conducive atmospheric conditions. The fact that air temperature was included first in the Full Data Wet model indicates that the effectiveness of the other variables in producing melt was largely dependent on the concurrent air temperature.

In Model H, Autumn Wet (Table 44), the beta value for wind speed decreased when air temperature was added, from 0.585 to 0.447. The beta value for relative humidity increased from 0.538 to 0.572 in the Full Data model (Aa) (Table 16) when air temperature was added and that for precipitation increased from 0.619 to 0.667 in the Autumn model (Ca) (Table 26). The importance of relative humidity in the Full Data model would have increased with decreasing air temperatures (the two were negatively correlated) because of a resulting increase in the vapour pressure gradient and therefore rates of condensation on the ice surface. In the Autumn model, high air temperatures during precipitation events indicates rainfall as opposed to snowfall and a larger precipitation heat flux. The $R^2$ value for wind speed and air temperature was negative in each case (as mentioned above) (Tables 12-14), so the decrease in the beta value for wind speed in the Autumn Wet model with the inclusion of air temperature is likely to be the result of the positive relationship between air temperature and wind speed in melt production.

Air temperature was not included as a predictor in either of the two summer models, excluded from the Summer (Ba) model with a significance of 0.425 and partial correlation of 0.184 (as the third most important predictor after wind speed and precipitation) (Table 22), and from the Summer Wet (Fa) model with the much lower significance of 0.069 and partial correlation of 0.542 (second in importance after wind speed) (Table 38). There is no evidence in any of the models for significant covariance between air temperature and any of the other variables. Interestingly, in Model Fb, Summer Wet Excluding Wind Speed, the excluded air temperature had a significance of 0.998 and partial correlation of 0.001 (Table 41). This indicates that variation in air temperature made little difference when not combined with variation in wind speed and that, because air temperature was always high enough for precipitation to fall as liquid, variation made little difference in this respect. In the 'enter' models for summer dry periods (Model G, Table 42), air temperature had the lowest significance. Together these results suggest that the influence of air temperature on the vapour pressure gradient, form of precipitation and heat of rain made it more important during precipitation events than any other time, that during dry periods the contribution of air temperature to melt via the sensible heat flux was low and that during summer the most important variation in atmospheric conditions was indeed turbulence in the boundary layer as discussed above.

### 2.14 Complex relationships – the beta statistics

Correlation between individual variables and stage was lower in every case in the single regressions (Chapter 3, Section 7.02) than they were in the multiple regression models (Chapter 3, Section 8.31). This indicates that the variables acted together in production of discharge (as discussed above). The following analysis looks at how the variables influenced each other using the change in beta values as presented in Chapter 3, Section 8.33. The analysis was done using the daily total data as the assumptions of a multiple regression model must be met for the beta statistic to be a valid diagnostic tool.

The beta statistic indicates the relative importance of each variable as a predictor in a model. Table 49 presents the beta values and corresponding relative importance of the predictors in each model. The relative importance of the variables changed depending on which sub-set of the data was being analysed, showing that the relationships between atmospheric variables and discharge production did not remain constant. The Tables and Figures in Chapter 3, Section 8.33 show the change in the magnitude of the relative contribution of each variable (the magnitude of the beta statistic) when one other was added as a predictor, indicting how the two variables influenced each other and how this influence changed under different conditions. Many of the relationships have been discussed above with reference to the diagnostic multiple regression models, so the following discussion is brief to avoid repetition.

#### 2.14a Wind speed:

As discussed above, wind speed and precipitation were highly covariant as a result of storm characteristics. This showed up again as a significant negative change in the wind speed beta values for each of the full data, summer and autumn models (Table 52 and Figure 69). This has made it impossible to say whether or not these two variables influence each others capacity to produce discharge.

The only other notable change in the beta value of wind speed occurred when relative humidity was added as a predictor in the full data analysis. The negative change of 0.102 indicates that the contribution of wind speed to the model decreased when relative humidity was added. As noted above, the wind speed and relative humidity records are positively correlated, and the decrease in beta would have been because they are each more effective when concurrently high.

### 2.14b Air temperature

The only large changes in air temperature beta values occurred in the summer model set (Table 50). The starting value for air temperature in this model was -0.008, changing to 0.553 with the inclusion of relative humidity, to 0.869 with the inclusion of wind speed, to -0.443 with the inclusion of shortwave radiation, and to 0.790 with the inclusion of precipitation. As discussed above, this indicates that the effectiveness of air temperature in melt production greatly increased when combined with high values of relative humidity and wind speed, that in summer the sensible heat flux was higher than it was in autumn and that the latent heat flux, and probably also the heat of precipitation, were both strongly influenced by air temperature. The negative change in beta with the inclusion of shortwave radiation indicates that the two variables do not contribute to each other's effectiveness and individually explain different parts of the variation in stage.

The fact that the beta value changed little in the autumn model set confirms that variation in air temperature diminished greatly in importance when it was low on average, that the sensible heat flux was low during autumn and temperature changes were primarily of import in their effect on the state of precipitation. It also suggests a greater importance for air temperature during summer than indicated in the summer models: that in these models the sensible heat flux was best represented by wind speed but that air temperature was nevertheless important in melt production.

### 2.14c Shortwave radiation

There were large changes in the beta statistic of shortwave radiation in all the model sets with the inclusion of relative humidity, wind speed and precipitation, in the full data set with air temperature and in the seasonal models with atmospheric pressure. All changes were positive except where air temperature was added in the full data model set (Table 53).

As discussed above, shortwave radiation is strongly negatively correlated with relative humidity, wind speed and precipitation, but those three variables are positively correlated and positively influential on each other. Naturally then, when shortwave radiation is low and any one of those three variables high, more runoff is likely to occur than when shortwave radiation is high. The change in beta with the inclusion of atmospheric pressure (to which shortwave radiation is positively correlated) may be an indication that net radiation increased in relative importance when conditions were dry, cool and clear, as they often are when atmospheric pressure is high because other energy sources are typically lesser in such conditions.

### 2.14d Atmospheric pressure

The beta statistics show that the predictive capacity of atmospheric pressure increased when precipitation was added (Table 54). The smallest difference was made in summer (a change of 0.097) and the highest in autumn (0.195). The $R^2$ values for atmospheric pressure and precipitation are negative (Tables 12-14). The beta statistic increased with the addition of relative humidity also, again with a greater change in autumn (0.140) than in summer (0.041). The $R^2$ values for atmospheric pressure and relative humidity are negative (Tables 12-14), and of higher magnitude for autumn than summer. As discussed above, this is an indication that the latent heat flux was greater during low pressure precipitation and/or humid events due to an intensification of the vapour pressure gradient. The difference in sensitivity of relative humidity to changes in atmospheric pressure were discussed above, and the same argument applies here; that is, the availability of latent heat was lower in autumn than in summer, and therefore more sensitive to changes in atmospheric pressure. It was argued above that this sensitivity was greatest in dry conditions, but the change in beta for autumn atmospheric pressure with the inclusion of precipitation indicates that it in fact existed in both dry and wet conditions.

The beta statistics for atmospheric pressure combined with wind speed are all negative, showing that as a pair they made a poor predictor of discharge. The change in beta with the addition of wind speed in autumn was significant however, with a value of 0.113. This is likely again to relate to the latent heat flux, increasing with low pressure and high wind speed.

In summer, the change in beta for atmospheric pressure changed -0.384 with the addition of shortwave radiation, while the addition of this variable had little effect in either the full data or autumn analyses. The two records for summer are not correlated (having a coefficient of 0.002). As discussed above, the importance of atmospheric pressure in effecting the latent heat flux was much lesser than it was in summer. The change in beta therefore indicates that changes in net radiation, with a much greater relative importance, swamped the less substantial contribution of changes in atmospheric pressure to runoff.

### 2.14e Relative humidity

Substantive changes in the beta value for relative humidity occurred in the full data model set with inclusion of shortwave radiation and precipitation, in the summer model set with inclusion of wind speed, shortwave radiation and precipitation, and in the autumn model set with inclusion of precipitation (Table 51 and Figure 68). The changes with wind speed and precipitation were negative, while the changes with shortwave radiation were positive. Relative humidity was negatively correlated with wind speed in the summer record (Table 13), negatively with shortwave radiation in the full data and summer regressions (Tables 12 and 13) and positively with precipitation in all three (Tables 12-14).

The positive change in beta with the inclusion of shortwave radiation indicates that the relative importance of the latent heat flux increased when the contribution of net radiation decreased and vice versa. It is unsurprising that this effect was more distinctive in summer than in autumn, when net radiation would have been greater and therefore of more importance to runoff production.

When relative humidity was high, precipitation was high and vice versa, and it is likely that in part it was this relationship that caused the importance of relative humidity to decrease in the models - while the absolute predictive capacity of the two variables in combination was in fact higher than for either alone (indicated by higher adjusted $R^2$ values when the two were included together in the models of Chapter 3, Section 8.31). The changes in beta were of a high magnitude: -0.143 the full data model set, -0.476 in the summer and -0.202 in the autumn, and the $R^2$ values for relative humidity and precipitation were comparatively high (0.210 in the full data, 0.411 in summer and 0.188 in autumn). Less condensation occurs on a wet surface than a dry one and it is likely that this phenomenon was also represented by the changes in the beta statistic. Furthermore, the relative importance of the latent heat flux would have decreased with the additional runoff component of rain, and possibly also meltwater from the precipitation heat flux.

### 2.14f Precipitation

The beta statistic for precipitation changed in the full data model set with inclusion of relative humidity and shortwave radiation, in the summer model set with wind speed and shortwave radiation and in the autumn model set with relative humidity and shortwave radiation (Table 55 and Figure 72). The changes with relative humidity were negative, that with wind speed was negative, and those with shortwave radiation were positive. Each of these changes mimic those seen in the beta values of shortwave radiation, relative humidity and wind speed and the relationships these changes represent discussed above with respect to the relevant variables.

### 2.15 Discharge production – Summary:

Overall, the results suggest that variation in discharge at Brewster Glacier was dominantly caused by shortwave radiation, precipitation and wind speed in summer, air temperature and precipitation in autumn, followed closely by relative humidity in both seasons. Net radiation was clearly the most important contributor to the energy balance equation on clear days, and especially important when these days were also dry. The latent heat exchange became most important on cloudy days and sensible heat - in its effect on the state of precipitation, the sensible heat flux at the ice surface and possibly also the precipitation heat flux – was most important during precipitation events. Net radiation was still the most important contributor to the energy balance equation in autumn when relative humidity was low, indicating that overall it is the most effective form of energy in melt production but that days of high net radiation receipt were less frequent during autumn than they were in summer (due to increased cloudiness, albedo and decreased solar angle). By mid-February 2006 the glacier had already received a full cover of snow (Figure 54) – an unusual occurrence (Mackintosh, pers. com.) - and this almost certainly decreased the relative importance of shortwave radiation in each of the models, particularly the autumn ones.

Air temperature alone was a poor predictor of discharge, indicating that alone it had little success in producing melt. When it was combined with high relative humidity, wind speed or precipitation its importance was greatly increased as was the runoff production of those latter. Wind speed was of greatest importance when total energy inputs were high, and had very little influence at all when they were low. Atmospheric pressure had a noticeable effect on the intensity of the latent heat flux when other energy inputs were comparatively low, and the latent heat flux diminished significantly during precipitation events.

During summer there was a high frequency of short-lived discharge events, indicating a comparatively high degree of instability in the drainage system. It is possible that the drainage system was most highly arborescent during this time but the clear discharge signal was more likely to have been the result of higher total runoff, least storage of water, least refreezing and a comparatively high degree of sensitivity of the ice to atmospheric conditions. The most important sources of energy during summer were net radiation, the turbulent latent heat flux and the turbulent sensible heat flux respectively, although, while the results are inconclusive, it is likely that precipitation was of greater importance than the turbulent energy exchange in producing runoff.

Atmospheric conditions controlled variation in discharge to a much lesser degree during autumn than they did in summer, because of an overall paucity of energy input. The sensitivity of discharge to air temperature was noticeably higher during this season, as too was that of atmospheric pressure in its effect on the latent heat flux and, as mentioned above, the relative contributions of the sensible and latent heat fluxes increased with the reduction of net radiation. The effectiveness of wind speed was lesser during autumn than it was in summer, due to lower average air temperatures, and other factors such as drainage from subsidiary channels in the drainage system, refreezing and melt water transmission delay due to a deeper snowpack had progressively more influence on the stage hydrograph.

These results are similar to those of other authors found for ice and snow environments in the Southern Alps. Moore and Owens (1984) found that high snow melt events in the Temple Basin catchment near the Main Divide of the Southern Alps occurred during warm, humid, windy conditions and that sensible and latent heat transfers dominated the energy budget. Prowse and Owens (1982) found that intense melt events occurred in similar conditions in the Craigieburn Range but that total net radiation was more important than the latent heat flux; total radiation and the sensible heat transfer of rain were the next most significant contributors respectively to the energy budgets of both studies. Prowse and Owens (1982) found that the direction and strength of wind made a substantive difference to the effectiveness of air temperature in snowmelt production at the Craigieburn Range by increasing the sensible heat transfer.

Neale and Fitzharris (1997), in a study of the energy balance and ablation at a site near Mueller Hut in Aoraki Mt Cook National Park, found that the sensible heat flux had little importance because of the dominance of cold, dry air. At Franz Josef Glacier Owens et al. (1986) found that shortwave radiation was the most important contributor to melt during clear sky, anticyclonic conditions, as also appears to be true at Brewster Glacier. Fitzharris et al. (1992a) suggests that altitude is an important factor in determining the relative importance of radiation and temperature. He asserts that at high altitudes, radiation is more important while at low altitudes air temperature is more important. Given that Brewster

Glacier is at neither low nor high altitude given the range of ice distribution in the Southern Alps, it makes sense that the dominance of each term should vary quite substantially with both daily and seasonal time frames given comparatively small changes in the magnitude of each energy source.

It is impossible to determine from the results of this study whether the melt produced during precipitation events was the result of a strongly positive vapour pressure gradient or the precipitation heat flux. Marcus et al. (1985) found that during a warm rainfall event at Franz Josef Glacier, the precipitation heat flux dominated the energy balance equation with the latent heat flux following. It is possible that during summer at Brewster Glacier the precipitation heat flux is dominant while in autumn the latent heat flux is, an interpretation supported by the results of both the single regressions and diagnostic multiple regressions. It is possible that the impact of raindrops also erodes snow, although this phenomenon is undocumented.

One phenomenon that has been very little discussed thus far is the effect of melt production through refreezing. Oerlemans (2001) asserts that "a 2m winter snowpack of uniform density at -10°C can … be brought to melting point by the melting and refreezing of only 12.5 cm of the snowpack." This is caused by the release of the latent heat of fusion during refreezing. Snowpacks of such a low temperature are rarely observed in Aotearoa New Zealand. Nevertheless, one might speculate that this phenomenon may be important in discharge production during cold rainfall events, particularly within the glacier drainage system itself, and may have contributed to maintaining the arborescence of the channel network.

## Section 3: Elucidation of the characteristics of the Brewster Glacier hydrological system

The changing lag times for different 'enter' type models (Table 56) and the change in amplitude of diurnal discharge variation (Figures 41-46) shed some light on the character of Brewster hydrological drainage system. Consistently shorter lag periods for each of the 'Wet' models compared to the corresponding 'Dry' models indicates the speed at which rainfall is communicated through the system to the proglacial channel, the extra time it takes for energy absorption at the ice surface to produce melt and for this meltwater to complete its passage to the proglacial channel.

There were consistently shorter lag times in summer than in autumn for both precipitation and non-precipitation models, and less diurnal variation in autumn than in summer in both 2005 and 2006 (Figures 41-46). This indicates either: 1) a change in arborescence of the drainage system, 2) a thicker snowpack, 3) lower water volumes and /or 4) lower efficiency of atmospheric variables in producing runoff. While Willis et al. (unpublished paper) inferred from a series of dye tracing experiments at Brewster glacier that the drainage system did indeed evolve from arborescent to non-arborescent with the onset of autumn, and Richards et al. (1996) found that increased channelisation of a drainage system decreased the lag time of response in streamflow, as discussed above the other results of this study do not support this hypothesis. Furthermore, the timing of peaks and troughs in the diurnal hydrographs does not exhibit seasonality and this suggests that what was observed was an absolute decrease in discharge with the onset of autumn rather than a change in the configuration of the drainage system. As discussed above, there was an absolute decrease in runoff quantity in the catchment in autumn, and more precipitation events occurred when air temperatures were below zero in autumn than in summer supporting the hypotheses that lower water volume and a thickened snowpack caused attenuation of water transmission.

Also discussed above is the process of energy absorption and release when a snow or ice surface is at or below the freezing point. The amount of energy required to effect an increase in the temperature of a mass below freezing is greater than it is to effect a change of the same magnitude in a mass above freezing. So, if the surface of Brewster Glacier was more often below the freezing point in autumn than in summer, a lag period between energy absorption and melt water production would be expected. Furthermore, lesser overall energy availability in autumn may also have contributed to extension of the stream response time by increasing the time required for sufficient energy for melt water production to be absorbed.

It is suggested above that the drainage system structure of Brewster Glacier underwent little evolution over the study period. While this may simply have been because the study covered a period too early in the glacier year to capture data on an evolution beginning in late autumn or winter, it may also be the result of a long-term shift in the configuration of the drainage network. When Willis et al. (unpublished paper) completed their dye tracing experiments at Brewster Glacier there were several main exit points from the glacier snout, whereas, as mentioned in the Introduction, there was only one when the field work for this study was carried out. The authors of the former inferred decreasing arborescence of the drainage system from summer to winter from the results of their tests, and vice versa. The glacial snout has been above lake level for only approximately twenty years (Anderson et al., 2008) and it may be conjectured that this has caused an evolution of the drainage system over that time. As mentioned in the Introduction, drainage system arborescence is generally associated with high channel pressure. As the glacier snout was submerged in the lake for a substantial period of time, drainage outlets may have been submerged and channel pressures therefore coupled with the lake rather than the atmosphere, reducing overall pressure in the drainage system. If this was the case, with a distributed drainage system being the result, the grounding of the glacier snout and resulting increase of pressure in drainage channels may have triggered a long-term evolution into a stable arborescent system only recently entering maturity as indicated by the single main drainage exit now evident.

While the results of this study shed no light on this particular problem, it is noted that the subglacial drainage system of Brewster Glacier is most probably a network of R-Channels as defined by Piotrowski (2006). The glacier has a bedrock base, very low velocities (around 20m per year – Mackintosh, pers. com.) with no recorded high velocity events and the exit channel is cut into glacier ice rather than bedrock or soft sediments. It is possible that these R-channels are currently comparatively stable and, aside from the accretion of ice at their walls (observed in the main drainage outlet in Spring 2006), evolve little over the course of the year.

Furthermore, most research into the drainage system and hydrology of glaciers has been completed in Switzerland (Campbell et al., 2006; Swift et al., 2005; Hubbard et al., 2003; Mair et al., 2001; Hubbard and Nienow, 1997) and Canada (Ramage et al., 2006; Bingham et al., 2005; Boon et al., 2003; Kavanaugh and Clarke, 2001) on polythermal or cold temperate glaciers. Given a climate regulated by the ocean, air temperatures in the Aotearoa New Zealand Alps are generally higher than they are in these northern locations, particularly in winter. It is plausible therefore that the degree to which the drainage systems of Aotearoa New Zealand glaciers constrict over winter could be lesser than that observed in Switzerland and Canada.

## <u>Section 4: Brewster proglacial stream and the Kidson atmospheric circulation indices</u>

### 4.0 Method reliability and limitations

As a diagnostic tool for the 2005-2006 period over which data was collected, the method used in this part of the analysis is entirely reliable. For discharge prediction the method may be qualitatively reliable, but as it has not been tested outside of the study period it is impossible to assert complete reliability. However, the results make sense given what is known about climate variability in the Southern Alps during different atmospheric circulations and this lends weight to the reliability of the indices for prediction of discharge in this and other glacierised catchments.

While there is statistical significance in the difference between stage in many of the classes, most of these also exhibit a high degree of internal variability – a high range in values. For this reason prediction of stage using the indices could only be qualitative and not quantitative.

### 4.1 Atmospheric circulation types and runoff production

The difference in average stage with circulation type broadly indicated that stage was higher in warm, wet conditions. This is also what was indicated by the distribution of stage when broken into the three groups, Trough, Blocking and Zonal, in which average stage of the Trough group was highest and of the Zonal lowest.

The highest stage event occurred during southwesterly circulation while trough northwesterly circulation had the highest average stage (Table 57) (the average stage for southwesterly circulation was a close second). The lowest stage event occurred during westerly circulation (with sixth highest average stage) and high southeasterly circulation had the both lowest average stage and the smallest maximum value. It is interesting that these do not correspond exactly to precipitation. The highest precipitation event occurred during southwesterly circulation but westerly circulation had the highest average precipitation (Table 62). Southwesterly circulation had the third highest average precipitation, while trough northwesterly actually had comparatively low average precipitation, seventh out of the eleven classes analysed. High southeasterly did have the lowest average precipitation and a fairly average maximum recorded value of precipitation.

Of the above circulation types only southwesterly and high southeasterly were significantly different to each other (at the 95% confidence level) (Tables 59 and 60). The distribution of trough northwesterly was entirely encompassed by that of both southwesterly and westerly (Figure 73), while high southeasterly was also entirely encompassed by the distribution of westerly and had a high degree of overlap with both the trough northwesterly and southwesterly distributions. Distribution of stage in the Trough and Zonal groups are the only of the groups that were statistically significantly different to each other (Table 61), and, given the above, the most that can be said with confidence is that Trough circulation types will produce highest discharge overall, that southwesterlies and northwesterly troughs will result in comparatively high runoff within this group, and that westerlies may sometimes result in high runoff.

As mentioned above, southwesterly circulation as defined by Kidson (2000) is characterised by strong pressure gradients and therefore high winds, cold air and high precipitation. Trough northwesterly circulation is typified by medium-low pressure gradients, comparatively warm, moist air and a medium level of precipitation. Both circulation types force air from circulation over the Tasman Sea across the Southern Alps, naturally tending to produce high wind speeds and precipitation in the mountains (Salinger, 1981).

The turbulent latent heat flux could possibly be of most importance to the energy balance equation during southwesterly circulation, given moist air and high wind speeds. The term is likely to increase in absolute importance during trough northwesterly circulation due to high air temperatures and high moisture content, but possibly decrease in relative importance given an increase of the sensible heat flux with higher air temperatures.

Westerly circulation is also typified by high pressure gradients, strong winds and orographic precipitation over the Southern Alps. Westerly circulation during the study period produced highest average precipitation and the highest precipitation event. This, together with the rank of westerly average stage, suggests that runoff during intense westerly storms is high (given a high turbulent convective heat flux and possibly a high precipitation heat flux combined with rainfall runoff), but that clear sky westerlies produce comparatively low runoff, possibly the result of low air temperatures and therefore a low sensible heat flux. The high southeasterly class had the lowest average precipitation and is typified by very low pressure gradients over the Alps, very low wind speeds and generally clear skies. This reinforces the conclusion that melt water production at Brewster is greatest when the local airmasses are warm, wet and turbulent.

These results are in part contrary to those of Fitzharris et al. (1992a) who found that, at the decadal resolution, ablation of glaciers in Aotearoa New Zealand was enhanced due to northerly flow over the period 1950-1979, while melt was restricted during summer 1980 due to stronger southerly and westerly airflows. The authors also determined that advance occurred over the periods 1982-1983 and 1986-1988 due to strong El Niño events that strengthened southwesterly airflow, lowered air temperatures and brought heavy precipitation. These results together with those of this study suggest an importance of the season in which the various circulation patterns occur. It is possible that during summer and early autumn, southwesterly and westerly airflow produce enhanced ablation that is more than amply made up for with low air temperatures and high precipitation with the same circulation type during winter and early spring.

Neale and Fitzharris (1997), in their study of snowpack melt in Aoraki Mt Cook National Park, found that northwesterly storms, characterised by high air temperatures and high wind speeds, produced most melt but that anticyclones were also important. Low levels of snow melt occurred during southwesterly conditions, during which clear skies resulted in high net radiation but also cool air which minimised melt. That study site is on the eastern side of the Main Divide of the Southern Alps, and being in the lee of westerly airflow may have made all the difference to the relative impact of northwesterly storms and of southwesterly air flow. In both cases, most of the moisture brought by airmasses from the Tasman Sea would have already been precipitated to the west and onto the Main Divide, such that on arrival at the Mueller study site they would be comparatively dry. At Brewster, the air may still retain sufficient moisture for high precipitation and high vapour pressure gradients to produce high melt and runoff.

The results of Moore and Owens (1984), Owens et al. (1986) and Bishop and Forsyth (1988) support those of this study. Moore and Owens (1984), in their study of the energy budget of the snowpack of Temple Basin, found that highest total energy input occurred during strong northwesterly circulation and lowest during weak southwesterly circulation and conclude that these relationships highlight the importance of turbulent heat exchanges which are most significant during warm, humid, windy conditions as provided by northwesterly airflow. Owens et al. (1986) found that high melt occurred at Franz Josef Glacier with anticyclonic easterly airflow and cyclonic northerly airflow. They inferred that anticyclonic easterly airflow is important at this site because air masses warm as they descend into the ablation zone (an effect that is unlikely to be important at the Brewster site being of higher altitude than the Franz Josef ablation zone and in a low gradient valley). Bishop and Forsyth, (1988), in their study of Dart Glacier, Tititea Mt Aspiring National Park recorded highest ice loss during warm northwesterly rainstorms, with up to five times the ice loss of fine sunny days.

## Section 5: Discharge and climate change

### 5.0 Data, reliability and limitations

As mentioned at the beginning of Section 11, Chapter 3, reliable estimates of glacial discharge variation through time account for all energy inputs and outputs, the effect each energy source has on the others with respect to discharge production, and changes in the glacier morphology (Hock, 2005; Oerlemans, 2001). Andrews (2006) asserts, “the critical mass balances affecting a glacier on a yearly or longer cycle are a product of the energy balance on the glacier’s surface, where for the majority of ice bodies the critical issue in summer losses is not temperature per se but the balance of net radiation.” – where in this case “net radiation” denotes the entirety of incoming and outgoing solar radiation. The analysis presented in this report was completed using only estimated changes in air temperature and precipitation between now and 2040 and 2090. As discussed above, a change in air temperature makes a difference to the effectiveness of relative humidity, precipitation and wind speed in discharge production (positive in every case). Therefore, even assuming constant glacier mass, there is likely to be greater discharge production with temperature and precipitation increases than have been estimated in here using statistical models based on present day relationships.

As discussed in the Introduction, Baisheng et al. (2003) suggest that glacial discharge increases during a period of glacial retreat until the glacier mass decreases past a threshold point at which time discharge decreases due to the decreased melt source area. Collins (1987) found that the regression coefficients for discharge changed through time, probably as a result of changes in the glacier mass. While Brewster Glacier is not currently retreating, it is in a long-term period of retreat (Anderson et al., 2008) and is expected to continue to retreat if temperatures continue to warm this century as predicted (Bernstein, 2007). Therefore, this pattern of a rise and subsequent fall in discharge as glacier size decreases can be expected in this catchment, although it is not accounted for in the quantitative analysis presented here.

### 5.1 Modelled response

Both the annual and total changes estimated for stage between 2007 and 2020 were tiny (Table 65). In fact, the estimated total change in average stage between 2007 and 2020 was comparable to the change in average stage recorded in 2006 and 2007 (an increase of 110mm). This suggests either that the models used were not robust, or simply that changes can be expected to be no greater overall than normal interannual variability (although superimposed). Possibly both are true.

However, it is important to note that the calculated values are averages, and that discharge during high temperature and/or high precipitation events may be more markedly different than the average. Averaging precipitation does render the signal less significant in overall discharge production than it is during precipitation events, when it is an important contributor (see above discussion). It is impossible to say how the percentage change in precipitation is temporally distributed and therefore how it might affect high flow events.

### 5.2 Physical model versus statistical model

Anderson et al. (2008) modelled the runoff from Brewster catchment using a linear reservoir model in which discharge was calculated from water storage volume, inflow to the reservoir and a coefficient for the rate of change of the reservoir's volume. The model includes three reservoirs accounting for storage of water as snow, firn or ice. The volume of water stored as snow, firn and ice was interpolated from measurements made over 2004-2006, as was the reservoir's rate of change, and the inflow coefficient was calculated from records of precipitation, relative humidity, wind speed, albedo and incoming shortwave radiation each for some substantial part of that same period.

The authors compared their modelled results with a ratings curve derived from the same record of measured discharge presented in this report. They acknowledge that the physical model consistently produced higher values of runoff than the ratings curve would lead one to expect (Figure 89).

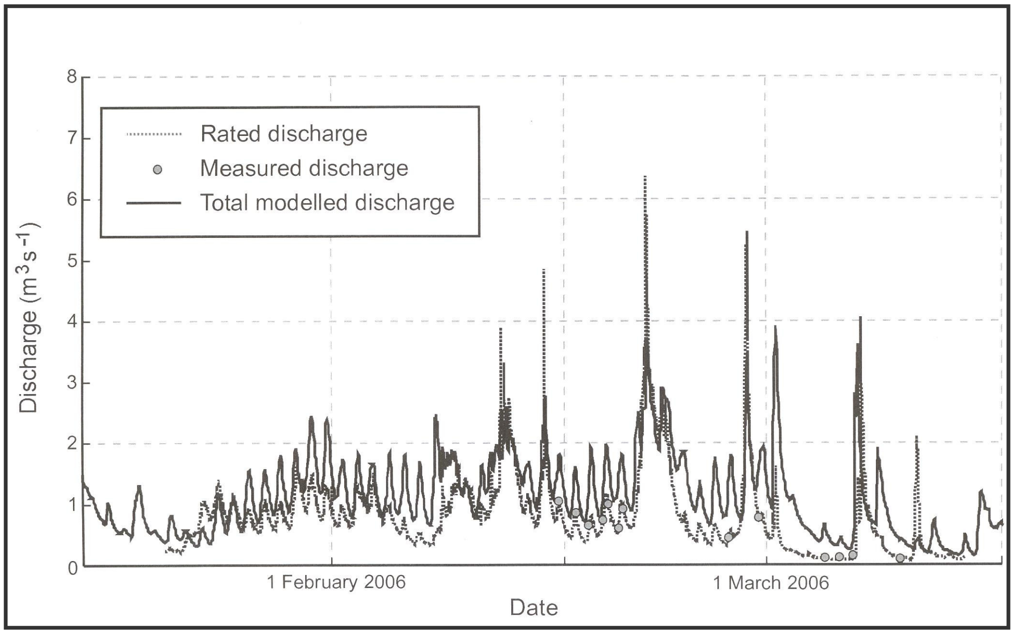


**Figure 90. Measured, rated and modelled discharge for mid and late summer 2006 at Brewster Proglacial stream. (Anderson et al., 2008)**

Total annual point runoff was calculated to be 7.3m over the 2004-2005 period and 7.9m over the 2005-2006 period. Multiplied by the surface area of Brewster catchment (3,600,000m$^2$) and consequently divided by the 31,536,000 seconds of a year, this equates to an average discharge of 0.8 and 0.9 cumecs respectively.

These values are approximately two thirds the 1.1 cumecs average calculated in this study (Table 3). The physically modelled estimate accounted for the entire year as opposed to only a few months as this study has, and during winter anecdotal evidence suggests discharge decreases to almost zero, so it is natural that the average for a full year is lower than that estimated for only summer and autumn months. It seems likely therefore that rather than an overestimation of discharge by the physical model, in fact the ratings curve used in Anderson et al.'s (2008) study underestimated discharge.

The problem with comparing the accuracy of the two methods in discharge production is the lack of a test period for the regression models presented here. For the period from which they were derived, they did produce more reasonable estimations of discharge than the physical model of Anderson et al. (2008) (Figures 61-66). However, when applied to periods outside of the study period, it is quite likely that the physical model would in fact produce results of greater accuracy because it uses inputs of actual water influx, rather than the proxy of atmospheric conditions used in the multiple regression models of this report.

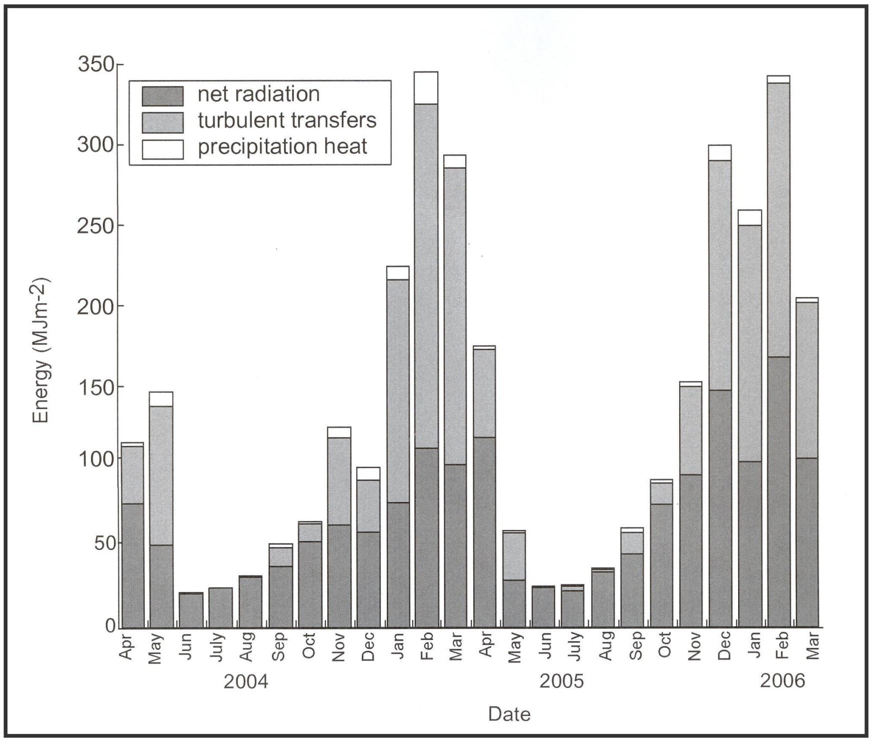


**Figure 91. Variation in source of energy for melt throughout a two-year study period at Brewster Glacier. Asymmetry in the annual pattern results from glacier surface feedbacks. The abrupt transition from dominantly ice to snow, which occurs in late summer or autumn, causes an increase in albedo and a decrease in surface roughness over large parts of the glacier simultaneously, resulting in reduced energy fluxes and hence lower ablation (Anderson et al., 2008).**

The authors of the physical model found that ice and snow melt peaked in summer with a distinct decrease towards the end of this period, which they attributed to limited distribution of residual snow and restricted energy available for ice melt. The energy inputs inferred from the study are shown in Figure 90, and support the interpretation given above that overall energy input decreased markedly over the study period in both 2005 and 2006, that precipitation heat had a high relative importance during summer and that the turbulent convective heat flux often dominated the energy balance equation.

Rainfall accounted for the largest proportion of total runoff in the physical model, with ice melt second and snow melt third, while acknowledging that the period of study was one of positive mass balance and that the importance of ice melt would increase during negative mass balance years (Figure 91 and Table 66). The importance of rainfall as a contributor to runoff is greater in the physical model than it is in the multiple regression models presented here. As discussed above, the models in this report almost certainly underestimated the contribution of rainfall because of the covariance of that record with others, and so it is likely that the physically-based model represented the contribution of rainfall runoff to overall discharge with more accuracy.

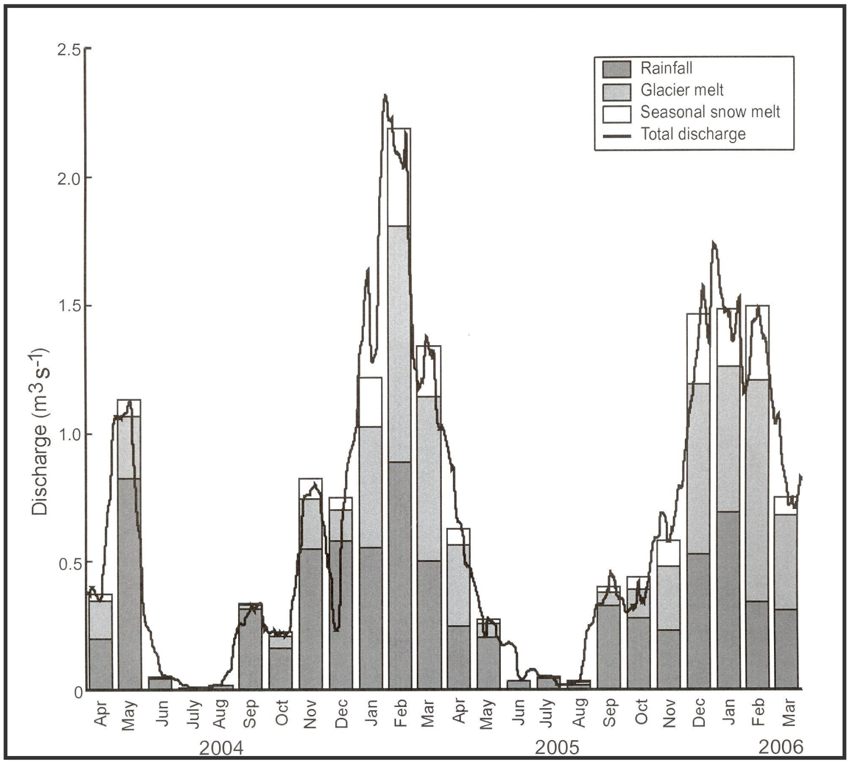


**Figure 92. Components of melt and run-off calculated by the energy balance and discharge models. For clarity a 1-month running mean is used to smooth the curves (from Anderson et al., 2008).**

**Table 66. Annual run-off components (from Anderson et al., 2008).**

| | Rainfall run-off (m) | Glacier melt (m) | Seasonal snow melt (m) | Total point runoff (m) |
|---|---|---|---|---|
| **2004-2005** | 4.0 (54 %) | 2.5 (34%) | 1.0 (14 %) | 7.3 |
| **2005-2006** | 4.5 (57 %) | 2.5 (32 %) | 1.0 (13%) | 7.9 |

The physical model indicates that runoff is highly sensitive to temperature changes, with an increase of 43% with a 1°C increase in temperature and a decrease of 27% with a 1°C decrease in temperature. It is less sensitive to precipitation changes, where a 10% increase in precipitation results in a 4% increase in runoff and 10% decrease leads to a 4% reduction of runoff. Again, these results are contrary to those from the study presented in this report, in which discharge appeared to have a very low sensitivity to both air temperature and precipitation changes. The short data record was one limitation on the predictive capacity of the multiple regression models, as was the fact that overall air temperatures in fact changed very little in the record making it difficult to determine sensitivity. Ultimately though, the results indicated that statistical models of this kind do not have the sensitivity required to accurately predict responses of a complex system to long-term input variability.

# Chapter 5: Conclusions

The research has allowed conclusions to be drawn with regard to each of the research questions outlined in Chapter 1. This chapter will address of these questions in turn.

## Primary

1. **Which are the most important atmospheric variables influencing discharge production?**

The order of importance of the atmospheric variables varied. The results suggest that overall, the relative importance of the variables, from greatest to least, was as follows:

1. Shortwave radiation
2. Relative humidity
3. Wind speed
4. Air temperature
5. Precipitation

However, given the results of Anderson et al.'s (2008) physically based model, the problems of covariance and underestimation in the precipitation record and the striking concurrence of the stage and precipitation records, it was concluded that precipitation is likely to in fact be of first equal (if not greater) importance with shortwave radiation.

The order of importance of each variable then changed depending on season. During summer it was concluded that this was:

1. Wind speed
2. Precipitation
3. Shortwave radiation

4a. Relative humidity

4b. Air temperature

The contribution of relative humidity and air temperature to the turbulent heat flux seemed to be near equal during summer. It was finally concluded that wind speed had a greater importance than precipitation and shortwave radiation simply because it was the sole variable included in the stepwise multiple regression models.

During summer, discharge was dominated by melt production by net radiation (shortwave radiation), with the turbulent convective heat flux – represented by wind speed, air temperature and relative humidity - a close second. The model results were inconclusive as to the relative importance of precipitation and wind speed in discharge production in summer. Both the highest stage event and the highest precipitation events occurred during southwesterly circulation. Highest average discharge occurred during trough northwesterly circulation however which had only the fifth highest average precipitation. This suggested that during large precipitation events rainfall runoff was the most important contributor to discharge while at other times, the degree of turbulence in the boundary layer climate was of greater significance. The latent heat flux was more important during summer that the sensible heat flux, and seemed to be of near equal importance to net radiation in melt production.

It was concluded that in autumn, the order of relative importance of the atmospheric variables was as follows:

1. Air temperature
2. Precipitation
3. Relative humidity
4. Shortwave radiation
5. Wind speed

The importance of wind speed sank when combined with low air temperatures and decreased surface roughness, while an inferred increase in cloudiness, lower solar declination and higher albedo together contrived to decrease the importance of shortwave radiation. Air temperature contributed to discharge production both through the sensible heat flux and by influencing the form of precipitation.

In autumn, precipitation runoff was still important but the contribution of sensible heat to the form of that precipitation increased to such an extent that the latter term's relative contribution increased beyond that of precipitation. The importance of wind speed diminished in this season, again superseded by air temperature and also relative humidity. The latent heat flux was of importance, and while the total amount of available sensible heat was important in its effect on runoff production during precipitation events, the latent heat dominated the turbulent heat flux. During dry periods, net radiation was again the most important source of energy for discharge production.

2. **What combination of atmospheric variables leads to highest/lowest discharge from the proglacial stream?**

Highest discharge occurred during warm, humid precipitation events – warm storms – and lowest in cold, dry conditions with little shortwave radiation receipt – cool, cloudy conditions in other words. Northwesterly cyclones, typified by warm, moist air, warm precipitation and high winds, produced highest average flows, and while the highest discharge event occurred during southwesterly circulation – typified by cool, relatively moist air, cold precipitation and high winds - it is likely that in the long-term northwesterly storms would prove to produce highest flow events. Having said this, it was concluded that southwesterly airflow did produce significant discharge events in summer and early autumn, primarily because of the intensity of precipitation, but that this decreased into autumn and winter as a result of colder air temperatures. Lowest discharge occurred during high southeasterly circulation, typified by cold, dry air and low wind speeds and westerly circulation also produced these conditions on occasion and thereby resulted in the smallest peak flow event.

3. **Can a statistical model of atmospheric variables be used to reliably predict discharge?**

It was concluded that during summer, when the relationship of atmospheric variables to discharge production is relatively straightforward, with sufficient data on which to base a model and a glacier in equilibrium, discharge predictions from a statistical model would be robust. The accuracy of predictions would decrease substantively during any other season because the relationship of atmospheric variability to discharge variability becomes more complicated. Furthermore, because the model developed in this study did not account for changes in glacier mass, flow or morphology, it would require regular updating to retain accuracy.

4. **Can an atmospheric classification scheme be used to reliably predict discharge?**

An atmospheric classification scheme can be used to give reliable predictions of relative average discharge production. Given a sufficient data base the method could be refined to provide quantitative predictions of both average discharge, peak flow frequency and an envelope for the magnitude of peak flows. Again changes in glacier mass, flow and morphology are likely to change the relationship between atmospheric circulation patterns and discharge production however such that prediction using circulation indices would have to use regularly updated data, largely defeating the purpose.

5. **Using a statistical model and atmospheric classification scheme, what changes to the discharge regime can be expected with predicted climate change?**

Unfortunately no predictions of changes to atmospheric circulation patterns were available for address of this question. The modelled changes led to the expectation of a minor increase in average discharge (no greater than ‘normal’ interannual variability) over the next twenty years given predicted changes in air temperature and precipitation in the Brewster region. However, the results of the diagnostic analysis indicated that that increase is in fact likely to be greater than the models suggest, as the impacts of air temperature on the efficacy of other atmospheric variables has been shown to be significant, but was unaccounted for in the modelled predictions.

**Secondary**

6. **What are the characteristics of the diurnal cycle of discharge from Brewster pro-glacial stream?**

During summer and autumn, peak flow occurred between 5pm and 7pm daily and low flows between 5am and 1pm. There was no significant development of either the timing of the peaks and troughs, nor the form of the diurnal hydrographs in any way excepting the magnitude of their amplitudes. This decreased substantially from summer to autumn, and the occurrence of a clear diurnal signal became less frequent. It was concluded that this was because of an overall reduction in discharge, the increasing influence of the supraglacial snowpack and possibly the drainage of high pressure subsidiary englacial channels.

**7. Is there evidence of a seasonal evolution of the drainage system? If so, what are the characteristics of this evolution?**

The only evidence for a seasonal development of the drainage system was the declining magnitude of diurnal fluctuations and frequency of clear diurnal fluctuations. Given no other evidence, it was concluded that the drainage system morphology evolved very little, if at all, over the course of the study period. The observed changes, as mentioned above, were more readily attributed to an overall reduction in discharge volume, the increasing influence of the supraglacial snowpack and possibly also the drainage of high pressure drainage channels. Having said this, theory suggests that if the main drainage channels emptied and drainage from high pressure subsidiary channels began that evolution of the drainage system into one more highly distributed may have been instigated. The results do not preclude the development of a non-arborescent drainage system over winter.

**8. Is there evidence in the diurnal hydrograph for an evolving influence of the supraglacial snowpack?**

As above, the decreasing frequency of clear diurnal fluctuations in the hydrograph over the study periods of both 2005 and 2006 suggested that the influence of the snowpack did increase with the onset of autumn. No change in the gradient of the rising limb of the diurnal hydrographs but falling limbs of increasing duration suggested that an increasingly deep snowpack retained a constant degree of 'ripeness', such that it had little effect on the transmission of water as energy input occurred, but that transmission of water produced at or after the peak of energy inputs was significantly attenuated by it. Furthermore, it is concluded that an increasingly thick snowpack through the seasons decreased surface roughness and that this had a negative impact on the influence of wind speed on the turbulent heat fluxes, and that increasing albedo from an extended snowpack resulting in lesser energy receipt and lower melt output.

**9. What is the extent of hydrological storage in the glacier and how does it influence the hydrograph of the pro-glacial stream?**

Lower $R^2$ values for stage and atmospheric variables in the hourly data than the daily suggested a high degree of short-term water storage and release. It is impossible to say from the results however whether the storage represented was in the form of pooled liquid water on, in or under the glacier or as snow or ice. Lower $R^2$ values for autumn than summer furthermore suggested that storage of melt and rainwater increased as energy inputs diminished, in this case suggesting pooling of liquid water. It is possible that refreezing of liquid water may also play a part in water storage during autumn, but this phenomenon ought to have produced some signal in the stage hydrograph, and none was identified.

**10. How do the real-time results compare with Anderson et al.s' (2008) model of energy balance and discharge?**

The values for average discharge calculated in this study were comparable to those calculated in Anderson et al.'s (2008), and the qualitative analysis of the energy budget in this study agreed in large part with the measured values in Anderson et al.'s (2008) paper. However, the results diverged in prediction of the effects of climate change on discharge production and it was concluded that those of this study were gross underestimates and that the sensitivity of the multiple regression models to changes in air temperature and precipitation was insufficient for accurate prediction.

# Chapter 6: Further Research

The hydrological system of Brewster Glacier would be further illuminated by the following research:

- Quantitative determination of the relative contributions of rainfall and melt to discharge, and from this the degree of water storage in the drainage system, at the hourly, daily, monthly and seasonal time scales.
- Comparison of snowfall records and the hydrograph form from the beginning of summer to the middle of winter to distinguish with greater detail the influence of the supraglacial snowpack on water transmission.
- Testing of the reliability of the models developed in this study by applying them to some future period over which discharge in Brewster catchment has been measured.
- Determination of whether or not drainage system evolution occurs over winter and spring through hydrograph analysis for those seasons.
- Relation of measured energy budgets to atmospheric circulation patterns over the catchment to further enable prediction of discharge using atmospheric circulation indices.

# **References**:


Alley, R., Lawson, D., Evenson, E. and Larson, G.; 2003; Sediment, glaciohydraulic supercooling, and fast glacier flow. *Annals of Glaciology*, 36, 135-141.

Anderson, B., Mackintosh, A., Stumm, D., George, L., Kerr, T., Winter-Billington, A. and Fitzsimmons, S.; 2008; Climate sensitivity of a high-precipitation glacier in New Zealand. *Journal of Geophysical Research* (submitted).

Anderson, personal communication; Dr Brain Anderson, Victoria University of Wellington.

Anderton, P.; 1973; *Estimation of snow storage and melt in the catchment of Lake Pukaki.* Water and Soil Division, Ministry of Works and Development, Christchurch.

Arnell, N.; 1994; Hydrology and Climate Change. In Ed.s: Calow, P. and Petts, G.E.; *The Rivers Handbook; Hydrological and Ecological Principles*. Blackwell Science, Oxford and London.

Arnold, N., Richards, K., Willis, I. and Sharp, M.; 1998; Initial results from a distributed, physically based model of glacier hydrology. In Ed.s Sharp, M., Richards, K. and Tranter, M.; *Glacier hydrology and hydrochemistry*. John Wiley and Sons Ltd.

Baisheng, Y., Yongjian, D., Fengjing, L. & Caohai, L.; 2003; Responses of various-sized alpine glaciers and runoff to climatic change. *Journal of Glaciology*, 49 (164), 1-7.

Barry, R.; 1992; *Mountain Weather and Climate; 2nd Edition*. Routledge, London.

Barry, R.; 2006; The status of research on glaciers and global glacier recession: a review. *Progress in Physical Geography*, 30(3), 285-306.

Bernstein, L., Bosch, P., Canziani, O., Chen, Z., Christ, R., Davidson, O., Hare, W., Huq, S., Karoly, D., Kattsov, V., Kundzewicz, Z., Liu, J., Lohmann, U., Manning, M., Matsuno, T., Menne, B., Metz, B., Mirza, M., Nicholls, N., Nurse, L., Pachauri, R., Palutikof, J., Parry, M., Qin, D., Ravindranath, N., Reisinger, A., Ren, J., Riahi, K., Rosenzweig, C., Rusticucci, M., Schneider, S., Sokona, Y., Solomon, S., Stott, P., Stouffer, R., Sugiyama, T., Swart, R., Tirpak, D., Vogel, C. and Yohe, G.; 2007; *Intergovernmental Panel on Climate Change; Fourth Assessment Report. Climate Change 2007: Synthesis Report. Summary for Policymakers.* Intergovernmental Panel on Climate Change.

Bingham, R., Nienow, P., Sharp, M. and Boon, S.; 2005; Subglacial drainage processes at a High Arctic polythermal valley glacier. *Journal of Glaciology*, 51, 15-24.

Bingham, R., Nienow, P., Sharp, M. and Copland, L.; 2006; Hydrology and dynamics of a polythermal (mostly cold) High Arctic glacier. *Earth Surface Processes and Landforms*. Wiley Interscience, DOI: 10.1002/esp.1374.

Bishop, G. and Forsyth, J.; 1988; *Vanishing Ice: An Introduction to Glaciers Based on a Study of the Dart Glacier.* New Zealand Geological Survey, DSIR, Dunedin.

Boon, S., Sharp, M. and Nienow, P.; 2003; Impact of an extreme melt event on the runoff and hydrology of a high Arctic glacier. Hydrological Processes, 17, 1051-1072.

Boulton, G. and Hindmarsh, R.; 1987; Sediment deformation beneath glaciers: Rheology and geological consequences. *Journal of Geophysical Research*, 92(B9), 9059–9082.

Braithwaite, R.; 2002; Glacier mass balance: the first 50 years of international monitoring. *Progress in Physical Geography*, 26, 76-95.

Braun, L. and Escher-Vetter, H.; 1996; Glacial discharge as affected by climate change. *Garmisch Partenkirchen, Interpraevent 1996*.

Brazel, A., Chambers, F., Kalkstein, L.; 1992; Summer energy balance on West Gulkana Glacier, Alaska, and linkages to a temporal synoptic index. *Zeitschrift fur Geomorphologie, Supplementband* 86, 15-34.

Campbell, F., Nienow, P. and Purves, R.; 2006; Role of the supraglacial snowpack in mediating meltwater delivery to the glacier system as inferred from dye tracer investigations. *Hydrological Processes*, 20, 969-985.

Chalmers, A.; 1982; *What is this thing called Science? 2nd ed.* Open University Press, Buckingham.

Chinn, T., Winkler, S., Salinger, M. and Haakensen, N.; 2005; Recent glacier advances in Norway and New Zealand: a comparison of their glaciological and meteorological causes. *Geografiska Annaler*, 87A(1), 141-157.

Chorley, R., Schumm, S. and Sugden, D.; 1984; *Geomorphology*. Methuen & Co., USA.

Chow, V.; 1964; *Handbook of Applied Hydrology*. McGraw-Hill, New York.

Clare, G.; Fitzharris, B., Chinn, T. & Salinger, M.; 2002: Interannual variation in end-of-summer snowlines of the Southern Alps of New Zealand, and relationships with southern hemisphere atmospheric circulation and sea surface temperature patterns. *International Journal of Climatology*, 22, 107-120.

Clarke, G.; 2005; Subglacial Processes. Annual Review; *Earth and Planetary Sciences*, 33, 247-276.

Collins, D.; 1987; Climatic fluctuations and runoff from glacierised Alpine basins. IN Eds. Soloman, S., Beran, M. and Hogg, W.; *The Influence of Climate Change and Climatic Change on the Hydrologic Regime and Water Resources (Proceedings of the Vancouver Symposium, August 1987)*, 168, 79-89.

Davie, T.; 2003; *Fundamentals of Hydrology. Routledge Fundamentals of Physical Geography*. Routledge, London.

Duchon, C. and Essenberg, G.; 2001; Comparative rainfall observations from pit and aboveground rain gauges with and without wind shields. *Water Resources Research*, 37(12), 3253-3263.

Dyurgerov, M. and Meier, M.; 2000; Twentieth century climate change: evidence form small glaciers. *PNAS*, 97(4), 1406-1411.

Evans, D.; 2004; Glaciers. *Progress in Physical Geography*, 28(2), 294-305.

Evans, D.; 2005; Glaciers. *Progress in Physical Geography,* 29(1), 114-121.

Fitzharris, B.; 1979; Snow Hydrology (In New Zealand). *Physical hydrology: New Zealand experience. Toebes memorial volume*, 23-43.

Fitzharris, B., Hay, J. and Jones, P.; 1992a; Behaviour of New Zealand glaciers and atmospheric circulation changes over the past 130 years. *The Holocene*, 2(2), 97-106.

Fitzharris, B., Owens, I. and Chinn, T.; 1992b; Snow and Glacier Hydrology. In Ed. Mosely, M.P.; *Waters of New Zealand*. New Zealand Hydrological Society, Wellington.

Fitzharris, B., Chinn, T., and Lamont, G.; 1997; Glacier balance fluctuations and atmospheric circulation patterns over the Southern Alps, New Zealand. *International Journal of Climatology*, 17(7), 745-763.

Fitzharris, B., Lawson, W. & Owens, I.; 1999; Research on glaciers and snow in New Zealand. *Progress in Physical Geography*, 23 (4), 469-500.

Fitzharris, B., Clare, G. and Renwick, J.; 2006; Teleconnections between Andean and New Zealand glaciers. *Global and Planetary Change*, doi:10.1016/j.gloplacha.2006.11.022.

Flowers, G. and Clarke, G.; 2000; An integrated modelling approach to understanding subglacial hydraulic release events. Annals of Glaciology, 31, 222-226.

Fountain, A.; 1996; Effect of snow and firn hydrology on the physical and chemical characteristics of glacial runoff. *Hydrological Processes*, 10, 509-521.

Fountain, A. & Walder, J.; 1998; Water flow through temperate glaciers. *Reviews of Geophysics*, 36(3), 229-328.

Francou, B., Ribstein, P., Saravia, R. and Tiriau, E.; 1995; Monthly balance and water discharge of an inter-tropical glacier: Zongo Glacier, Cordillera Real, Bolivia, 16°S. *Journal of Glaciology*, 14(137), 61-67.

Gardiner, V. and Dackombe, R.; 1983; *Geomorphological Field Manual*. George Allen and Unwin, London.

Gelman, A. and Hill, J.; 2007; *Data Analysis Using Regression and Multilevel/Hierarchical Models*. Cambridge University Pres, New York.

Gordon, S., Sharp, M., Hubbard, B., Willis, I., Smart, C., Copland, L., Harbor J., and Ketterling, B.; 2001; Borehole drainage and its implications for he investigation of glacier hydrology: experiences from Haut Glacier d'Arolla, Switzerland. *Hydrological Processes*, 15, 797-813.

Gregory, J. and Oerlemans, J.; 1998; Simulated future sea-level rise due to glacier melt based on regionally and seasonally resolved temperature changes. *Nature*, 391(29), 474-476.

Hannah, D., Gurnell A. and McGregor, G.; 2000; Spatio-temporal variation in microclimate, the surface energy balance and ablation over a cirque glacier. *International Journal of Climatology*, 20, 733-758.

Hannah, D., Gurnell, A. and McGregor, G.; 2003; A methodology for investigation of the seasonal evolution in proglacial hydrograph form. *Hydrological Processes*, 13, 2603-2621.

Haresign, E. and Warren, C.; 2005; Melt rates at calving termini: a study at Glaciar Leon, Chilean Patagonia. *Geological Society Special Publication*, 242, 99-109.

Harrison, W. and Post, A.; 2003; How much do we really know about glacier surging? *Annals of Glaciology*, 36, 1-6.

Hay, J. and Fitzharris, B.; 1988; A comparison of the energy-balance and bulk-aerodynamic approaches for estimating glacier melt. Journal of Glaciology, 34, 145-153.

Hessell, J.; 1983; Climatic effects on the recession of the Franz Josef Glacier (New Zealand). New Zealand Journal of Science, 26(3), 315-320.

Hochstein, M., Claridge, D., Henrys, S., Pyne, A., Nobes, D. & Leary, S.; 1995; Downwasting of the Tasman Glacier, South Island, New Zealand: changes in the terminus region between 1971 and 1993. *New Zealand Journal of Geology and Geophysics*, 38, 1-16.

Hock, R.; 2005; Glacier melt: a review of processes and their modelling. *Progress in Physical Geography*, 29(3), 362-391.

Hock, R. and Hooke, R.; 1983; Evolution of the internal drainage system in the lower part of the ablation area of Storglaciären, Sweden. *Geological Society of America Bulletin*, 105, 537-546.

Hodgkins, R.; 2001; Seasonal evolution of melt-water generation, storage and discharge at non-temperate glacier in Svalbard. *Hydrological Processes*, 15, 441-460.

Hooke, R.; 1989; Englacial and subglacial hydrology: A qualitative review. *Arctic and Alpine Research*, 21 (3), 211-233.

Hooker, B. and Fitzharris, B.; 1999; The correlation between climatic parameters and the retreat and advance of Franz Josef Glacier, New Zealand. *Global and Planetary Change*, 22(1-4), 39-48.

Hubbard, B. and Nienow, P.; 1997; Alpine subglacial hydrology. Quaternary Science Review, 16, 939-955.

Hubbard, B., Hubbard, A., Madar, H., Tison, J-L., Grust, K. and Nienow, P.; 2003; Spatial variability in the water content and rheology of temperate glaciers: Glacier de Tsanfleuron, Switzerland. *Annals of Glaciology*, 37, 1-6.

Huntington, T.; 2006; Evidence for the intensification of the global water cycle: Review and synthesis. *Journal of Hydrology*, 319, 939-955.

Jansson, P., Hock, R., Schneider, T.; 2003; The concept of glacier storage; a review. *Journal of Hydrology*, *Journal of Hydrology* 282 (1-4), pp. 116-129.

Kaiser, C.; 1952; *An essay on Method*. Rutgers University Press, New Jersey.

Kavanaugh, J. and Clarke, G.; 2001; Abrupt glacier motion and reorganization of basal shear stress following the establishment of a connected drainage system. *Journal of Glaciology*, 47(158), 472-480.

Kerr, personal communication; Tim Kerr, Canterbury University of Christchurch.

Kidson, J.; 2000; An analysis of New Zealand synoptic types and their use in defining weather regimes. *International Journal of Climatology*, 20, 299-316.

Kirkbride, M.; 1993; The temporal significance of transitions from melting to calving termini at glaciers in the central Southern Alps of New Zealand. *The Holocene*, 3(3), 22-240.

Klok, E. and Oerlemans, J.; 2002; Model study of the spatial distribution of the energy and mass balance of Morteratschgletscher, Switzerland. *Journal of Glaciology,* 48(163), 505-518.

Kulessa, B. and Murray, T.; 2003; Slug-test derived differences in bed hydraulic properties between a surge-type and a non-surge type Svalbard glacier. *Annals of Glaciology*, 36, 103-109.

Lamont, G., Chinn, T. and Fitzharris, B.; 1999; Slopes of glacier ELAs in the Southern Alps of New Zealand in relation to atmospheric circulation patterns. *Global and Planetary Change*, 22(1-4), 209-219.

Land Information New Zealand; 1999; 'Haast Pass'. *NZMS 260; Sheet G38*.

Lingle, C. and Fatland, D.; 2003; Does englacial water storage drive temperate glacier surges? *Annals of Glaciology*, 36, 14-20.

Mackintosh, A.; personal communication; Dr Andrew Mackintosh, Victoria University of Wellington.

Mair, D., Nienow, P., Willis, I. and Sharp, M; 2001; Spatial patterns of glacier motion during a high velocity event: Haut Glacier d'Arolla, Switzerland. *Journal of Glaciology* 47(156), 9-20.

Mair, D., Sharp, M. and Willis, I.; 2002; Evidence for basal cavity opening from analysis of surface uplift during a high velocity event: Haut Glacier d'Arolla, Switzerland. *Journal of Glaciology*, 48(161), 208-216.

Marcus, M., Moore, R. and Owens, L.; 1985; Short-term estimates of surface energy transfer and ablation on the lower Franz Josef Glacier, South Westland, New Zealand. *New Zealand Journal of Geology and Geophysics*, 28, 559-567.

McConchie, J; personal communication; Dr Jack McConchie, Victoria University of Wellington.

Menzies, J.; 1995; Glaciers and Ice Sheets. In Ed. Menzies, J.; 1995; *Modern Glacial Environments: Processes, Dynamics and Sediments; Glacial Environments, Volume 1*. Butterworth Heinemann, UK.

Moore, R. and Owens, I.; 1984; Controls on advective snowmelt in a maritime alpine basin. *Journal of Climate and Applied Meteorology,* 23, 135-142.

Moore, R. & Demuth, M.; 2001; Mass balance and streamflow variability at Place Glacier, Canada, in relation to recent climate fluctuations. *Hydrological Processes*, 15, 3473-3486.

Mosley, M. and McKercher, ; 1992; Streamflow. In Ed. Maidment, D.R.; *Handbook of Hydrology*. McGraw Hill, U.S.A.

Motyka, R., Hunter, L., Echelmeyer, K. and Conner, C.; 2003; Submarine melting at the terminus of a temperate tidewater glacier, LeConte Glacier, Alaska, U.S.A. *Annals of Glaciology*, 36, 57-65.

Mullan, B.; personal communication; Dr Brett Mullan, The New Zealand National Institute of Water and Atmospheric Research.

Munro, D.; 2000; Progress in glacier hydrology; a Canadian perspective. *Hydrological Processes*, 14, 1627-1640.

Neale, S. & Fitzharris, B.; 1997; Energy balance and synoptic climatology of a melting snowpack in the Southern Alps, New Zealand. *International Journal of Climatology*, 17, 1595-1608.

Oerlemans, J.; 1997; Climate sensitivity of Franz-Joseph Glacier, New Zealand, as revealed by numerical modelling. *Arctic and Alpine Research,* 29(2), 233-239.

Oerlemans, J.; 2000; Holocene glacier fluctuations: is the current rate of retreat exceptional? *Annals of Glaciology*, 31, 39-44.

Oerlemans, J.; 2001; *Glaciers and Climate Change*. Swets and Zeitlinger, Lisse.

Oerlemans, J.; 2005; Extracting a climate signal from 169 glacier records. *Science*, 308, 675-677.

Oerlemans, J., Bjornsson, H., Kuhn, M., Obleitner, F., Palsson, F., Smeets, C., Vugts, H and de Wolde, J.; 1999; Glacio-meteorological investigations on Vatnajokull, Iceland, summer 1996: An overview. *Boundary Layer Meteorology*, 92, 3-26.

Oerlemans, J. & Reichert, B.; 2000; Relating glacier mass balance to meteorological data using a seasonal sensitivity characteristic. *Journal of Glaciology*, 46 (152), 1-6.

Oerlemans, J. and Grisogono, B.; 2002; Glacier winds and parameterisation of the related surface heat fluxes. *Tellus*, 54(A), 440-452.

Oerlemans, J. and van den Broeke, M.; 2002; Foreword: Katabatic flows over ice sheets and glaciers. *Tellus*, 54(A), 439-439.

Oke, T.; 1978; *Boundary Layer Climates*. Methuen and Co., London.

Owens, I., Marcus, M. and Moore, R.; 1986; Temporal variations of energy transfers over the lower part of Franz Joseph Glacier. *Proceedings of the Twelfth New Zealand Geography Conference*, Christchurch.

Paterson, W.; 1994; *The Physics of Glaciers, 3rd Edition.* Redwood Books, Trowbridge.

Paul, F., Kaab, A., Maisch, M., Kellenberger, T. and Haeberli, W.; 2004; Rapid disintegration of alpine glaciers observed with satellite data. *Geophysical Research Letters*, 31, 1-4.

Pilgrim, D. and Cordery, I.; 1992; Flood runoff. In Ed. Mosley, M.P.; *Handbook of Hydrology*. McGraw Hill, U.S.A.

Piotrowski, J.; 2006; Groundwater under ice sheets and glaciers. In Ed. Knight, P.G.; *Glacier Science and Environmental Change*, Blackwell, Oxford.

Popper, K.; 1959; *The Logic of Scientific Discovery*. Hutchinson and Co, London.

Prowse, T. and Owens, I.; 1982; Energy balance over melting snow, Craigieburn Range, New Zealand. *Journal of Hydrology (NZ),* 21, 133-147.

Ramage, J., McKenney, R., Thorson, B., Maltais, P. and Kopczynski, S.; 2006; Relationship between passive microwave-derived snowmelt and surface-measured discharge, Wheaton River, Yukon Territory, Canada. *Hydrological Processes*, 20, 689-704.

Raper, S., Brown, O. & Braithwaite, R.; 2000; A geometric glacier model for sea-level change calculations. *Journal of Glaciology*, 46(154), 357-368.

Raymond, C.; 1987; How do glaciers surge? *Journal of Geophysical Research*, 92(B9), 9121-9134.

Richards, K., Sharp, M., Arnold, N., Gurnell, A., Clark, M., Tranter, M., Nienow, P., Brown, G., Willis, I. and Lawson, W.; 1996; An integrated approach to modelling hydrology and water quality in glacierised catchments. *Hydrological Processes*, 10, 479-508.

Salinger, M.; 1981; *New Zealand Climate: The Instrumental Record*. PhD Thesis, Victoria University of Wellington.

Salinger, M., Heine, M. and Burrows, C.; 1983; Variations of the Stocking (Te Wae Wae) Glacier, Mount Cook, and climatic relationships. *New Zealand Journal of Science*, 26, 321-338.

Schaefli, B. Hingray, B., Niggli, M. and Musy, A.; 2005; A conceptual glacio-hydrological model for high mountainous catchments. *Hydrology and Earth System Sciences*, 9, 95-109.

Scheidegger, A.; 1991; *Theoretical Geomorphology; third, completely revised edition*. Springer-Verlag, Austria.

Sharp, M.; 2005; Subglacial drainage. In Ed. Anderson, M.; *Encyclopaedia of Hydrological Sciences*. John Wiley and Sons, Hoboken, N.J.

Shreve, R.; 1972; Movement of water in glaciers. *Journal of Glaciology*, 11, 205-214.

Sieck, L., Burges, S. and Steiner, M.; 2007; Challenges in obtaining reliable measurements of point rainfall. *Water Resources Research*, 43, art. no. W01420.

Singh, P., Haitashya, U., Ramasastri, K. and Kumar, N.; 2005; Diurnal variations in discharge and suspended sediment concentration, including runoff delay characteristics, of the Gangotri Glacier in the Garhwal Himalayas. *Hydrological Processes*, 19, 1445-1457.

Stull, R.; 1988; *An Introduction to Boundary Layer Meteorology*. Kluwer Academic Publishers, Netherlands.

Sturman, A. and Tapper, N.; 2006; *The Weather and Climate of Australia and New Zealand*, Second Edition. Oxford University Press, Victoria.

Swift, D., Nienow, P., Spedding, N. and Hoey, T.; 2002; Geomorphic implications of subglacial drainage configuration: rates of basal sediment evacuation controlled by seasonal drainage system evolution. Sedimentary Geology, 149, 5-19.

Swift, D., Nienow, P., Hoey, T. and Mair, D.; 2005; Seasonal evolution of runoff from Haut Glacier d'Arolla, Switzerland and implications for glacial geomorphic processes. *Journal of Hydrology,* 309, 133-148.

Takeuchi, Y., Naruse, R;, Satow, K. and Ishikawa, N.; 1999; Comparison of heat balance characteristics at five glaciers in the Southern Hemisphere. *Global and Planetary Change*, 22, 201-208.

Walder, J. and Driedger, C.; 1995; Frequent outburst floods from South Tahoma Glacier, Mount Rainier, U.S.A.: relation to debris flows, metrological origin and implications for subglacial hydrology. *Journal of Glaciology*, 41(137), 1-10.

Watson, R. and the Core Writing Team IPCC; 2001; *IPCC Third Assessment Report: Climate Change 2001; Synthesis Report; Summary for Policymakers*. Intergovernmental Panel on Climate Change, Geneva, Switzerland.

Willis, I., Arnold, N. and Brock; B.; 2002; Effect of snowpack removal on energy balance, melt and runoff in a small supraglacial catchment. Hydrological Processes, 16, 2721-2749.

Willis, I., Lawson, W., Owens, I. and Jacobel, B.; Unpublished paper. Subglacial drainage system structure and morphology of Brewster Glacier, New Zealand.

Xia, Y. and Xu, G.; 2007; Impacts of systematic precipitation bias on simulations of water and energy balances in Northwest America. *Advances in Atmospheric Sciences*, 24(5), 739-749.

# Appendix 1.

Air temperature, relative humidity, wind speed and shortwave radiation recorded at Brewster proglacial lake in summer and autumn 2005 and 2006, and atmospheric pressure in the catchment calculated for the same period.

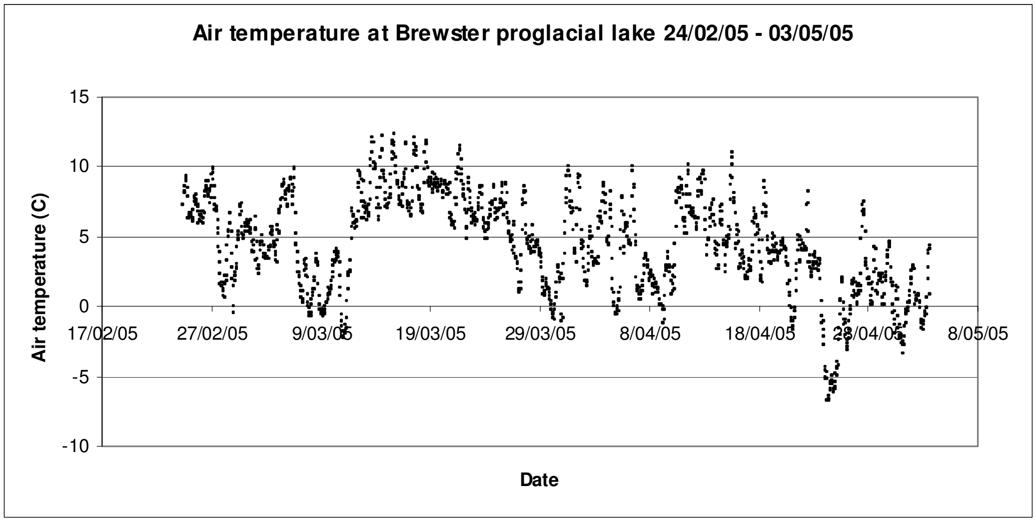


**Figure A1. Air temperature at Brewster proglacial lake from 2 February to 3 May 2005.**

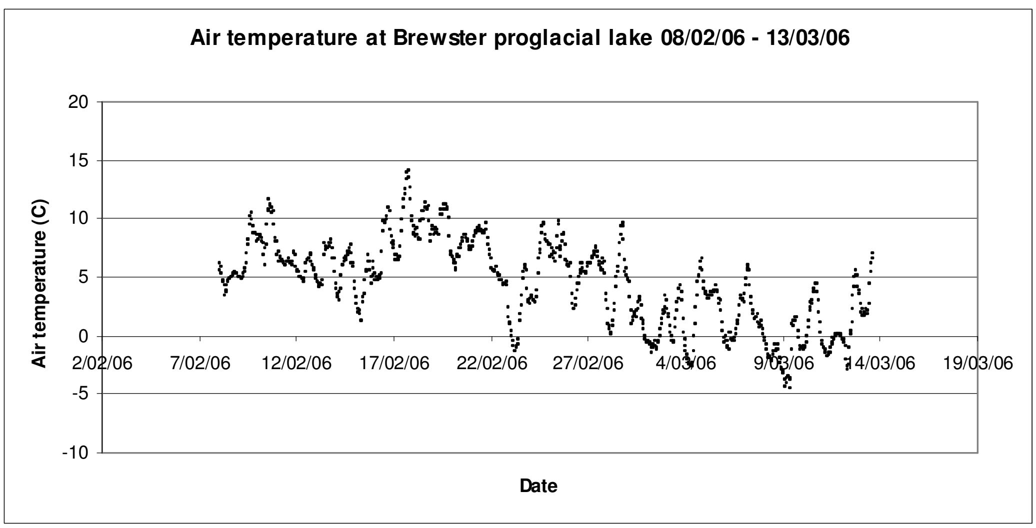


**Figure A2. Air temperature at Brewster proglacial lake from 8 February to 13 March 2006.**

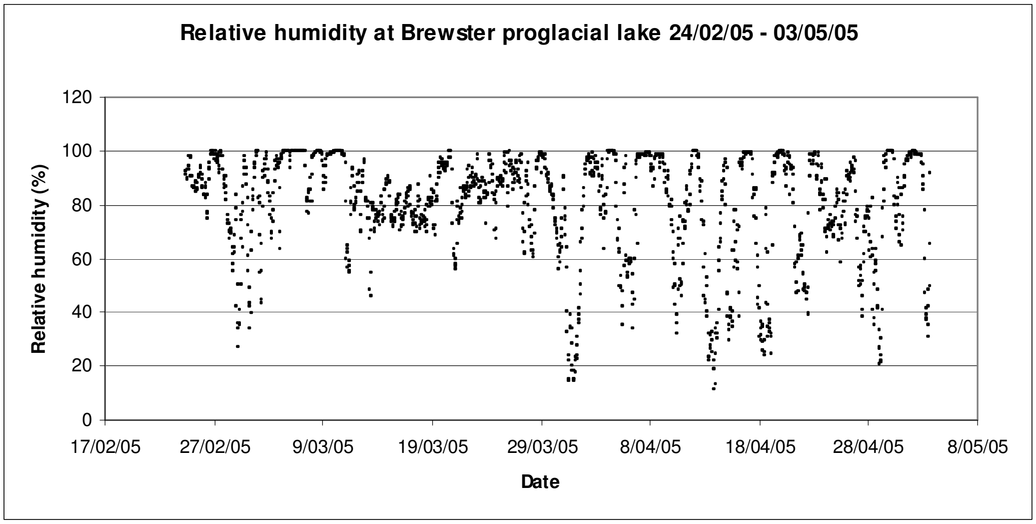


**Figure A3. Relative humidity at Brewster proglacial lake from 24 February to 3 May 2005.**

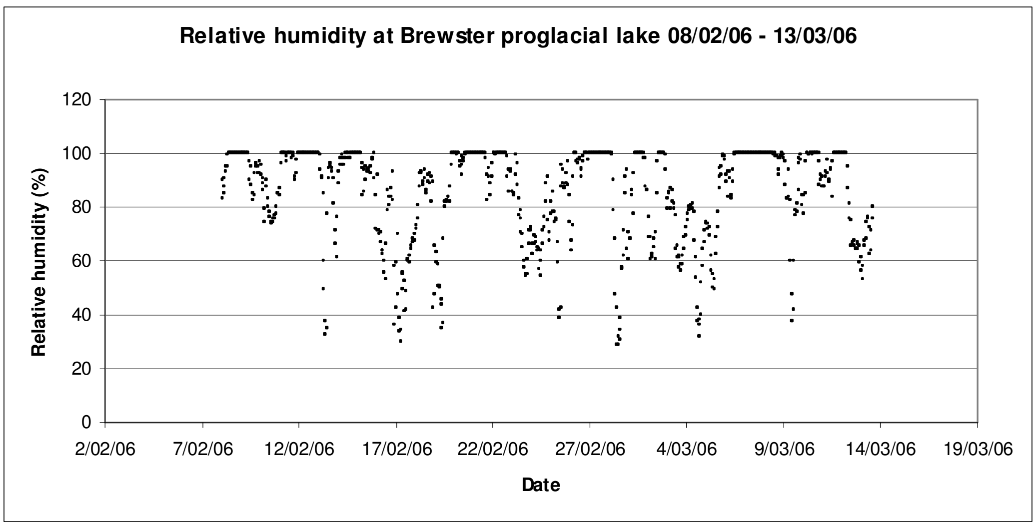


**Figure A4. Relative humidity at Brewster proglacial lake from 8 February to 13 March 2006.**

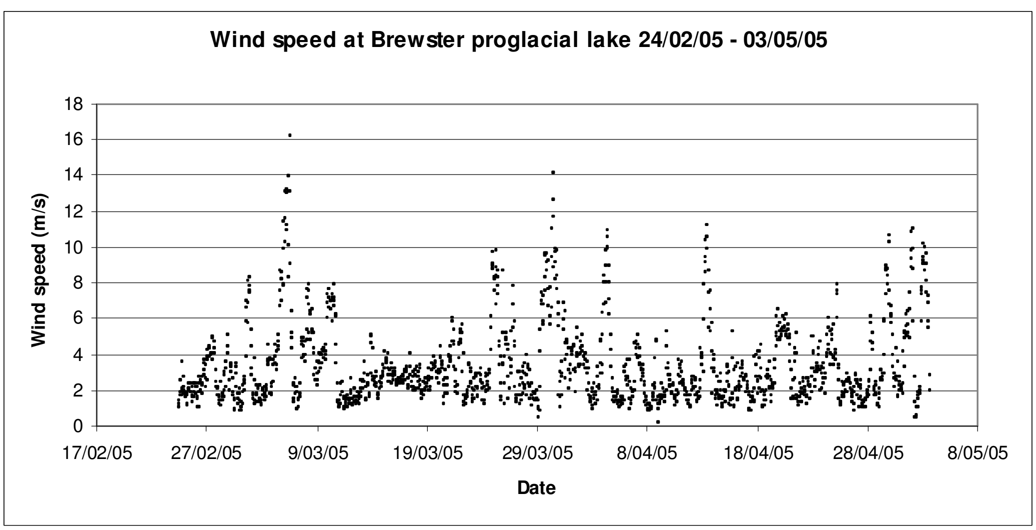


**Figure A5. Wind speed at Brewster proglacial lake from 24 February to 3 May 2005.**

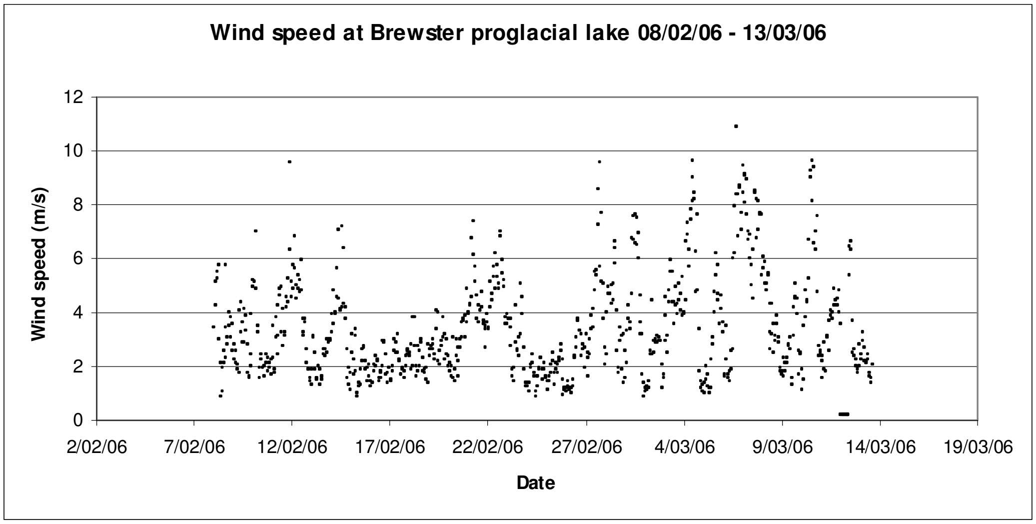


**Figure A6. Wind speed at Brewster proglacial lake from 8 February to 13 March 2006.**

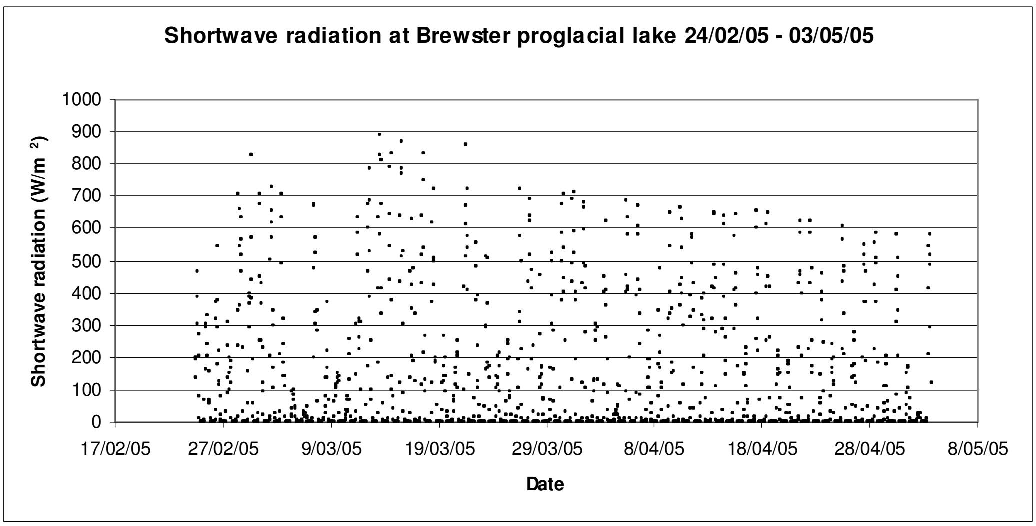


**FigureA7. Shortwave radiation at Brewster proglacial lake from 24 February to 3 May 2005.**

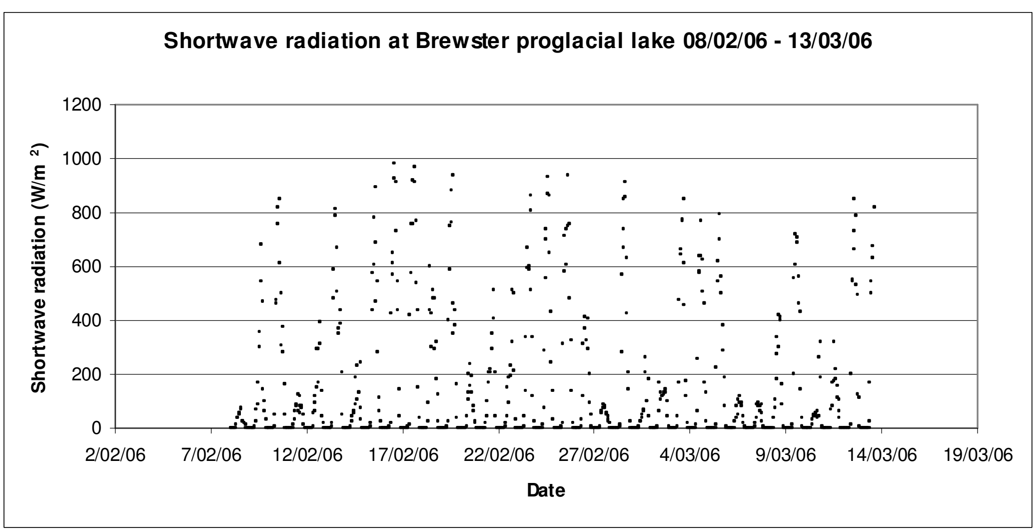


**Figure A8. Shortwave radiation at Brewster proglacial lake from 8 February to 13 March 2006.**

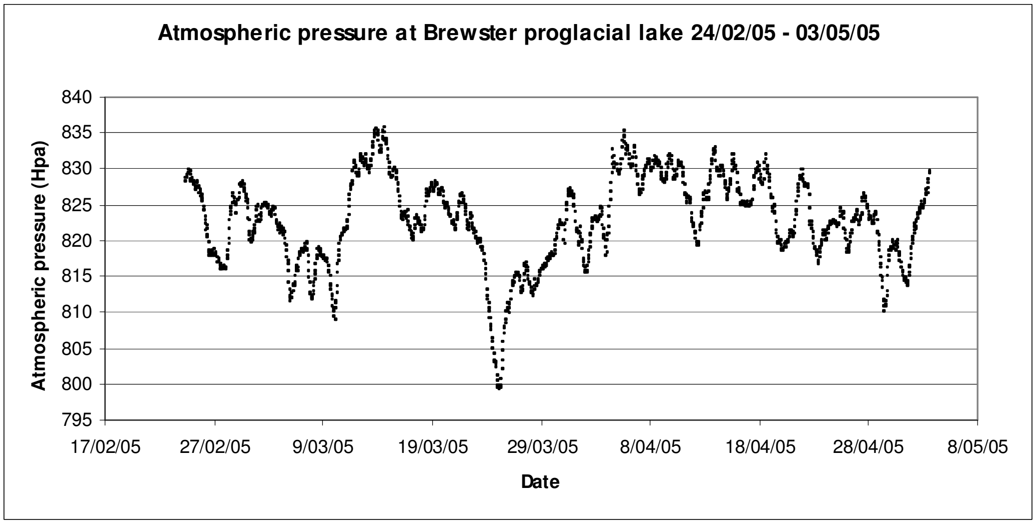


**Figure A9. Atmospheric pressure at Brewster proglacial lake from 24 February to 3 May 2005.**

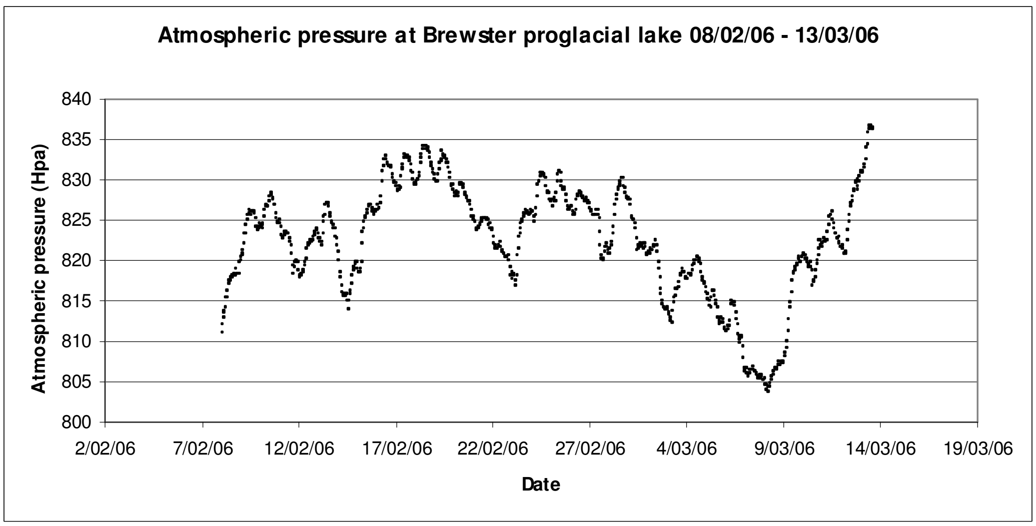


**Figure A10. Atmospheric pressure at Brewster proglacial lake from 8 February to 13 March 2006.**

# Appendix 2.

ANOVA statistics, normal p-plots of residuals and studentised versus standardised residuals for each 'stepwise' model.

### Model Aa: Full data '60%'

**Table A1: ANOVA for model Aa.**

| Model | | Sum of Squares | df | Mean Square | F | Sig. |
|---|---|---|---|---|---|---|
| 1 | Regression | 177909133.165 | 1 | 177909133.165 | 26.002 | .000 |
| | Residual | 437890417.530 | 64 | 6842037.774 | | |
| | Total | 615799550.695 | 65 | | | |
| 2 | Regression | 278492872.812 | 2 | 139246436.406 | 26.008 | .000 |
| | Residual | 337306677.883 | 63 | 5354074.252 | | |
| | Total | 615799550.695 | 65 | | | |
| 3 | Regression | 330314661.864 | 3 | 110104887.288 | 23.912 | .000 |
| | Residual | 285484888.831 | 62 | 4604594.981 | | |
| | Total | 615799550.695 | 65 | | | |
| 4 | Regression | 367011021.990 | 4 | 91752755.498 | 22.497 | .000 |
| | Residual | 248788528.705 | 61 | 4078500.471 | | |
| | Total | 615799550.695 | 65 | | | |
| 5 | Regression | 395414135.936 | 5 | 79082827.187 | 21.530 | .000 |
| | Residual | 220385414.759 | 60 | 3673090.246 | | |
| | Total | 615799550.695 | 65 | | | |

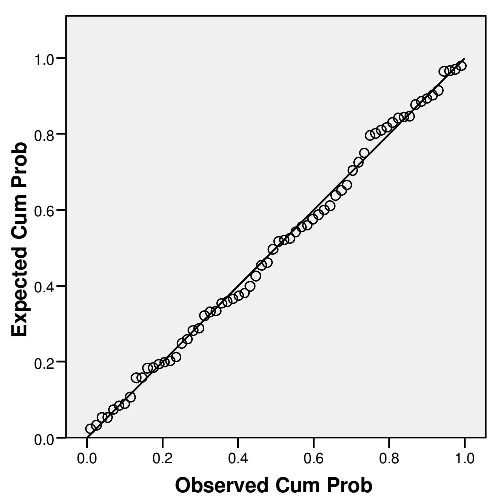


**Figure A11: Normal P-P scatterplot of regression standardized residual showing the distribution of model Aa residuals.**

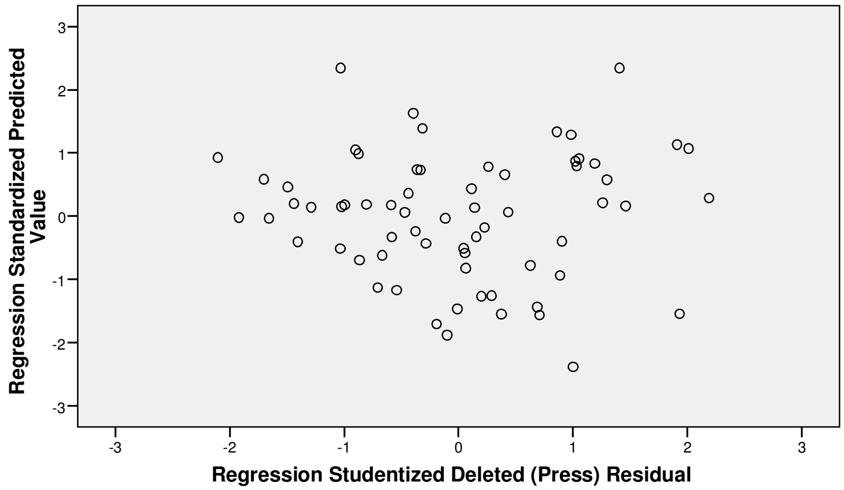


**Figure A12: Studentized residual versus standardized predicted residuals, indicating the spread of model Aa residual variance.**

## Model Ba: Summer 90% 'stepwise'

**Table A2: ANOVA for model Ba.**

| Model | | Sum of Squares | df | Mean Square | F | Sig. |
|---|---|---|---|---|---|---|
| 1 | Regression | 70426741.390 | 1 | 70426741.390 | 56.536 | .000 |
| | Residual | 24913969.272 | 20 | 1245698.464 | | |
| | Total | 95340710.663 | 21 | | | |

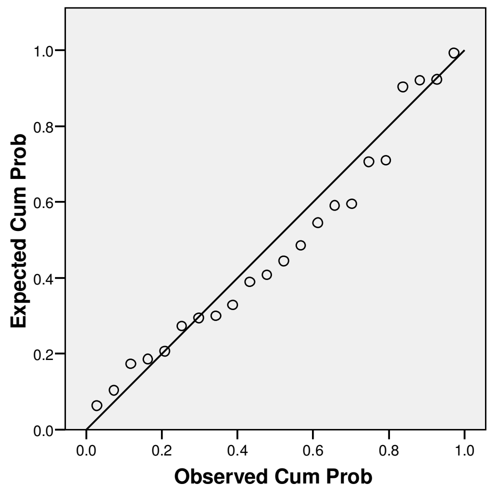


**Figure A13: Normal P-P plot of regression standardized residuals showing the distribution of model Ba residuals.**

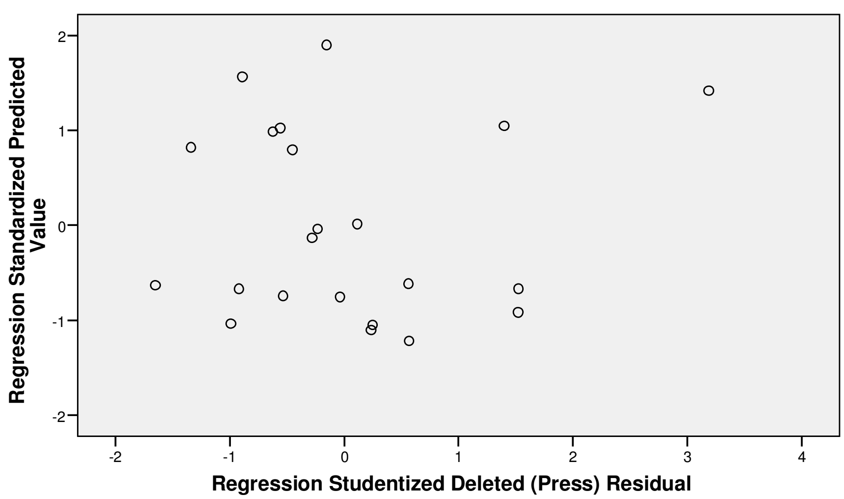


**Figure A14: Studentised residual versus standardized predicted residual indicating the spread of model Ba residual variance.**

## Model Ca: Autumn 60% ‘stepwise’

**Table A3: ANOVA for model Ca.**

| Model | | Sum of Squares | df | Mean Square | F | Sig. |
|---|---|---|---|---|---|---|
| 1 | Regression | 142595937.024 | 1 | 142595937.024 | 29.756 | .000 |
| | Residual | 230023921.255 | 48 | 4792165.026 | | |
| | Total | 372619858.279 | 49 | | | |
| 2 | Regression | 176663773.498 | 2 | 88331886.749 | 21.186 | .000 |
| | Residual | 195956084.781 | 47 | 4169278.400 | | |
| | Total | 372619858.279 | 49 | | | |
| 3 | Regression | 205873863.735 | 3 | 68624621.245 | 18.931 | .000 |
| | Residual | 166745994.544 | 46 | 3624912.925 | | |
| | Total | 372619858.279 | 49 | | | |
| 4 | Regression | 226073041.959 | 4 | 56518260.490 | 17.355 | .000 |
| | Residual | 146546816.320 | 45 | 3256595.918 | | |
| | Total | 372619858.279 | 49 | | | |

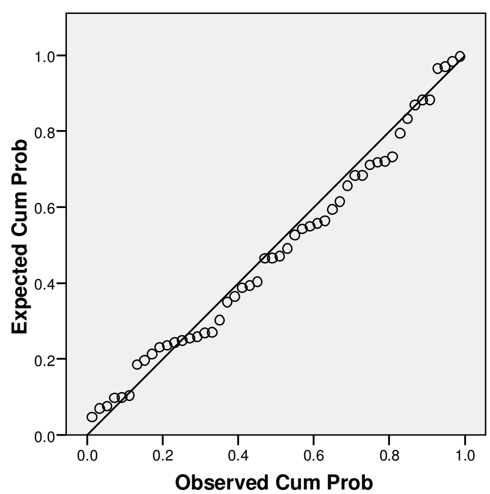


**Figure A15: Normal P-P plot of regression standardized residuals showing the distribution of residuals of model Ca.**

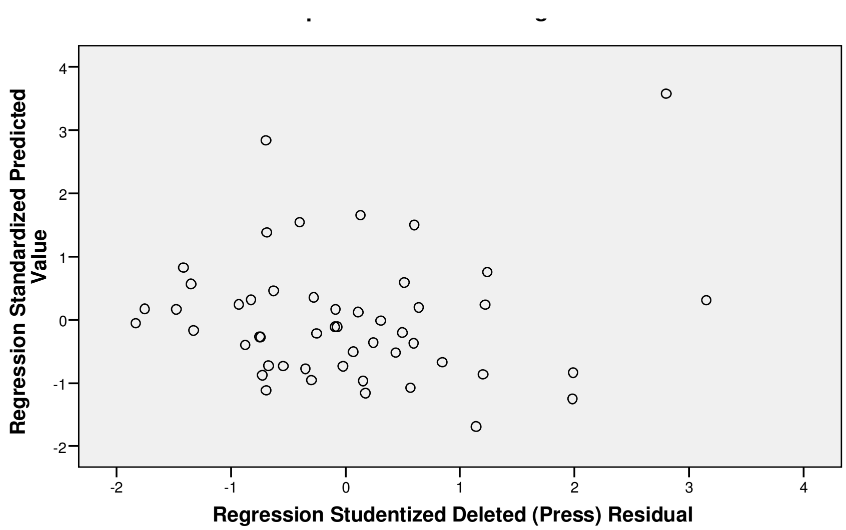


**Figure A16: Studentized residual versus standardized predicted residual indicating the spread of model Ca residual variance.**

## Model D: Full data wet 'stepwise'

**Table A4: ANOVA for model D.**

| Model | | Sum of Squares | df | Mean Square | F | Sig. |
|---|---|---|---|---|---|---|
| 1 | Regression | 215301241.377 | 1 | 215301241.377 | 28.745 | .000 |
| | Residual | 307086392.124 | 41 | 7489912.003 | | |
| | Total | 522387633.501 | 42 | | | |
| 2 | Regression | 295745042.409 | 2 | 147872521.205 | 26.098 | .000 |
| | Residual | 226642591.092 | 40 | 5666064.777 | | |
| | Total | 522387633.501 | 42 | | | |
| 3 | Regression | 324905454.278 | 3 | 108301818.093 | 21.388 | .000 |
| | Residual | 197482179.223 | 39 | 5063645.621 | | |
| | Total | 522387633.501 | 42 | | | |
| 4 | Regression | 403274563.793 | 4 | 100818640.948 | 32.164 | .000 |
| | Residual | 119113069.708 | 38 | 3134554.466 | | |
| | Total | 522387633.501 | 42 | | | |

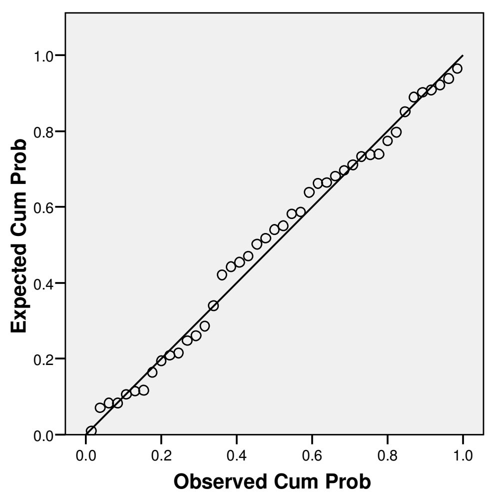


**Figure A17: Normal P-P plot of regression standardized residual showing the distribution of model D residuals.**

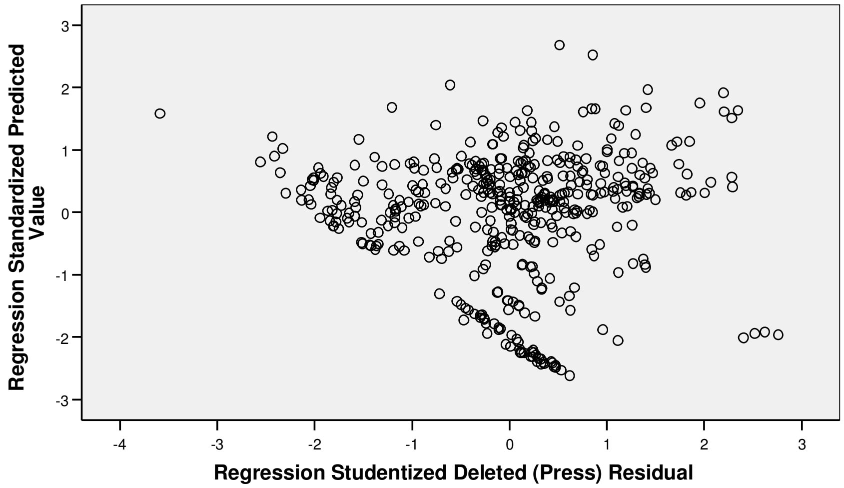


**Figure A18. Studentized residual versus standardized predicted residual indicating the spread of model D residual variance.**

**Model E: Full data dry 60% ‘stepwise’**

**Table A5: ANOVA for model E.**

| Model | | Sum of Squares | df | Mean Square | F | Sig. |
|---|---|---|---|---|---|---|
| 1 | Regression | 28276050.280 | 1 | 28276050.280 | 8.522 | .006 |
| | Residual | 106174483.525 | 32 | 3317952.610 | | |
| | Total | 134450533.805 | 33 | | | |
| 2 | Regression | 65256887.107 | 2 | 32628443.554 | 14.618 | .000 |
| | Residual | 69193646.698 | 31 | 2232053.119 | | |
| | Total | 134450533.805 | 33 | | | |

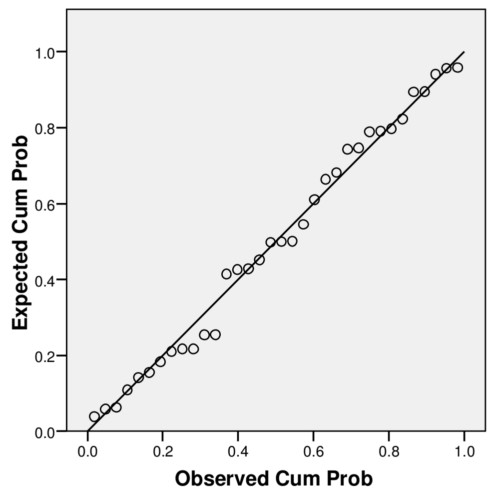


**Figure A19: Normal P-P plot of regression standardized residuals showing the distribution of model E residuals.**

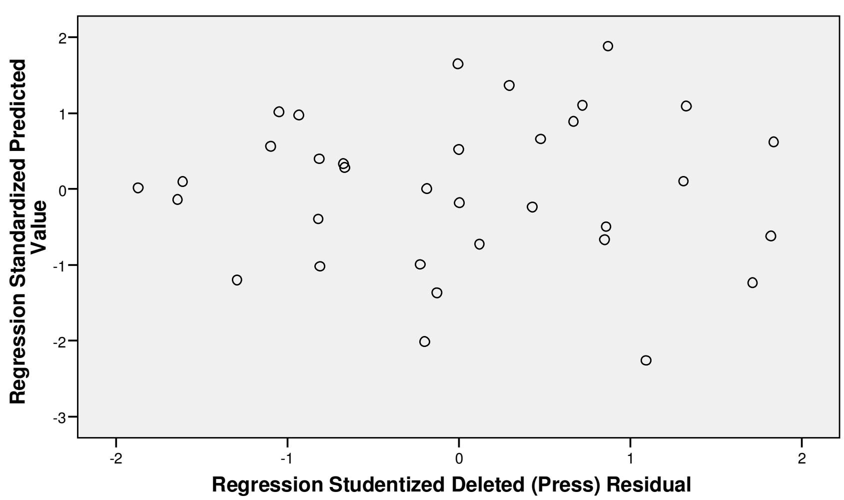


**Figure A20: Studentized residual versus standardized predicted residual, indicating the spread of model E residual variance.**

## Model Fa: Summer wet 'stepwise'

**Table A6: ANOVA for model Fa.**

| Model | | Sum of Squares | df | Mean Square | F | Sig. |
|---|---|---|---|---|---|---|
| 1 | Regression | 28419478.017 | 1 | 28419478.017 | 15.693 | .002 |
| | Residual | 19920702.659 | 11 | 1810972.969 | | |
| | Total | 48340180.675 | 12 | | | |

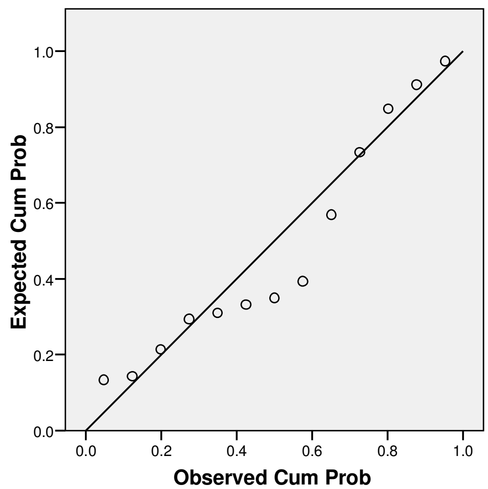


**Figure A21: Normal P-P plot of regression standardized residuals showing the distribution of model Fa residuals.**

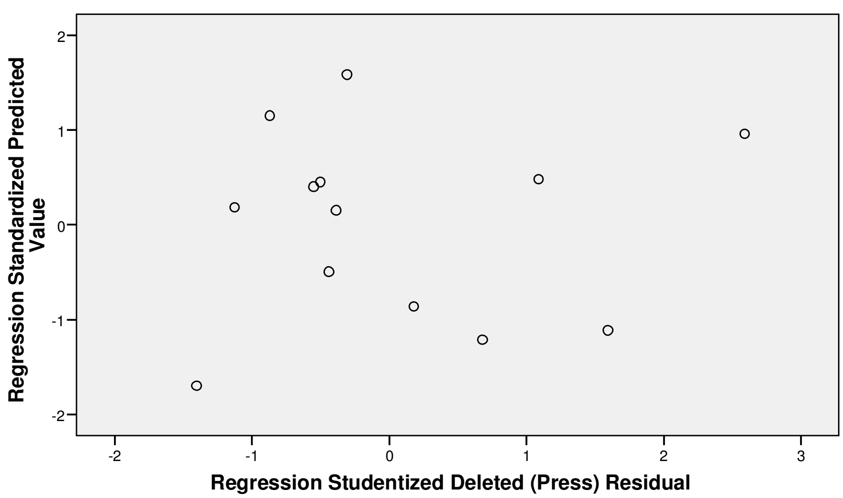


**Figure A22: Studentized residuals versus standardized predicted residuals indicating the spread of model Fa residual variance.**

## Model Fb: Summer wet 'stepwise' (excluding wind speed)

**Table A7. ANOVA for model Fb.**

| Model | | Sum of Squares | df | Mean Square | F | Sig. |
|---|---|---|---|---|---|---|
| 1 | Regression | 15857150.119 | 1 | 15857150.119 | 5.370 | .041 |
| | Residual | 32483030.556 | 11 | 2953002.778 | | |
| | Total | 48340180.675 | 12 | | | |

## Model H: Autumn wet 'stepwise'

**Table A8: ANOVA for model H.**

| Model | | Sum of Squares | df | Mean Square | F | Sig. |
|---|---|---|---|---|---|---|
| 1 | Regression | 112038766.864 | 1 | 112038766.864 | 14.554 | .001 |
| | Residual | 215553629.847 | 28 | 7698343.923 | | |
| | Total | 327592396.712 | 29 | | | |
| 2 | Regression | 174348367.947 | 2 | 87174183.974 | 15.359 | .000 |
| | Residual | 153244028.765 | 27 | 5675704.769 | | |
| | Total | 327592396.712 | 29 | | | |
| 3 | Regression | 210583161.655 | 3 | 70194387.218 | 15.598 | .000 |
| | Residual | 117009235.057 | 26 | 4500355.194 | | |
| | Total | 327592396.712 | 29 | | | |
| 4 | Regression | 239662815.541 | 4 | 59915703.885 | 17.035 | .000 |
| | Residual | 87929581.171 | 25 | 3517183.247 | | |
| | Total | 327592396.712 | 29 | | | |
| 5 | Regression | 256967836.394 | 5 | 51393567.279 | 17.465 | .000 |
| | Residual | 70624560.317 | 24 | 2942690.013 | | |
| | Total | 327592396.712 | 29 | | | |
| 6 | Regression | 254542450.101 | 4 | 63635612.525 | 21.778 | .000 |
| | Residual | 73049946.611 | 25 | 2921997.864 | | |
| | Total | 327592396.712 | 29 | | | |

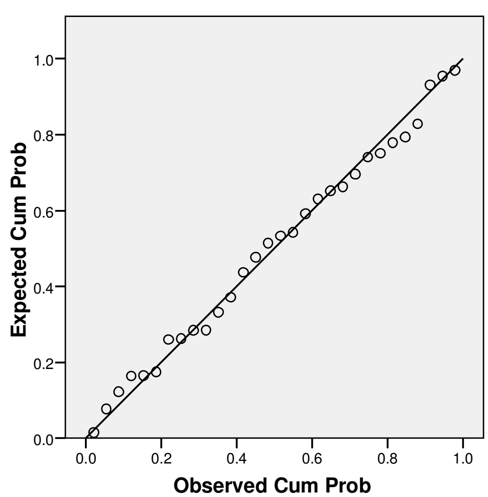


**Figure A23: Normal P-P plot of regression standardized residual showing the distribution of model H residuals.**

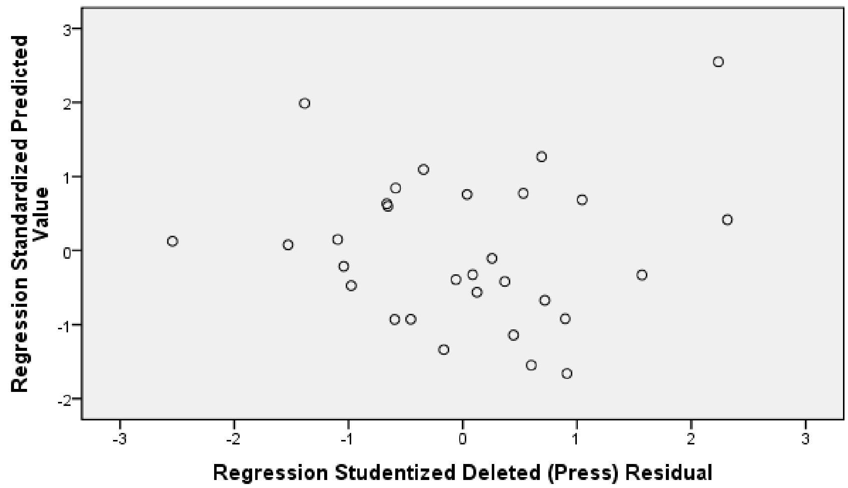


**Figure A24: Studentized residual versus standardized predicted residual indicating the spread of model H residual variance.**

**Model I: Autumn dry 65% 'stepwise'**

**Table A9: ANOVA for model I.**

| Model | | Sum of Squares | df | Mean Square | F | Sig. |
|---|---|---|---|---|---|---|
| **1** | Regression | 9161788.422 | 1 | 9161788.422 | 4.715 | .038 |
| | Residual | 60241469.225 | 31 | 1943273.201 | | |
| | Total | 69403257.647 | 32 | | | |
| **2** | Regression | 21702101.117 | 2 | 10851050.559 | 6.824 | .004 |
| | Residual | 47701156.530 | 30 | 1590038.551 | | |
| | Total | 69403257.647 | 32 | | | |
| **3** | Regression | 28655132.712 | 3 | 9551710.904 | 6.798 | .001 |
| | Residual | 40748124.935 | 29 | 1405107.756 | | |
| | Total | 69403257.647 | 32 | | | |

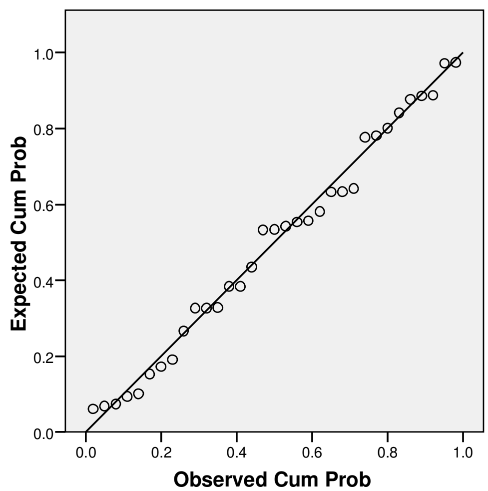


**Figure A25: Normal P-P plot of regression standardized residuals showing the distribution of residuals in model I.**

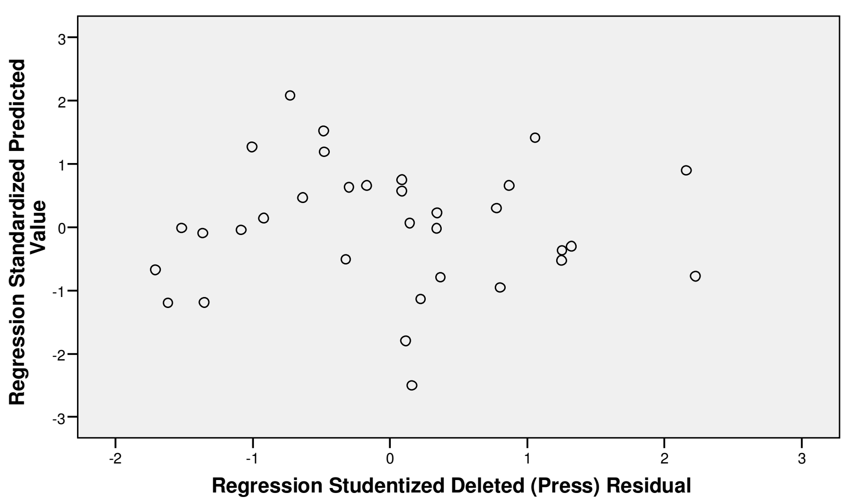


**Figure A26: Studentized residuals versus standardized predicted residuals indicating the spread of model I residual variance.**